INVESTIGATING THE ROLE OF GAMMA-AMINOBUTYRIC ACID (GABA) IN SEDATION: A COMBINED ELECTROPHYSIOLOGICAL, HAEMODYNAMIC AND SPECTROSCOPIC STUDY IN HUMANS

Dr. Neeraj Saxena

Thesis submitted in partial fulfilment of the requirement

for the Degree of

Doctor of Philosophy

at

Cardiff University

2017

School of Medicine

ACKNOWLEDGEMENTS

I would start off by thanking my supervisors Professors Judith Hall and Richard Wise. This work would not have been possible without the inspiration, guidance, support and mentoring provided by them over this long journey. They kept the faith, despite the slow progress at times, and always managed to find solutions for seemingly insurmountable problems. Also, thanks to Professor Krish Singh for his invaluable advice during various stages of this work.

Thanks to CUBRIC and all the scientists based in CUBRIC who provided an immensely stimulating and supportive environment to carry out this research. Special thanks to Suresh Muthukumaraswamy, John Evans, Ana Diukova and Tommaso Gili who helped me understand and learn the basics of neuroimaging techniques and help run the rather complex studies, surprisingly, smoothly. Also, thanks to Kevin Murphy, Ian Driver and Gavin Perry for their expertise and advice, especially at crucial moments. Thanks to other CUBRIC members including Peter Hobden, Spiro Stathakis, Cyril Charron, Martin Stuart and Angela who went out of their way to help me with the scanning, IT and other organisational issues. I also thank my anaesthetic colleagues, Danielle Huckle and Sarah Bell who provided anaesthetic support during these studies.

I also thank my employers (Cardiff University and Cwm Taf University Health Board) for providing support, for me to be able to spend time towards my thesis while carrying out my other clinical and academic responsibilities. I also thank National Institute for Social Care and Health Research (now Health Care Research Wales) for funding some of my research time.

Last, but by no way the least, I thank all the volunteers who participated in these research studies and gave up their time to contribute towards the progress of science.

KEY WORDS

Mechanisms: Anaesthesia, Sedation; GABA; Neuroimaging: Magnetoencephalography, Magnetic Resonance Spectroscopy, Functional MRI, BOLD, Arterial Spin Labeling

In loving memory of my father who inspired me to never stop learning.

SUMMARY

A better understanding of the mechanisms of anaesthesia and sedation are expected not only to improve the understanding of the neural correlates of consciousness but also to help improve safety from the complications of anaesthesia/ sedation and develop safer drugs and objective brain function monitoring systems. Neuroimaging modalities such as functional MRI, magnetoencephalography and MR spectroscopy provide complimentary information about brain functions and can help interrogate brain activity in a living human brain. Most anaesthetic drugs act by enhancing the inhibitory actions of GABA in the brain. Most neuroimaging research has focused on anaesthetic-induced unconsciousness, with only few investigating the earliest levels of sedation-induced altered consciousness.

The work in this thesis used a range of advanced neuroimaging modalities to investigate the role of GABA (through a GABA-ergic drug, propofol), during mild sedation, in humans. This was performed as a series of experiments within two, sequential, scanning sessions, MEG followed by fMRI, in the same participants.

Propofol resulted in a dissociation of the visual gamma band response (decreased evoked, increased induced power). This was related to a reduced BOLD fMRI response but there were no changes in MRS detectable GABA concentration. Response to multisensory stimulation also revealed interesting changes with MEG and fMRI. Functional connectivity analyses showed changes in connectivities of the posterior cingulate cortex (key hub of default-mode network) and thalamus with each other and other key brain regions. Resting state networks were identified with MEG too, which revealed interesting increases in connectivity in certain band- limited networks while motor networks showed no change. Perfusion fMRI using arterial spin labelling revealed a global and regional reduction in perfusion, highlighting some of the key regions (frontal cortex, precuenus, PCC and thalamus) involved in sedation.

DECLARATION

This work has not been submitted in substance for any other degree or award at this or any other university or place of learning, nor is being submitted concurrently in candidature for any degree or other award.

Signed …… 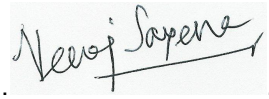 … (candidate) Neeraj Saxena

Date …20.09.2017……

STATEMENT 1

This thesis is being submitted in partial fulfillment of the requirements for the degree of …PhD

Signed ……  … (candidate) Neeraj Saxena

Date …20.09.2017……

STATEMENT 2

This thesis is the result of my own independent work/investigation, except where otherwise stated, and the thesis has not been edited by a third party beyond what is permitted by Cardiff University's Policy on the Use of Third Party Editors by Research Degree Students. Other sources are acknowledged by explicit references. The views expressed are my own.

Signed …… 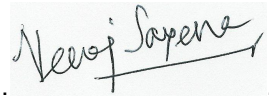 … (candidate) Neeraj Saxena

Date …20.09.2017……

STATEMENT 3

I hereby give consent for my thesis, if accepted, to be available online in the University's Open Access repository and for inter-library loan, and for the title and summary to be made available to outside organisations.

Signed …… 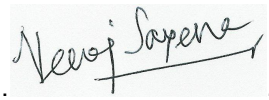 … (candidate) Neeraj Saxena

Date …20.09.2017……

Dissemination of Findings

Published – peer reviewed papers

1. Gili, T., Saxena, N., Diukova, A., Murphy, K., Hall, J. E. & Wise, R. G. 2013. The thalamus and brainstem act as key hubs in alterations of human brain network connectivity induced by mild propofol sedation. *J Neurosci,* 33**,** 4024-31.

2. Saxena, N., Muthukumaraswamy, S. D., Diukova, A., Singh, K., Hall, J. & Wise, R. 2013. Enhanced Stimulus-Induced Gamma Activity in Humans during Propofol-Induced Sedation. PLoS One, 8, e57685.

Conference Abstracts

1. Saxena, N., Diukova, A., Venzi, M., Gili, T., Huckle, D., Bell, S., Wise, R. G. & Hall, J. E. 2012. Endogenous brain oscillations during sedation: Initial results of a magnetoencephalography and functional magnetic resonance imaging study. Anaesthetic Research Society Meeting 2011 London. *British Journal of Anaesthesia*, 721.

2. Gili, T., Saxena, N., Diukova, A., Murphy, K., Hall, J. & Wise, R. 2012a. Mapping alterations in cortical and subcortical functional connectivity induced by light sedation. . *OHBM Proceedings*.

3. Gili, T., Saxena, N., Diukova, A., Murphy, K., Hall, J. & Wise, R. 2012b. Mild sedation alters eigenvector centrality of BOLD FMRI in the thalamus and brainstem *OHBM Proceedings*.

4. Gili, T., Saxena, N., Diukova, A., Murphy, K., Hall, J. & Wise, R. 2012c. Physiological noise correction may help to detect changes in brain activity during mild sedation. . *OHBM Proceedings*.

5. Saxena, N., Diukova, A., Venzi, M., Gili, T., Huckle, D., Bell, S., Wise, R. G. & Hall, J. E. 2012. Endogenous brain oscillations during sedation: initial results of a magnetoencephalography and functional magnetic resonance imaging study. *British Journal of Anaesthesia,* 108, 721P.

6. Saxena, N., Gili, T., Huckle, D., Bell, S., Hall, J. & Wise, R. Mild propofol sedation reduces frontal lobe and thalamic cerebral blood flow: an arterial spin labelling study. BJA Research forum, 2016 London. *British Journal of Anaesthesia*, e841.

Papers to be submitted

1. Mild propofol sedation reduces frontal lobe and thalamic cerebral blood flow: an arterial spin labeling study.

Invited presentations

1. Society of Intravenous Anaesthesia- Annual Scientific Meeting-2014: Neurobiology of sedation: what can we learn from functional neuroimaging?

2. Royal College of Anaesthetists – Jubilee Current Concepts Symposium 2013: Rising stars in anaesthesia, pain and critical care, London- Depth of sedation and anaesthesia: What does neuroimaging tell us?

3. Anaesthesia Post fellowship study day, Cardiff, 2013- Anaesthesia and consciousness: Insights from neuroimaging.

CONTENTS

LIST OF TABLES AND FIGURES

Tables

Figures

LIST OF ABBREVIATIONS

5-HT	5- hydroxytryptamine
AAGA	Accidental awareness under general anaesthesia
ACC	Anterior cingulate cortex
Ach	acetylcholine
AMPA	α-amino-3-hydroxy-5-methyl-4-isoxazole-propionic acid
ASL	Arterial spin labelling
BOLD	Blood oxygen level dependent
CBF	Cerebral blood flow
CO_2	Carbon dioxide
CT	Cortico-thalamic
CUBRIC	Cardiff University brain research imaging centre
CV	Coefficient of variance
DA	Dopamine
DBP	Diastolic blood pressure
DMN	Default mode network
DpME	Deep mesencephalic reticular formation
ECD	Equivalent current dipole
EEG	Electroencephalography
EPI	Echoplanar imaging
FLIRT	FMRIB's linear registration tool
fMRI	functional MRI
FSL	FMRIB's software library package
FSPGR	Fast Spoiled Gradient-Recalled-Echo (pulse sequence)
GABA	Gamma- Aminobutyric acid
Gal	Galanin
GBR	Gamma band response
GFP	Global field power
Glut	Glutamate
GM	Grey matter
HA	Histamine
HR	Hear rate
HRF	Haemodynamic response function
Hz	Hertz
ICA	Independent component analysis
ICU	Intensive care unit
K+	Potasssium ion
LC	Locus coeruleus
LDT	Laterodorsal tegmentum
MAP	Mean arterial pressure
MCE	Minimum current estimate
MCS	Minimally conscious state
MEG	Magnetoencephalography

MEGA-PRESS	MEscher-GArwood Point –RESolved Spectroscopy
MNE	Minimum norm estimates
MNI	Montreal Neuroimaging institute
MnPO	Median preoptic nucleus
mPFC	Medial prefrontal cortex
MR	Magnetic resonance
MRI	Magnetic resonance imaging
NAP	National audit project
NE	Norepinephrine
NMDA	N-Methyl-D-aspartate
NREM	Non- rapid eye movement
O_2	Oxygen
OAA/S	Observer's assessment of alertness/ sedation
Ox	Orexin/ hypocretin
PASL	Pulsed arterial spin labelling
PCC	Posterior cingulate cortex
PET	Positron emission tomography
PnO	Pontine reticular nucleus oral part
PPT	Pedunculopontine tegmentum
PTSD	Post-traumatic stress disorder
RAS	Reticular activating system
REM	Rapid eye movement
RF	Radiofrequency
RN	Raphae nuclue
ROI	Region of interest
RSN	Resting state network
SAM	Synthetic apertune magnetometry
SBP	Systolic blood pressure
SCN	Suprachiasmatic nucleus
SD	Standard deviation
TC	Thalamo-cortical
TCI	Target controlled infusion
TE	Echo time
TMN	Tuberomamillary nucleus
TR	Repetition time
UWS	Unresponsive wakefulness syndrome
VLPO	Ventrolateral preopotic nucleus
vPAG	Ventral periaqueductal gray
WM	White matter

Chapter 1 : Introduction and Literature review

"*Gentlemen! This is no humbug."*

W. G. Morton, on 16th October, 1846, used ether to facilitate a painless dental extraction. This, first reported, demonstration of anaesthesia, stunned the audience and led the impressed surgeon to proclaim, "this is no humbug" (Haridas, 2016). The ground-breaking impact of this discovery was immediately obvious and it rapidly became popular for all kinds of surgeries. Ability of certain drugs to transiently, reversibly and controllably alter consciousness and provide pain relief has made surgeries safer and made advances in surgical procedures possible; things, which could not have been contemplated without anaesthesia. General anaesthesia is given to nearly a million human beings, all over the world, every single day; yet, mechanisms of anaesthesia continue to be a 'humbug' in some sense.

1.1 Consciousness and anaesthesia

The basic tenets of anaesthesia include the components of unconsciousness, amnesia and immobility. A more comprehensive definition of anaesthesia, however, may include suppression of reflexes, analgesia, muscle relaxation, prevention of nausea and vomiting and even prevention of long-term side effects such as postoperative delirium (confusional state with impairment of memory and attention) (European Delirium and American Delirium, 2014) or postoperative cognitive dysfunction (deficits in one or more discrete areas of mental state, such as attention, concentration, executive function, memory, visuospatial ability and psychomotor speed over a period of weeks to months) (Rasmussen et al., 2001, Urban and Bleckwenn, 2002).

Unconsciousness, for anaesthetists, means unresponsiveness to verbal command, tactile stimuli or even painful stimuli. While it is clear that unresponsiveness does not really mean unconsciousness, it provides a practical endpoint for anaesthetists (Sanders et al., 2012). Beyond the practicalities of anaesthesia, unconsciousness may be difficult to define, since 'consciousness' itself continues to be difficult to explain and define. In philosophical terms, the subjective experience which makes someone conscious

continues to be a ‘hard- problem’ to define, let alone study in a systematic manner (Chalmers, 1995).

Indeed, anaesthetic drugs, producing a state of altered consciousness can be used as a neurophysiological probe, as suggested by Henry Beecher, to study consciousness (Beecher, 1947). This proposition is increasingly bearing fruit, with rapid advances in neuroimaging tools and analytic methods.

According to Baar’s ‘global workspace theory’ the human brain can be compared to a theatre, where ‘selective attention’ shines a spotlight over various competing conscious and unconscious processes (Baars et al., 2003). Various hierarchically organised networks synchronise various neuronal workspaces. For example, the area involved in attention being the prefrontal cortices and sensory cortices may have their workspaces, while other brain regions such as the parietal cortex, doing unconscious processing provides the ‘context’. An alternative theory (Information Integration theory) by Tononi, proposes that consciousness corresponds to the capacity of a system to integrate information (Tononi, 2004). This further depends upon two key concepts- ‘differentiation’- availability of a large number of conscious experiences and ‘integration’- the unity of each such experience. Mashour proposed, as an extension of the information integration theory, a ‘cognitive unbinding theory’ of anaesthesia where isolation of neural activity results in anaesthesia (Mashour, 2013). Some aspects of these theories have been able to explain the neuroimaging findings of anaesthesia, and these findings in return have helped consolidate these theories of consciousness.

1.2 Mechanisms of anaesthesia

Early theories of anaesthetic action, presumed that all anaesthetic drugs worked in the same way and resulted in a global suppression of neural activity (‘wet blanket theory’). However, it soon became clear that regional selectivity may exist and so some brain regions may be more crucial than others.

Meyer and Overton, showed that the lipophilicity (solubility in Olive oil) of anaesthetic drugs correlated with their anaesthetic potencies. This led to the hypothesis that the neuronal lipid bilayer was the key site of action of anaesthetic drugs and appeared to provide the basis for a 'unitary' site of action. This further led to numerous theories of how the anaesthetic agents may act with the lipid bilayers (Kopp Lugli et al., 2009). These theories could not explain all aspects of anaesthetic actions and so the focus shifted to alternate targets. Protein targets emerged as valid targets for anaesthetic drugs, and the rapid discovery of the range of potential protein targets meant that a unitary protein molecule as target for anaesthetic actions was unlikely.

1.2.1 Molecular targets for anaesthetic drugs

There are multiple receptors that target sites for anaesthetic drug actions.

Gamma (γ)- Aminobutyric acid (GABA) receptors are the main inhibitory receptors and are targeted by most anaesthetic drugs. GABA-A receptors are heteromeric structures with 2α, 2β and 1γ units. The γ-subunit may be replaced by variants such as δ subunits (Farrant and Nusser, 2005, Hevers and Luddens, 1998). The receptors with the γ unit are commonly located in the post-synaptic membranes while those with the δ units are heavily present in the extra-synaptic sites (Nusser et al., 1996). It is the subunit structure and their locations that determine most of the actions of the anaesthetic agents. The synaptic release of GABA in response to nerve stimuli, resulting in the fast phase synaptic inhibition is well known (phasic release). More recently, a 'tonic' form of inhibition resulting from extra-synaptic release and action of GABA has been identified. As the extra-synaptic receptors are not usually saturated and also because they desensitise less as compared to the post-synaptic receptors, they are more efficient targets for anaesthetic drugs to produce their 'inhibitory' actions (Bianchi et al., 2002, Mody et al., 1994).

Importance of GABA receptor subunits is further exemplified in the hippocampal GABA receptors, with α-5 subunits, which are highly sensitive to anaesthetic drugs (Sur et al., 1999). This may be responsible for the early-amnesic effects of anaesthetic drugs. Similarly, GABA-A receptors with α-4 subunits may account for the amnesic effects of

volatile agents (Rao et al., 2009). Sedative effects of anaesthetic drugs are also highly dependent on the subunit structure of the GABA receptors. Replacement of the asparagine residue at position 265 in the β-2 or β-3 GABA-A receptor subunit with serine or methionine, respectively, rendered GABA-A receptors containing these subunits relatively insensitive to etomidate or propofol (Reynolds et al., 2003). Similarly, α-1 subunit's specific constitution is essential for the sedative properties of benzodiazepines (Rudolph et al., 1999). Gaboxodol's sedative actions are dependent on the presence of α-4 and δ subunits in the thalamic ventrobasal neurons (Chandra et al., 2006). Hypnotic (unconsciousness) actions by anaesthetic drugs are dependent on the β-2 and β-3 subunits (Reynolds et al., 2003). Immobility, an essential component of anaesthesia, is mediated through the spinal GABA-A receptors with the β-3 subunits (Zeller et al., 2007). Volatile anaesthetics act through multiple receptors including GABA-A. GABA receptors containing α-1 and β-3 subunits have been shown to be important binding sites for the action of volatiles (Mihic et al., 1997).

Glutamate is the major excitatory neurotransmitter in the brain. It acts on N-Methyl-D-aspartate (NMDA) and non-NMDA receptors (which include AMPA: α-amino-3-hydroxy-5-methyl-4-isoxazole-propionic acid and kainite receptors). These non-NMDA receptors are responsible for the fast phase of the excitatory post-synaptic potentials. Anaesthetic drugs usually have no effect on these non-NMDA receptors. NMDA receptors, however, are responsible for the slow phase of the post-synaptic potential and are affected by anaesthetic drugs such as ketamine, xenon and nitrous-oxide. Ketamine's main actions on the NMDA receptors are thought to be of non-competitive antagonism. Xenon and nitrous oxide also act on NMDA receptors by competing with the glycine binding subunit of the NMDA receptor (Dickinson et al., 2007).

Potassium ion (K^+) channels may also contribute to the anaesthetic actions of the volatile agents, as they may directly activate or enhance the activity of the two-pore domain family of K^+ channels (Gray et al., 1998). Other ion channels such as hyperpolarisation –activated cyclic nucleotide-gated channels which help maintain synchrony of neuronal networks and also generation of spontaneous rhythm in 'pacemaker' neurons may also be anaesthetic targets (Biel et al., 2009). Volatile agents,

propofol and ketamine: all have been shown to inhibit the activities of these channels (Chen et al., 2009).

Through these potential molecular targets, anaesthetics may modulate neuronal function by a variety of mechanisms. They can reduce neuronal excitability and disrupt the flow of information between neurons. This may be the key mechanism of drugs acting on GABA receptors. Anaesthetic agents may also alter long-term potentiation, which normally occurs through pre- and post-synaptic firing occurring coincidentally, resulting in strengthening of the excitatory synapses. This occurs through the stabilisation of glutamate receptors in postsynaptic membrane and growth of new synapses. Finally, anaesthetic agents may alter the balance of the excitatory and inhibitory activity in neuronal networks leading to changes in network oscillatory activity (discussed further in Section 1.4).

1.3 Sleep and anaesthesia

Research into un-consciousness mechanisms can be looked into through alterations in consciousness induced during physiological (such as sleep), pharmacological (such as sedation and anaesthesia) and pathological conditions (such as epilepsy and vegetative states). Indeed, there is a fair degree of overlap among those conditions.

The phrase “now you will go off to sleep”, is commonly used by anaesthetists as they administer anaesthesia. Anaesthetic- unconsciousness is related to natural sleep, by patients and clinicians alike, as it provides a sense of comfort and reversibility. While sleep has been defined as a naturally occurring, periodic state of rest during which consciousness of one’s environment and responses to external stimuli are largely suspended (Franks and Zecharia, 2011), it cannot be completely characterised without referring to its elements such as spontaneous movements, variations in muscle tone, response to command, self perception, mental imagery, thermodynamic control and reversibility upon external stimulation (Bonhomme et al., 2011). While there are key differences between natural sleep and anaesthetic-induced ‘sleep’, there are enough commonalities, which has provided a substrate for further research into anaesthetic mechanisms.

1.3.1 Target brain sites for anaesthetic drug actions

Anaesthetics, in part, produce their effects by stimulating natural sleep promoting pathways. Some of the key brain regions, responsible for maintaining the sleep-wake homeostasis have been studied in detail and the effect of anaesthetic drugs on those have been evaluated. The key nuclei lie in the brainstem (forming part of the Reticular Activating System- RAS), and subcortical (hypothalamus and thalamus) regions have been described below.

Locus Coeruleus

Locus Coeruleus (LC) is situated in the brainstem and has the highest collection of noradrenergic neurons in the brain. It innervates diffusely to other parts of the brain, including directly to the cortex, thalamus, hypothalamus, basal forebrain, amygdala, hippocampus and other subcortical systems. Firing of the LC neurons promote wakefulness through actions on the medial septum, medial preoptic area and substantia innominate in the basal forebrain (Berridge, 2008). It also switches the tone of the thalamo-cortical neurons from a 'burst' pattern (as in sleep) to a 'spiking' pattern supporting wakefulness.

Raphe nuclei (RN)

These nuclei are the brain's major source of serotonin. It may exert biphasic influences on arousal, such as its effect on sleep-active ventrolateral preoptic nucleus (VLPO), where it inhibits half of the neurons while it stimulates the other half (Gallopin et al., 2005).

Ventral periaqueductal gray

It has wake active dopaminergic neurons, so drugs increasing dopamine increase wakefulness. Ventral periaqueductal gray (vPAG) efferents go to arousal state regulation regions including the basal forebrain, orexinergic neurons in the perifornical hypothalamus, midline thalamic and intralaminar thalamus, laterodorsal tegmentum, as well as the sleep-active Ventrolateral preoptic nucleus (VLPO) (Lu et al., 2006).

Laterodorsal tegmentum (LDT) and pedunculopontine tegmentum (PPT)

These nuclei constitute the major cholinergic nuclei in the brainstem and promote wakefulness or rapid-eye-movement (REM) sleep. They innervate the midline and intralaminar thalamic nuclei and thalamic reticular nuclei and alter thalamic activity from 'bursting' to 'spiking' (Steriade et al., 1990). They send projections to the pontine reticular formation and fire mainly during REM sleep. They also have GABA-ergic neurons (Fuller et al., 2007) which promote REM sleep and so may be influenced by GABA-ergic drugs.

Pontine reticular nucleus

Here Rapid Eye movement (REM)-ON generating nuclei are found, however, they can promote wakefulness too. They receive cholinergic, orexinergic and GABA-ergic inputs. Increased GABA promotes wakefulness as demonstrated with anaesthetics (Vanini et al., 2008).

Tuberomamillary nucleus

The brain's sole histaminergic signalling nucleus has widespread connections. Tuberomamillary nucleus (TMN) neurons display state-dependent firing patterns with maximal rates of discharge occurring during wakefulness, slower rates in NREM sleep, and minimal activity during REM sleep (John et al., 2004). Fluctuating levels of GABA modulate activity of TMN neurons and have been shown to produce hypnosis but not complete anaesthesia (Nelson et al., 2002).

Hypocretin/ orexin neurons

These are wake-promoting neurons and show maximal activity during wakefulness (Mileykovskiy et al., 2005). They project to all monoaminergic groups and basal forebrain, midline thalamic and other regions and participate in modulating emergence from anaesthetics (Kelz et al., 2008, Peyron et al., 1998).

Basal forebrain

Basal forebrain contains acetylcholinergic neurons (wake-active) and receive input from the brainstem and hypothalamic arousal-promoting nuclei and project to the cerebral cortex (Jones and Cuello, 1989). Physostigmine, an acetylcholinesterase inhibitor has

been shown to reverse the effects of sevoflurane anaesthesia (Plourde et al., 2003). Basal forebrain also contains GABA-ergic neurons (sleep-active) which too project to the cerebral cortex, especially to the inhibitory interneurons (Freund and Meskenaite, 1992). These neurons also have α2 adrenergic receptors and are inhibited (during wakefulness) by noradrenergic projections form the LC (Modirrousta et al., 2004).

Ventrolateral preoptic nucleus

Ventrolateral preoptic nucleus lies in the anterior hypothalamus and is reciprocally interconnected to wake promoting nuclei, including histaimnergic TMN, serotonergic RN, noradrenergic LC, cholinergic LDT and PPT and orexinergic neurons of hypothamaus. They contain GABA and so can reciprocally inhibit wake-active ascending Reticular Activating system (Szymusiak and McGinty, 2008).

Median preoptic nucleus

Medin preoptic nucleus (MnPO) has sleep-active GABA-ergic neurons which play a role in sleep initiation and fire before the onset of sleep (Suntsova et al., 2002). Endogenous somnogens stimulate MnPO and it sends inhibitory signals to other systems such as orexinergic system or hypothalamus (Szymusiak and McGinty, 2008).

Thalamo-cortical system

The thalamo-cortical system (TC) receives input from dorsal pathway and wake-active regions of hypothalamus. TC system comprises of three types of neurons, which form interlocking positive and negative feedback loops. TC neurons send excitatory glutamatergic input to the other two populations: the reticular thalamic neurons and the corticothalamic (CT) neurons. The CT neurons send depolarizing glutamatergic feedback to the TC neurons (forming the positive feedback loop) and excitatory input to the reticular neurons (forming the negative feedback loop, since the reticular neurons are GABA-ergic and innervate the TC neurons) (Steriade, 2003). Both reticular and TC neurons receive monoaminergic and cholinergic input from the brainstem, but with opposing results. TC neurons are depolarized, while reticular neurons are hyperpolarized. During wakefulness, on-going depolarisation of the TC neurons results in a ‘tonic’ firing pattern while during sleep they become hyperpolarised and produce a ‘bursting’ pattern of activity. During this phase they prevent transmission of sensory

stimuli to the cortex (Alkire et al., 2000). Anaesthetic drugs have been shown to affect these thalamo-cortical systems in wide ranging sets of experiments (Alkire et al., 1995a, Alkire et al., 2000, Alkire et al., 2007, Byas–Smith, 2002, Ching et al., 2010a, Vijayan et al., 2013a, Akeju et al., 2014, Alkire et al., 1997, Alkire et al., 1999, Byas-Smith et al., 2002, Ni Mhuircheartaigh et al., 2013, Schreckenberger et al., 2004).

Interactions between brainstem, wake-sleep circuits and the cortex

The section above provides an overview of the literature on potential anaesthetic action on the brain regions, which regulate physiological consciousness states, including the brainstem, wake-sleep circuits and the thalamo-cortical systems. As these systems do not work in isolation, interactions between these systems are likely to contribute to the unconsciousness related to anaesthesia.

It has been proposed (John and Prichep, 2005) that anaesthetics work by suppressing brainstem influence of the RAS on the thalamus and cortex. Further depression of mesolimbic-dorsolateral prefrontal cortex interactions leads to blockade of memory storage. Further depression of the RAS releases its inhibition of the nucleus reticularis of the thalamus, resulting in closure of thalamic gates (especially in the diffuse projection system) by hyperpolarizing GABA-mediated inhibitory action of the nucleus reticularis (increases inhibitory action), thereby blocking thalamo-cortico-thalamo-cortical reverberations. This possibly decreases perception. Further anaesthetic action results in uncoupling of parietal–frontal transactions (coherence decreases), and blocks cognition. Suppression of prefrontal cortex reduces awareness. These changes are unlikely to follow a precise sequence but it is conceivable that brainstem actions precede those on the cortical-subcortical activity.

The experiments in this thesis have focused mainly on local actions of the GABA-ergic drug (propofol) on human cortical and subcortical activity. Any effect on the brainstem function or that on primary afferents (e.g. primary order neurons or spinal level activity) has not been directly studied. While this presents a limitation of the present set of experiments, it reflects the limits of current neuroimaging techniques (in the temporal and spatial domains to study finer brainstem and spinal level function). However, as the

current non-invasive neuroimaging techniques evolve further, it may be possible to study these finer brain functions too, in the near future.

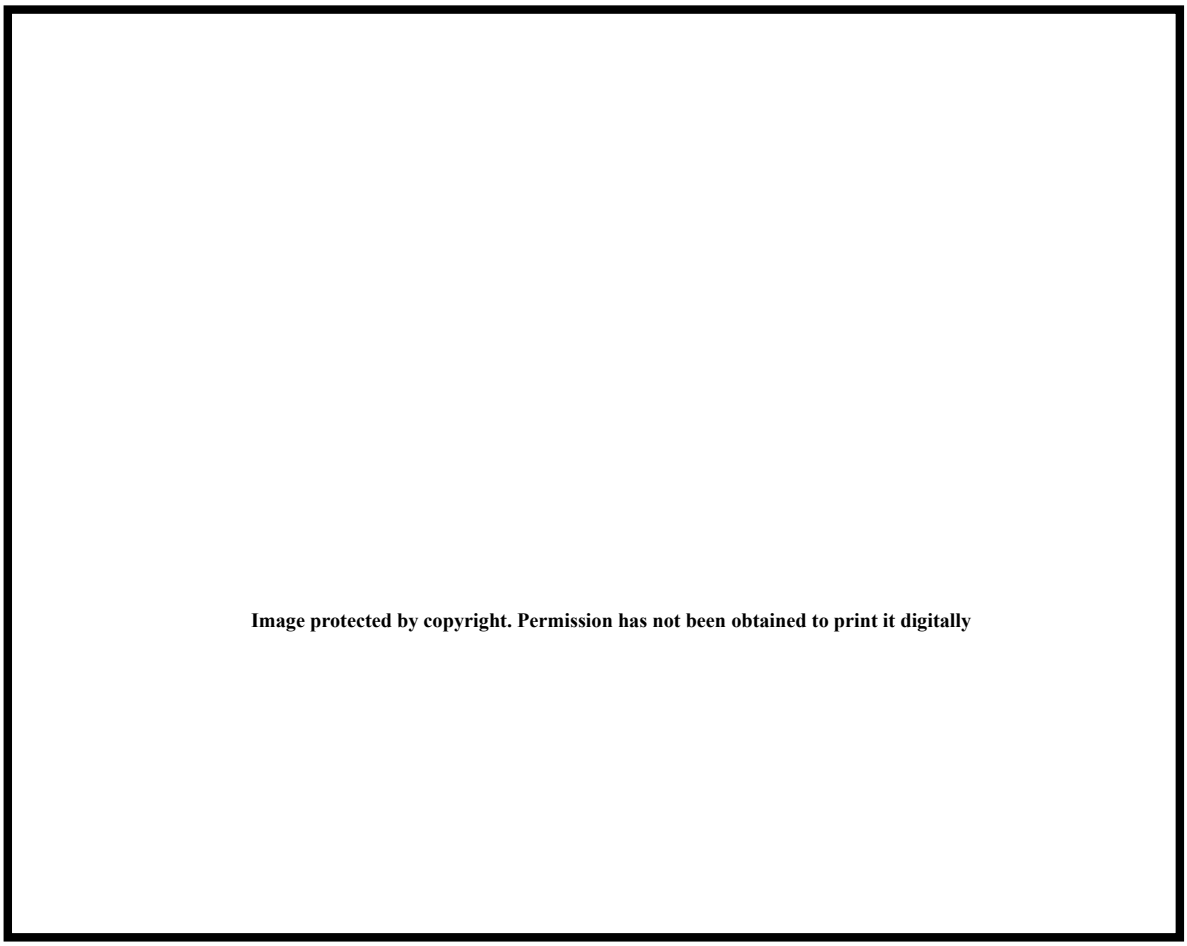

Figure 1-1: Figure showing sagittal view of brain demonstrating some of the key areas involved in anaesthesia and sleep.

Inset highlights key arousal systems with neurotransmitters involved in sleep or wakefulness. Sleep-active loci are shown in light blue. When wake-active systems (shown in red) are firing they antagonize the sleep-active groups. Conversely, when sleep-active neurons are active, they mutually antagonize the wake-active regions to further reinforce sleep. Anesthetic drugs are known to interact with this circuitry to produce hypnosis. 5-HT: serotonin; ACh: acetylcholine; DA: dopamine; GABA: γ-aminobutyric acid; Gal: galanin; HA: histamine; Glut: glutamate; NE: norepinephrine; BF: basal forebrain; DpME: deep mesencephalic reticular formation; LC: locus coeruleus; LDT laterodorsal tegmentum; MnPO: Median preoptic nucleus; mPFC: medial prefrontal cortex; Ox: orexin/hypocretin neurons in lateral, perifornical, and posterior hypothalamus; PnO: pontine reticular nucleus oral part; PPT pedunculopontine tegmentum; RN: raphe nuclei; SCN: suprachiasmatic nucleus; TMN: tuberomammillary nucleus; VLPO ventrolateral preoptic nucleus; vPAG: ventral periaqueductal gray. Adapted from (Moore and Kelz, 2011)

1.4 Cortical cytoarchitecture and cell assemblies: generation of brain rhythms

The human neocortex is a thin, and extended, convoluted sheet of tissue with a surface area of ~2600 cm^2, and thickness 3–4 mm. It contains up to 28 $x10^9$ neurons and approximately the same number of glial cells. Cortical neurons are connected with each other and with cells in other parts of the brain by a vast number of synapses, of the order of 10^{12} (Mountcastle, 1997). The neurons in the neocortex are structured in relatively well-defined horizontal layers (6 laminae) and vertical columns. The basic unit of the neocortex is a 'minicolumn', a narrow chain of neurons extending through the layers, perpendicular to the pial surface. Each minicolum contains 80-100 neurons (a lot more in the striate cortex). Cortical columns are formed by minicolumns bound together by short-range horizontal connections. Putting these columns in macroscopic perspective, assuming that a column with a diameter of 40μm contains 100 cells, the cortical surface that would correspond to 50,000 cells (which is the number expected to produce the weakest magnetic current of 10nAm) should form a patch with about 0.63 mm^2 in area. If this cortical patch had a circular form, then its diameter would be about 0.9 mm (Lopes da Silva, 2010).

While the neocortex contains hundreds of types of cells, they may, broadly, be classified as 'projection neurons' and 'interneurons'. Projection neurons are glutamatergic, pyramidal neurons that project to other cortical, subcortical and subcerebral regions (Figure 1-1). Interneurons are GABA-ergic and make local, short-distance connections (Molyneaux et al., 2007). The basis of the columnar arrangement, in sensory cortices, is that each column receives selective input from the relay thalamic nuclei. Activities, both excitatory and inhibitory, in these cortical pyramidal cells are observed on Electroencephalography (EEG) (Kirschstein and Kohling, 2009). Pyramidal cells in different layers may have further differentiation of roles depending on the inputs ending in those and the afferent sources (Figure 1-2). For example, the visual evoked potentials are generated from the activity of the layer IV (Kraut et al., 1985) while the visual gamma band responses result from the activities of layers II, III and IV (Xing et al., 2012).

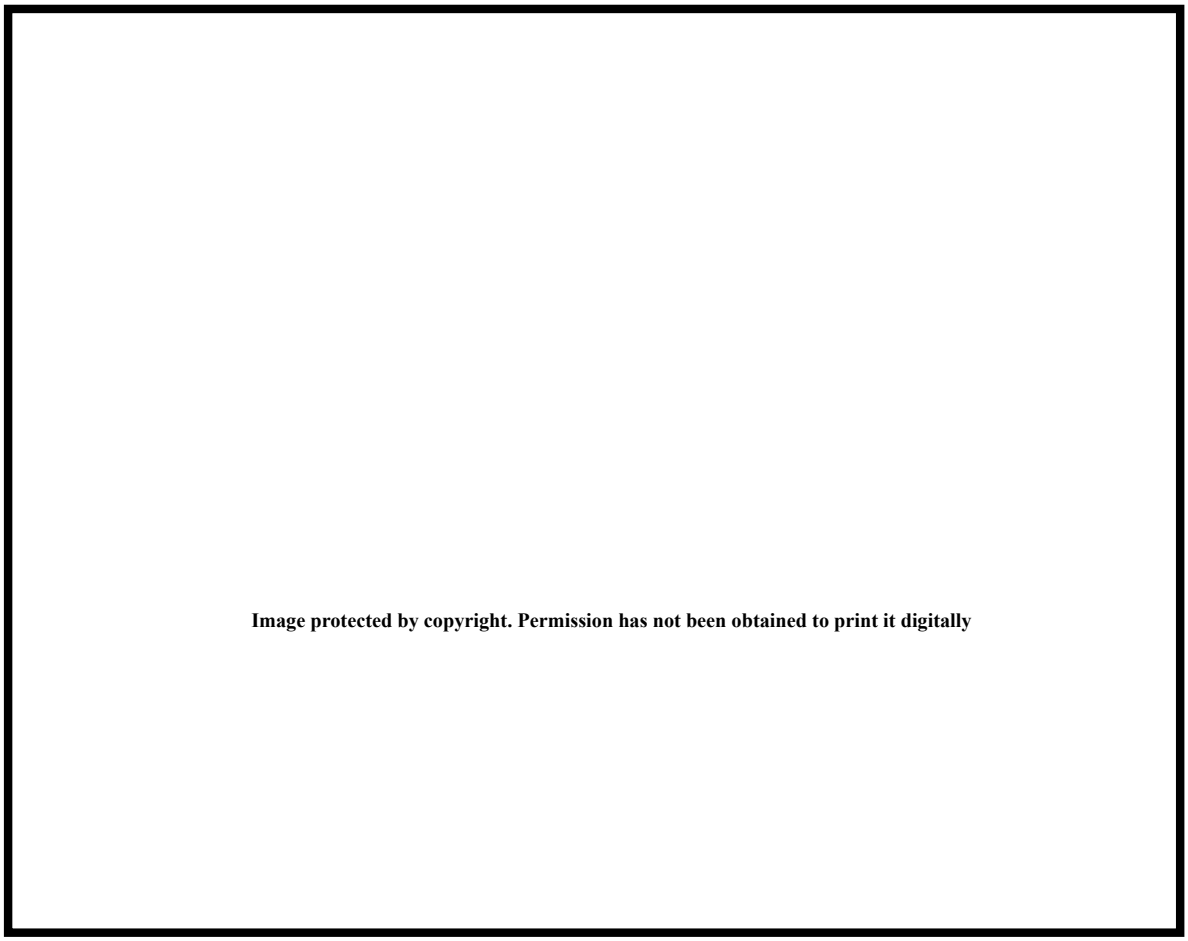

Figure 1-2: Cortical laminar structure: basic circuits.
Blue and grey fibres are afferents, interneurons are green and efferents are red. Adapted from Lynch, 2013 (Lynch, 2013)

Inhibitory interneurons, typically, have short ranges and influence neurons close-by. They also have short latencies and faster action potentials than pyramidal cells. These cells, thus, prevent runaway excitation of pyramidal cells. There is feed-forward inhibition, such that a rapidly occurring inhibitory potential limits the time window for summation of excitatory inputs to generate action potentials. There is feedback inhibition too, where excitation of the pyramidal cell excites the interneuron which inhibits the pyramidal cell (Figure 1-3) (Mohler, 2002). This mechanism results in the oscillatory action potentials, which are then recorded as the EEG/ Magnetoencephalography (MEG) rhythms.

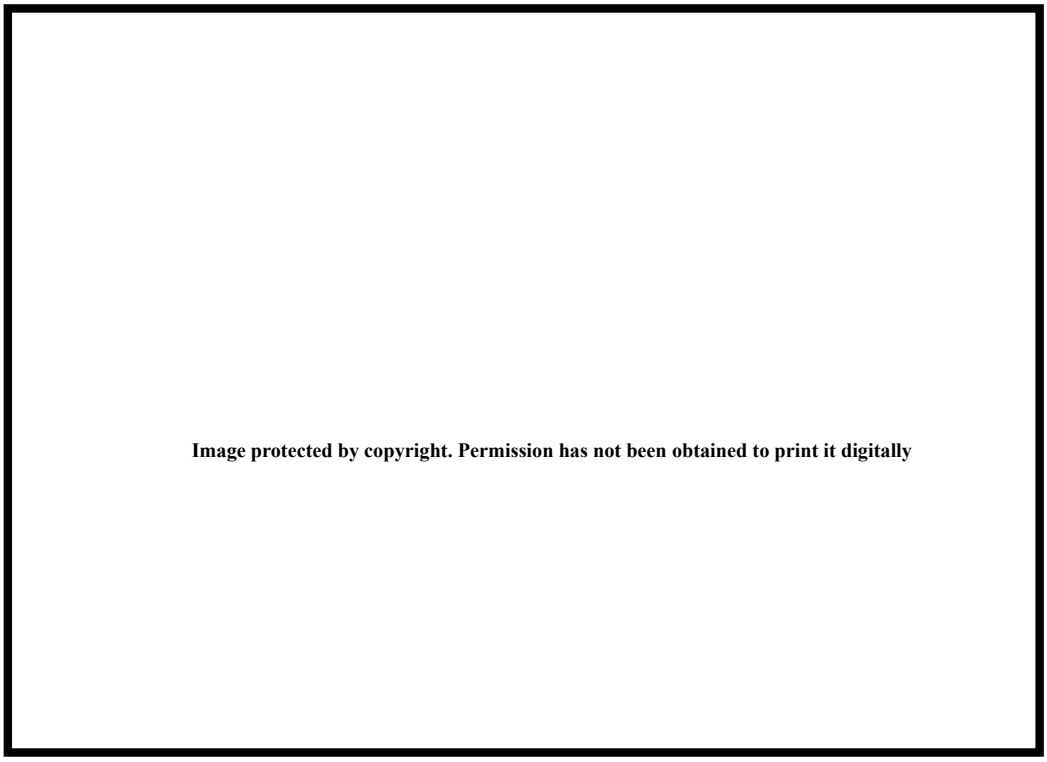

Figure 1-3: Scheme of feedforward and feedback inhibition
Pyr: Pyramidal cells. Adapted from Mohler, 2002 (Mohler, 2002).

1.5 Using advances in neuroimaging techniques

As is clear from the previous sections that neuronal assemblies, in microscopic scale, interact with each other, in microsecond time scales, to produce the behavioural changes associated with anaesthesia. In-vivo study of such changes in humans is close to impossible. Advances in neuroimaging techniques have provided a non-invasive window into such neuronal changes, albeit, occurring at a macroscopic, large scale, network-level. The advantages and strengths of different neuroimaging techniques are discussed in more detail in Chapter 2.

1.6 Insights into anaesthetic action from neuroimaging research

Neuroimaging techniques, in humans, have been used to confirm the findings of animal (in vivo/ in vitro) research; but also to generate testable hypotheses. Some of the earliest neuroimaging studies used positron emission tomography (PET) to study

pharmacodynamic effects on the brain and also to study cerebral perfusion changes, especially in terms of their usefulness for neuro-anaesthesia, or in patients with a raised intracranial pressure. PET was therefore, naturally, used to study perfusion and metabolic changes to study anaesthetic mechanisms. The neuroimaging literature may be divided into specific questions, in relation to different consciousness levels and different anaesthetic drugs, which the neuroimaging researchers have attempted to answer.

1.6.1 Is the anaesthetic effect global or regional?

Some of the early theories of anaesthetic mechanism suggested a 'global suppression' by drugs resulting in unconsciousness. However, neuroimaging studies demonstrated that there was not only a global reduction in cerebral metabolism and perfusion, but also that different anaesthetics affect different regions preferentially. In one of the first studies of its kind, Alkire et al, during propofol anaesthesia, showed reduced global metabolism along with some regions more depressed than others (Alkire et al., 1995b). Inhalational anaesthetic agents isoflurane and halothane revealed a significant global suppression of neuronal activity (Alkire et al., 1997, Alkire et al., 1999). There was a greater global suppression and regional suppression of cortical metabolism with less effect on basal ganglia and midbrain with propofol as compared to the inhalational agents. Sedative doses of propofol and sevoflurane reduced perfusion in the cuneus, precuneus, posterior limbic system and the thalamus or midbrain, with propofol causing additional reduction in frontal and parietal regions (Kaisti et al., 2002). Jeong et al described the changes as propofol affecting the neocortex more while sevoflurane affected the paleocortex and telencephalon more (Jeong et al., 2006).

Halothane and isoflurane, drugs with similar chemical structure, appeared to have different effects on perfusion in different regions (Reinstrup et al., 1995). Even within GABA-ergic intravenous anaesthetic drugs, different molecules may have different actions on the brain. Propofol at sedative doses decreases cerebral blood flow (CBF) in the right-sided anterior brain whereas thiopental decreased CBF mainly in the left cerebellum. At hypnotic concentrations both drugs decrease CBF in the posterior

cortical regions. Also, at these concentrations propofol reduced thalamic blood flow but thiopental did not (Veselis et al., 2004b).

These studies demonstrated the regional effects of anaesthetic agents and pointed towards mechanistic differences between propofol and inhalational groups of drugs.

1.6.2 Relating molecular mechanisms to neuroimaging findings

The key differences in propofol and the commonly used inhalational anaesthetic agents is that while propofol has mainly GABA-ergic activity, inhalational drugs work through a number of other receptors. Cerebral metabolic changes with propofol correlated with the GABA receptor density (i.e. areas with greater GABA receptors, showed greater reduction in activity) but not with isoflurane, which produced metabolic changes correlating with the muscarinic (acetylcholinergic) receptor density (Alkire and Haier, 2001). These findings further provided proof of different receptor mechanisms of the two main groups of anaesthetic agents.

1.6.3 Neural correlates of suppression of sensations and cognition

Anaesthetic unconsciousness includes reversible cognitive and sensorimotor failure. Neuroimaging studies have been done during specific tasks to investigate changes in brain activity and the effect of anaesthetic drugs on the regions involved with escalating doses.

During isoflurance anaesthesia, blunting of noxious and normal sensory stimuli were shown while some sensory cortical and thalamic activity persisted during lower (sedative) doses (Antognini et al., 1997). Similarly, at sub-anaesthetic doses, isoflurane was shown to affect specific areas including the right anterior insular and intraparietal sulcus while performing a visual search task while the sensory cortical and subcortical regions were unaffected (Heinke and Schwarzbauer, 2001). With propofol, brain responses to a vibrotactile stimulus decreased in a dose-dependent manner in the cortical and subcortical regions (Bonhomme et al., 2001). Thalamic activity was lost completely only at the doses producing unconsciousness. Propofol related dose-

dependent suppression of primary cortical activity has been shown by multiple groups (Dueck et al., 2005, Veselis et al., 2005). Similarly, dose related suppression of brain activity in higher-order regions has been shown by most of these studies. Thalamic activity is lost later as sedative depth progresses; however, it stays unclear if thalamic suppression is a cause or consequence of cortical suppression. While some of these studies supported the concept of a 'thalamic switch of consciousness', other neuroimaging modalities have revealed other contenders as the key anatomical sites for switching consciousness on-off, or a lack of any such specific brain site (See Section 1.6.7).

1.6.4 Neural correlates of amnesia

Amnesia is a key component of anaesthesia and has therefore been an area of interest. The focus has been on studying anaesthetic effect on brain regions known to be involved in memory and the sequence of amnesia induced as a part of anaesthetic process.

Midazolam (a benzodiazepine (BZD), another GABA-ergic drug), is commonly used for procedural sedation provides good anterograde amnesia. Decreased CBF in the left middle temporal gyrus, left dorsolateral prefrontal cortex and bilateral orbitofrontal cortex were shown during midazolam infusion (Reinsel et al., 2000), however activity on prefrontal cortex was not associated with amnesia (Bagary et al., 2000). Lorazepam (another BZD) and scopolamine (anticholinergic drug) produced amnesia and suppressed activity in the hippocampus, fusiform gyrus and inferior prefrontal cortex (Sperling et al., 2002).

Right sided prefrontal and parietal areas were involved in the amnesic effects of propofol sedation, while medial temporal lobes were more resistant, suggesting an indirect effect of propofol on centres known to be key for memory (Veselis et al., 2002). During an auditory recall task it was shown that primary and association auditory cortical areas remain active during propofol anaesthesia but the regions associated with processing and recall, bilateral planum temporale, were suppressed at sedative doses (Plourde et al., 2006). Davis et al., studied the brain responses to different states of

speech, comprehension and recall (Davis et al., 2007). They showed that superior and middle temporal gyri were related to speech perception and active during the mild sedation stage but not during deep sedation. Activation of the inferior frontal and posterior temporal responses corresponded to comprehension and was absent even during mild sedation.

These studies have therefore helped understand some of the key steps in the anaesthetic cascade with specific effects on key brain regions involved in memory and recall.

1.6.5 Atypical anaesthetic drugs

Anaesthetic drugs with different (non-GABA-ergic) actions, such as ketamine, nitrous oxide, xenon and dexmedetomidine are associated with quite different behavioural and central effects. Most of these drugs are not useful as sole anaesthetics (except ketamine) but they are useful as sedatives and as a component of multimodal anaesthesia. Neuroimaging studies of the altered consciousness induced by these drugs have also provided a valuable insight into the mechanisms of anaesthesia and the differences with typical anaesthetic drugs.

Ketamine is an NMDA antagonist and produces a state of 'dissociative' anaesthesia where patients are immobile, amnesic and do not experience pain. However, they appear awake, although detached from the surroundings and may also be able to talk. PET demonstrated a dose dependent CBF increase in the anterior cingulate, thalamus, putamen and frontal cortex while the greatest relative increase occurred in the anterior cingulate cortex (ACC), insula and frontal cortex (Langsjo et al., 2003).This increase in perfusion was associated with an increase in neuronal metabolism (Langsjo et al., 2005, Langsjo et al., 2004). Blood oxygen level dependent -functional magnetic resonance imaging (BOLD-fMRI) studies also demonstrated task related deactivations in specific brain regions with ketamine (Abel et al., 2003a, Abel et al., 2003b) while its analgesic effects were correlated with a reduced activity in the insular cortex and thalamus (Rogers et al., 2004).

Like ketamine, nitrous oxide has been shown to increase cerebral metabolism. Inhalation of nitrous oxide (20%) was associated with significant activation in the anterior cingulate cortex, while deactivation was found in the posterior cingulate, hippocampus, parahippocampal gyrus, and visual association cortices (Gyulai et al., 1996). Unlike ketamine and nitrous oxide, xenon was shown not to increase metabolism. Xenon resulted in a metabolic suppression and also cortical and sub-cortical CBF decreases (Rex et al., 2008, Rex et al., 2006).

Dexmedetomidine is an α-2 adrenergic agonist, which produces characteristic sedation wherein patients are easily arousable even from deeper stages of unconsciousness. PET showed a dose dependent global and regional decrease in CBF with dexmedetomidine (Prielipp et al., 2002). Clonidine, another α-2 adrenergic agonist, was shown to reduce acts on the prefrontal, orbital and parietal association cortex, precuneus, posterior cingulate and thalamus (Bonhomme et al., 2008).

These neuroimaging findings show how different receptor mechanisms affecting different brain regions may produce the same behavioural outcomes, i.e. altered consciousness. While this does not completely shift the focus away from having a single common final pathway of anaesthetic unconsciousness, it shows that there may be a number of different paths in terms of approaching it.

1.6.6 Connectivity between brain regions

As the understanding of the anaesthetic effects on the brain regions (and their metabolism and perfusion) has improved, the focus has moved on to the interaction of different brain regions underlying anaesthesia. This has been facilitated by discovery of the temporal coherence in the activity of various brain regions, resting state networks and the advances in mathematical modelling, being able to predict the influence of one region over another.

Network connectivity studies have studied higher-state (those serving higher cognitive functions) and basic-state (those serving primary sensory functions) functional networks and consistently demonstrated a disruption of higher state networks earlier in the

anaesthetic cascade while the lower-state networks (primary function) maintained their activities even during deeper stages of sedation and anaesthesia (Boveroux et al., 2010, Liang et al., 2015, Martuzzi et al., 2010, Mhuircheartaigh et al., 2010, Stamatakis et al., 2010).

While functional connectivity provides a useful measure of the potential relationship between different brain regions, efforts have been made to identify more direct measures and to be able to demonstrate causal influence of one site on the other to establish the sequence of effects. EEG changes following transcranial magnetic stimulation (TMS) induced stimulation showed that during midazolam sedation the spread of cortical activity was much limited to the stimulation site (Ferrarelli et al., 2010). This demonstrated a direct measure of loss of cortical connectivity from the stimulation site, associated with midazolam. The direction of connectivity within the fronto-parietal networks has also been of interest. The feed-forward connections relay incoming sensory information while the feedback projections help select and interpret those. During the anaesthetic state the feed-forward information transfer may continue however the feedback gets reduced and may be responsible for the unconsciousness (Imas et al., 2005). Computational modelling has shown this directional suppression of feedback activity as a common step between different classes of anaesthetics including ketamine, sevoflurane and propofol (Lee et al., 2013b). During propofol induced anaesthesia feed-forward connectivity persists suggesting that sensory information continues to flow (Ku et al., 2011).

Combining information from neuroimaging tools (as is the focus of this thesis) has also provided valuable information about the temporal and spatial sequence of changes in the anaesthetic cascade. Slow wave EEG-activity (1Hz) of cortical neurons emerged at the point of loss of consciousness with propofol and was associated with thalamo-cortical dissociation (Ni Mhuircheartaigh et al., 2013).

1.6.7 Consciousness switch

A great deal of research has focused on identifying a key brain area which results in consciousness, a so called 'consciousness switch'. Neuroimaging techniques have provided a tool to investigate if indeed there is such a brain region.

Thalamus had been known to be the gateway to the cortex and therefore naturally appeared to be a contender. Thalamic microinjection of nicotine was able to reverse sevoflurane induced unconsciousness in mice (Alkire et al., 2007). Selective lesions of the medial thalamus can produce coma while stimulation of the central thalamus can restore consciousness (Schiff, 2008, Schiff, 2009). Most neuroimaging literature, as discussed above, shows thalamus to be more resistant to anaesthetic effects than the cortical areas, suggesting that thalamic suppression is related to anaesthetic unconsciousness. However, more detailed analyses and recent anaesthetic literature has challenged this view. It is unclear whether thalamic suppression is a cause of unconsciousness, or the consequence of cortical suppression (and therefore unconsciousness) or an equal participant (Mashour and Alkire, 2013a).

Precuneus, which forms a key node of the default mode network has also been suggested by some as the key region maintaining consciousness. As one of the brain areas with highest resting metabolism, it is one of the commonly affected areas in sedation/ anaesthesia (Cavanna and Trimble, 2006). Physostigmine induced reversal of propofol sedation was associated with increased perfusion of thalamus and precuneus (Xie et al., 2011). More recently the right dorsal anterior insular cortex has been proposed as the cortical gate associated with anaesthesia (Warnaby et al., 2016).

These neuroimaging studies have certainly contributed to the understanding of anaesthetic mechanisms, the similarities and differences between different anaesthetic compounds and the value of using the strengths of different neuroimaging modalities. These have informed some of the experimental design used in this thesis.

1.7 Need for understanding mechanisms of sedation and anaesthesia

While anaesthetic drugs may be used as a consciousness probe to understand consciousness better, there are other obvious and pressing needs for this area of research. The bench to bedside translation of this area of research holds promise for clinicians in some of these areas.

1.7.1 Disorders of consciousness

Coma has been defined as a state of profound unconsciousness associated with markedly depressed cerebral activity, a loss of the ability to maintain awareness of self and environment combined with markedly reduced responsiveness to environmental stimuli, and a loss of the ability to perceive and respond. This essentially means a lack of wakefulness and awareness. Coma, for most people, leads on to irreversible loss of brain stem function or brain death. If only wakefulness returns, patients may be in a state of unresponsive wakefulness syndrome (UWS: earlier called 'vegetative state'). When patients show return of limited signs of awareness without consistent communication with the environment, they are called to be in a state of minimal conscious state (MCS). These states are different from the locked-in syndrome, where patients have all cognitive functions, but an inability to perform movements except with their eyes (Kirsch et al., 2016).

These conditions are not just challenging for clinical management but also pose a diagnostic challenge. Wrong diagnosis and classification of altered consciousness states can be as high as 40 % (Schnakers et al., 2009). Owen et al, demonstrated presence of consciousness in a young woman, who was believed to be in a vegetative state, by using activation of relevant brain regions on fMRI on verbal commands (Owen et al., 2006). This not only exposed the limited understanding of brain function but also challenged the commonly held behaviour-driven definitions of 'awareness'. Further neuroimaging testing revealed awareness and also potentially ability to communicate in a small group of patients with minimally conscious states (MCS) (Monti et al., 2010). Similar to pharmacological sedation, neuroimaging has revealed disruption of functional connectivity in the default-mode network (DMN) and other fronto-parietal resting state

networks in patients with UWS/MCS (Noirhomme et al., 2010, MacDonald et al., 2015). Recovery from UWS/MCS has also been shown to correlate strongly with functional connectivity strength of the PCC/ precuneus (Wu et al., 2015). Differentiating MCS from UWS has implications in terms of prognosis, but also ethical and legal in terms of care and decision-making. Indeed, it has been suggested that neuroimaging could be used to facilitate neurorehabilitaiton in such group of patients (Laureys et al., 2006).

It is clear that differentiating the various conditions of pathological alterations in consciousness is critical in terms of prognosis and overall better quality of care of these patients. Neuroimaging techniques have shown value where explicit behaviour has been unable to help. It is expected that better understanding of the neurophysiology of consciousness will help this particular group of patients.

1.7.2 Complications of anaesthesia and sedation

Critically ill patients, being managed in Intensive Care units (ICU), experience a number of traumatic experiences during their stay. These include activities such as airway instrumentations, placing intravenous / arterial lines, catheterisation and nursing care. Most critically ill patients are kept sedated to help them cope with being bed-bound, dependent and to tolerate mechanical ventilation. Post-traumatic stress disorder (PTSD) is fairly common in ICU survivors and while the causes could be many, use of benzodiazepine sedatives and 'frightening' ICU experiences are common contributors.

The trauma of their clinical condition is compounded by other neurological consequences, such as delirium. Delirium, is an acute and fluctuating disturbance of consciousness and cognition, a common manifestation of acute brain dysfunction in critically ill patients, occurring in up to 80% of the sickest of these patients (Girard et al., 2008). This delirium makes the stay distressing; it also has long-term consequences including dementia and death. This forms one of the key elements of the 'triad' of ICU management- pain, agitation and delirium. It has been proposed that sedation should be used only after this triad has been managed. Sedation itself can cause delirium and different sedatives have been shown to affect the incidence and outcomes of delirium

(Reade and Finfer, 2014). Dexmedetomidine has been shown to reduce the incidence of ICU delirium when compared with midazolam. It has been suggested that dexmedetomidine's non-GABA-ergic actions, in promoting the natural sleep pathways, helps avoid this complication (Pandharipande et al., 2007).

Similarly delirium may occur following surgery (post anaesthesia delirium) and has been reported to be as common as 54% in patients undergoing major elective non-cardiac surgery (Sanders et al., 2011). Certain anaesthetic drugs such as benzodiazepines, opioids and inhalational agents are more likely to be associated with delirium (Hernandez et al., 2017).

It is likely that a better neurophysiologic understanding of delirium and development of cleaner anaesthetic drugs will benefit a large group of surgical and critically ill patients.

1.7.3 Awareness during anaesthesia

During general anaesthesia, patients expect to be unconscious and amnesic to their surgical experience. Clinically, ensuring amnesia and immobility (which is easily achievable by giving high enough doses) needs to be balanced against overdosing patients, which may cause cardiovascular compromise or delayed recovery. This is where anaesthesia becomes a skillful 'art'. A better understanding of the brain functions which anaesthetic drugs are meant to block can support this art further.

The consequences of accidental awareness during anaesthesia include experiencing excruciating pain during the procedure and may have long term neuropsychiatric sequelae like PTSD (Ghoneim, 2000). National Audit Project-5 (NAP-5), one of the largest surveys of its kind identified the incidence of accidental awareness under general anaesthesia (AAGA), its consequences and the factors related to it (Cook et al., 2014). They found that although the incidence of AAGA was low, its impact can be substantial, with patients experiencing long term distress and psychological consequences including PTSD. This was commoner and worse in those patients who experienced paralysis (due to the neuromuscular drugs administered) during AAGA. NAP recently reported a high degree of awareness during procedures carried out under

sedation. This report reflects a failure of explanation on the part of the anaesthetist rather than the failure of sedation. While amnesia is not always a goal of procedural sedation it would be useful to provide that with reliability and be able to monitor that.

Co-relational depth of anaesthesia monitors have been developed for use during anaesthesia and sedation. These are usually indices derived from EEG activity. These monitoring systems have, however, not been widely popular due partly to the unfamiliarity of anaesthetists with the underlying EEG, but, mainly due to a lack of clear understanding of the mechanistic link between anaesthetic drugs and their targets of activity. Also, such monitors (and indeed EEG indices) fail to reflect the effects of certain drugs that increase EEG activity as opposed to decrease it, with increasing drug effect. Therefore, a reliable depth of unconsciousness/ anaesthesia monitor that would work with all types of anaesthetic drugs would improve the safety and quality of anaesthetic practice. Indeed, it has been suggested that a comprehensive understanding of the mechanisms of pharmacological, physiological and pathological consciousness may result in development of a 'consciousness-meter' (Boly et al., 2013).

With increasing pressures on anaesthetic departments providing clinical cover in non-operating areas it is increasingly difficult. Sedation, when administered by non-anaesthetists is associated with a much higher morbidity and mortality (Quine et al., 1995). If a reliable, responsive sedation monitoring system could be developed, it is envisaged that the safety profile of sedatives in non-anaesthetic hands may increase thus widening the safe practice that patients enjoy in the hands of anaesthetists.

1.8 Conclusions

The contents of this chapter provide the relevant background for the experiments in this thesis. Understanding of the complexities of some of the receptor mechanisms and targets of anaesthesia, brain regions and current neuroimaging literature is required to formulate the hypotheses in the following chapters. The focus of this thesis is on mild sedation, which is clearly distinct from anaesthetic unconsciousness. While mild sedation is the first step towards the loss of consciousness in response to anaesthetic drugs, it may also have more in common with other disorders where cognition and

memory is affected. A range of advanced neuroimaging tools are used in this thesis in an attempt to bring together the metabolic, haemodynamic and electrophysiological characteristics of mild sedation to understand its neural correlates. This will undeniably assist in understanding the basic mechanisms of sedation. This may, in turn, help developments of monitoring techniques to help make sedation safer in clinical practice.

Chapter 2 : Introduction to techniques: General materials and methods

Each experimental chapter reported in this work involved administering of propofol (GABA-ergic drug) in a controlled manner and collecting neurophysiological and haemodynamic data using a range of neuroimaging tools. This chapter provides a more detailed background of the drug and its administration. It also provides a more detailed background of the neuroimaging modalities, their unique characteristics and application in the subsequent experiments. Each following thesis chapter describes the experimental paradigm and analytic steps, which complements the information provided in this chapter.

2.1 Participants

This section describes the experimental characteristics, including that of the participants, drug choice, administration and safety measures.

2.1.1 Recruitment

The project was assessed and approved by the Cardiff University's Ethical Committee (MRSREC no 09/58) and complied with the guidelines of the Declaration of Helsinki. Experiments in the project involved healthy volunteers who were recruited through the standard recruiting channels of Cardiff University Brain Research and Imaging Centre (CUBRIC), as approved by the Ethics Committee. This included contacting previous volunteers who had participated in CUBRIC research and were willing to be contacted for other neuroimaging research. Flyers asking for volunteers were also placed within the Cardiff University departments. An advertisement was also placed through the Cardiff University online notice board, the target audience of which included all Cardiff University staff and students. The first 20 responders were sent the information sheets, medical assessment questionnaire and invited for an initial visit if they met the eligibility criteria. The initial visit included confirmation of eligibility criteria (as

below), their understanding of the experiments and the risks involved. They were taken around the scanner suites to familiarise them with the MR and MEG scanners. They were given an opportunity to lie in the 'mock' MR scanner (benching) to provide them a realistic feel of lying in an MR scanner. This was done as it reduces participant anxiety and also the risk of drop-outs during the study session. No study session was arranged within at least one week after the consenting/ familiarisation process to give the participants enough time to change their mind if they wished to.

2.2 Inclusion and exclusion criteria

The inclusion criteria included:

- Participant willing and able to give informed consent for participation in the study.
- Male participants, aged 18 -50 years.
- In good health and not on any regular medications (American Society of Anesthesiologists : ASA grade 1)
- Fluent English speaker
- Registered with a GP (the GP will not routinely be informed of the volunteer's participation)

Only male participants were included in these experiments. This was done as one of the main hypotheses in these experiments involved investigating the MR detectable GABA concentration. There was evidence that variation in Magnetic Resonance Spectroscopy (MRS) measures of GABA, in human brain, was related to the different stages of the menstrual cycle in female subjects (Harada et al., 2010, Epperson et al., 2002). This would have been an additional, difficult to control, confound. Also, the study by Muthukumaraswamy et al (Muthukumaraswamy et al., 2009), which had formed the basis of a section of this thesis had been performed on male volunteers only. Due to these considerations, it was decided to restrict recruitment only to male participants.

The exclusion criteria included:

- Any of the commonly accepted contraindications to MRI scanning or MEG, for example, severe claustrophobia, presence of incompatible metallic implants, a pacemaker etc.
- Involvement in another drug study or recent involvement in another drug study in the last two weeks
- Inadequate understanding of verbal and written information in English, sufficient to complete an MRI safety screening.
- Clinically significant condition such as obesity, chronic pain, psychiatric or neurological condition.
- History of:
    - Intolerance/ allergy to propofol
    - Drug dependency
    - Cardiovascular, respiratory, cerebrovascular disease or gastrointestinal disorders (such as acid reflux), as determined by the anaesthetist on the study.
    - Participants, with a potentially difficult airway (based on external assessment) who are likely to be at a greater risk of airway obstruction, such as those with a history of snoring, sleep apnoea, obesity or facial features such as micrognathia etc. were excluded at the recruitment stage.

2.2.1 Financial compensation

Participants were paid £10 per hour for their inconvenience. They were also provided food and refreshments following the experiments, as they had been fasting prior to that. They were also offered a taxi to drive them home or reimbursed such costs.

2.2.2 Care of participants

In preparation for the experimental session, all participants were prepared as if they were attending for a surgical procedure (which would require a full anaesthetic). This

was done as a safety precaution as one of the risks with sedation studies is of overdosing, which may create an 'anaesthetic' state. Such a state would be associated with loss of airway reflexes and potential for regurgitation of gastric contents and potential pulmonary aspiration. While the chances for this are very low, the potential severity of harm is quite significant. All participants were therefore instructed to fast for at least 6 hours prior to the session. They were allowed to have clear fluids up to 2 hours prior to the experiment. Following the experimental sessions, all participants were monitored for an hour till the effects of sedation had worn off completely. They were provided with food and drink when they were able to do so. They were discharged home, with an escort, with advice to contact the researchers/medical team in case of any problems. They were instructed not to drink alcohol or operate any machinery for the next 24 hours.

2.3 GABA-ergic drug- Propofol

2.3.1 Investigating mild sedation

General anaesthesia is defined as a controlled, reversible alteration of consciousness induced by pharmacological agents. This state is characterised by unconsciousness, amnesia and lack of movement to a surgical stimulus. This is usually associated with respiratory suppression and loss of protective airway reflexes. While general anaesthesia usually has a well-defined end-point (generally, lack of eyelash reflex in clinical practice), end-points of altered consciousness states prior to reaching general anaesthesia, are more difficult to define and depend on the context. For procedural sedation, the earliest states of sedation involve anxiolysis, followed by deeper stages of sedation, such as 'conscious sedation', where the patient maintains purposeful contact with the operator, either on verbal contact or gentle prodding (Martel and Barnett, 2015) but may be amnesic to the experience. At further deeper stages of sedation, the patient responds purposefully only on repeated or painful stimulation. At such deep stages of sedation the patients start losing control of their airway and their ventilation may be depressed. As is clear from this, sedation is a continuum and specific end-points for different stages of sedation are difficult to define with objective certainty.

Various sedation scales have been developed to help classify the different levels of sedation for clinical and research use. Observer's Assessment of Alertness/ Sedation (OAA/S) scale was developed by Chernik et al and has been used extensively (Chernik et al., 1990). A modification of the OAA/S scale (Thomson et al., 2009) has been used in these experiments (Figure 2-1). To study mild sedation, it was agreed to target the earliest identifiable level of sedation (OAA/S level of 4). This state is characterised by a participant responding lethargically to normal verbal commands and having a 'mild slowing or thickening' of the speech.

Assessment categories		
Responsiveness	**Speech**	**Composite score level**
Responds readily to name spoken in normal tone	Normal	5 (Alert)
Lethargic response to name spoken in normal tone	Mild slowing or thickening	4
Responds only after name is called loudly and/or repeatedly	Slurring or prominent slowing	3
Responds only after mild prodding or shaking	Few recognisable words	2
Does not respond to mild prodding or shaking	–	1 (Deep Sleep)

Figure 2-1: Modified Objective Assessment of Alertness/ Sedation Scale.
Adapted from Thomson et al (2009).

2.3.2 Choice of drug

Most of the anaesthetic agents act through GABA-ergic mechanisms. While volatile (inhalational agents) are the commonest anaesthetic drugs used to 'maintain' anaesthesia, they are rarely used for 'initiating' anaesthesia or providing sedation. Their administration also requires specialist equipment, such as vapourisers and breathing circuits. Therefore the choice of drug, for this series of experiments, was limited to commonly use intravenous agents.

Benzodiazepines (such as midazolam and diazepam) are commonly used for peri-procedural sedation. Midazolam can be used intravenously and the relatively short onset, peak and half-life would allow easy titration of drug effects. They work only

through the GABA receptors and may be considered the best drug for investigating GABA-ergic mechanisms. However, benzodiazepines are not considered anaesthetic drugs in the true sense and are never used as a sole anaesthetic drug. The pharmacokinetic models for delivering midazolam are less well studied as compared to those of propofol making it less practical to administer. In clinical practice, propofol is the commonest drug used for 'initiating' anaesthesia and is increasingly being used for peri-procedural sedation. Considering all these factors propofol was chosen as the drug of interest, to study the role of GABA, in the human brain, in producing mild sedation.

2.3.3 Drug administration

Sedatives delivered intravenously can be administered using an intermittent bolus technique or as a continuous infusion. Continuous infusions may be delivered using pharmacokinetic models in which the rate of delivery is altered automatically to achieve a desired plasma concentration (target controlled infusion- TCI), considering the distribution and elimination pharmacokinetics of the drug. A number of such models have been developed for propofol of which Marsh's (Marsh et al., 1991) and Schnider's (Schnider et al., 1998) are the most commonly used ones. While there are differences in how these models have been derived and therefore the calculations they use to decide infusion rates, no one model is considered superior to the other, especially for low doses in healthy young volunteers (Absalom et al., 2009). Marsh model, which has been extensively tested and is more commonly used in clinical practice, was therefore chosen for these experiments.

Propofol (Propofol-Lipuro 1%, Braun Ltd.) was administered using an Asena-PK infusion pump (Alaris Medical, CareFusion Ltd.) using a TCI based on the Marsh pharmacokinetic model (Marsh et al., 1991). Infusion was started targeting an effect-site concentration of 0.6 mcg/ml. Once the target was reached, 2 min were given for further equilibration. Drug infusion was increased in 0.2 mcg/ml increments until the desired level of sedation was achieved. Sedation level was assessed at every two-minute intervals by an anaesthetist blinded to the infusion level. At the desired sedation a second assessor confirmed the level.

2.3.4 Drug effects and monitoring

2.3.4.1 Haemodynamic changes

Most anaesthetic drugs induce hypotension as anaesthesia is induced. The degree of hypotension varies among anaesthetic drugs and is usually dose-dependent. Propofol causes hypotension both by peripheral vasodilation, reducing systemic vascular resistance and also by reducing the contractility of the heart (Claeys et al., 1988, Gauss et al., 1991, Robinson et al., 1997). Hypotension is common at anaesthetic doses of propofol but uncommon with conscious sedation doses. The degree of hypotension may also be related to the rate of drug administration, which is lower using a target controlled infusion (TCI) as opposed to a bolus injection. The likelihood of hypotension was low considering the amount required for mild sedation and the use of a TCI pump. Neurovascular coupling, which forms the basis of some of the neuroimaging modalities, in particular BOLD-fMRI, is largely unaffected by propofol (Veselis et al., 2005).

2.3.4.2 Airway and breathing control

Respiratory suppression is also a requirement of anaesthesia and therefore a desirable element of the effects of anaesthetic drugs. Propofol causes significant respiratory depression at anaesthetic doses but less so with sedative doses (Goodman et al., 1987). This is also dependent on the dose and rate of delivery. Doses required for mild sedation are unlikely to cause significant respiratory depression. Irrespective of this, oxygen was supplied to all participants at 2 litres/ minute through nasal cannulae and expired carbon-dioxide measured to monitor ventilatory depression.

Airway obstruction may occur as a consequence of a sedated state, especially with volunteers lying in a supine position. Airway obstruction may further worsen respiratory depression. Conscious/mild sedation is characterised by participants being able to maintain their oral/pharyngeal tone, therefore, the likelihood of airway obstruction was perceived to be low. Participants who are likely to be at a greater risk of airway obstruction, such as those with a history of snoring, sleep apnoea, obesity or facial features such as micrognathia etc. were excluded at the recruitment stage.

2.3.4.3 Monitoring for side effects

The order of experiments was chosen with MEG experiments being first and followed by the MRI session, at least one week apart. All the volunteers had been given an opportunity to lie in the mock MRI scanner as part of the consenting process to reduce any apprehension about the scanning environment. The MEG scanning session involved participants lying on the flattened bed of the MEG scanner. Herein the participant's head is inside the MEG helmets but the rest of the face is exposed and easily accessible. This served as an additional opportunity to ensure safety with the sedation protocol of participants prior to their MRI scanning session.

Participants were monitored throughout the scanning sessions by one senior anaesthetist, who was not involved in data collection, following the Minimum Monitoring Standards, as recommended by the Association of Anaesthetists (Checketts et al., 2016). Heart rate (continuous), non-invasive blood pressure (every 5 minutes), oxygen saturation, and concentrations of expired (end-tidal) carbon dioxide were monitored using a MR-compatible, Veris MR Vital Signs monitoring system (MEDRAD Radiology). The volunteer was able to alert the experimenters and anaesthetist at any time using a voice call over the continuously active intercom system. Standard operating procedures were in place to stop study session if there was increasing sedation, reduced respiratory rate, desaturation (blood oxygen saturation levels of less than 90% while breathing air enriched with 2 litres of oxygen per minute), a drop in pre-baseline blood pressures of more than 20% or if the participant developed any intolerance to propofol. Volunteers were monitored for at least one hour following the cessation of propofol infusion.

2.4 Experimental design

The experiments were performed in two sessions, with the same participants. Following recruitment, consenting and 'benching' as required, the first session was the MEG session while the second one was the MR session. This order was maintained

throughout the study and the gap between the two scanning sessions was at least one week.

The schematic below (Figure 2-2, Figure 2-3) describes the sequence of data collection within the two sessions. The different data collected in the two scanning sessions have been described as separate experiments, within the thesis, as they test/ investigate separate hypotheses.

2.4.1 MEG session

An anaesthetist inserted a cannula in a vein of the hand/arm of the volunteer before entry to the MEG suite. Median nerve localisation was done for the somatosensory task. The electrodes were placed to produce a robust adduction of the thumb, in a non-painful, repetitive twitch. Once inside the MEG suite, the volunteer lay on the MEG trolley and were positioned supine for the scanning. Monitoring was applied as in Section 2.3.4.3. The first half of the scanning was done in the *Awake* state without any drug infusion. Participants performed a visual and auditory reaction time test at the start and the end of the session. They were presented with various stimuli (Figure 2-2) and were asked to perform various tasks.

Propofol infusion was then started and increased slowly till the desired level of sedation was achieved. The starting target plasma concentration was 0.6 mcg/ml, as administered using the Marsh pharmacokinetic model. Once the target concentration was achieved, two minutes were allowed to pass, for further equilibration, before increasing the target level by a further 0.2 mcg/ml. This sequence was continued till the desired level of sedation was achieved.

Once mild sedation (assessed using an OAA/S level of 4; Figure 2-1) was achieved the second part of the scanning (*Sedated* state) commenced. This included the same tasks and stimuli as the *Awake* session.

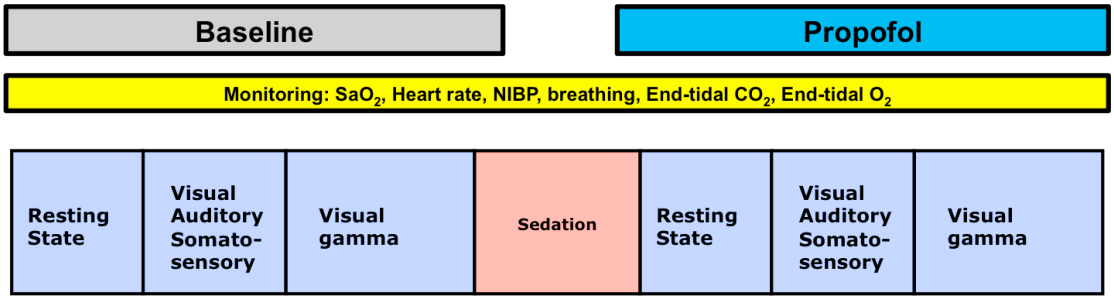

Figure 2-2: Schematic of the MEG Session

At the end of the scanning in the *Sedated* session, propofol infusion was stopped and the infusion line disconnected. After waiting for a few minutes the participant was supported to sit-up and once they were comfortable and recovered enough, assisted to walk out of the MEG suite. They were monitored for a further period of about 1 hour to ensure recovery from drug effects.

The MRI session followed at least 1 week after the MEG session to allow a complete "washout" period in which the drug naturally clears from the system.

2.4.2 MRI session

Participants had their scalps prepared for application of an MR compatible EEG cap (BrainAmp MR, BrainProducts, Munich, Germany). EEG data was collected throughout the MR scanning session, but not analysed as part of this thesis.

A cannula on the dorsum of the hand was then placed. Electrodes were placed to stimulate the median nerve. Once inside the MR suite, the volunteer lay on the MR trolley and were positioned for the scanning. Respiratory bellows and cardiac monitoring for the MR scanner were applied as standard. Further physiological monitoring was applied as in Section 2.3.4.3. The first half of the scanning was done in the *Awake* state without any drug infusion. Participants performed a visual and auditory reaction time test at the start and the end of the session. They were presented with various stimuli (Figure 2-3) and were asked to perform various tasks.

Propofol infusion was then started and continued as for the MEG session. Once mild sedation was achieved, scanning and stimuli were repeated (Figure 2-3). Termination of infusion and participant recovery were performed as in the MEG session.

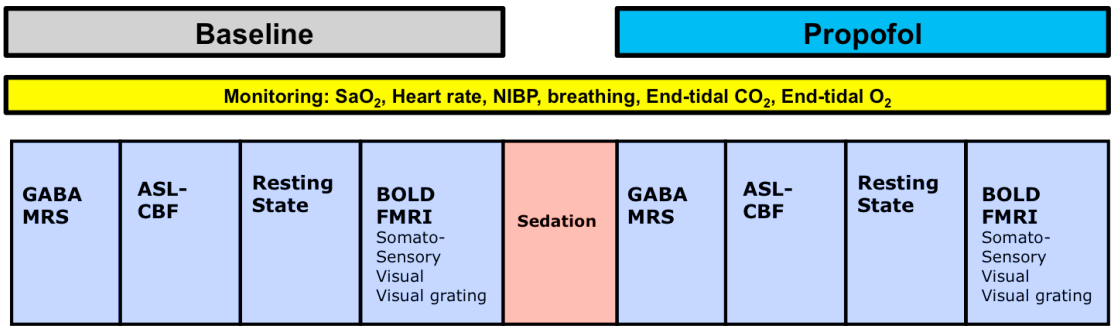

Figure 2-3: Schematic of the MR session

2.5 Functional Neuroimaging

Functional brain imaging broadly refers to include the full range of techniques, which may be used to define physiological changes accompanying brain activity. In vivo methods help gather information at the level of larger neuronal assemblies and pathways. This is unlike the in-vitro methods, which allow study of individual neuronal level function. These techniques, therefore, provide an extension from microscopic level study of brain function and help understand brain function at a larger-scale, macroscopic level and provide the bridge between understanding of cellular function and clinical/ behavioural responses to those.

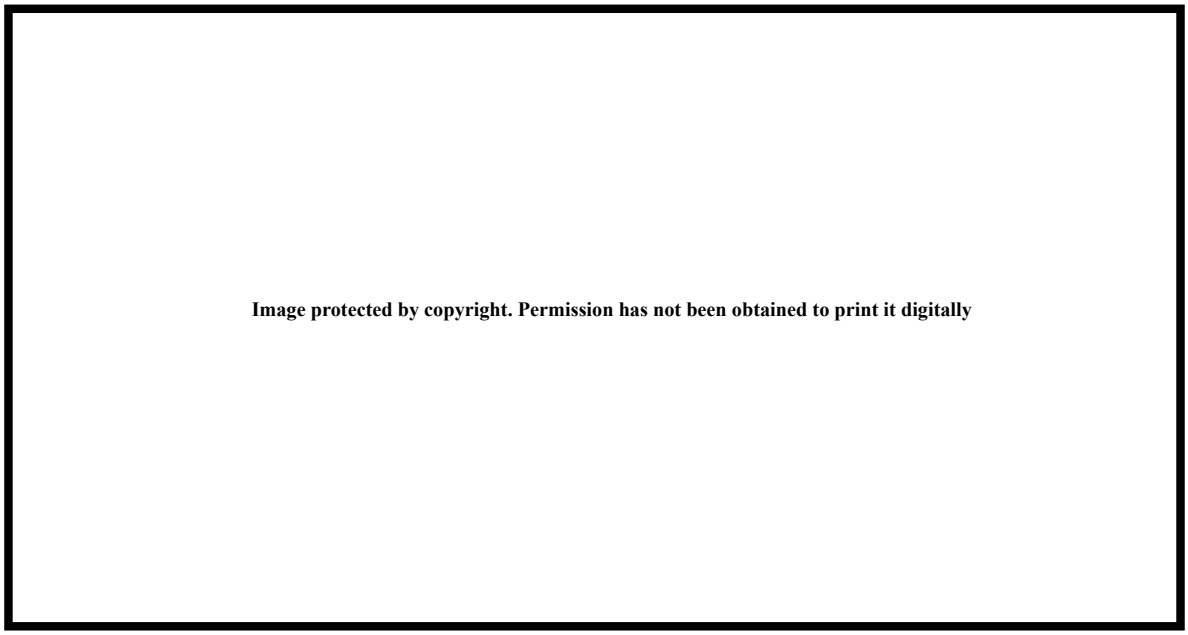

Figure 2-4: Functional brain mapping tools.
Relative ranges of the tools in temporal and spatial domains. Adapted from Cohen and Bookheimer (1994)

The aspiration of neuroimaging techniques is to provide a complete spatiotemporal description of the distribution of the various activities in the brain. Currently this is not feasible by any individual neuroimaging modality, however, using modalities in a complementary manner may go some distance in providing a comprehensive understanding of neural functions. Such a complementary use of neuroimaging modalities forms the basis of this work.

2.5.1 Functional MRI

2.5.1.1 Principles of MRI

Nuclei with an uneven number of nucleons (sum of protons/ neutrons) develop a magnetic moment when placed in a magnetic field. They act as a dipole and may rearrange themselves in a higher energy state (opposite to the background field) or lower energy state (in line with the field). This magnetisation has a characteristic frequency in relation to the oscillating radiofrequency, known as the Larmor frequency.

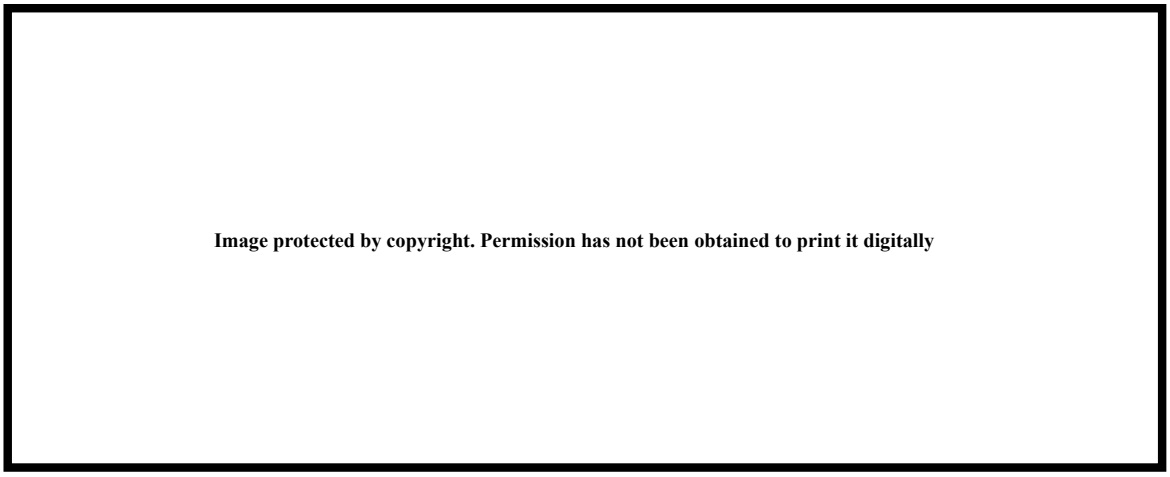

Figure 2-5: Direction of magnetic spins (M) changing with applied magnetic field (B0)
Adapted from Noll (2001)

When radiofrequency (RF) magnetic field is applied in a perpendicular direction, these nuclei get 'excited'. Once the nuclei are excited they return back to the low energy state by emitting RF. Transition between the 2 energy states results in emission or absorption of energy. Frequency of released energy depends upon the magnetic field and the resonance of the nuclei is specific to those; this information can be used to identify / map specific groups of nuclei.

This relaxation also depends upon its interaction with adjoining nuclei (lattice). This relaxation process (time) is referred to as T1 (spin-lattice relaxation time). This process has a relaxation time – rate constant of 1/T1. For example, tissue has a shorter T1 than water; therefore by altering repetition time (TR) (providing increasingly inadequate time for complete relaxation) different tissues may be preferentially captured. As nuclei start

relaxing, each nucleus' relaxation affects the magnetic field slightly. All this combined over larger volumes leads to a loss of coherence of the signal intensity. This 'spin-spin' interaction is referred to as T2 relaxation time, which is an intrinsic property of a nucleus in a particular environment. Grey matter has longer T2 than white matter. By increasing echo time (TE) the signal from tissues with a longer T2 increases. The rate of decay changes as molecules pass through zones with different local field gradients. These changing local field gradients lead to more rapid decay (e.g. tissue close to blood vessels), referred to as T2* relaxation time. So, in areas of rapidly changing fields T2* can be shorter than T2. All these principles are used to identify different tissues with MRI.

2.5.2 Spatial localisation

Spatial localisation of these nuclei is achieved by altering magnetic field gradients in different axes (x and y, where z axis is the main magnetic field, for e.g in the axis of the bore of a typical MR scanner). By altering these gradient fields and their timings, frequency shifts and phase shifts can be induced which are then captured to help localise different tissues in the 3 dimensions.

2.5.3 Physiological basis of fMRI

To be able to detect changes brain function a contrast is required. It is known that with increasing neuronal activity there is an increase in regional blood flow to provide for the metabolic requirements of the neurons. This 'neurovascular coupling' forms the basis of studying changes in blood flow as a surrogate for neuronal activity in the form of a Blood Oxygen Level Dependent (BOLD) contrast.

BOLD utilises the magnetic susceptibility of Haemoglobin (Hb); since deoxygenated Hb is paramagnetic, while fully oxygenated Hb is diamagnetic. The paramagnetic deoxy-Hb alters the static magnetic field making the protons precess at different frequencies causing more rapid phase dispersal and decay of NMR signal. This alters the T2* signal and intensity. With increasing neuronal activity, as glucose and oxygen get utilised, there is a compensatory increase in CBF (oxygenated blood). An increasing

oxygenated blood should reduce the inhomogeneity of the magnetic field (reducing relative deoxyHb concentration) and therefore increase T2* decay time resulting in increased signal intensity. This appears as in increase in BOLD signal intensity, in response to neuronal activity and forms the basis of fMRI.

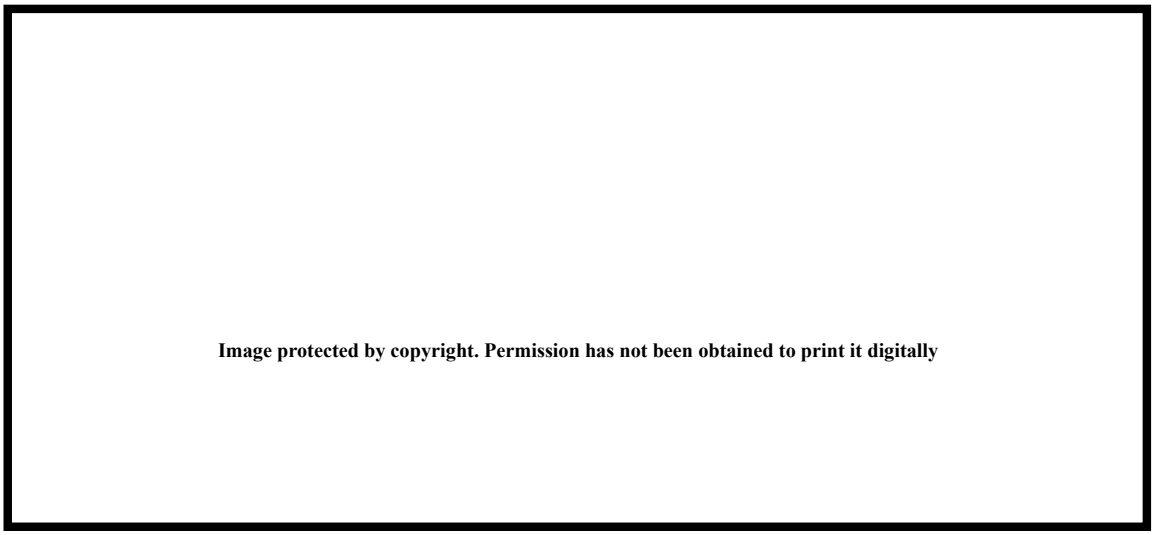

Figure 2-6: Echo-Planar Imaging sequence
RF-Radiofrequency pulse, Gy: phase encoding gradient , Gx: Frequency encoding gradient. Adapted from Noll (2001).

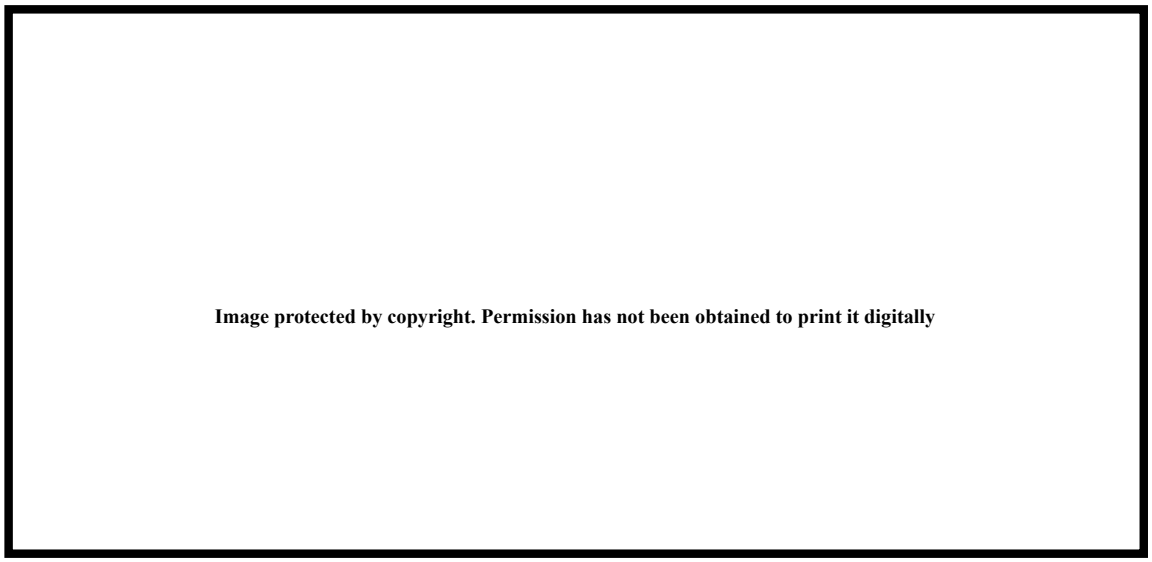

Figure 2-7: Schematic of a typical BOLD response.
This represents a brief initial dip, followed by a robust positive response followed by a slower post-stimulus undershoot. Adapted from Hoge and Pike (2001).

The haemodynamic response, which forms the basis of BOLD, however, does not follow the neuronal changes linearly. Each response has different components as shown

in Figure 2-7. The maximum observed amplitude of the BOLD response is about 5% for primary sensory stimulation and about 0.1-0.5% for cognitive tasks at 3T. The onset of the haemodynamic response occurs within 1-2 seconds, peaks within 4-6 seconds of the stimulus and returns to baseline by 12-20 seconds. There is occasionally an initial dip that occurs within the first 1-2 seconds and represents the oxygen consumption before changes in blood flow and volume occur. A post-stimulus undershoot may persist for up to 20 seconds after the stimulus (Hoge and Pike, 2001).

The precise mechanisms of this 'neurovascular coupling' are also not completely understood. Synaptic activity, dendritic activity and to a much lesser extent direct neuronal activity have been shown to be responsible for the haemodynamic activity, seen as BOLD. Although excitatory activity is more likely to produce a BOLD signal there is plenty of evidence that inhibitory activity (or that associated with no measurable macroscopic electrophysiological activity) may still result in a BOLD signal. To further add to the complexity, there is a range of factors, both physiological and technical, which may influence the resulting in the signal intensity as observed on MRI (Figure 2-8).

2.5.4 Resolution of BOLD-fMRI

Resolution in fMRI is limited by its signal to noise ratio (SNR). For MRI, SNR depends on the pixel size, the slice thickness and the k-space readout time. Accordingly, the typical fMRI pixel size is 3–4 mm, although with higher field magnets (for e.g. 7T) it can be increased substantially. Functional MRI's temporal resolution is limited by haemodynamic response time; typically the BOLD response has a width of ~3s and a peak occurring ~5–6s after the onset of a brief neural stimulus. This is much slower than the underlying neural processes, and temporal information is thereby heavily blurred. Although by using techniques such as jittering event-related stimuli and with appropriate analysis methods, temporal inferences in the range of 100ms may be achieved (Glover, 2011).

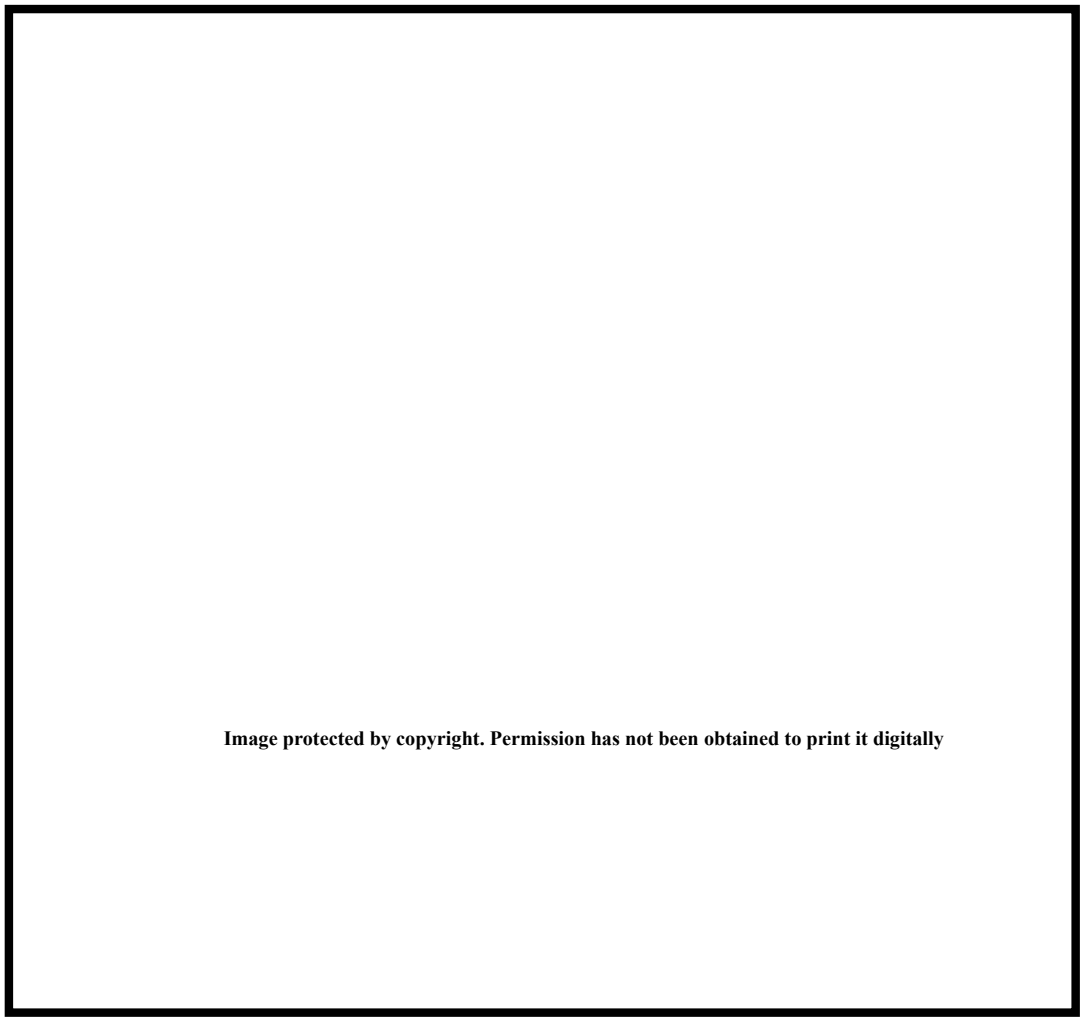

Figure 2-8: Schematic showing the interactions affecting the BOLD response. Positive/ negative arrows indicate positive/ negative correlations between the parameters. Bold arrows represent the significant modulators. Adapted from Noll (2001)

2.5.5 Designing BOLD-fMRI experiments

The most basic method of designing BOLD based fMRI experiments involves a 'subtraction' method, wherein the change in the BOLD signal between two conditions or populations is deemed as a difference in neuronal activity. Since the change in BOLD in response to a task is about 0.5- 3%, repeated stimuli are required to achieve a reasonable signal. Also, since BOLD provides a relative change (in percentage terms) a baseline state is required.

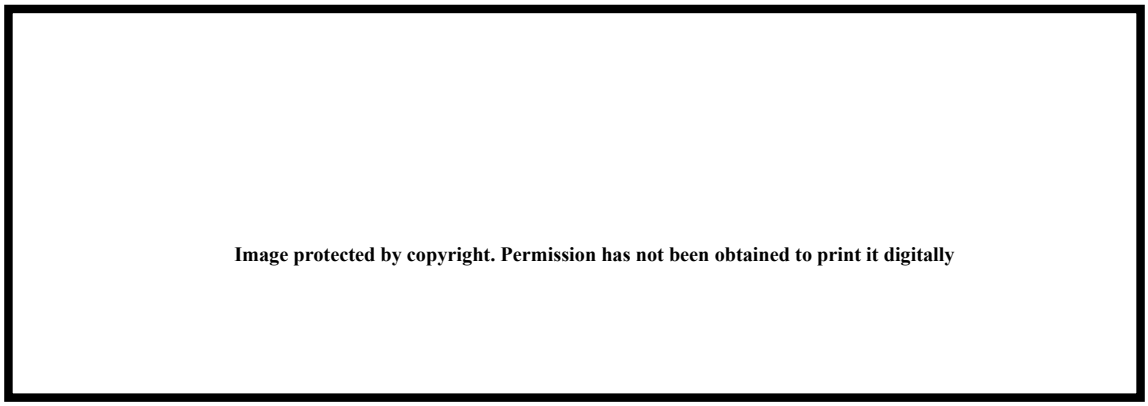

Figure 2-9: Typical BOLD haemodynamic response to repetitive stimuli
This diagram represents the BOLD fMRI timeseries in an active voxel. Blue trace is the signal from the voxel while the red trace is the stimulus timeseries. Adapted from Poldrack et al. (2011).

The haemodynamic response is modelled around the stimulus design and averaged over a number of trials (Figure 2-9).

2.5.6 Analysing fMRI data

The basic principles of analysing fMRI data is to compare the BOLD signal change in different brain regions and compare them across conditions or groups, using appropriate statistical tests. However, to be able to do so, the data has to be pre-processed to reduce the artefacts and noise components, to enhance the signal available for analysis and also prepare the data to be compared across different subjects.

The sequence of these pre-processing steps may vary depending on the software package used, however, the principles remain similar. FMRIB's software library package (FSL) was used for most of the fMRI analysis in this thesis and so most steps have been described in its context.

2.5.6.1 Quality control

This involves a quality check to ensure that the data are not corrupted by artifacts, such as scanner spikes, ghosting or excessive head motion.

2.5.6.2 Distortion correction

The most common method of fMRI acquisition, Echo-planar imaging (EPI) suffers with field inhomogeneties (B_0), especially at air-tissue interfaces and results in signal drop-outs and distortions. Correction of distortions requires information from field maps required to 'unwarp' the EPI.

2.5.6.3 Motion correction

Even the most compliant participant's head will move involuntarily (for example during breathing, swallowing etc.). Head motion can induce various forms of errors. Bulk movement of the head shifts the images in relation to the reference. Occasionally, movement of the protons in a different slice occurs where their excitation level may be different to that expected by the scanner resulting in inaccurate identification of the tissue (spin history effect). The correction therefore involves estimating the degree of motion and then using interpolation and transformation to adjust the slices in relation to the reference slice. In FSL, motion correction is performed using FLIRT (FMRIB's Linear Registration Tool) by applying rigid-body (using six parameters) transformations or its non-linear transformation counterpart- FMRIB's Linear Registration Tool (FNIRT).

2.5.6.4 Physiological noise correction

Other sources of noise in fMRI data can be introduced through normal physiological activity. The pulsatile blood flow due to heartbeat and chest movements during breathing can introduce changes in blood flow and alterations in magnetic field, indirectly affecting the BOLD response.

Corrections for these artefacts have been done using techniques which involve removal of the low frequency time-locked oscillations in relation to the heartbeats and breathing, as identified by a pulse oximeter, respiratory belt or even measured end-tidal CO_2 and O_2 traces (Birn et al., 2006, Glover et al., 2000, Murphy et al., 2011a), as employed in this thesis.

2.5.6.5 Slice timing correction

Functional MRI analysis assumes that all brain slices were acquired at the same time point. As this is not the case, correction of the timing of the slices is required. This is done by choosing a reference slice and interpolating data from other slices to match the timing of the reference slice. Slice timing correction has some disadvantages too, as it may result in propagation of artefacts into other slices and is therefore not carried out in acquisitions with short TR.

2.5.6.6 Spatial normalization (spatial registration)

Since the anatomy of different individuals varies with respect to each other, spatial normalisation (also called registration) is required to be able to combine their data for group analysis.

This involves removing of the non-brain tissues and alteration in the various dimensions of the image to match it to a reference image. In FSL it is usually done using FLIRT (FMRIB's linear registration tool) (Jenkinson et al., 2002). Functional (EPI) images are first registered to the individual's high resolution T1 weighted structural scan. A rigid body transformation is used for within subject registrations with 7 degrees of freedom (x, y, z translations, side-side, front-back, up-down rotations and a single global scaling) and sinc interpolation. After registration to subject space, an affine transformation with 12 degrees of freedom (six for rigid body transformation and an additional three scalings and three skews) registered the data to a standard space template (MNI 152 T1 1mm brain, Montreal Neurological Institute, Quebec, Canada. Further non-linear transformation can be done to account for small-scale changes, using more advanced level tools (in FSL, it is done using FMRIB's non-linear registration tool-FNIRT)(Andersson et al., 2007b).. Typically FLIRT is used for within subject registration, for e.g. when registering functional data to subject's structural data. FNIRT, on the other hand is used to refine the registration of a structural image to a standard-space image such as a template brain (after application of FLIRT). These steps

have been carried out in for the first level (within subject) analyses in all chapters of the thesis. Further group-level analyses have been conducted in the standard space.

The steps above involve registration of the whole-brain EPI data. When analysing data with a narrow field of view (such as that of the visual cortex in Chapter 3), a multistage registration process is required. The first stage is to acquire an EPI of the whole brain using the same imaging parameters so that the image with the narrow FOV can be registered with this image. Further registration proceeds as described in the paragraph above.

2.5.6.7 Spatial smoothing:

This step involves applying a filter to reduce high frequency information to 'blur' the images, with a view of increasing SNR. This helps reduce the mismatch between individual datasets, for the purpose of group analysis, although at the cost of spatial resolution.

2.5.6.8 Temporal filtering:

Temporal filtering involves filtering of the data in time to remove high and low-frequency noise. Low pass filtering is not always applied as it may reduce the strength of the signal of interest.

2.5.6.9 Statistics: modelling and inference

The basic tenet of fMRI is to analyse each voxel's time series to see if the BOLD signal changes in response to any intervention. For a simple 'on/ off' block design, it may take the form of subtracting the averaged responses between the on and off states. Since simple statistics may ignore the temporal structure of the BOLD-HRF and therefore general linear model (GLM) based analyses are considered more appropriate. This involves comparing the time courses of the voxels to an 'expected' model of HRF (Webster, 2017).

A very simple example of linear modelling is y(t)=a*x(t)+b+e(t).

Here y(t) is the data as a function of time. x(t) is the model, a is the parameter estimate for x(t), i.e., the value that the square wave (of x) must be multiplied by to fit the square wave component in the data. b is a constant, usually corresponds to the baseline (rest) intensity value in the data. e is the error in the model fitting.

For each voxel, this model, generates a parameter estimate (PE) depending upon how well the data fits the model. These voxel-wise PEs may be plotted into statistical maps by dividing them by the estimate error (t value). Statistical transformation converts these t-values into Z values (Gaussianised t values) which is the commonly used statistical nomenclature in neuroimaging. So, a Z value of 2 means that the data is 2 standard deviations away from 0. Z –values represent how strongly each voxel's data is related to the explanatory variable. With more than one explanatory variables they can be modelled in different (linear) combinations and then contrasted to identify which have a stronger effect than the others.

Comparing the results between groups is more difficult, as with a large number of voxels there is a high chance of a false positive result. Bonferroni correction for the entire number of voxels could prevent that, but that would be too conservative, as the voxels are not truly independent of each other. The practical compromise, therefore, is to use 'cluster –level' (a predefined number of voxels forming a cluster) thresholding, where Gaussian field theory is used to estimate probability based on the cluster size and the initial statistical threshold chosen (Woolrich et al., 2001). Thresholded activation maps can be visualized by setting an appropriate Z value (for e.g. Z= 2.3).

Group comparisons may then be done using 'fixed effects' or 'mixed effects'. Mixed effects is commonly used as it takes into consideration the between subject and between session variability and therefore provides information more representative of the wider population. FEAT uses FMRIB's Local Analysis of Mixed Effects (FLAME) for this.

2.5.6.10 Functional Connectivity analysis

The section above describes common analytic techniques of data, especially those investigating changes in specific regions of the brain. Increasingly neuroimaging data is being used to study changes in the way different brain regions communicate with each other. This involves studying the change in the BOLD response in relation to a 'task-free' or 'during task' period and correlating the time-courses of discrete and distant brain-regions. The different options for such functional connectivity between different brain regions are as follows (van den Heuvel and Hulshoff Pol, 2010).

Seed based functional connectivity involves choosing a region of interest (seed) and estimating the correlation of its BOLD timeseries with other parts of the brain (specific regions or the entire brain), thus creating a whole-brain voxel-wise functional connectivity map of covariance with the seed. In this thesis, correlation of timeseries has been limited to grey matter. White matter or CSF have not been used as regressors. While reasonably straightforward and statistically robust, it has its limitations. Other low frequency oscillations (such as physiological, respiratory, haemodynamic fluctuations) can create confounds. Also, selection of seed requires a strong a priori hypothesis and variations in seed selection can influence results.

Model free or independent component analysis (ICA), do not require a specific a priori hypothesis. This technique can search the whole brain for changes in connectivity patterns. ICA methods are designed to search for a mixture of underlying sources that can explain the resting- state patterns, looking for the existence of spatial sources of resting-state signals that are maximally independent from each other. These two approaches have been used with fMRI and MEG data in this thesis.

More advanced techniques include graph based network anlayses. A particular network architecture, which is commonly emphasised in this emerging field, is small-worldness (Watts and Strogatz, 1998). The small-world property is a qualitative description of a network characterized by high levels of local clustering and short path lengths linking all nodes of the network. This constitutes a particularly attractive model of brain network organization, since it can account for the combination of both specialized and

distributed information processing, as well as minimizing wiring cost in brain circuitry (Achard et al., 2006, Sporns and Honey, 2006). Given the small-world properties of the human brain, graph- based methods provide a valuable tool for elucidating network structures. Node centrality is a key concept in network analysis, of which one is eigenvector centrality, which, identifies nodes that play central roles among highly connected nodes of the network (Lohmann et al., 2010).

2.6 Arterial Spin Labelling – MRI

Cerebral blood flow (CBF) changes correlate well with brain function and therefore changes in CBF can be used to study brain activity in different physiological and pathological states. Arterial spin labelling (ASL) is one such technique of measuring CBF non-invasively.

This technique involves using endogenous water as the magnetic contrast to measure CBF. The proton spins of blood arterial water are 'labelled', i.e. their magnetisation altered (saturated or inverted). A 'control' image of a voxel (or slice) is taken which represents tissue and blood water. Following a time delay a 'labelled' image is taken of the water to allow tagged blood to diffuse into the tissue. The difference between the magnetisations of the 'labelled' blood and control images is proportional to the blood flow and represents the ASL signal.

All CBF measurements rely on compartmental modelling and tracer kinetics following the flow of tracer through the arterial tree prior to venous washout. Advantages of ASL include utilisation of an endogenous tracer, i.e. arterial water, thus avoiding the risks with exogenous tracers. ASL can be repeated over time and can therefore follow disease progression and longitudinal drug action. ASL also produces an absolute measurement of CBF and better spatial and temporal resolution than most other modalities.

2.6.1 Types of ASL

The different types of ASL differ based on the methods of magnetic labelling of inflowing blood.

2.6.1.1 Continuous ASL

This involves proton labelling in a thin slice at the neck level including continuous pulsed RF application for 2-4 seconds and also a gradient and a magnetic field gradient in the direction of flow. The advantage of CASL is an improved SNR, but the downside is a high level of energy deposit on the molecules. In practice, the RF amplifiers of most modern scanners are not able to deliver the necessary pulse durations, so the scheme is little used.

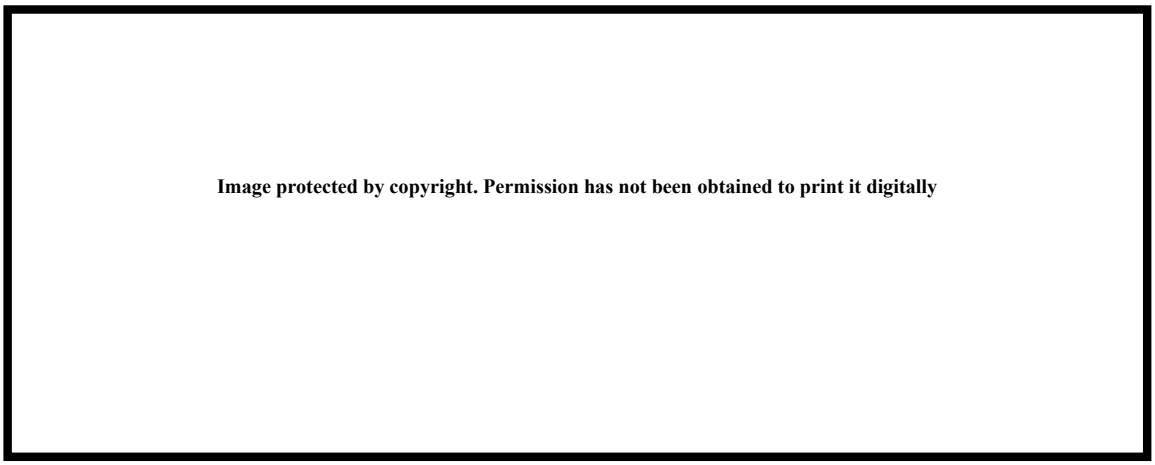

Figure 2-10: Principle and stages of Arterial Spin Labelling.
Adapted from Ferre et al. Ferre et al. (2013)

2.6.1.2 Pulsed ASL (PASL)

This uses shorter pulses of RF. This is more widely used since it is easier to implement. Shorter labelling times means less energy is deposited. Drawbacks include lower SNR, high sensitivity to transit times and slice profile artefacts. The basis of PASL is an echo-planar MR imaging readout but with arterial labelling (on or off for label and control respectively) in a slab proximal to the imaging slices. A number of flavours of PASL exist of which we have used PICORE QUIPPSII. PICORE improves the profile of the

labelling and QUIPPS (Wong et al., 1998) reduces the sensitivity to the arterial transit time.

2.6.2 BOLD vs ASL

BOLD is a susceptibility based method that creates a 'functional' T2* image by exploiting local in-homogeneities in the magnetic field due to change in relative concentrations of Oxy and Deoxy Hb. Both BOLD and ASL use endogenous tracers; BOLD has higher SNR, is more suited for event related designs, especially where absolute quantification is not required.

2.6.2.1 Advantages of ASL

ASL has certain advantages making it more suitable in certain conditions/ experiments.

- Spatial localization: BOLD signal is a complex result of the interplay between CBF, cerebral blood volume (CBV) and oxygen consumption (with signal resulting from capillaries, but also from veins. ASL signal is all related to intravascular component, making it more specific.
- Signal quantification: Baseline values before and after activation are possible with ASL and therefore absolute quantification (in physiologically meaningful units) is possible.
- Power spectrum: BOLD has a noise spectrum 1/f ; i.e. higher amplitudes at lower frequency making it unsuitable to study events with frequency less than 0.1 Hz. ASL requires pair wise subtraction and so is frequency independent.
- Susceptibility effects: BOLD is susceptibility dependent, using Gradient Echo-Echoplanar imaging resulting in artefacts at tissue-bone or tissue-air boundaries. ASL can use Spin-Echo sequences, or other imaging readouts, to reduce such artifacts.

2.7 Magnetic Resonance Spectroscopy

Magnetic resonance spectroscopy is a technique, which allows detection and quantification of metabolites, *in-vivo*, using the magnetic properties of its molecules.

2.7.1 Signal generation

In a magnetic field, nuclei orient themselves in a specific pattern and release energy as they revert back to a low energy state. The electron cloud surrounding these nuclei, shield them from the magnetic field and therefore may affect their behaviour in that magnetic field. The precession frequency of these nuclei, which depends on the magnetic field and their specific gyromagnetic ratio is altered by the electron cloud, as it reduces their precession frequency. This change in frequency is known as 'chemical shift'. This is quantified as the ratio of the frequency of the molecule to that of the frequency of a reference molecule multiplied by a constant factor (dependent on the scanner and acquisition characteristics). This chemical shift is reported in International units (in parts per million (ppm)) and therefore, regardless of scanner strength, always has the same position on the chemical-shift axis. However, since the frequency of the reference molecules may vary between scanners, the concentration is reported in ppm in institutional units. The usual reference molecules are inert compounds, such as water or N-acetyl aspartate (NAA) or creatine. In this thesis, as is standard practice in CUBRIC, water was used as the reference molecule. Metabolite (GABA) concentrations were, therefore, referenced to water within the same voxel (internal referencing). This is considered an appropriate technique as the participants were healthy volunteers and the study was of a crossover design. When considering patient populations or comparing different groups, 'external referencing' with a standard reference metabolite (such as quantities of metabolite in a phantom) may be more appropriate.

A typical MR spectral plot displays the chemical shift (in ppm) on the x-axis with the peaks of the signal amplitude, with the area under the peak representing the concentration of the metabolite. The quality of the spectra is determined by the line width (spectral resolution) and by the SNR that determines the peak of the height of metabolite peaks in comparison to noise. This SNR may be increased by increasing

field strength, voxel size or longer acquisitions. Spectral quality is affected by the variations in magnetic field induced by magnet imperfections or proximity to regions of high magnetic susceptibility such as bone, water, CSF or haemorrhages.

Dispersion of the metabolite signal in relation to chemical shift axis is limited and so signals from different metabolites may overlap and those metabolites with larger (greater concentration) signals tend to obscure those with smaller signals. GABA being one of the less abundant molecules tends to get obscured. GABA molecules appear as multiplets, which are overlapped by higher concentration molecules, such as Creatine at 3ppm, NAA at 2 ppm and Glutamine and Glutamate at 2.3 ppm.

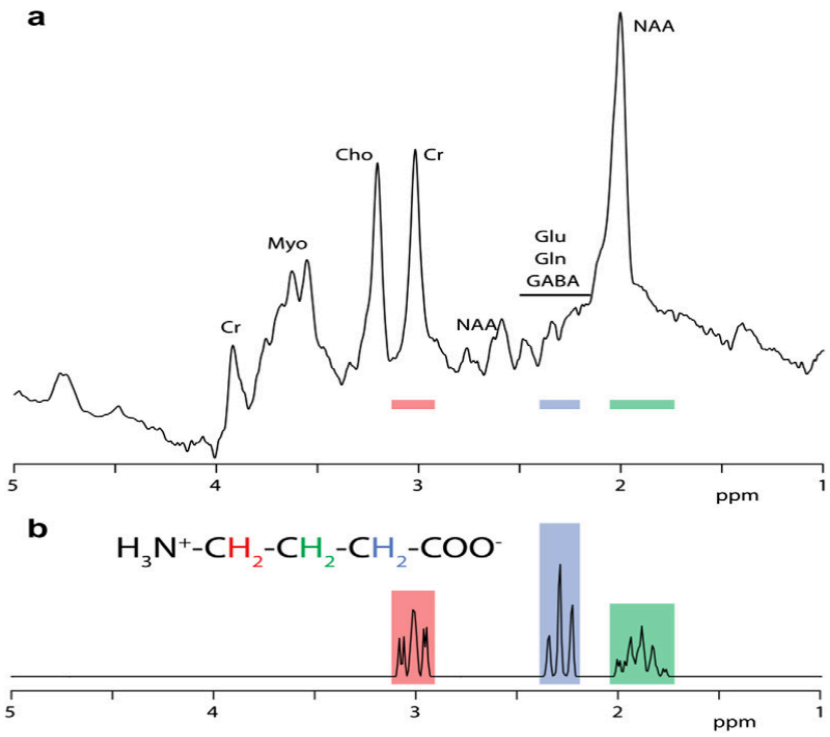

Figure 2-11: MR spectra of GABA.
a) Shows peaks corresponding to the various molecules, including N-Acetylaspartate, Creatine and GABA. b) shows simulated MR spectrum at 3T. Coloured bars represent the same molecular groups in a and b. Adapted from Puts and Edden (2012).

Most of the MRS signal (like MRI) is derived from the hydrogen atoms as they are not only abundant but also form part of different functional groups with specific resonant frequencies. The coupling relationship between different hydrogen ions and atoms (for example the number of bonds between them) help determine the position of these on the

chemical shift axis. Sub-peaks can be identified within a molecule especially if they have more than one hydrogen atom depending on their direction of spins. So, if both spins are 'up' the resulting frequency may be higher than that of the overall molecule while if both spins are 'down' it may result in a lower frequency. With more than two hydrogen atoms, multiple sub peaks are produced (multiplet). This spin-spin coupling or 'J-coupling' can result in flatter and broader peaks making it more difficult to identify and measure metabolites.

2.7.2 Signal acquisition: GABA edited spectroscopy

In typical MRS experiments a single voxel or volume is excited (single voxel MRS) using a combination of selective pulses in different directions. While this is the commonest technique, other techniques such as a hybrid technique involving simultaneous MRS imaging (Magnetic resonance spectroscopic imaging or chemical shift imaging) may also be used. Single voxel spectra are usually acquired using either Point –RESolved Spectroscopy (PRESS) or Stimulated Echo Acquisition Mode (STEAM). In this thesis PRESS was used for single voxel spectroscopy.

GABA peaks occur at 1.9 ppm and 3 ppm. The GABA molecules at 3 ppm are coupled with the molecules at 1.9 ppm. An 'editing' pulse applied at 1.9 ppm affects the spectra of GABA at 3 ppm. The difference in the spectra with the pulse 'on' (with coupling altering the spectra) and pulse 'off' (no change) gives a measure of the concentration of GABA (at 3 ppm), combined Glx (glutamine, glutamate peaks at 3.75 ppm) along with other J-coupled macro-molecule peaks (Puts and Edden, 2012). Water is the most abundant molecule; so suppressing the water molecules is required and is done through applying an even number of 180-degree re-phasing pulses at the frequency of the water molecule, de-phasing its signal. This is the commonly termed MEGA-PRESS (MEscher-GArwood – PRESS) sequence and has been used in the experiments of this thesis (Mullins et al., 2014). One major limitation of this method is that insufficiently selective editing pulses results in co-editing of macromolecular (MM) signal at 3 ppm (due to a coupling to a signal at 1.7 ppm that is partially inverted by the editing pulses) as well as other metabolite species such as homocarnosine; the edited GABA signal is therefore widely referred to as GABA+ (Harris et al., 2014).

2.8 Magnetoencephalography

Magnetoencephalography (MEG) is a neuroimaging technique where the changes in the magnetic field induced by the electrical activity in the brain is recorded. Although MEG activity is closely related to EEG activity, in contrast to neuroelectric activity (as measured by EEG), the neuromagnetic activity is much weaker. It has required decades of development of sophisticated tools to be able to detect and record such activity. David Cohen, first recorded the human alpha oscillations in 1968 and went on to develop the superconducting technology for MEG measurements in 1972 (Singh, 2006).

2.8.1 Signal generation

Neuronal activity from an individual neuron is far too weak to be measured outside the brain and therefore synchronous activity of a large enough group of neurons is required to generate a measurable electrical or magnetic signal. It is estimated that nearly 25mm^2 of cortical sheet has a high enough number of neurons to be able to produce such a signal.

This neuroelectric activity generated, generally, is a combination of action potentials and the slower synaptic potentials in the dendrites. However, due to the short duration and erratic activity of actions potentials, it is unlikely that they contribute much to the synchronised neural activity as measured by MEG. The post-synaptic potentials (PSPs) generated in the dendritic cells need to be oriented appropriately such that the net current flows do not cancel themselves out (as would happen in randomly, uniformly distributed dendrites). This requirement makes the apical dendrites of pyramidal cells as the most likely sources of such MEG measurable neural activity (Figure 2-12).

2.8.2 EEG vs MEG

As the neuro-magnetic signals picked up by MEG are somewhat different form those detected by EEG, the two techniques present their own distinct advantages and potential disadvantages. MEG sources are mainly PSPs, while EEG detects conductor currents

(as the brain tissue, skull and scalp will generate secondary currents) as well as the PSPs. The magnetic fields generated by the secondary currents tend to nullify themselves and therefore MEG is considered better at identifying primary currents. As shown in Figure 2-12, current sources in radial direction are not observable in MEG, although it has been suggested that this represents only a small fraction of the overall neural activity (Hillebrand and Barnes, 2002). The main advantage of MEG is that it is unaffected by the conductivity through skull and scalp tissue and the size or shape of the skull which could create confounds between subjects in experiments using EEG. The main disadvantage of MEG is that since the magnetic field drops exponentially with distance, it is most sensitive to superficial cortical structure but its abilities to detect from deeper structures is poorer, although researchers have been able to successfully study deeper structures with MEG.

2.8.3 MEG systems

As MEG measures very tiny magnetic field changes it may be influenced very easily by magnetic noise generating sources. The core element of a MEG system is a highly sensitive magnetic field detector- superconducting quantum interference device (SQUID). Such SQUIDS are placed close to each other to cover the entire skull (usually 275-300) and are linked to pickup coils. All these are housed in a single liquid dewar reservoir, which maintains their superconducting properties at 4.2^{o} K. The design of the pickup coils also plays a role in the quality and type of data generated. The commonly used design of pickup coils includes magnetometers, planar gradiometer and axial gradiometers. A magnetometer consists of a single loop of wire connected to a SQUID and for a dipole current source it produces a map with maximum and minimum on either side of the dipole. A first order gradiometer is formed when two magnetometer loops of opposite orientation are combined. They detect changes in magnetic fields across the two loops. Radial gradiometer have the two loops oriented parallel to the dipole source and produce similar field patterns as a magnetometer. Planar gradiometers have the pickup loops oriented perpendicular to the dipole source and produce field maps with peaks directly over the source. The gradiometers have an advantage over magnetometers in that they are less sensitive to environmental noise as they measure the

difference between the coils. Also, planar gradiometer field maps are easier to comprehend as they represent a single maxima below the sensor.

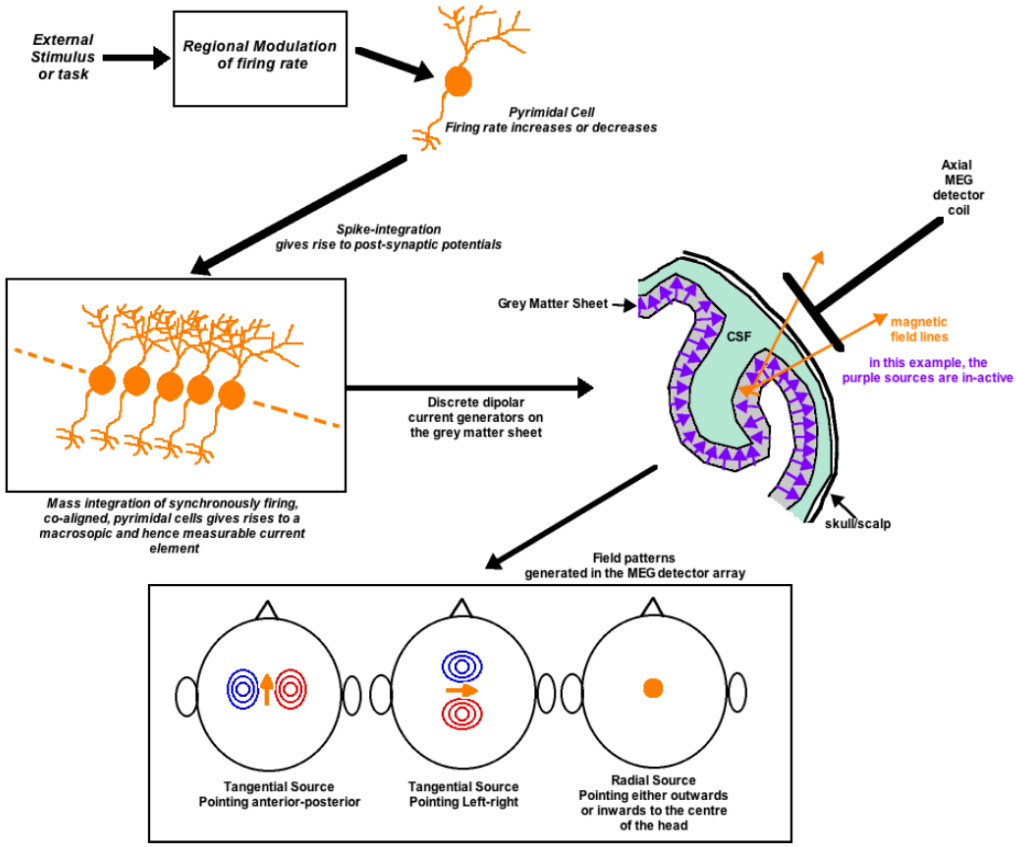

Figure 2-12 : Schematic of generation of neuromagnetic fields depending upon source
Top panel showing how the neuromagnetic fields are generated from a population of dendritic cells firing synchronously. Bottom panel showing how tangential sources may be captured but radial sources are not. Adapted from Singh (2006).

2.8.4 Acquiring MEG data

Since there may be variable relationship between the skull/ scalp anatomy and the brain, well-defined surface anatomical locations are identified to help localise the head position in relationship to the MEG helmet. This is achieved by placing fiducial markers

on the prominent landmarks such as the nasion and the tragus of the ears, bilaterally. To perform localisation analysis, further anatomical MRI scans are collected where these landmarks are identified to help co-register the brain anatomy with the MEG data.

2.8.5 MEG data analysis

In a typical MEG experiment, the MEG equipment collects data from about 275 channels, simultaneously, over a period of several minutes. During this time experimental manipulations are done. This continuously collected data is then divided into temporal 'epochs' based on similar stimulation paradigms. In simple MEG experiments this data is averaged in the time domain resulting in retention of the neural activity occurring at the same time point in every epoch, in relation to the stimulus (phase-locked) while the irregular ones get averaged out. These averaged peaks are then used for further analysis.

Steady state evoked response occurs when stimulus is presented with a fixed frequency resulting in oscillatory response at the stimulation frequency (as in Chapter 3) or its harmonic response. Although some of the most commonly used techniques in MEG/ EEG literature, the limitation of evoked responses is that it reveals only that neural activity which is time and phase locked but loses activity with a 'jitter' i.e. varying time lag. Studies of primary cortical activity are therefore well suited for such activities, while cognitive activities that may have inter and intra- individual variation do not produce such useful results. If this epoched data is averaged in the Fourier domain (averaging the time frequency content of each trial) it can reveal increases or decrease in power in the frequency bands, referred to as 'induced effects' (as in Chapter 3), which is usually not phase locked but time locked to the stimulus.

MEG signals are recorded in sensor space and then converted to source space for further analysis. Converting to source space poses the 'inverse problem'. Inverse problem refers to predicting the neuronal sources of electrical/ magnetic activity as detected on the skull surface. Due to the numerous confounding factors and infinite possible combinations of sources possible, a 'unique' solution is difficult to establish without having further information about the spatial and temporal content of the acquired data.

The ‘forward problem’, as opposed to the inverse problem, refers to predicting the magnetic field generated form a source from a known location, magnitude and orientation.

2.8.5.1 Source localisations (inverse problem solutions)

A simple ‘inverse problem’ solution used with evoked responses (few peak latencies) is the modelling of single equivalent current dipole (ECD), assuming that a single small patch generates the MEG detected current. This ECD appears as a dipole (in axial gradiometer assembly) and is located at the midpoint of these two maxima. More complex arrangements of such models are possible to study fit of MEG data over a range of latencies.

Further solutions of the ‘inverse problem’ involve dipole fitting, where dipoles are simulated at a given source location to result in a magnetic field which matches closest with the data. Further dipoles are added if a close enough match is not generated. A minimum norm estimate (MNE) technique aims to provide the best solution with minimum overall power while a minimum current estimate (MCE) technique aims to solve the problem with the minimum number of sources. Unlike the MCE and MNE techniques, which attempt to estimate the amplitude of all modelled source locations simultaneously, with beamformer based techniques the source activity is estimated, at arbitrarily defined voxel levels, by multiplying spatial filters with measured data.

Synthetic aperture magnetometry (SAM) is one such beamforming technique. SAM involves producing beamformers (or weighting vectors) to estimate the contributions from the different brain regions to the data captured as magnetic fields outside the skull. For example raw MEG data consists of time series of magnetic fields (number of gradiometers x many data points). The signal source will have a magnetic field recordable by MEG sensors, with different sensors having different sensitivities depending on their location (proximity to source) and orientation (lead field). The magnetic fields recorded at any particular sensor are a mixture of all the lead fields. SAM tries to estimate the source activity in a particular location assuming that it is some weighted linear mixture of recorded signals (weighting vectors or beamformers).

The whole brain is divided into 3D volume of points. At each voxel a time series could be plotted depending on the weighing vectors. In SAM, the weighting vectors for voxels are generated independently of each other. These weighing vectors are generated using the covariance matrix, which represents the degree of correlation in each channel of the recording. The SAM algorithm uses the data covariance and the lead fields to generate beamformers while trying to minimise power variance of the virtual sensor.

For SAM used in these experiments, a single global covariance matrix is estimated from the entire dataset and a single set of weights calculated from this. Virtual sensors are then constructed at each source location and then band-pass filtered to the frequency band of interest, time windows applied and then differential power images calculated.

2.9 Choice of neuroimaging techniques and synopsis of methods used

The sections above have explained the basics of the neuroimaging techniques used in this thesis. Previous studies have employed one of these neuroimaging techniques. A multimodal neuroimaging technique has been employed in this research to exploit the unique advantages of each individual modality, such as excellent temporal resolution of MEG along with the excellent spatial resolution of fMRI. This would help integrate the findings from these multimodal techniques and provide complementary information in studying the electrophysiological, haemodynamic and neurochemical changes with propofol sedation, in the same population. This would also allow inter-relationships between different techniques, instead of being restricted to one, as in previous studies.

In Chapter 3 the relationship between GABA concentration changes, gamma oscillations, and BOLD-fMRI changes to a visual stimuli has been tested (hypotheses 1-3). This necessitated the use of GABA-MR spectroscopy, MEG and BOLD-fMRI sessions. In Chapter 4, cortical responses to multisensory stimulation were evaluated in the electrophysiological and haemodynamic domains (hypothesis 4) and necessitated the use of MEG and fMRI sessions. In Chapter 5, changes in resting state brain activity was evaluated in the electrophysiological and haemodynamic domains (hypothesis 5) and necessitated the use of BOLD-fMRI and MEG. In Chapter 6, cerebral perfusion

during sedation was assessed (hypothesis 6). This necessitated the use of ASL technique. The specific hypotheses are as follows:

Hypothesis 1: Propofol sedation increases the GABA concentration in key cortical and subcortical brain regions, measurable by MRS (tested in Chapter 3)

Hypothesis 2: Propofol sedation results in a change in visual gamma band activity, measurable by MEG, which is correlated to the changes in GABA concentration (tested in Chapter 3)

Hypothesis 3: Propofol sedation results in a change in visual cortical BOLD response, measured using MRI and is correlated with changes in visual gamma band responses and GABA levels (tested in Chapter 3)

Hypothesis 4: Mild propofol sedation reduces the neural activity of the primary sensory cortices (visual, auditory and sensorimotor). This will be evident as reduced BOLD activations on fMRI in those regions and reduced evoked fields on MEG in the respective sensory domains.

Hypothesis 5: Mild propofol sedation reduces the functional connectivity in the Default Mode networks and the thalamo-cortical networks without affecting the functional connectivity of the sensori-motor networks using fMRI.

Hypothesis 6: Mild propofol sedation will be associated with a reduction in CBF in the frontal cortex, precuneus, posterior cingulate cortex and the thalamus.

2.10 Sample size calculation

A formal power calculation was not performed, due to the exploratory nature of the work. Fifteen participants were recruited with the aim of obtaining complete scan datasets on 12 of them. This estimation was done, based on previous literature involving

pharmacological fMRI and MRS studies studying alterations in consciousness and MRS studies, as follows:

- The aim is to estimate the BOLD fMRI signal response (percent signal change) both voxel-wise and in regions of anatomical interest e.g. auditory cortex, in response to stimulation and the modulation of this by sedation. This is expected to be of the order of 0.5% (+/- 0.3%SD) for auditory stimulation based on pilot data previously acquired. To detect a reduction in the auditory activity of the order of 50% of this response would require at least 9 subjects (1-tailed test, $P<0.05$, 80% power). A target of 12 subjects was therefore chosen, in this exploratory study, to provide a little extra power. Other sedation and anaesthesia studies involving fMRI have used similar sample sizes (Stamatakis et al., 2010, Boveroux et al., 2010, Mhuircheartaigh et al., 2010).

- Coefficient of variance of GABA values was shown to be 9% (within subject,) in the visual cortex using the MEGA-PRESS technique, in a repeatability study (Evans et al., 2010). Using this information, a sample size of 7 subjects, is likely to provide adequate power to detect a difference of 10% within subjects.

- In a study correlating GABA concentration, visual gamma responses and BOLD response, (Muthukumaraswamy et al., 2009) which provided one of the key hypotheses, 12 subjects provided an adequate sample to identify and correlate the three modalities.

Chapter 3 : Effects of mild propofol sedation on cortical and subcortical GABA levels, neural oscillations and BOLD signal

3.1 Abstract

Gamma-aminobutyric acid (GABA) is the main inhibitory neurotransmitter in the humans. Propofol, like most anaesthetics, is known to cause anaesthesia and sedation through its GABA-ergic actions. There is evidence of relationship between brain GABA levels with visual induced gamma band frequency and BOLD response to visual stimulation. In a series of experiments, using multimodal neuroimaging techniques, the effect of mild propofol sedation was explored on cortical and subcortical GABA levels, neural oscillations (especially induced and evoked visual gamma oscillations) and the BOLD signal in response to a visual stimulus. Furthermore, the relationship between these metabolic, neural and haemodynamic markers was explored in the context of propofol sedation.

The results revealed the following findings during mild propofol sedation

- GABA+ (GABA plus co-edited macromolecules), as detected by magnetic resonance spectroscopy, did not change in the cortical (occipital) or subcortical (thalamic) regions during mild propofol sedation.
- An increase in visually-induced gamma band responses, increased alpha amplitude suppression, and a concurrent reduction in the visually evoked response, was seen with magnetoencephalography. A significant negative correlation between the peak spike gamma frequency with occipital GABA+ concentration was seen during the *Sedated* state but not with the sustained gamma band frequencies.
- A reduced BOLD signal was seen at the peak voxel, in visual cortex on visual stimulation, during propofol sedation. While there was a trend towards an inverse relationship between GABA+ concentration and BOLD signal change (during visual activation), no clear cut relationship existed during sedation, nor was there a well-defined relationship between the BOLD response and gamma band response.

3.2 Background and Rationale

3.2.1 GABA and its physiology

Gamma-aminobutyric acid (GABA) is the most widely distributed inhibitory neurotransmitter in the human brain. GABA is produced from glutamate by glutamic acid decarboxylase (GAD) and is metabolised to succinic acid semialdehyde by GABA transaminase (GABA-T) and further broken down to succinate. GABA is synthesised in the presynaptic neurons and stored, locally, in vesicles. On activation, these GABA molecules are released in the synaptic space where they act on GABA receptors, on the postynaptic membranes, or diffuse out into the extracellular space to act on extrasynaptic GABA receptors. GABA production, in the presynaptic neurons, is facilitated by the enzyme L- glutamic acid decarboxylase. Once released in the synaptic cleft, GABA is removed by GABA transporters. The metabolism and activity of GABA is regulated by a feedback balance between its production, release and re-uptake (Nutt, 2006).

There are two main types of GABA receptors; fast acting ionotropic GABA-A and GABA-C receptors and slower acting metabotropic GABA-B receptors. GABA-A receptors are the predominant types within the brain and present on about 20-50% of all central synapses (Chu et al., 1990). GABA acts on GABA-A receptors to increase chloride ion (Cl^-) conductance which produces hyperpolarisation of the neurones and thus promotes inhibition (Concas et al., 1991).

3.2.2 Proton Magnetic resonance spectroscopy (MRS) and its ability to study GABA changes

MRS is the only technique that allows non-invasive study of endogenous GABA, in vivo. While this developing field of proton MRS in vivo is still reliant on methodological constraints, it has proven to be a reliable, robust and repeatable technique (Evans et al., 2010). MRS detectable GABA-ergic inhibitory processes have been shown to influence the BOLD- haemodynamic response function (HRF) responses that form the basis of fMRI studies (Muthukumaraswamy et al., 2012). MRS-GABA

concentration, as the macroscopic surrogate of cellular level neurotransmitter function, has been shown to influence various physiological and psychological functions (Puts et al., 2011, Sumner et al., 2010). MRS has been useful in demonstrating altered GABA concentration in clinical conditions such as epilepsy, panic disorder, manic-depression (Goddard et al., 2004b, Petroff et al., 1996, Sanacora et al., 1999) and also the modulation of GABA concentrations by pharmacological compounds known to work on the GABA system such as vigabatrin, gabapentin, topiramate and levitaracetam (Petroff et al., 1999a, Petroff et al., 1999b, Petroff and Rothman, 1998, Puts and Edden, 2012) .

Most anaesthetic drugs (with the exception of certain drugs such as ketamine and dexmedetomidine) produce their central inhibitory action through GABA-ergic / GABA facilitatory mechanisms; but their entire range of molecular actions is not clearly understood. While some drugs such as benzodiazepines and barbiturates act only on GABA receptors, inhalational anaesthetic agents act on other receptors including acetylcholine (Ach), histamine, serotonin, AMPA and glycine receptors (Rudolph and Antkowiak, 2004). Propofol (2,6-diisopropylphenol) is one of the most commonly used anaesthetic and sedative drugs in current clinical practice and functions primarily on GABA receptors. While propofol exerts a small amount of activity on nAch, AMPA and NMDA receptors as well as sodium channels its principal mechanism of action is thought to be via potentiation of GABA-A receptors (Trapani et al., 2000). In vitro, it potentiates GABA evoked hyperpolarizing Cl- currents and at higher concentrations may directly activate Cl^- currents at GABA receptors. Its site of action is distinct from that of the benzodiazepine and has recently been shown to be within the beta subunit and consists of both the beta 3 homopentamers and alpha 1 beta 3 heteropentamers (Yip et al., 2013). It increases GABA binding and slows its rate of dissociation from the GABA receptors. It also has presynaptic and postsynaptic mechanisms where it has been shown to increase both spontaneous and K+ stimulated release from synaptosomes and it inhibited GABA uptake in a dose dependent and reversible manner (Orser et al., 1994, Rudolph and Antkowiak, 2004, Sanna et al., 1995, Whittington et al., 1996, Collins, 1988). .It also has a significant effect of potentiating the extrasynaptic tonic inhibitory currents (Bai et al., 2001). Some of these mechanisms of propofol action (for example, inhibition of GABA reuptake) are expected to, transiently, increase local

concentrations of GABA. Measurement of this change in local GABA concentration may provide a useful surrogate measure of propofol's local activity.

3.2.3 Propofol and MRS-GABA

Little evidence exists on the use of MRS in exploring GABA-ergic effects of propofol on the human brain. GABA concentration was shown to be increased following propofol induced unconsciousness (average plasma concentration of propofol 3 mcg/ ml) in most brain areas (Zhang et al., 2009). While the greatest increase occurred in the hippocampus (57.6%), motor cortex showed an increase of about 36%, while the thalamus showed a 22% increase. There was a concomitant decrease in glutamate and choline measures in all brain regions at anaesthetic doses. At sedative doses, however, there were no significant increases in GABA concentration. Ramani et al (Ramani et al., 2011) have also reported an increase in thalamic GABA concentration with propofol doses (2 mcg/ ml concentration) producing unconsciousness.

Following the hypothesis that the change in GABA concentration is indeed related to propofol's activity on reducing synaptic GABA reuptake, GABA concentration would be expected to increase linearly with the propofol dose. Zhang et al (Zhang et al., 2009) used small voxel sizes (1.5 cm^3), low magnet strength (1.5T) and smaller number of acquisitions and therefore it is possible that they were unable to detect a change in GABA concentration at sedative levels of propofol due to their technique (with low sensitivity) and small sample size (type 2 error). The sensitivity of MRS can be increased by increasing magnet strength, increasing voxel volume, acquisition time or a combination of these, as all of these tend to increase the signal to noise ratio (Puts and Edden, 2012). Using a more sensitive GABA detection methodology, changes in GABA concentration during propofol related sedation might be studied more robustly and reliably.

3.2.4 Link between visual cortical GABA concentration and visual gamma band oscillations

Muthukumaraswamy et al demonstrated that MRS measured- GABA levels in the visual cortex were directly proportional to the peak gamma frequency (measured using Magnetoencephalography (MEG)) localised to the visual cortex and was inversely related to the blood oxygen level dependent (BOLD) signal (on MRI) in response to a visual stimuli (Muthukumaraswamy et al., 2009). It was suggested that GABA levels represented inhibitory potential and a higher inhibitory activity (i.e. high GABA level) reduced the excitation/ inhibition balance resulting in the filtering of the dominant high frequency oscillations, as proposed by Brunel and Wang (Brunel and Wang, 2003). This interesting and novel finding forms the basis of this set of experiments. Further background to the modulatory role of propofol in task induced neural oscillatory activity is discussed in the introduction to Experiment 2, in this chapter.

3.3 Hypotheses

1. Propofol sedation increases the GABA concentration in key cortical and subcortical brain regions, measurable by MRS (tested in Experiment 1).

2. Propofol sedation results in a change in visual gamma band activity, measurable by MEG which is correlated to the changes in GABA concentration (tested in Experiment 2).

3. Propofol sedation results in a change in visual cortical BOLD response, measured using MRI and is correlated with changes in visual gamma band responses and GABA levels (tested in Experiment 3).

3.4 Experiment 1: Changes in occipital and thalamic GABA concentration with mild propofol sedation

3.4.1 Introduction

Both cortical and subcortical (especially thalamic) activities are modulated during sedation and anaesthesia (Alkire et al., 1997, Alkire et al., 1999). While it is still disputed whether cortical suppression precedes thalamic suppression or vice versa, propofol has clearly been shown to act on the cortical regions and thalamus (Fiset et al., 1999). Occipital cortex (as the cortical area) and thalamus were chosen to study GABA level changes as likely sites of propofol action.

Occipital lobe is a common choice of brain region in MRS – GABA studies. This possibly represents a technical limitation as measurements that use a surface receive-coil are most conveniently carried out in this location, especially due to good magnetic field homogeneity. Similarly those that use a volume coil often have best SNR in this location due to proximity to the coil elements, providing a stable measurement and a better chance of finding an effect (Puts and Edden, 2012). Occipital (visual) cortex has high GABA receptor density and is therefore likely to be sensitive to GABA modulation. Also, this choice was, specifically, based on previous work by Muthukumaraswamy et al (Muthukumaraswamy et al., 2009), to explore the relationship between MRS GABA concentration, gamma band response and BOLD-HRF during visual stimulation (Experiments 2 and 3).

Thalamus, as a brain region has been less extensively studied for MRS-GABA changes due to technical and signal-to-noise (SNR) limitations. Zhang et al (Zhang et al., 2009), however, were able to demonstrate a reduction in thalamic GABA levels with propofol anaesthesia.

3.4.2 Aims

The aims of Experiment 1 were to evaluate MRS measurable changes in GABA levels in the cortical (occipital) and subcortical (thalamus) regions and their alterations with mild propofol sedation.

3.4.3 Methods

3.4.3.1 Participants

Fifteen right-handed, healthy, male volunteers (mean age 26 years; range 20–41 years) participated in this study after giving informed consent. They were recruited following a detailed screening procedure. Medical screening was performed to ensure that all subjects were in good physical and mental health and not on any medications (American Society of Anesthesiologists grade 1). Any volunteer with complaints of regular heartburn or hiatus hernia, known or suspected allergies to propofol (or its constituents), regular smoker, or who snored frequently or excessively, or who had a potential difficultly in managing airways was excluded. Volunteers were instructed to follow standard pre-anaesthetic fasting guidelines. They avoided food for 6 hours and any fluids for 2 hours before the experiments. Following the experiments they were monitored until they recovered from the effects of sedation and were discharged with safety advice after they fulfilled all day-case anaesthesia discharge criteria (Verma et al., 2011). All participants underwent two MRI scans within the same session, the first before and the second during intravenous propofol administration while they remained at rest. No behavioural task was presented apart from asking volunteers to remain still with their eyes closed and to try not to fall asleep.

GABA concentration has been shown to vary according to the menstrual phase in women with GABA being less during the luteal phase than the follicular phase, in non smoking women and also postpartum women (Epperson et al., 2006, Epperson et al., 2002, Epperson et al., 2005). These factors would have been difficult to control and could potentially have confounded the findings. It was therefore decided to include only male participants in this study. All participants were compensated for their participation.

3.4.3.2 Monitoring, drug administration and sedation assessment

Propofol (Propofol-Lipuro 1%, Braun Ltd.) was administered using an Asena-PK infusion pump (Alaris Medical, CareFusion Ltd.) using a target-controlled infusion based on the Marsh pharmacokinetic model (Marsh et al., 1991). Infusion was started targeting an effect-site concentration of 0.6 mcg/ml. Once the target was reached, 2 min were given for further equilibration. Drug infusion was increased in 0.2 mcg/ml increments until the desired level of sedation was achieved. Sedation level was assessed by an anaesthetist, blinded to the level of propofol being administered, using the modified Observer's assessment of alertness/sedation (OAA/S) (Chernik et al., 1990). The sedation endpoint was an OAA/S level of 4 (slurred speech with lethargic response to verbal commands). The average targeted propofol plasma concentration, required to achieve the desired level of sedation was 1.2 +/- 0.2 mcg/ml. All subjects were monitored throughout the experiments by two qualified anaesthetists (Table 3-1). Heart rate, noninvasive blood pressure, oxygen saturation, and concentrations of expired (end-tidal) carbon dioxide were monitored using Veris MR Vital Signs monitoring system (MEDRAD Radiology).

Visual and auditory reaction times were also recorded as an additional, objective measure to differentiate between the *Awake* and *Sedated* states. Participants were instructed to press a button as soon as they saw a 'cross' appear on the screen (visual reaction time) and as soon as they heard a beep (auditory reaction time). The reaction times were tested at the beginning of the overall scanning session, at the end of the session and an additional set halfway through the scanning during the second (*Sedated* state) session.

3.4.3.3 MRS acquisition

All MR scanning was done at CUBRIC. The MR scanner was a GE Signal HDx 3 Tesla (General Electric Healthcare, Chalfont St. Giles, UK), and used an 8- element head coil for receive and the body coil for transmit. Prior to MRS acquisition, a $1mm^3$ isotropic-resolution T1-weighted anatomical scan (FSPGR) was acquired to determine voxel placement. GABA-edited MR spectra were acquired using the MEGA-PRESS sequence

(Edden and Barker, 2007, Mescher et al., 1998) in two (3 cm^3) volumes in the midline occipital regions and midline thalamus regions as shown in Figure 3-1 and Figure 3-2 respectively (positioning detailed below). The parameters used were; repetition time (TR) = 1.8 s, echo time (TE)= 68 ms, 332 transients of 4096 data points; receiver bandwidth = +/- 2KHz; a 16 ms editing pulse was placed alternately at 1.9 ppm and 7.5 ppm during *on* and *off* transients. Eight unsuppressed acquisitions were collected at the end of MEGA-PRESS scan to serve as internal concentration (and phase) reference and automatic first order shimming was done for all scans (Evans et al., 2013). The acquisition time was approximately 10 min for each scan.

Voxels of 3x3x3cm were positioned in occipital cortex (Figure 3-1) across the two hemispheres, with the lower edge aligned with the bottom of the occipital lobe, the anterior edge aligned with the parieto-occipital sulcus and the posterior edge as much within the cortex as possible. Axial, sagittal and coronal extent was carefully viewed to avoid inclusion of cerebrospinal fluids (CSF) within the lateral cerebral ventricle and the trough into the volume of interest (VOI), as much as possible.

The thalamus was identified from the 3D T1-weighted structural scan (FSPGR). The horizontal plane of the thalamus voxel was defined to be in line with the anterior cingulate- posterior cingulate plane, with the centre of the voxel set to the midline of the brain (left-right) and the apparent midpoint of the thalamus in the anterior-posterior and superior-inferior directions (Figure 3-2).

Since the participants were moved out of the MR scanner between *Awake* and *Sedated* scans (to administer and assess sedation) a structural (FSPGR) scan and the voxel placement were repeated during each session.

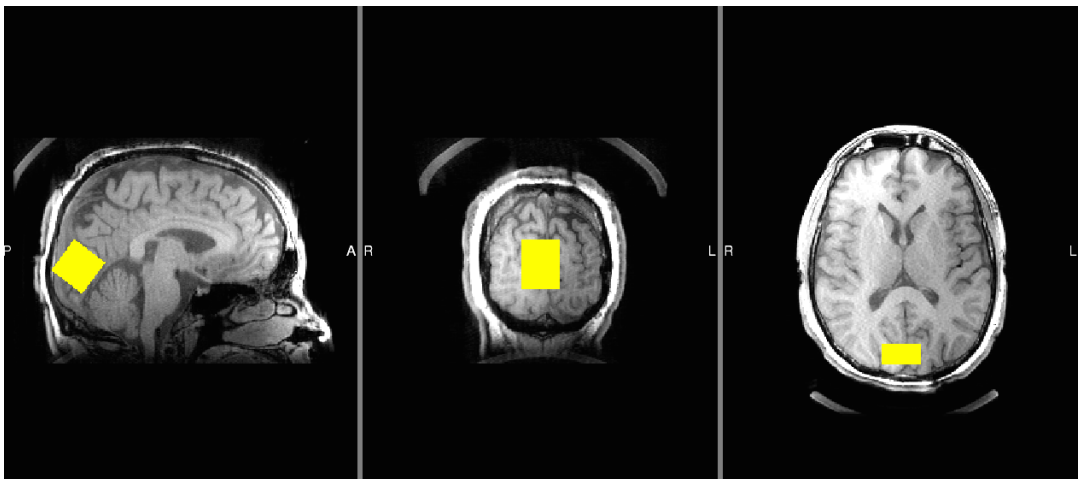

Figure 3-1: Anatomical localisation of the occipital voxel

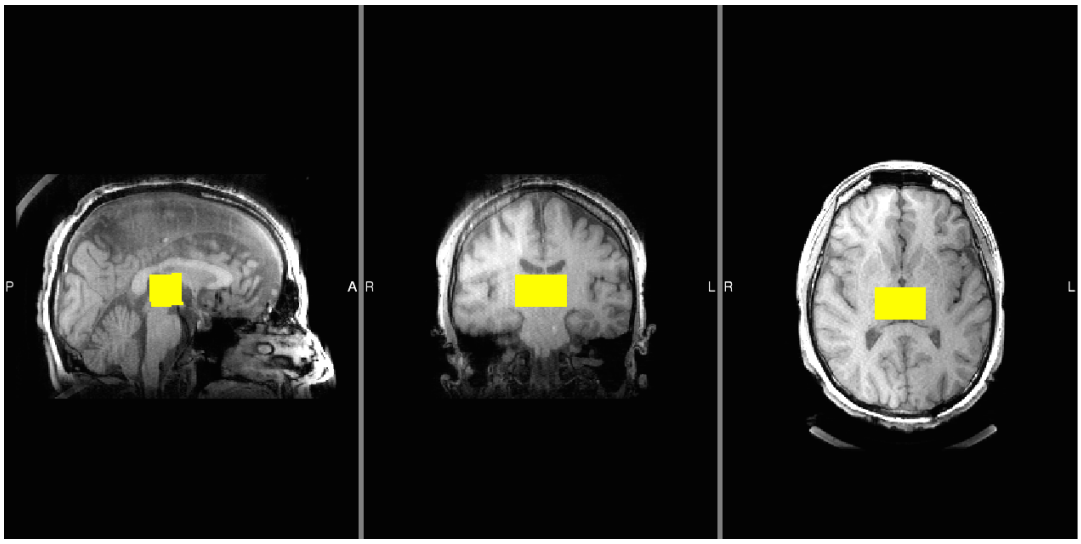

Figure 3-2: Anatomical localisation of the thalamus voxel

3.4.3.4 MRS data analysis

All analyses were performed using the GABA Analysis Toolkit (Gannet) (http://gabamrs.blogspot.co.uk/) in Matlab. Each dataset was zero-filled 8 times, line broadened with a 4Hz exponential function and automatically phased, with minor manual adjustments where necessary (mean manual phase correction = 3.0 degrees). The difference spectra were analysed by fitting a Gaussian function to the edited spectrum over the range 2.75 ppm to 3.55 ppm using a nonlinear least squares fit. The integral of the Gaussian peak was designated GABA+, as it represents both GABA and

co-edited macromolecular signal (Henry et al., 2001). GABA+ values were calculated using both creatine and water as internal concentration references. Those with reference to water are reported here. For the water reference, the water integral is determined using similar procedure with a Voigt lineshape. The ratio of GABA+ integral to water integral was then converted to institutional units using a constant correction factor to account for the effective visibility of water (Kreis et al., 1993), differences in T_1 and T_2 (Edden et al., 2012), and editing efficiency and is reported here.

The estimated fit error, is calculated from the standard deviation of the fit residuals (expressed as a percentage of peak height) of the GABA+ fit and water fit and is also reported.

3.4.3.4.1 Voxel segmentation and grey matter fraction

The high-resolution T_1-weighted images were segmented into grey matter (GM), white matter (WM), and cerebral spinal fluid (CSF) compartments using the segmentation tool in the commercial software package FSL 4.1 (FMRIB Software Library). Subsequently, the volumetric tissue contribution for each oblique voxel was determined and the relative contributions of GM and WM were calculated using in-house software. The GABA+ values from this grey matter component are reported here.

3.4.3.4.2 Statistics

Paired t-tests (in Microsoft Excel) were used to compare the changes in the haemodynamic and respiratory parameters, occipital GABA+ and thalamic GABA+ levels during '*Awake*' and '*Sedated*' states. Relationships between variables were explored further using correlation analyses.

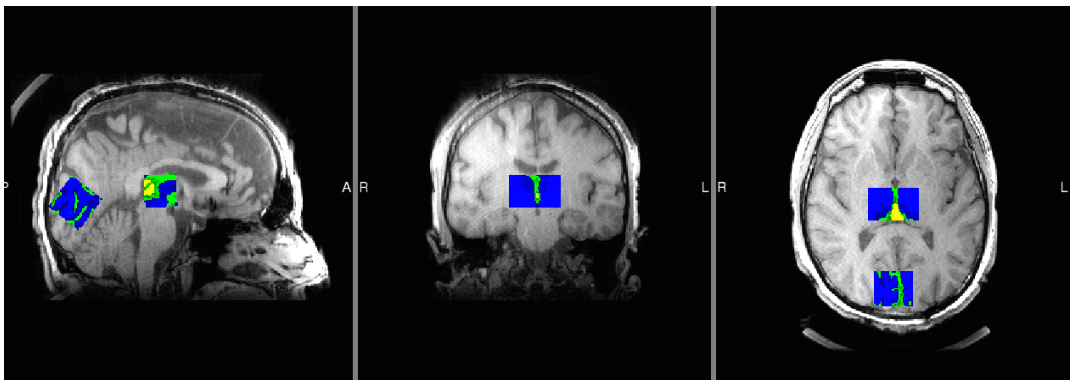

Figure 3-3: Segmented voxel masks (Blue- grey matter; green- white matter, yellow- CSF)

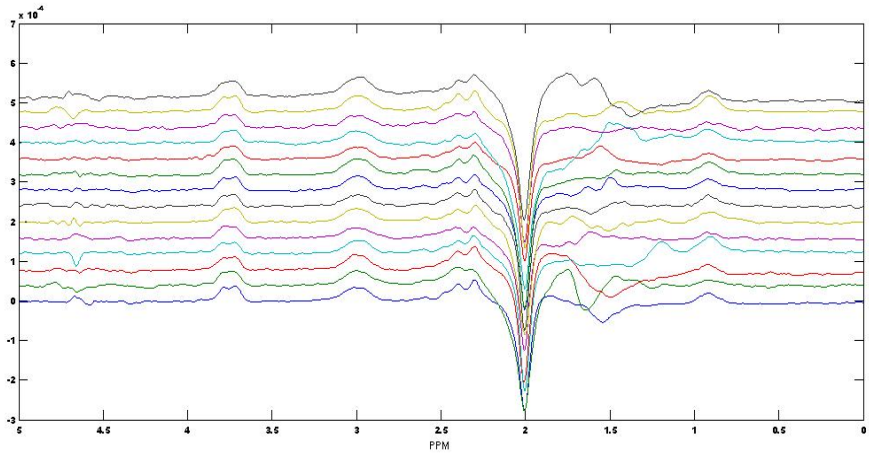

Figure 3-4 : Spectra from all participants from the occipital voxel (*Awake*)
(GABA signal appears as a Gaussian shaped peak at 3 ppm)

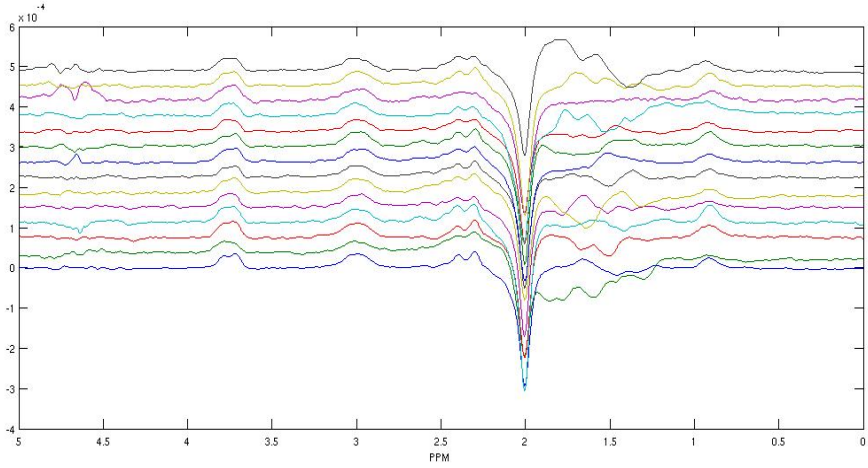

Figure 3-5: Spectra from all participants from the occipital voxel (*Sedated*)
(GABA peak at 3 ppm)

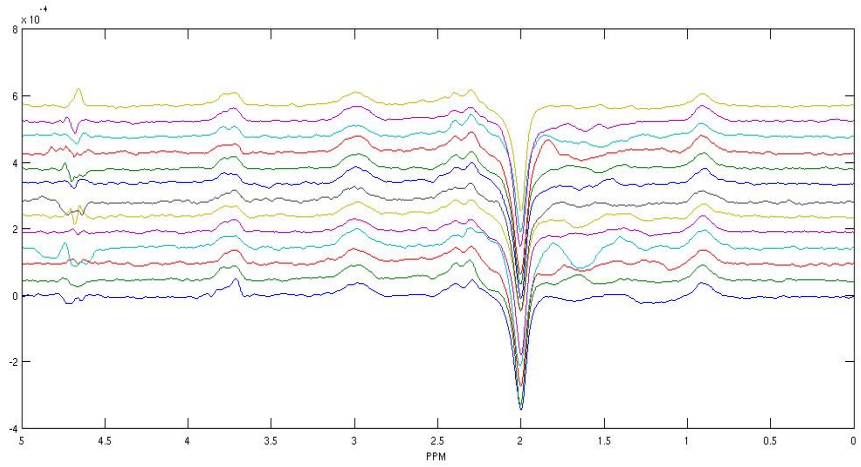

Figure 3-6: Spectra from all participants from the thalamic voxel (*Awake*)
(GABA peak at 3 ppm)

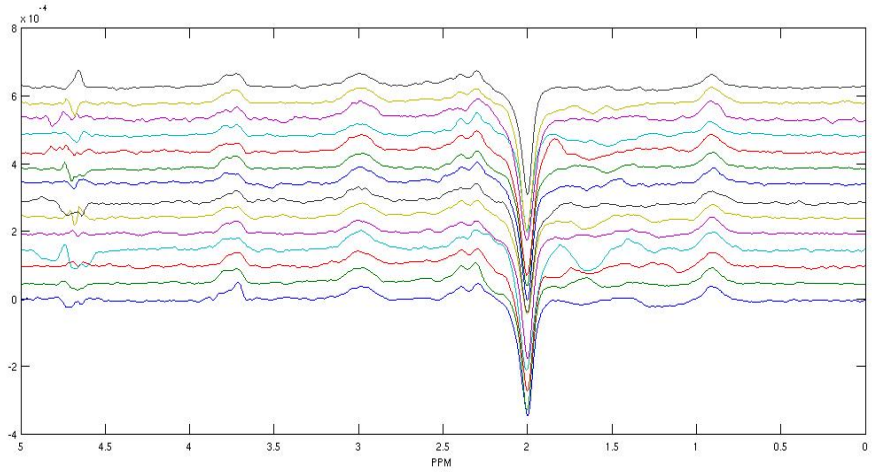

Figure 3-7 Spectra from all participants from the thalamic voxel (*Sedated*)
(GABA peak at 3 ppm)

3.4.4 Results

There were no significant effects of propofol sedation on haemodynamic or respiratory parameters (Table 3-1). There was a significant slowing of the reaction times (both visual and auditory) following sedation (Table 3-2). The mean (SD) propofol target concentration was 1.2 (0.2) mcg/ml.

Table 3-1: Physiological Data

Mean (SD) across subjects of physiological recordings measured before and during sedation. Paired t-test revealed no significant differences between *Awake* and *Sedated* states. HR, Heart rate; SBP, systolic blood pressure; DBP, diastolic blood pressure; MAP, mean arterial pressure; SpO_2, oxygen saturation.

	Awake	*Sedated*
HR (bpm)	56 (7)	55 (7)
SBP (mmHg)	123 (10)	119 (9)
DBP (mmHg)	71 (8)	70 (8)
MAP (mmHg) %	95 (8)	92 (7)
SpO_2 %	98 (1)	98 (1)

Table 3-2: Reaction times

[Paired t-test (2 tailed) revealed significant differences between *Awake* and *Sedated* states]. Both visual and auditory reaction times decreased (slowed) with sedation)

	Awake	*Sedated*	P value
Visual reaction time (seconds)	0.4192 (0.1009)	0.5563 (0.2973)	0.039
Auditory reaction time (seconds)	0.3306 (0.0779)	0.4271 (0.1845)	0.022

3.4.4.1 GABA values

One participant's data (both occipital and thalamic, during *Sedated* state) were lost during collection while another participant's thalamic data during sedation session were lost due to excessive head movement.

The occipital GABA+ did not show any change (paired t-test) during *Sedated* as compared to the *Awake* state [Mean (SD); *Awake* = 1.8314 (0.2926) to *Sedated* =1.8343 (0.2148)]

The thalamic GABA+ also did not show any change during *Sedated* as compared to the *Awake* state [Mean (SD); *Awake* = 2.1392 (0.1910) to *Sedated* =2.1301 (0.3882)]

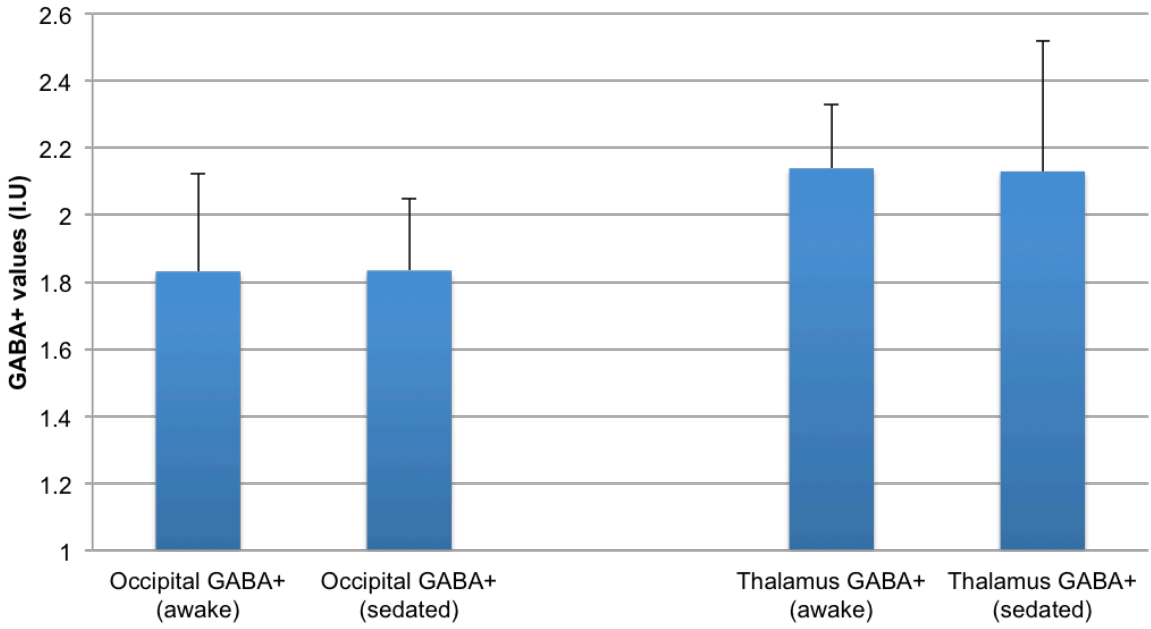

Figure 3-8 GABA+ values of the occipital and thalamic regions (Mean with SD)

3.4.4.2 Tissue fraction

There was no significant difference between the grey matter tissue fraction of the occipital or thalamus voxels between the *Awake* and *Sedated* states.

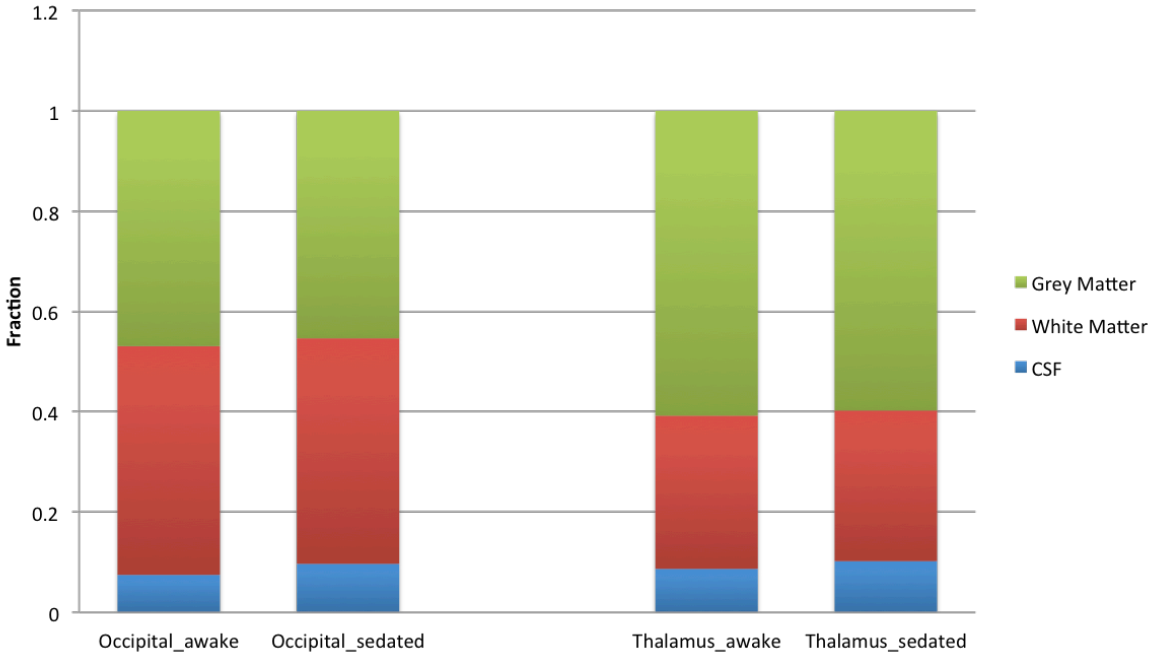

Figure 3-9: Relative tissue composition of the MRS voxels

3.4.4.3 Reliability

The between subjects coefficient of variance (CV: SD/ mean) for the occipital voxel-*Awake* was 15.9% while that for occipital voxel-*Sedated* (N=14) was 11.7%. CV for thalamus voxel-*Awake* was 8.9% while that for thalamus voxel-*Sedated* (N=13) was 18.2%.

3.4.4.4 GABA spectra fit error

The overall fit error (%; mean (SD)) for the occipital voxels was 6.5 (1.5)% and for the thalamic voxel was 8.7 (1.2)% and there was no statistical difference between the fit errors between *Awake* and *Sedated* sessions.

3.4.4.5 Dependence of reaction times on GABA+ levels

While there was a trend of dependence of the baseline visual reaction times on the *Awake* occipital GABA+ concentration (R= 0.488; P= 0.076) and the change in visual

reaction times on *Awake* thalamic GABA+ levels (R= -0.49; P=0.08); neither of them was statistically significant. No other correlations with the visual or auditory reaction times with *Awake* and *Sedated* GABA+ levels were suggestive of a potential relationship.

Since there were no changes in occipital or thalamic GABA+ levels following sedation, no further correlations with difference in regional GABA+ levels were attempted.

3.4.5 Discussion

This experiment, using a more sensitive MRS – GABA detection technique (c.f. (Zhang et al., 2009)) was unable to demonstrate a significant change in GABA+ concentration in either the cortical (occipital) or the subcortical (thalamus) brain regions during mild propofol sedation.

While it is difficult to prove a null result; taken together with other work (Zhang et al., 2009, Ramani et al., 2011) it appears that MRS detectable GABA concentration does not change with propofol-induced sedation but increases only when propofol induces anaesthesia/ unconsciousness. If this is indeed true, this is an interesting finding, suggesting that the GABA concentration does not change in a linear response to the propofol dose but rather changes as a measurable step once consciousness is lost (and therefore may be a potential biomarker of consciousness).

However, the alternative, i.e. the inability of the current experimental design to detect a change in GABA concentration or an actual unlikelihood of change in GABA concentration associated with mild propofol sedation also needs to be considered. The hypothesis of an increase in GABA concentration was generated based on the, very limited, literature available (Ramani et al., 2011, Zhang et al., 2009). There is some evidence of propofol potentially affecting GABA levels by increasing presynaptic and postsynaptic GABA, both in spontaneous and K+ stimulated release from synaptosomes and inhibiting GABA uptake in a dose dependent and reversible manner (Orser et al., 1994, Rudolph and Antkowiak, 2004, Sanna et al., 1995, Whittington et al., 1996, Collins, 1988). However, the main action, in humans, appears to be on the GABA

receptors by increasing the activity of GABA on those receptors. Indeed, if the main action, at clinically relevant doses, is prolongation of GABA activity without an actual change in concentration, such a negative result, as observed in this experiment would not be surprising.

However, the MRS findings of GABA levels and known actions of GABA-ergic drugs are not always straightforward. If the GABA-ergic actions of benzodiazepines are considered, they too facilitate GABA receptor's inhibitory function, albeit at different binding sites than propofol. Interestingly, acute administration of clonazepam (Goddard et al., 2004a) in healthy volunteers resulted in a decrease in GABA levels in the occipital cortex while zolpidem (an atypical benzodiazepine) (Licata et al., 2009) produced a reduction in thalamic GABA levels. These findings suggested additional activity of benzodiazepines on decreasing GABA production and availability. However, tiagabine, an antiepileptic drug known to inhibit GAT-1 enzyme and therefore reduce synaptic breakdown of GABA, did not show any change in GABA concentration on MRS. These, somewhat conflicting reports, highlight the limitations of the current understanding of the cellular level significance of the macroscopic MRS detectable measures of GABA. While the MRS detects overall macroscopic level GABA concentration, in a unit voxel, it is still unable to differentiate between the synaptic and cytoplasmic pools of GABA, especially if some of these pools are more tightly bound to other 'macromolecules' making them less likely to be detected within the spectrum (Stagg et al., 2011). This variation is further confounded by the tonic GABA activity at extracellular sites. So, although, studies successfully demonstrating a link between cortical MRS – identifiable GABA and physiologic, pharmacologic and psychological effects are reassuring, the current technique might be limited in identifying changes in GABA concentration where the overall GABA pool size remains relatively constant. This could have been a reason for failure to detect a change in GABA concentration in our experiment if there was only a 'reshuffling' of the GABA molecules at the synaptic and cytoplasmic level. It is also possible that at sedative doses of propofol there is a facilitation of the tonic GABA currents (Bai et al., 2001) without a significant change in MRS measurable GABA levels, which, preferentially, tends to measure the cytoplasmic pool (Maddock and Buonocore, 2012).

The sensitivity of a technique such as MRS would always be questioned, if it produces negative findings. In this study 256 acquisitions were collected in 27 ml voxels each, at 3T as compared to 128 acquisitions in 3.375 ml voxels at 1.5 T by Zhang et al (2009). This would result in a substantially increased signal –to-noise ratio, improving the sensitivity of detection. If the 22% increase in thalamic GABA at propofol concentrations of 3mcg/ ml (Zhang et al., 2009) was indeed a linear dose related increase; in this experiment (mean propofol concentration of propofol being 1.2 mcg/ ml) there should have been about a 10% increase from baseline in the GABA concentration. A *post-hoc* power calculation suggests that the current experimental design would have been able to detect a 7% change (CV 8.9% of thalamic GABA+) or more with a sample size of 13 subjects. The CV and spectra fit errors in this experiment are also within reasonably acceptable limits (Bogner et al., 2010, Evans et al., 2010). All these factors point towards the absence of a false negative result.

3.5 Experiment 2 ; Visual evoked and induced gamma oscillations: changes with mild propofol sedation

3.5.1 Background and rationale

3.5.1.1 Significance of gamma band oscillations and relationship with GABA

Gamma oscillations in the 30-80 Hz range have been implicated in a wide number of functions including, memory (Jensen et al., 2007), attention (Tallon-Baudry and Bertrand, 1999) and consciousness (Singer, 2001), and are thought to be disturbed in schizophrenia (Uhlhaas and Singer, 2010). Both neurophysiological data and modelling studies provide convergent evidence that the most plausible mechanism for the generation of temporally-organised gamma activity is in reciprocally connected neuronal networks containing an interconnected mixture of pyramidal cells, stellate cells and GABA-ergic inhibitory interneurons (Bartos et al., 2007, Traub et al., 1996). Consistent with this, gamma oscillations recorded from primary visual cortex slices in vitro have been shown to be modulated by drugs that target GABA-A receptors as well as drugs that target glutamatergic AMPA and NMDA receptors (Oke et al., 2010) and acetylcholine receptors (Rodriguez et al., 2004). Muthukumaraswamy et al (2009) have demonstrated a relationship between the resting GABA concentration in the human visual cortex and the peak gamma frequency originating in the visual cortex. Gamma oscillations have thalamo-cortical and cortico-cortical origins and the differences in evoked and induced visual gamma oscillations can therefore provide a probe to investigate the thalamic and cortical actions of anaesthetic drugs. (Ribary et al., 1991, Castelo-Branco et al., 1998)

3.5.1.2 Gamma band activity and propofol

Most of the information about propofol's in vivo modulation of gamma oscillatory activity is based on investigating spontaneous EEG activity after loss of consciousness. Loss of spatiotemporal organisation of gamma oscillations and information integration capacity has been shown at anaesthetic doses of propofol (Lee et al., 2009b). However,

Murphy et al (2011b) showed a persistently increased gamma activity with increased connectivity between the regions of the default-mode network (DMN) during propofol anaesthesia challenging the role of gamma oscillations in predicting consciousness. The relationship between spontaneous gamma activity, stimulus-induced activity and potential muscle artefacts in the spontaneous EEG also remains unclear (Whitham et al., 2008, Whitham et al., 2007). The effect of sedation on visual gamma oscillations has not been tested previously, nor has the modifiability of visual gamma, in vivo, been demonstrated.

3.5.1.3 Other oscillatory bands

Alpha band activity is closely related to the gamma band activity, especially in the occipital cortex (Osipova et al., 2008, Jensen et al., 2014). While alpha activity is associated with an inhibitory function, in response to a task, it is suppressed to allow high frequency oscillations to transmit information. This reduced alpha band power in response to stimuli (event related desynchronisation- ERD) has been well studied (Pfurtscheller and Lopes da Silva, 1999, Dujardin et al., 1993, Boiten et al., 1992). Alpha band ERD has also been shown proportional to the attention involved in the task, emphasising its role in cognitive processing (Suffczynski et al., 2001).

Thalamo-cortical neurons may be responsible for the generation and maintenance of the alpha band oscillations (Suffczynski et al., 2001). Modelling studies have suggested the action of propofol, on these neurones, at unconsciousness producing doses, causes a suppression of posterior alpha and emergence of frontal alpha rhythms (Vijayan et al., 2013b, Hindriks et al., 2011).

3.5.2 Introduction

In this experiment, knowing the GABA-ergic mechanisms involved in generation of gamma oscillations; the GABA-ergic activity of propofol sedation is explored by studying its actions on visual-task induced gamma oscillations. ERD of alpha oscillations are also studied to evaluate reciprocal change (in relation to gamma oscillations) and its importance in anaesthesia related unconsciousness, as a marker of

anaesthetic thalamo-cortical actions. These changes in gamma oscillations may also be able to help discriminate the temporal sequence of thalamo-cortical actions and site-specificity (if any) of propofol's actions.

3.5.3 Hypothesis

Propofol sedation results in an increase in gamma band activity, reduction in alpha band activity, measurable by MEG, which is related to the changes in GABA concentration.

3.5.4 Aims

In this experiment we investigated a) the modifiability of stimulus-induced gamma activity, during mild propofol sedation and b) its relationship with GABA concentration (from Experiment 1)

3.5.5 Methods

3.5.5.1 Participants

The same fifteen male volunteers (mean age 26 years; range 20-41 years) who participated in Experiment 1, also took part in this experiment. This MEG session (Experiment 2) was conducted preceding Experiment 1 as part of the overall experimental design. The time interval between the 2 experiments was at least 1 week to ensure total clearance of the drug and return of normal physiological functioning of the participant. All these participants had provided informed consent for this experiment, met the inclusion criteria and had no contra-indications to the drug (as described in Experiment 1- Methods 3.4.3) or MEG environment.

3.5.5.2 Monitoring, drug administration and sedation assessment

Drug administration, monitoring and sedation assessment were essentially similar to that in Experiment 1 with only slight differences due to the MEG environment.

Throughout the experiments, all participants were monitored in accordance with guidelines from the Association of Anaesthetists of Great Britain and by two medically qualified anaesthetists. HR, BP, SpO_2 and $EtCO_2$ were monitored using Veris MR Vital Signs monitoring system (MEDRAD Radiology) and recorded every 5 minutes. The monitoring system was located outside the magnetically shielded room. The connecting cables passed through waveguides into the magnetically shield room. This monitoring setup was tested and found to add no noise to the MEG signals. The monitoring anaesthetist observed the participants through a video monitor and maintained verbal contact, as required, through an intercom system.

Volunteers were instructed to follow standard pre-anaesthetic fasting guidelines. They avoided food for six hours and any fluids for two hours before the experiments. Of the two anaesthetists supervising the sessions, one was solely responsible for participant monitoring and was not actively involved in the experiment. Intravenous access (20 gauge) was obtained on the dorsum of the right hand and physiological monitoring (HR, BP, SpO_2 and $EtCO_2$) was instituted. Nasal cannulae were used for sampling of expired and inspired gases and the administration of oxygen, as required. Propofol (Propofol-Lipuro 1%, Braun Ltd., Germany) was administered using an Asena ®- PK infusion pump (Alaris Medical, UK) using a target controlled infusion based on the Marsh-pharmacokinetic model (Marsh et al., 1991). While participants lay supine in the magnetically shielded room, infusion was started targeting an effect-site concentration of 0.6 mcg/ml. Once the target was reached 2 minutes were allowed to ensure reliable equilibration. Drug infusion was then increased in 0.2 mcg/ ml increments until the desired level of sedation was achieved. Sedation level was assessed by an anaesthetist, blinded to the level of propofol being administered, using the modified Observer's assessment of alertness/ sedation (OAA/S)(Chernik et al., 1990). Sedation endpoint was an OAA/S level of 4 (slurred speech with lethargic response to verbal commands). The same anaesthetist assessed this endpoint on every occasion to ensure consistency of the depth of sedation achieved. Reaction times in response to auditory and visual stimuli were also recorded during the *Awake* and *Sedated* states both before and after completion of the stimulation paradigm.

3.5.5.3 Stimulation paradigm

Once steady state sedation was achieved, participants were presented with a visual stimulus consisting of a vertical, stationary, maximum contrast, three cycles per degree, square-wave grating presented on a mean luminance background. The stimulus was presented in the lower left visual field and subtended 4° both horizontally and vertically. A small red fixation square was located at the top right hand edge of the stimulus, which remained on for the entire stimulation protocol (Muthukumaraswamy, 2010, Swettenham et al., 2009). The stimulus was presented on a projection screen controlled by Presentation®. The duration of each stimulus was 1.5-2 s followed by 2 s of fixation only. Participants were instructed to fixate for the entire experiment and in order to maintain attention were instructed to press a response key at the termination of each stimulation period. Responses slower than 750 ms triggered a brief visual warning for participants. 100 stimuli were presented in a recording session and participants responded with their right hand. Each recording session took approximately 10 min and was carried out before sedation (*Awake* state) and then repeated during sedation (*Sedated* state). The *Awake* state recordings were always carried out before the *Sedated* session on the same day.

3.5.5.4 MEG acquisition and analysis

Whole head MEG recordings were made using a CTF 275-channel radial gradiometer system sampled at 1200 Hz (0–300 Hz bandpass). An additional 29 reference channels were recorded for noise cancellation purposes and the primary sensors were analysed as synthetic third-order gradiometers (Vrba and Robinson, 2001). Three of the 275 channels were turned off due to excessive sensor noise. At the onset of each stimulus presentation a TTL pulse was sent to the MEG system. Participants were fitted with three electromagnetic head coils (nasion and pre-auriculars), which were localised relative to the MEG system immediately before and after the recording session. Each participant had a 1mm isotropic T_1 weighted MRI scan available for source localisation analysis. To achieve MRI/MEG co-registration, the fiduciary markers were placed at fixed distances from anatomical landmarks identifiable in participants' anatomical MRIs

(tragus, eye centre). Fiduciary locations were verified afterwards using digital photographs.

Offline, data were first epoched from -1.5 to 1.5 s around stimulus onset and each trial visually inspected for data quality. Data with gross artefacts, such as head movements and muscle clenching were excluded from further analysis. Two source localisations were performed on each dataset using synthetic aperture magnetometry, one for induced responses (SAM), and one for evoked responses (SAMerf). Correspondingly, two global covariance matrices were calculated for each dataset, one for SAM (40 – 80 Hz) and one for SAMerf (0 – 100 Hz). Based on these covariance matrices, using the beamformer algorithm (Robinson and Vrba, 1999), two sets of beamformer weights were computed for the entire brain at 4mm isotropic voxel resolution. A multiple local-spheres (Huang et al., 1999) volume conductor model was derived by fitting spheres to the brain surface extracted by FSL's Brain Extraction Tool (Smith, 2002).

For gamma-band SAM imaging virtual sensors were constructed for each beamformer voxel and student *t* images of source power changes computed using a baseline period of -1.5 to 0 s and an active period of 0 to 1.5 s. Within these images, the voxel with the strongest power increase (in the contralateral occipital lobe) was located. To reveal the time–frequency response at this peak location, the virtual sensor was repeatedly band-passed filtered between 1 and 150 Hz at 0.5 Hz frequency step intervals using an 8 Hz bandpass, 3rd order Butterworth filter (Le Van Quyen et al., 2001, Muthukumaraswamy et al., 2010). The Hilbert transform was used to obtain the amplitude envelope and spectra were computed as a percentage change from the mean pre-stimulus amplitude (-1.5 to 0 s) for each frequency band. This relative-change baseline provides a control for between-recording and between-participant effects (for example, different head positions in the MEG), as well as correcting for the 1/f nature of unbaselined MEG source estimates (Gross et al., 2012). From these spectra, the time courses of alpha (8-15 Hz) and gamma (40–80 Hz) were extracted and submitted to non-parametric permutation tests using 5000 permutations (Maris and Oostenveld, 2007, Nichols and Holmes, 2002). Permuted *t* statistics were corrected for multiple comparisons using cluster-based techniques with an initial cluster forming threshold of $t = 2.3$. This approach allowed the examination of the temporal profile of oscillatory spectral

modulations as well as controlling for potential contamination of early-evoked response components into the alpha band. To examine pre-stimulus amplitudes the time-frequency spectra were recomputed with no baseline correction and the average amplitudes of alpha (8–15Hz), beta (15–40 Hz) and gamma (40–80 Hz) in the pre-stimulus period (-1.5 to 0 s) were calculated.

For SAMerf, the computed evoked response was passed through the 0-100 Hz beamformer weights and SAMerf images (Robinson, 2004) generated at 0.01 s intervals from 0.05 to 0.015s. The image (usually 0.08 to 0.09 s or 0.09 to 0.1 s) with the maximal response in visual cortex was identified and the maximal voxel selected as the peak location for virtual sensor analysis. For time-domain analysis, the evoked field was computed for this virtual sensor (-0.2 to 0 s baseline, 40 Hz lowpass filter) and the peak amplitude and latency of the M100 and M150 responses quantified. A spectral analysis of the evoked field using the same time-frequency techniques as above was also performed. The evoked frequency response in the 0-0.2 s period was obtained for each condition and analysed using same statistical methodology.

3.5.6 Results

There were no differences in the haemodynamic and ventilator parameters between the *Awake* and *Sedated* groups. The mean (SD) propofol target concentration was 1.07 (0.19) mcg/ml.

3.5.6.1 Key press- reaction times

Participants showed significantly (p = 0.001) slower key presses to stimulus offset during propofol sedation (Mean (SD): 355 (42) ms) compared to the *Awake* state (Mean (SD): 277 (33) ms). They also missed significantly more (p = .002) key presses during sedation (Mean (SD): 6.1 (4.7)) compared to the *Awake* state (Mean (SD): 1.3 (1.0)).

3.5.6.2 Correlation between resting GABA and gamma band

The relationship between resting occipital GABA+ values (from Experiment 1) and gamma band frequency (spike and sustained) were explored. The *Sedated* occipital GABA+ levels were inversely correlated with the peak spike gamma frequency during the *Sedated* state ($r = -0.55$; $P<0.05$) while there was a trend towards significance of the correlation between *Awake* occipital GABA+ and peak spike gamma frequency during the *Awake* state ($r= -0.51126$, $P = 0.061$) (Figure 3-10).

There was no relationship between peak 'sustained' gamma frequency with occipital or thalamic GABA+ levels (*Awake* or *Sedated*).

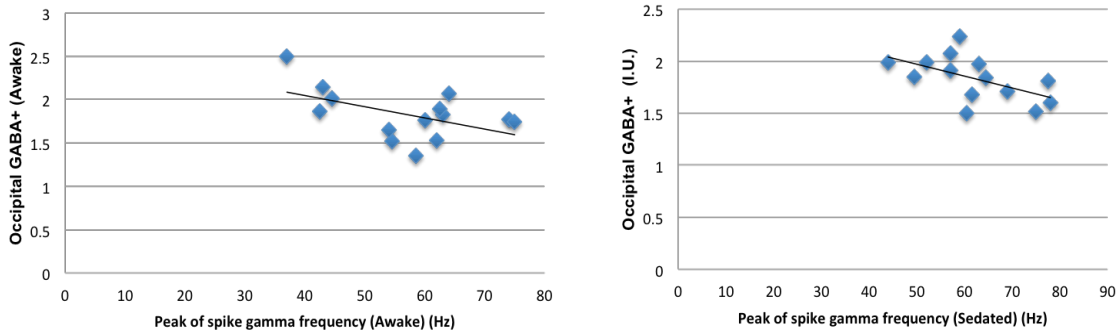

Figure 3-10: Scatter plots between peak spike gamma frequency and Occipital GABA+ levels during *Awake* and *Sedated* states

3.5.6.3 Evoked and Induced activity

Figure 3-11a shows grand-averaged source reconstructions for gamma band (40–80 Hz) responses to presentation of the grating stimulus during *Awake* and *Sedated* states respectively. As expected, both reconstructions locate the sources in the medial visual cortex in the quadrant opposite to the side of visual stimulation. The grand-averaged peak locations of the responses were located in adjacent source reconstruction voxels (4 mm voxel size). From the peak locations identified in individual source localisation images, source level activity was reconstructed and time-frequency spectra computed. The grand-average of these time-frequency spectra are displayed in Figure 3-11b. These show the typical morphology following this type of visual stimulus: there is an initial

transient broadband (50 to 100 ms) amplitude increase in the gamma frequency (40 Hz) range, followed by a longer lasting elevation of gamma frequency amplitude in a narrower frequency range. In the lower frequencies, there exists a sustained alpha amplitude decrease that commences around 200 ms, and a low frequency onset response, which is indicative of the evoked response. In Figure 3-11c the extracted gamma (40–80 Hz) and alpha (8–15 Hz) amplitude time-courses are plotted. During propofol sedation there was significantly elevated ($p = 0.01$, corrected) gamma band activity between 0.15 to 0.61 s corresponding to a 59.8% increase in amplitude. Similarly, during propofol sedation there was significantly ($p < 0.01$, corrected) more alpha amplitude decrease between 0.230 to 1.25 s corresponding to a 94.0% increase in stimulus- induced alpha suppression.

3.5.6.4 Evoked activity

In Figure 3-12a, the time-frequency response of the source-level evoked response is presented for both *Awake* and *Sedated* states and in Figure 3-12b the frequency spectra of these are presented for 0 to 0.2 s time window (i.e. where Figure 3-12a indicates that bulk of evoked activity occurred). Figure 3-12b indicates significantly less evoked power in the *Sedated* state. Figure 3-12c presents the time- averaged evoked responses and demonstrates significant reductions in both the amplitude of the M100 (46%) and M150 (94%) components during propofol sedation. We also noted significant ($t = 3.16$, $p = 0.007$) slowing of the M100 component. The M150 component was reduced to such a level during propofol sedation that we were unable to adequately quantify latency for a number of participants. Figure 3-13 demonstrates that there was no shift in peak gamma frequency, while peak alpha frequencies could not be reliably estimated across participants.

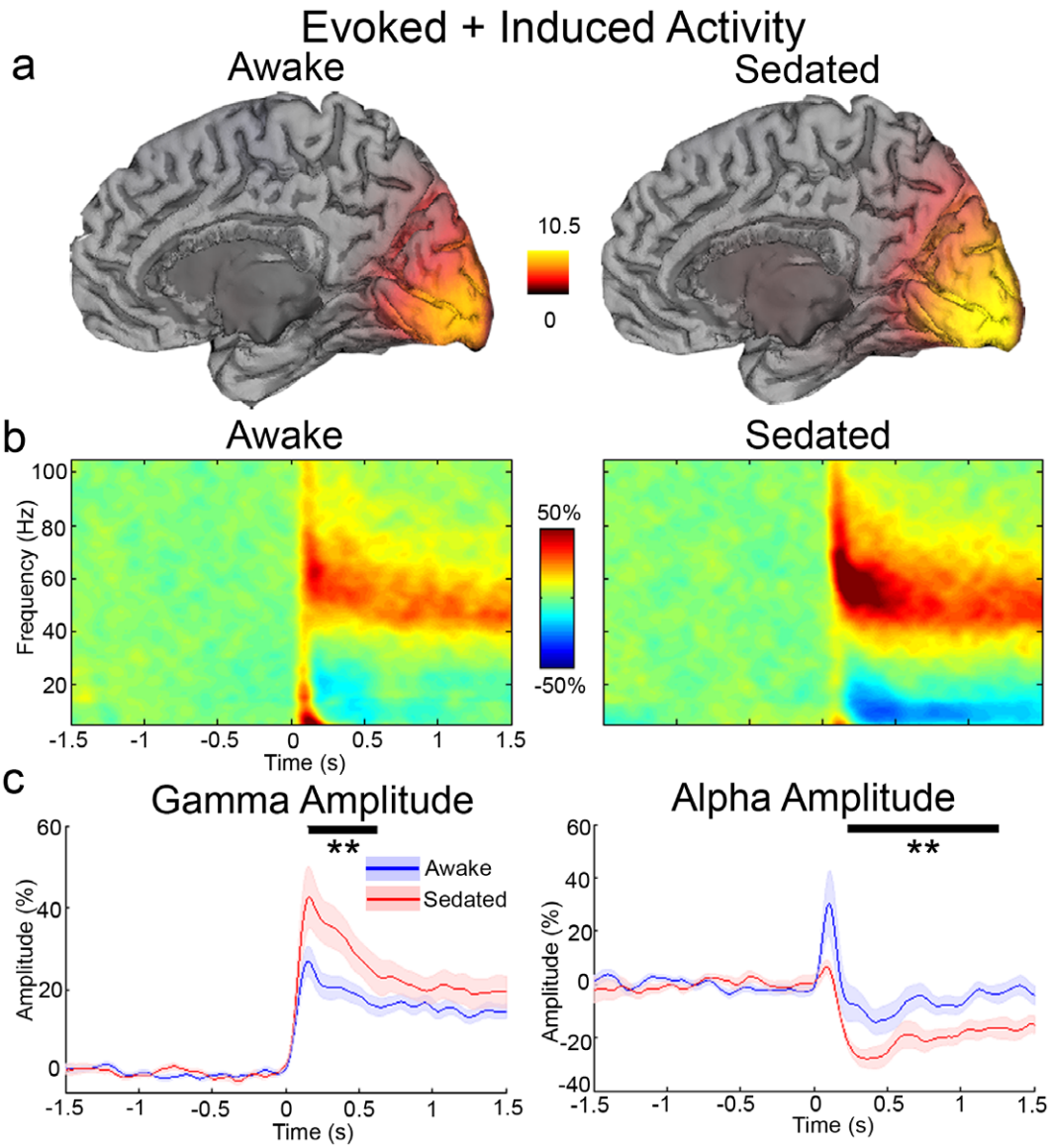

Figure 3-11: Summary of total (evoked plus induced) amplitude differences in the experiment.

a) Grand-averaged source localisation of gamma oscillations (40–80 Hz) for *Awake* and *Sedated* states respectively. Units are t statistics. The peak source location for the gamma band was at MNI (mm) co-ordinate [15 -95 7] for *Awake* and [17 -97 1] for *Sedated* (adjacent SAM voxels). b) Grand-averaged time-frequency spectrograms showing source-level oscillatory amplitude (evoked + induced) changes following visual stimulation. Spectrograms are displayed as percentage change from the pre-stimulus baseline. c) Envelopes of oscillatory amplitude for the gamma (40–80 Hz) and alpha (8–15 Hz) bands respectively. Time-periods with significant differences between the *Awake* and *Sedated* states are indicated with a black bar (*p <005, **p <0.01, ***p <0.001, shaded areas represent SEM).

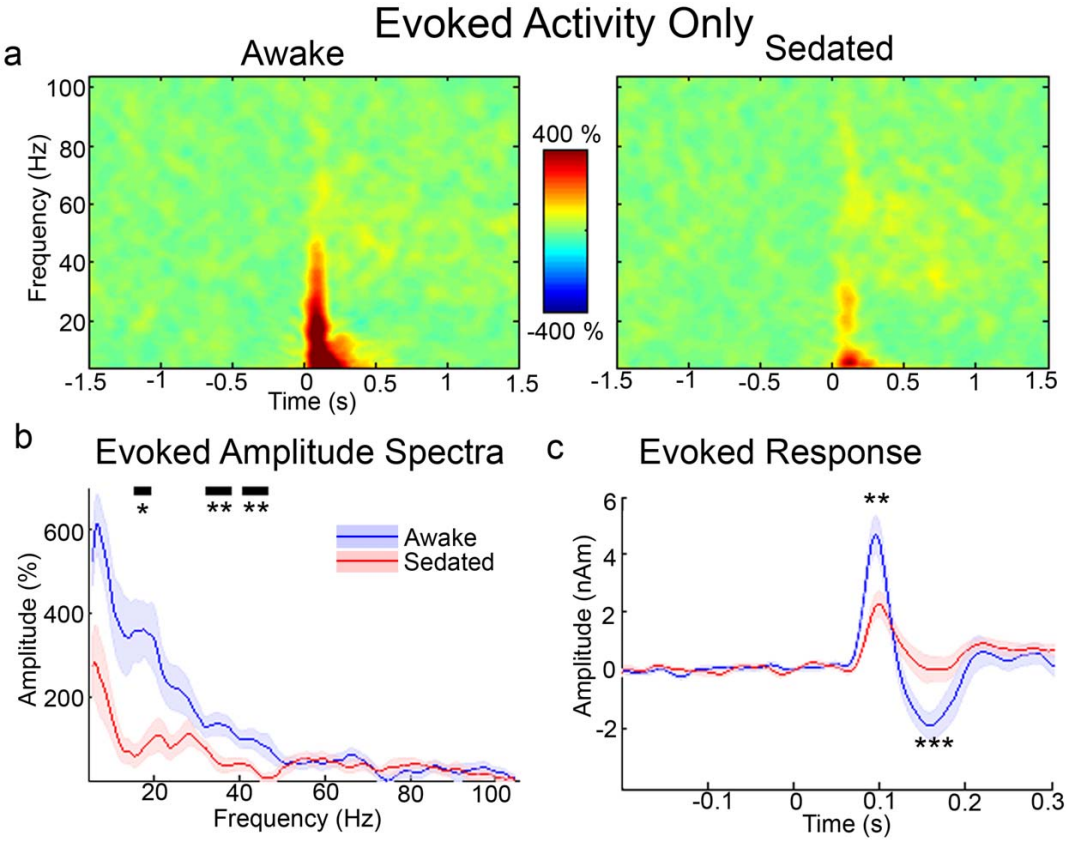

Figure 3-12: Summary of evoked amplitude differences in the experiment.
a) Grand-averaged time-frequency spectrograms showing source- level oscillatory amplitude changes for the evoked response. b) Evoked amplitude spectra for the 0–0.2 s time period. c) Source-level time-averaged evoked responses for *Awake* and *Sedated* states. Significant differences were seen in the amplitude of the M100 and M150 responses (*p <0.05, **p <0.01, ***p <0.001, shaded areas represent SEM).

3.5.6.5 Changes in baseline activity

Changes in the baseline power spectrum were examined for their possible role in driving the alpha and gamma activity changes. To do this, the absolute amplitudes of the virtual sensor amplitude spectra in the baseline period were computed. No changes were seen in baseline gamma or alpha amplitude but an increase in resting beta amplitude (p = 0.05) (Figure 3-13c-e) was seen.

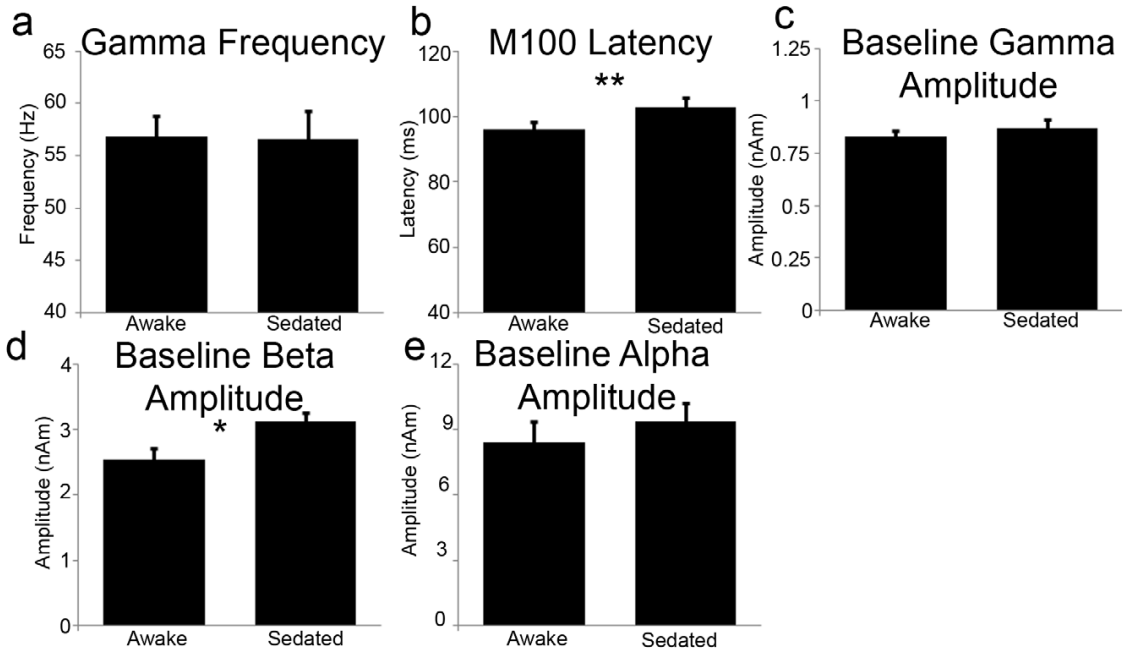

Figure 3-13: Bar charts showing peak (a) gamma frequency, (b) M100 Latency, and baseline, (c) gamma, (d) beta and (e) alpha amplitudes.
(*p,.05, **p,.01, ***p,.001, bars represent SEM).

3.5.6.6 Exploratory correlation analysis

Further exploratory correlational analyses were done between each of the parameters found to be significantly modulated by propofol (differences in, reaction time, gamma amplitude, alpha amplitude, M100 latency, M150 latency, and beta baseline amplitude). The only correlation that emerged was between M100 latency differences and alpha amplitude differences ($r = 0.57$, $p<0.003$).

3.5.7 Discussion

This experiment has two key findings

- During mild propofol sedation there is an increase in visually-induced gamma band responses, increased alpha amplitude suppression, and a concurrent reduction in the visually evoked response compared to the *Awake* state.
- A significant negative correlation between the peak spike gamma frequency with occipital GABA+ concentration during the *Sedated* state (and a trend towards significance between the occipital GABA+ and peak spike gamma frequency during the *Awake* state) but no relationship of GABA+ with the sustained gamma frequencies

The increase in visually-induced gamma band responses, increased alpha amplitude suppression, and a concurrent reduction in the visually evoked response during propofol sedation is a novel finding. This provides an in vivo demonstration in humans, that stimulus-induced gamma oscillations in visual cortex can be modified pharmacologically. The increase in induced gamma and alpha stimulus reactivity occurred concurrently with a reduction in the evoked response, that is, the evoked and induced responses showed a pharmacologically-induced dissociation. One particularly striking feature of this dissociation is that this occurred in the same MEG data. This suggests that these two MEG responses may reflect the activity of different generator populations in primary visual cortex or that these generators are differentially pharmacologically sensitive. Indeed, in primary visual cortex gamma band responses are primarily generated in layers II, III and IV (Xing et al., 2012), whereas early evoked responses are mostly generated in layer IV (Kraut et al., 1985). The present dissociation appears comparable to the dissociation between ERP and the gamma responses recorded during an adaptation (double pulse paradigm) task, using subdural recordings. While there was a reduction in the ERP the gamma-band response remained constant (Privman et al., 2011). An important aspect of this dissociation is that it argues against other, more prosaic, interpretations of the data. For example, it may be argued that the reduction in the M100 amplitude evoked response is due to reduced task vigilance, attention (Kahlbrock et al., 2012) as participants' state of consciousness changed. However, these effects would also decrease the amplitude of oscillatory responses

(Kahlbrock et al., 2012, Swettenham et al., 2009). The concurrent increase in oscillatory signals is therefore inconsistent with such arguments. Another possibility is that the decreased evoked responses observed here might be due to altered fixation control during propofol sedation. However, loss of fixation control would be expected to decrease the amplitude of both the evoked response (Di Russo et al., 2002) and the gamma-band response (Perry et al., 2013, Swettenham et al., 2009) whereas these components change in opposite directions in this data.

EEG studies of the resting spectra during mild propofol sedation demonstrate decreased posterior alpha and increased central beta power (Gugino et al., 2001). Increased sedation levels are marked by increased delta and theta power and frontal alpha with increased peak frequency (Feshchenko et al., 2004). Neural modelling of the changes in the resting EEG spectra during propofol anaesthesia suggest that these are caused by increased inhibition within local interneuron circuits (Ching et al., 2010b, Hindriks and van Putten, 2012). While the scalp EEG is a mixture of many generators, the advantage of the MEG beamformer approach used here is that it allows activity from a spatially confined region of interest to be analysed (Vrba and Robinson, 2001). The baseline spectra in the primary visual cortex virtual sensors demonstrated only a relatively minor increase in beta power and no changes in resting gamma or alpha activity. As such, the event-related amplitude changes demonstrated here do not appear to be related to baseline spectral changes with the drug. The other advantage of the well-validated MEG beamfomer (Brookes et al., 2005, Hoogenboom et al., 2006, Muthukumaraswamy et al., 2010) approach used here is that one can be very confident that the gamma-band activity here does not reflect the influence of muscle activity, be it from microsaccades (Fries et al., 2008, Yuval-Greenberg et al., 2008), or neck/head muscles (Whitham et al., 2008).

While a broadband frequency range was used to identify the virtual sensor the changes in evoked resposnes; the induced response virtual sensor was identified using frequency in the gamma band range. The induced resposnes were therefore ‘optimised’ for gamma band changes. This was done as these were the changes of primary focus in the experiment. This gamma band ‘optimised’ virtual electrode was then used to characterise alpha/ beta band activity. It is possible that using a specific frequency range

to identify peak activity voxel as virtual electrode for further evaluating the alpha band would have been localised to a different voxel and may have been more informative, for that frequency band.

Based on the results of Muthukumaraswamy et al (2009), it was hypothesized that peak sustained gamma frequency would increase with propofol but instead the gamma amplitude increased. There was no change in GABA+ also seen in the sequential MR experiment (Experiment 1). The questions about the sensitivity of MRS have been discussed previously (Section 3.4.5). Based on the same reasoning it is possible that the original relationship observed by Muthukumaraswamy et al (2009) could have been influenced by a number of anatomical, biochemical or even genetic variables. In particular, recently Schwarzkopf et al. (Schwarzkopf et al., 2012) found across individuals, that gamma frequency correlates with the surface area of V1 defined by retinotopic mapping with fMRI, suggesting anatomical factors may have driven our previous results. However, another recent study using structural estimates of V1 area did not find such a relationship (Perry et al., 2013). Since MEG and MR experiments were done on different days, albeit on the same participants, the stability of GABA measures, within subject, may also influence the results. MRS detectable GABA has been shown to be stable throughout a day and did not shown any diurnal variation (Evans et al., 2010). Similarly, GABA measurements have been shown to be stable over longer periods as long as 7 months (Near et al., 2014). It is therefore unlikely that any of the relationships between MEG measures and GABA may be accounted for by variations in GABA measurements over time.

Although gamma amplitude and frequency are not correlated across individuals (Muthukumaraswamy et al., 2010) across experimental manipulations they often change together and perhaps they should not be viewed as isolated parameters. For example, in both animals (Gray et al., 1990) and humans (Swettenham et al., 2009) it has been shown that moving stimuli lead to gamma oscillations of both higher frequency and amplitude. Similarly, when the contrast of stimuli changes, induced gamma oscillations (dynamically) change in both amplitude (Hall et al., 2005a) and frequency (Ray and Maunsell, 2010). In addition, stimuli of different spatial frequency elicit not only different gamma amplitudes (Adjamian et al., 2004) but also alter the spectral shape of

the gamma response (Hadjipapas et al., 2007). Finally, recent computational modelling studies suggest that individual variability in both areal integration across V1 columns and synaptic excitation/inhibition (Chambers et al., 2012, Pinotsis et al., 2013) can drive variability in induced visual gamma frequency, suggesting a possible dependence on multiple parameters.

Propofol's mechanism of action is primarily through GABA-ergic activity by enhancing its inhibitors actions, among other roles, as discussed in Section 3.2.3. Computational modelling (Wang and Buzsaki, 1996) suggests that gamma activity can be generated by networks of gap junction connected interneurones (Galarreta and Hestrin, 1999) providing large synchronised IPSPs to excitatory cells (Hasenstaub et al., 2005). Indeed, in barrel cortex, driving fast-spiking interneuron activity, but not pyramidal cell activity, selectively amplifies gamma activity (Cardin et al., 2009). Given all of these previous results, the amplified gamma response observed here seems most likely to be caused by the potentiation of GABA-A activity by propofol. Gamma amplitude changes could result from the enhancement of either phasic or tonic GABA currents, as propofol amplifies both (Feng and Macdonald, 2004, Houston et al., 2011, Jeong et al., 2011) and both can modify gamma activity (Cardin et al., 2009, Mann and Mody, 2011).

Another interesting observation in this experiment was the negative prediction of the resting GABA+ concentration on the peak spike gamma frequency during both the *Awake* and *Sedated* states. While the spike (transient) and sustained gamma activity appear to be generated from different sources, they are strongly related to each other in terms of frequency and amplitude (Gaetz et al., 2012). While Muthukumaraswamy et al (2009) demonstrated a positive correlation between resting GABA concentration and peak of sustained gamma frequency they did not find a similar relationship with the spike frequency. However, considering the expected relationship between spike and sustained gamma frequency an inverse relationship of spike frequency with GABA+ concentration, as discovered in this experiment, is counter-intuitive. This does, however, suggest a relationship with GABA-ergic activity in the visual cortex and the evoked response. Due to its temporal characteristics, the gamma spike is considered to represent the early visual pathway while the sustained gamma represents a cortico-cortical synchronous response to the visual stimulation (Castelo-Branco et al., 1998),

but the exact significance of these two components is unclear. Since the GABA+ concentration did not change with propofol sedation, in these experiments, it would only be speculative to predict how spike gamma frequency would have changed with it, if at all.

3.6 Experiment 3: Changes in visual BOLD signal with mild propofol sedation

3.6.1 Rationale and background

3.6.1.1 Vision and effect of sedation on vision

Vision (visual perception and awareness) is one of the key senses and an important component of 'consciousness'. The visual pathway is organised in a hierarchical fashion with the visual signals passing onward from the retina to the primary visual cortex and then onto the higher areas in the dorsal and ventral visual pathways. Different brain structures within this pathway have different functional sensitivities and specificities. Moving forward within this pathway, the receptive fields become larger and their specificity for stimuli changes, with higher areas becoming more responsive to complex stimuli (Baars and Gage, 2010).

Vision appears to be one of the most sensitive sensations and earliest to be affected, pharmacologically, within the spectrum of altered consciousness related to sedation and anaesthesia, as evident by the visual reaction times being slowed before the auditory reactivity (Kim et al., 2004). Sedation, depending upon the depth, is characterised by the loss of visual perception, awareness and recall. Clinically this manifests as blurred vision, sluggish eye movements, slowed visual reaction times and eventually, inability to keep the eyes open (motor effect). The neuroimaging correlates of these behavioural changes are measurable using neuroimaging techniques. Cortical activity of primary sensory cortices is preserved, albeit reduced, even during deeper stages of anaesthesia while activity of the higher association cortical areas is suppressed early (Heinke and Schwarzbauer, 2002). Alkire et al (Alkire et al., 1995b) demonstrated reduced cerebral metabolism in the occipital cortex (greater than global metabolic suppression) at anaesthetic doses of propofol. At sedative doses of propofol, Sun et al (Sun et al., 2008) found a 15% reduction in occipital lobe metabolism. Ramani et al (Ramani et al., 2011) used arterial spin labelling (ASL) to demonstrate a reduced visual cortical activation following sub-anaesthetic doses of sevoflurane. Other GABA-ergic drugs such as alcohol (Levin et al., 1998), pentobarbital (another anaesthetic drug) (Martin et al.,

2000) and zolpidem have also been shown to diminish the BOLD response to a visual stimulation. This suppression of vascular response seems to correlate with suppression in neuronal activity as measured by EEG/ MEG, as demonstrated by an increase in latency and reduced amplitude to visual (and other sensory stimuli) (Ghita et al., 2013, Iohom et al., 2001). Of the evoked responses, visual evoked potentials have been least studied for depth of anaesthesia/sedation as compared to other sensory modalities.

3.6.1.2 Functional relationship of BOLD signal, GABA concentration and gamma band oscillations

BOLD- functional MRI (fMRI) signal forms the basis of most fMRI studies, yet, the precise nature, source and mechanism of this haemodynamic response is still a topic of research. The BOLD signal correlates with the local field potential (weighted average of synchronised dendro-somatic components of the input signals) of a neuronal population (Kayser et al., 2004, Logothetis et al., 2001) with possibly some contributions from the spiking activity of such neuronal populations (Zaehle et al., 2009). This field potential may well be influenced by numerous chemical factors that further confound the vascular response to this neural activity. To provide convergent and coherent understanding of the human in-vivo neurophysiology through macroscopic neuroimaging tools, this relationship between neuronal activity and its resulting vascular response needs to be established.

It has been suggested that the inhibitory inter-neuronal population may have a major role to play in the generation of this BOLD response in relation to high frequency oscillations in the gamma band (Niessing et al., 2005). Tightly synchronised discharges in the gamma frequency range result in periodic inhibition of the pyramidal cells, which synchronises their discharge to the depolarising membrane potential oscillations. So, when gamma frequency oscillations are generated, the interneuronal discharges are phase locked to the oscillations and their activity increases with the oscillatory frequency. In humans, BOLD signal and gamma band response (GBR) have been shown to be similarly spatially located following a visual task suggesting similar sources/ origin (Muthukumaraswamy and Singh, 2008). A similar contrast tuning

relationship exists between BOLD and gamma band amplitude (Hall et al., 2005b) but this relationship is not universally linear or predictable (Muthukumaraswamy and Singh, 2009, Muthukumaraswamy and Singh, 2008). Muthukumaraswamy et al (2009) demonstrated an inverse relationship between the peak gamma sustained response frequency and the BOLD response, which appeared to be mediated by the resting GABA concentration.

GABA, as an inhibitory neurotransmitter (along with Glutamate, an excitatory neurotransmitter) plays a significant role in the BOLD responsiveness, although the exact mechanism is still unclear. GABA interneurons may act as local integrators of neurovascular coupling by transmuting incoming neuronal afferents into vascular responses (Cauli et al., 2004, Vaucher et al., 2000). In rats, increased GABA concentrations (by GABA transaminase inhibitor, vigabatrin) is associated with a reduced BOLD response (Chen et al., 2005). In humans, GABA concentration as measured by MRS, has been shown to be inversely correlated to the BOLD signal (Donahue et al., 2010, Hu et al., 2013).

Based on this information, BOLD- fMRI response to a visual task was studied and compared during the awake state and during propofol sedation.

3.6.2 Hypothesis

Propofol sedation results in a reduction in BOLD response, measured using fMRI and this reduced BOLD signal correlates with changes in visual gamma band responses and GABA concentration.

3.6.3 Aims

The aims of Experiment 3 were to evaluate changes in BOLD response to a visual task during mild propofol sedation and its relationship with the GABA concentration (*Awake* and *Sedated*; from Experiment1) and peak gamma band frequency and amplitude (*Awake* and *Sedated*; from Experiment 2).

3.6.4 Methods

This experiment was performed during the same session as Experiment 1 (Session MRI) and so the participant characteristics, drug administration and sedation assessment are the same as reported in Section 3.4.3.

3.6.4.1 Visual stimulus

A visual stimulation task comparable to the experiment 2 (4.4.3.2) was implemented. Visual stimuli consisting of vertical, stationary, maximum-contrast, 3 cycles per degree, square-wave gratings were presented on a mean luminance background. These stimuli were presented in the lower left visual field and subtended 4° both horizontally and vertically, with the upper right corner of the stimulus located 0.5° horizontally and vertically from a small red fixation point. Participants were instructed to maintain fixation for the entire experiment and, to maintain attention, were instructed to press a response key as fast as possible at the termination of each stimulation period. The duration of each stimulus was 1.5–2 s followed by 10 s of fixation cross only, with 42 events presented in the session. The stimuli were controlled by a Visage and presented via a Canon Xeed SX60 (1024 x 768 pixel resolution, 60 Hz refresh) projector.

3.6.5 MRI acquisition and analysis

Magnetic resonance (MR) data were acquired on a 3T GE scanner with an 8-channel receive-only head RF coil. For each participant a 3D FSPGR scan with 1 mm isotropic voxel resolution was obtained. fMRI data were acquired using a gradient echo EPI sequence taking 30 axial slices at 3 mm isotropic voxel resolution centred over the visual cortex using a 64 x 64 matrix size, TE of 35 ms, 90° flip angle, and TR of 2 s.

fMRI data processing was carried out using FEAT (Expert Analysis Tool) Version 5.98, part of FSL (FMRIB's Software Library, www.fmrib.ox.ac.uk/fsl). The following pre-statistics processing was applied; motion correction using MCFLIRT (Jenkinson et al., 2002), non-brain removal using BET (Smith, 2002), spatial smoothing using a Gaussian kernel of FWHM 5mm; grand-mean intensity normalisation of the entire 4D dataset by

a single multiplicative factor; highpass temporal filtering (Gaussian-weighted least-squares straight line fitting, with sigma=50.0s). The GLM was used to model a 2/10 s boxcar for each stimulus, after convolution with a standard haemodynamic response function (gamma function) to account for haemodynamic effects. Time-series statistical analysis was carried out using FILM with local autocorrelation correction (Woolrich et al., 2001). Z (Gaussianised T/F) statistic images were thresholded using clusters determined by Z>2.3 and a (corrected) cluster significance threshold of P=0.05 (Worsley, 2001). Registration to high resolution structural and standard space images was carried out using FLIRT (Jenkinson et al., 2002, Jenkinson and Smith, 2001). Registration from high resolution structural to standard space was then further refined using FNIRT nonlinear registration (Andersson et al., 2007a, Andersson et al., 2007b).

Higher level analysis was carried out using FLAME (FMRIB's Local Analysis of Mixed Effects) stage 1(Beckmann et al., 2003, Woolrich, 2008, Woolrich et al., 2004). Z (Gaussianised T/F) statistic images were thresholded using clusters determined by Z>2.3 and a (corrected) cluster significance threshold of P=0.05 (Worsley, 2001).

FSL was used to view the statistical parametric maps and the areas of BOLD signal differences were identified by using the Harvard-Oxford cortical and subcortical atlases. Group-level peak activation voxel was identified as the area of maximal activation with the two datasets combined (*Awake* and *Sedated*). This group –level peak location was transformed back to individual subject's space and the percentage BOLD signal change was calculated. This BOLD amplitude change was compared between the 2 groups used paired t-test in MS Excel.

3.6.6 Results

One subject's data had to be discarded due to excessive movement, resulting in a total of 14 paired datasets for analysis.

Head movement was compared between the two sessions using paired t-test. This revealed no significant difference between the two groups (p= 0.39, 2-tailed).

The location of the peak voxel, on combined dataset group level, was identified in the right occipital pole (MNI_152 voxel coordinates 29, 16, 39). The BOLD signal at this voxel reduced significantly from the *Awake* to the *Sedated* state [Mean (SD): 2.18 (1.13)% to 1.40 (1.23)%, $p < 0.005$, 2 tailed). However, further whole brain level, paired, voxelwise comparison at a statistical level of $P < 0.05$ (FWE corrected) was unable to detect any difference between the *Awake* and *Sedated* states.

The mean thresholded activation maps displayed on a template MNI brain are shown in Figure 3-14 *(Awake* state) and Figure 3-15 *(Sedated* state). As expected activation patterns are seen in the right occipital cortex in both groups. Activation is also seen in the left sensorimotor cortex representing the right finger motor movement (button press) as part of the task. Activation is also seen in the left occipital cortex in the *Sedated* group which probably represents a loss of attention/ focus as a result of sedation resulting in bilateral activation. However this activation also did not reach significance at the whole brain level.

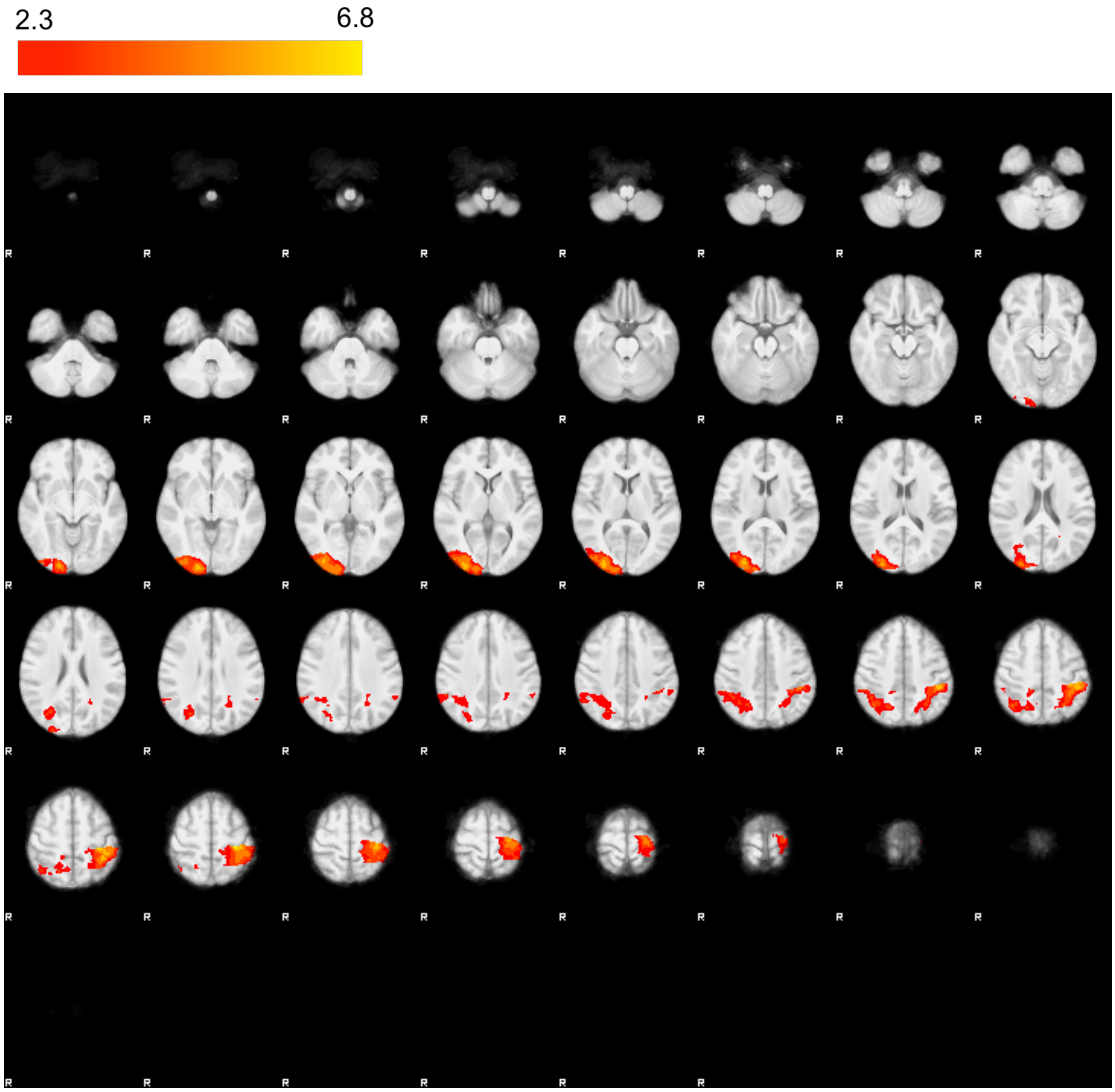

Figure 3-14: Group mean map showing activation of regions following a visual grating stimulus (*Awake* state)
Z (Gaussianised T/F) statistic images were thresholded using clusters determined by Z > 2.3 and a corrected (cluster) significance threshold of P= 0.05

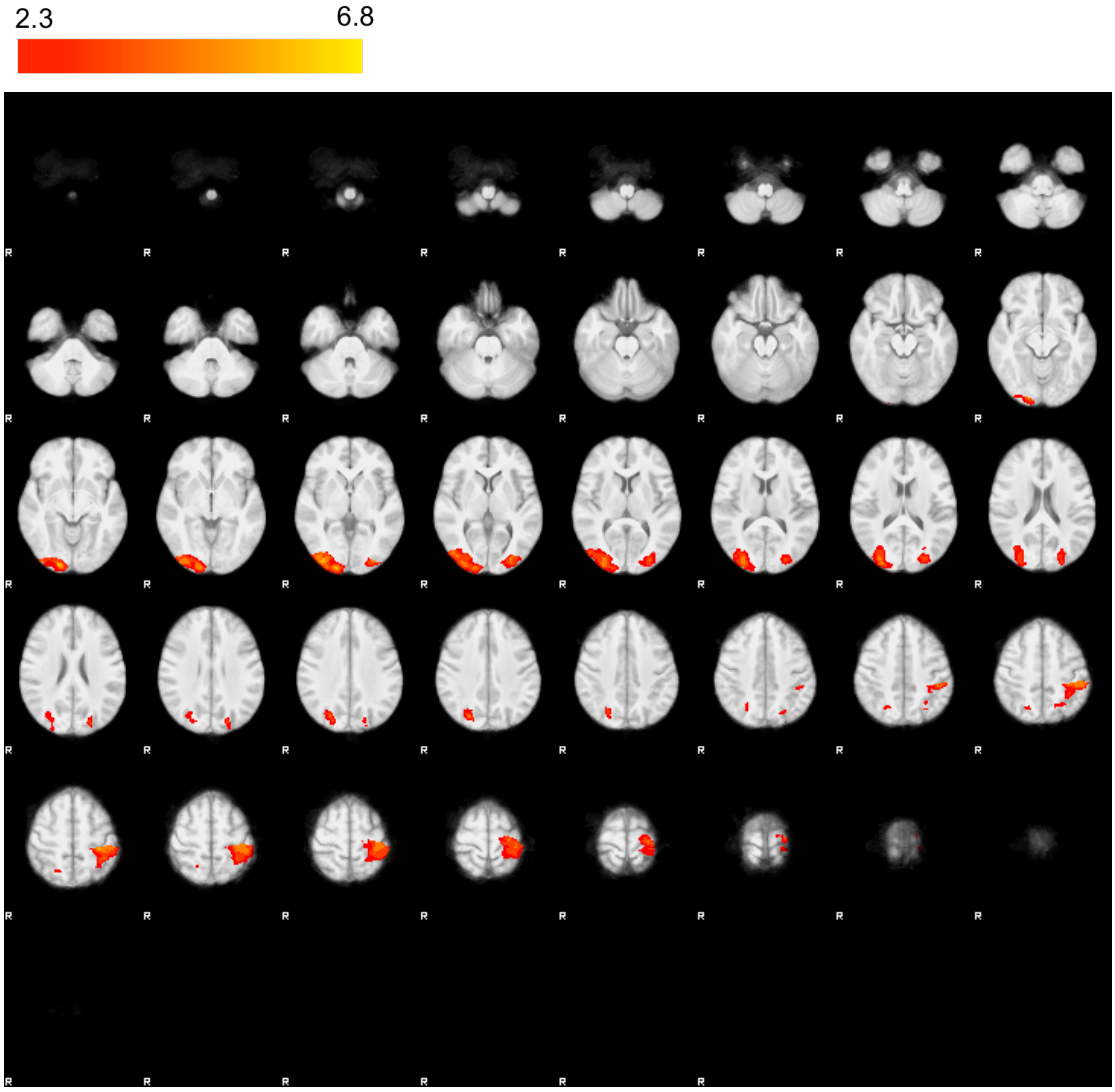

Figure 3-15: Group mean map showing activation of regions following a visual grating stimulus (*Sedated* state)

Z (Gaussianised T/F) statistic images were thresholded using clusters determined by Z > 2.3 and a corrected (cluster) significance threshold of P= 0.05

Table 3-3: Locations of peak activations, with their Z values (*Awake* and *Sedated* states)

On MNI atlas

Awake state			MNI_152 voxel coordinates		
		Z stat	x	y	z
	Occipital pole (R)	6.19	29	16	39
	Postcentral and precentral gyrus (L)	6.17	61	48	65
Sedated state					
		Z stat	x	y	z
	Occipital pole (R)	5.53	36	16	32
	Postcentral and precentral gyrus (L)	5.29	62	48	64
	Lateral occipital cortex (L)	4.85	60	19	38

There was a moderate, but not statistically significant, correlation across the group between the BOLD signal in the group (*Awake* + *Sedated*)-defined peak occipital voxel in the *Awake* state with the *Awake* occipital GABA+ concentration (experiment 1) (R= -0.374; p = 0.09) but not during the *Sedated* state GABA+ and BOLD signal change.

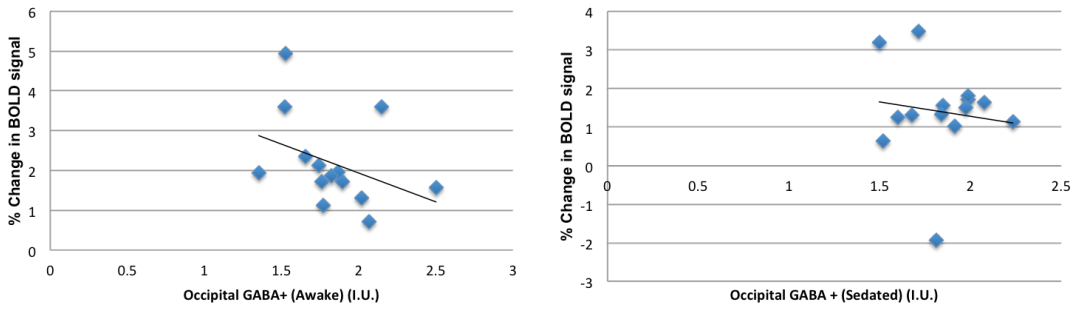

Figure 3-16: Scatter plots between and BOLD signal change (%) and Occipital GABA+ levels during *Awake* and *Sedated* states

There was no evidence of a relationship between the BOLD signal change and the gamma band parameters including spike and sustained frequency and power.

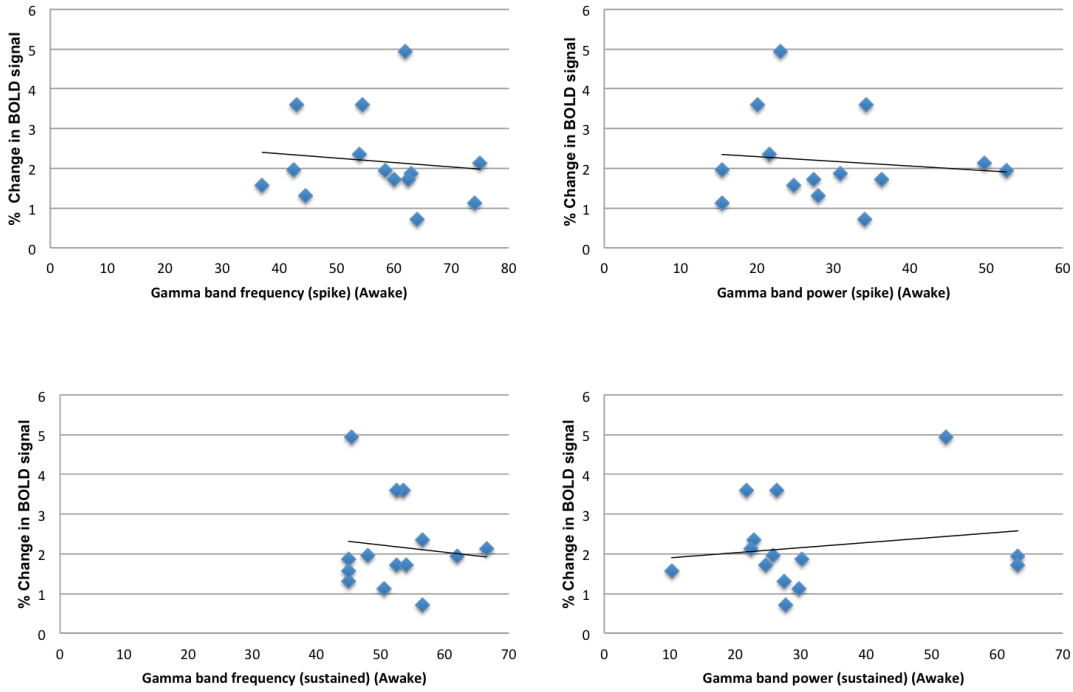

Figure 3-17: Scatter plots between and BOLD signal change (%) and visual gamma band characteristics (spike and sustained power and frequency) during *Awake* and *Sedated* states

3.6.7 Discussion

There was a significant reduction in the percentage change in the BOLD signal within the peak voxel in the occipital cortex following mild propofol sedation. This was an expected finding based on previously published experiments and other findings in this series of experiment including a reduction in visual reaction times and reduced visual evoked potentials.

A subsequent whole brain analysis was performed; however, this difference within the peak voxel, did not survive statistical correction for multiple comparisons at the whole brain level. The difference between the 'peak voxel' comparison and the 'whole brain' analysis could be explained by a number of factors. Statistical inference in neuroimaging studies can vary depending on the question asked and the willingness to accept type 1 or type 2 errors. Due to the high number of voxels involved and the lack of true independence of each voxel from the other family –wise error correction techniques have been applied for fMRI studies. The choice of region of interest (ROI) can influence the outcome, as might have been the case in this analysis (a single voxel instead of the whole brain). Arguably, a further, selective ROI analysis, limited to the primary visual cortex may have provided further insight into strength of change, but was not attempted to limit further 'multiple testing'.

The experimental design in the series of visual experiments was similar to that of Muthukumaraswamy et al (2009). The visual grating stimulus was chosen as it reliably produces visual gamma band oscillations and also produces a reasonable change in task induced BOLD signal (and was therefore required to relate the BOLD data with MEG data). Arguably, a 'stationary grating' visual pattern is not the strongest stimuli to study visual cortical activation (Fox and Raichle, 1984, Iidaka et al., 2004, Thomas and Menon, 1998) and most published visual experiments, to study drug-induced changes, have employed a flashing/reversing checkerboard (Licata et al., 2011, Martin et al., 2000). This choice of a 'weak' activator could have resulted in a 'floor' effect. While such a 'floor effect' if present, did not manifest itself on a single voxel level analysis, but could have been compounded by multiple testing at the whole brain level resulting in loss of significance. Another possible reason, for not finding a significant change at

the whole brain level, could be that following sedation, the resulting longer reaction times may have altered the haemodynamic response function resulting in a larger amplitude as in response to a stronger, compensatory effort in task performance (Yarkoni et al., 2009).

3.6.7.1 BOLD signal and GBR

There was no relationship identified between the BOLD signal changes and the gamma band parameters in the *Awake* state. Further comparison with the BOLD signal change during *Sedated* state and gamma band parameters was therefore not performed. The relationship between gamma band and BOLD signal is not straightforward. The GBR and BOLD have been shown to have similar spatial source location for the visual stimuli (Muthukumaraswamy and Singh, 2008) but seem to respond differently to stimulus characteristics including spatial frequency, temporal frequency, luminance and colour contrasts (Muthukumaraswamy and Singh, 2009, Swettenham et al., 2009). The relationship is further complicated by the various parameters of the GBR, (induced or evoked; frequency or amplitude) which may or may not predict BOLD signal changes (Singh, 2012). Yet, failure to replicate the findings of Muthukumrasawamy et al (2009), in the *Awake* state, with a similar experimental paradigm, was surprising.

With a reduced visual evoked field activity (as found in experiment 2, section 3.5.6.4) a reduced BOLD signal would have been predicted. This was found at the peak voxel level in the visual cortex. This relationship may be explained by a similar observation where it was shown that the haemodynamic response to an electrophysiological activity was limited to a smaller area than the larger cluster of change observed (Arthurs and Boniface, 2003).

Alternatively, the lack of BOLD change at the whole-brain level may be explained by the metabolic changes associated with the GBR response. Since the GBR following sedation resulted in dissociation between the evoked and induced responses, i.e. a reduction in evoked activity with an increase in induced gamma amplitude (suggesting local synchronicity), it is possible that an increase local neuronal activity countered this reduction (in evoked activity) and resulted in no change or a limited net change in local

neuronal metabolic activity. The proposed mechanisms linking the LFP changes in neuronal assemblies in the generation of BOLD signal (Niessing et al., 2005, Kayser et al., 2004, Logothetis et al., 2001) suggests that maintenance of this local excitation/ inhibition balance at the visual cortical level may indeed be the cause of a maintained BOLD signal, following sedation.

The peak voxels estimated by SAM for GBR analyses were different to the peak voxel identified for BOLD analysis. They were separated by about 20mm. The choice of peak voxel for BOLD analysis was chosen at the group level by averaging data between *Awake* and *Sedated* states. This was different for the GBR, which was estimated at subject level. This difference in analytic processing may have accounted for some of the results.

3.6.7.2 BOLD signal and GABA concentration

There was a moderately strong inverse correlation between the *Awake* occipital GABA+ levels and the BOLD signal change. Although not as strong as that reported by Muthukumaraswamy et al (2009), yet, reassuring. Some of the possible reasons for the absence of a stronger relation could be related to sensitivity of GABA measurements as discussed in section 3.4.5. The relationship between bulk MRS GABA measures and BOLD signal is also unlikely to be simply linear. As Donahue et al (Donahue et al., 2010) have demonstrated, the CBF weighted ASL tends to be positively correlated to GABA levels unlike the BOLD signal which is strongly inversely correlated. This suggests a complex interplay of excitation/ inhibition balance manifesting as a BOLD signal change depending on the basal GABA-ergic inhibitory tone. Since propofol induced mild sedation did not result in any measurable change in occipital GABA concentration it would be speculative to predict its precise role in the reduced/ maintained BOLD signal during the *Sedated* state. The correlation between the GABA+ concentration and BOLD signal in the *Awake* state was lost during the *Sedated* state (Figure 3-16) further suggesting the role of other, unidentified mediators between the two parameters.

3.7 Limitations

This ambitious experimental design attempted to bring together the functionality of diverse but inter-related neuroimaging techniques to relate the complex neurovascular and metabolic interplay induced by pharmacological sedation. While all neuroimaging techniques have their own limitations, which may have been compounded by relating together the results from different modalities, this series of experiments may be improved upon further, by some of the modifications, as below

- Increasing sample size: The absence of GABA+ concentration change, as discussed previously, is unlikely to be due to a sample size effect. However, with a larger sample size the expected variance of GABA measurements would have been lower and so the confidence in the results could have been higher.

- Eye tracking in MEG experiment: As discussed in section 3.5.7, loss of attention could be a confound in the visual task experiment. Although it is unlikely to be a source of the results found, eye tracking during such experiments would provide more robust and reliable data of eye fixation.

- Order effect: All *Sedated* sessions followed *Awake* sessions and so an 'order effect' cannot be ruled out. Since recovery from sedation / anaesthesia may have significant neurophysiological differences from a pre-sedation awake state, there was no valid option of avoiding this. It would, however, have been interesting and useful to study the recovery characteristics of the measures collected in these experiments. While this would have made these sessions prohibitively lengthy, simpler or more focussed questions may be better posed in experimental designs including the entire range of sedation and recovery.

- Different levels of sedation: While this series of experiments focussed on mild sedation, some of the positive findings and negative findings (for e.g. GABA changes) could have been further explored if different levels of sedation were studied, providing a dose-response relationship.

3.8 Conclusions

This series of experiments has attempted to study the complex relationship between neurochemistry (GABA concentration), electrophysiology (GBR) haemodynamic activity (BOLD signal) and their modulation with mild propofol sedation. This has produced the following key findings.

- MRS detectable GABA+ concentration does not change in the cortical (occipital) or subcortical (thalamic) regions during mild propofol sedation.
- During mild propofol sedation there is an increase in visually-induced gamma band responses, increased alpha amplitude suppression, and a concurrent reduction in the visually evoked response compared to the *Awake* state.
- A significant negative correlation between the peak spike gamma frequency with occipital GABA+ concentration during the *Sedated* state (and a trend towards significance between the occipital GABA+ and peak spike gamma frequency during the *Awake* state) but no relationship was found between the GABA + concentration and the sustained gamma band frequencies.
- BOLD signal is reduced at the peak voxel, in visual cortex on visual stimulation, during propofol sedation.
- While there was a trend towards an inverse relationship between GABA+ concentration and BOLD signal change (during visual activation), no clear cut relationship existed during sedation, nor was there a well-defined relationship between the BOLD resposne and GBR.

Chapter 4 : Cortical responses to multisensory stimulation and effect of propofol sedation

4.1 Abstract

Mild sedation, as the first step towards anaesthetic-induced unconsciousness, involves a gradual suppression of sensory perception and cognition. Mild sedation is characterised by a slurred speech and reduced visual and auditory responsiveness.

In a series of experiments, using multimodal neuroimaging techniques, the effect of mild propofol sedation was explored on electrophysiological responses to multisensory stimulation, using MEG, and haemodynamic changes in cortical reactivity, using BOLD-fMRI.

The results revealed a reduction in visual evoked fields but no change in auditory or somatosensory evoked fields. BOLD-fMRI revealed a reduction in cortical responses in the sensorimotor cortex but not in auditory or visual cortices, in response to respective stimuli.

4.2 Background and rationale

Sedation is characterized by increasing loss of visual, auditory and sensory perception, memory and speech. As sedation deepens, anaesthetic unconsciousness encompasses functional, reversible loss of all sensory and most motor modalities. The neurophysiological correlates of sedation can therefore be studied by studying the changes in some of these sensory modalities during pharmacological sedation.

Traditionally, EEG, due to its millisecond temporal sensitivity, has been used to study cortical responses to anaesthetic effects. MEG provides a similar window into brain function while avoiding some of the limitations of EEG; such as lower spatial resolution and possible interference from the skull (see Section 2.8.2). Also, due to its spatial accuracy, BOLD-fMRI is increasingly being used to investigate neurophysiologic correlates of altered consciousness and anaesthetic effects. Most studies have focused on unconsciousness or deeper levels of sedation. Very few studies have investigated the earliest stages of pharmacological sedation and no previous work has used MEG to interrogate the cortical responses to sensory stimulation during sedation.

This experiment was therefore undertaken to use the complementary information provided by BOLD-fMRI and MEG to investigate changes in primary cortical activity, involved in basic sensory processing and the effect of mild propofol sedation. This study was conducted as a two-part, sequential fMRI/ MEG study (as described previously in Section 2.4).

4.3 Hypotheses

Mild propofol sedation reduces the neural activity of the primary sensory cortices (visual, auditory and sensorimotor). This will be evident as reduced BOLD activations on fMRI in those regions and reduced evoked fields on MEG in the respective sensory domains.

4.4 Experiment 1

4.4.1 Introduction

Evoked potentials are changes in electrical potential, recorded in the nervous system, in vivo, in response to a stimulus. The change in these potentials during the time course of a stimulus response represent the neural processing occurring at different stages of the neuronal pathway and represents the functional integrity of these anatomical pathways. More specifically, 'event related potentials' (ERP) (or their MEG equivalent- 'event related fields' (ERF)) are evoked potentials to a specific stimulus. When ERPs/ERFs are used for experimental or clinical reasons, responses to visual, auditory or somatosensory stimuli are commonly measured.

4.4.1.1 Visual evoked potentials/ fields

Recorded visual evoked potentials (VEPs), in response to visual stimulation, consist of positive-negative deflections designated by capital letters followed by a number indicating the average latency. The two most frequent waves are designated N70 (negative wave occurring at about 70 msec) and P100 (positive wave occurring at around 100 msec). Often, a positive wave around 50 msec, named P50, precedes N70. MEG recordings demonstrate a similar pattern (Teyler et al., 1975). The source modelling of N70/ P100 suggests that the N70 originates from the primary visual cortex while the P100 originates from the extrastriate visual areas (Slotnick et al., 1999, Di Russo et al., 2002).

Visual evoked potentials are the least well studied evoked potentials in the anaesthetic literature. Most anaesthetic agents including halothane, isoflurane and nitrous oxide have been shown to alter VEPs by increasing their latencies and reducing amplitudes (Sebel et al., 1984, Sebel et al., 1986), however diazepam and fentanyl on their own do not (Loughnan et al., 1987). This suggests both drug specific and dose dependent effects on VEPs.

4.4.1.2 Auditory evoked potentials/ fields

Figure 4-1 represents the anatomical origins of the different components of the auditory evoked responses (AER). Those of importance to study cortical responses are the middle- latency and late / delayed latency evoked responses.

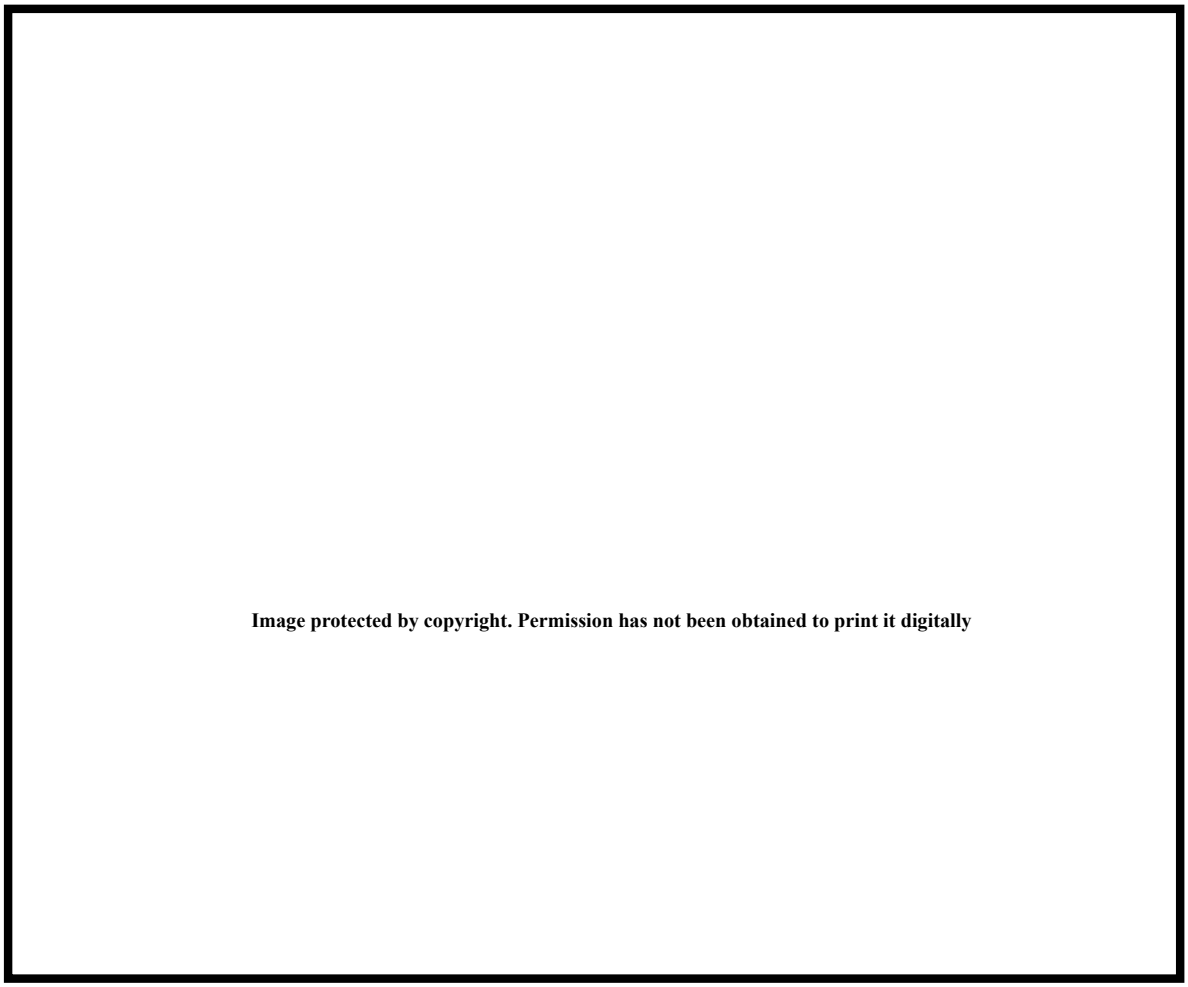

Figure 4-1: Auditory evoked response.
This diagram represents the nomenclature used to denote the phases of the AER and the anatomical components of the pathway associated with those. Adapted from Thornton and Sharpe (1998).

Similar middle- and long-latency auditory evoked fields (AEF) are generated in the auditory cortex with MEG. The waves are depicted with letters (for eg, N_am, P_am, N_bm, P_am respectively) or with their usual peak latencies (N19m, P30m, N40m, P50m), with the long-latency AEF being P50m, N100m and P200m. The P19m and P30m have been shown to originate from the medial Heschl's gyrus while the P50m is generated more

lateral from the Heschl's gyrus (Scherg et al., 1989, Yvert et al., 2001, Hashimoto et al., 1995, Pelizzone et al., 1987).

AER have been widely studied as a marker of anaesthetic depth. A dose dependent reduction in AER has been shown, with both Na and N100 potentials being sensitive to changes in doses of propofol (Ypparila et al., 2004, Tooley et al., 1996, Savoia et al., 1988). Midazolam (another GABA-ergic, sedative drug) has also been shown to produce changes in AER at sedative concentrations (Brunner et al., 2002, Brunner et al., 1999).

4.4.1.3 Somatosensory evoked potentials/ fields

Figure 4-2 represents the anatomical origins of the different components of the somatosensory evoked responses (SSER). Early SSER peaks also referred to as "short latency" SSERs are considered to be the most useful for the study of neurological activity as they are the least variable among participants with intact nervous systems, free from pathology and considered to represent the normal population. Short latency refers to the peaks and troughs present within the first 40 ms following a single stimulation to the upper limb, and less than 50 ms for the lower limb.

In human MEG studies, the earliest SI response to median nerve stimulation peaks at 20ms and may continue for 100-180 ms. Activation of SII usually peaks at 70- 100ms and may continue up to 200ms (Lin and Forss, 2002). Early electrophysiological components of SI, such as N20 or P27 (or its magnetic counterpart of M20 or M35), refer to the fundamental somatosensory neural response to changes in afferent inputs. It has been shown that the M20 is generated in the Brodmann's area 3b of the SI (Inui et al., 2004), however, the generator for M35 is unclear. It has been suggested that the M35 may originate from the overlapping activities of Broadmann's areas 3b, 4 and 1 (Inui et al., 2004), or area 4 of the primary motor area (Kawamura et al., 1996).

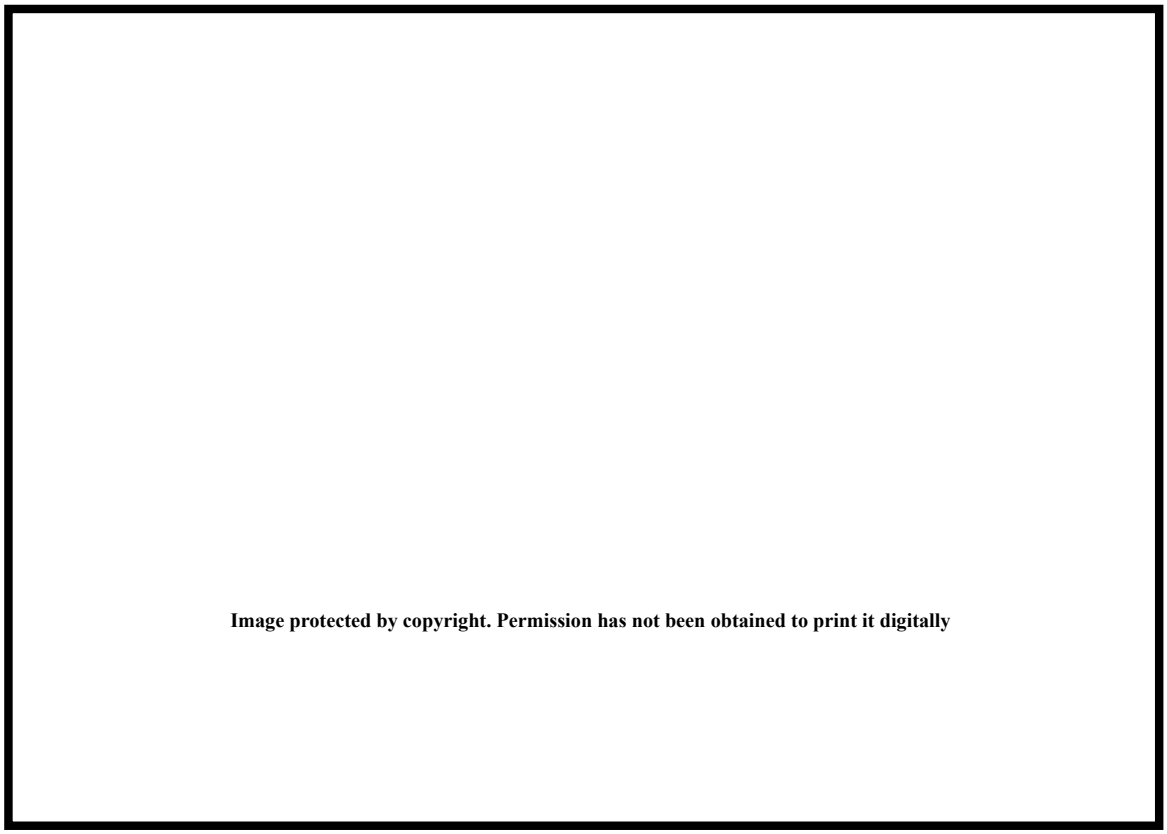

Figure 4-2: Somatosensory evoked response.
The diagram shows waveforms obtained on median nerve stimulation at the wrist. Recording electrodes placed at A) the somatosensory cortex and B) the seventh vertebra. Adapted from Thornton and Sharpe (1998).

GABA-ergic drugs such as thiopental reduce amplitude of latencies of SSERs (Koht et al., 1988). Inhalational agents appear to affect the SSEP more than propofol; with propofol having minimal effect on latencies or amplitudes of N29, P40 and N50 (Boisseau et al., 2002) while nitrous oxide appeared to reduce the SSER greater than isoflurane (Thornton et al., 1992), suggesting some degree of drug specificity in SSERs.

4.4.2 Aims

The aims of experiment 1 were to

- Study the changes in cortical evoked activity in response to visual, auditory and sensorimotor stimulation, following propofol sedation, using MEG.

4.4.3 Methods

4.4.3.1 MEG data collection

This experiment was performed as a part of the data collection for experiments described previously (Chapter 3) and therefore the methods for participant inclusions, monitoring, drug administration and sedation assessment were the same as stated in part (Section 3.4.3.2).

The participants were fifteen, male, healthy volunteers (mean age 26 years; range 20-41 years). This MEG session was conducted preceding MRI session (Experiment 2 in this chapter) as part of the overall experimental design. The time interval between the 2 experiments was at least 1 week to ensure total clearance of the drug and return of normal physiological functioning of the participant. All these participants had provided informed consent for this experiment, met the inclusion criteria and had no contra-indications to the drug or MEG/MRI environments (as described in Section 2.3). All participants were instructed to lie still with their eyes open and attend to the tasks. The sequence of data acquisition was always *Awake* state followed by *Sedated* state.

4.4.3.2 Stimulation paradigm

During the *Awake state* and following steady-state sedation (*Sedated state*), the following stimuli were presented in a sequential, block design. This sequence was maintained for all participants in both sessions.

Sensorimotor: For somatosensory stimulation, the median nerve was stimulated, transcutaneously, at the left wrist (duration 0.1 ms, inter-stimulus interval 0.4 ms) using a constant-current generator (Digitimer^{TM}). The stimulus intensity exceeded the motor threshold producing a clear twitch of the thumb, although without being painful. The stimulation intensity was individually defined and was kept constant through both the sessions. Each recording took 5 minutes.

Visual: A checkerboard, reversing at 4Hz was presented on a projection screen controlled by Presentation®. Participants were instructed to fixate on a small red cross at the middle of the screen for the entire experiment. Each recording session took about 5 minutes (n=800).

Auditory: Brief auditory tones were presented, binaurally (1 kHz sine tone pulses, n = 200, duration 150ms, rising/decay time 5ms, ISI 210 ms, NHL 90dB) and transmitted via pneumatic headphones (tube diameter 5mm, length 3m). This recording session lasted about 5 minutes.

4.4.3.3 MEG acquisition and analysis

Whole head MEG recordings were made using a CTF 275-channel radial gradiometer system sampled at 1200 Hz (0–300 Hz bandpass). An additional 29 reference channels were recorded for noise cancellation purposes and the primary sensors were analysed as synthetic third-order gradiometers (Vrba and Robinson, 2001). Three of the 275 channels were turned off due to excessive sensor noise. At the onset of each stimulus presentation a TTL pulse was sent to the MEG system. Participants were fitted with three electromagnetic head coils (nasion and pre-auriculars), which were localised relative to the MEG system immediately before and after the recording session.

Offline, data were first epoched around stimulus onset (VEF: -0.05 to 0.25s, AEF: -0.1s to 0.4s, SSEF: -0.05s to 0.25s) and each trial visually inspected for data quality. Data with gross artefacts, such as head movements and muscle clenching were excluded from further analysis. This data was then averaged across participants and plotted topographically (Figure 4-5, Figure 4-6, Figure 4-7).

Global field power (GFP) was used to explore the changes further. GFP provides a global and spatially unbiased measure of the field strength at the scalp and avoids the problems of varying latencies and amplitudes at different sensor level or that of variable reference electrodes (Murray et al., 2008, Pourtois et al., 2008). Global field power was calculated with this averaged data and paired t-tests were done at each time point for differences between the two states, using in-house Matlab scripts.

4.4.4 Results

One participant's data had to be excluded from AEF and SSEF analysis, while two participants' data had to be excluded from the VEF analysis, due to missing data. Therefore the final number of subjects was 14 for AEF and SSEF and 13 for VEF.

There were no differences in the haemodynamic and ventilatory parameters between the *Awake* and *Sedated* groups. The mean (SD) propofol target concentration was 1.07 (0.19) mcg/ml. There was a significant reduction in reaction times during the *Sedated* state (Section 3.5.6.1).

Evoked response peaks were identified in all domains, especially in the *Awake* state, comparable to that expected, based on the EEG literature (Table 5-1). The responses were more variable in the *Sedated* state, especially in the AEF domain. This made it difficult to identify and label response peaks in the *Sedated* state, and precluded any quantitative analysis of changes in latencies of these responses between the *Awake* and *Sedated* states.

There was a significant reduction in the global field power of the VEF during the *Sedated* state as compared to the *Awake* state (Figure 4-4). This significant difference persisted between 0.08- 0.12 ms following the stimulus. AEFs showed a brief (non-significant) reduction in global field power, around the M100 peak (Figure 4-6). There were no significant differences in the SSEF global field power at any time point (Figure 4-8).

Table 4-1: Evoked responses: identifiable peaks and differences between *Awake* and *Sedated* states

	Awake Peaks identified at time point (s)	Possible EEG / MEG equivalent	*Sedated* Peaks identified at time point (s)	Qualitative differences
VEF	70	N70/M70	72	Delayed second peak
	90	P100/ M90	150	
	120 (maximum)	M120		
AEF	40	N40/M40		No change in latencies
	65	P50/M65	67	
	100 (maximum)	N100/M100		
SSEF	22	N20/M20	22	No change in latencies
	90		47	
			100	

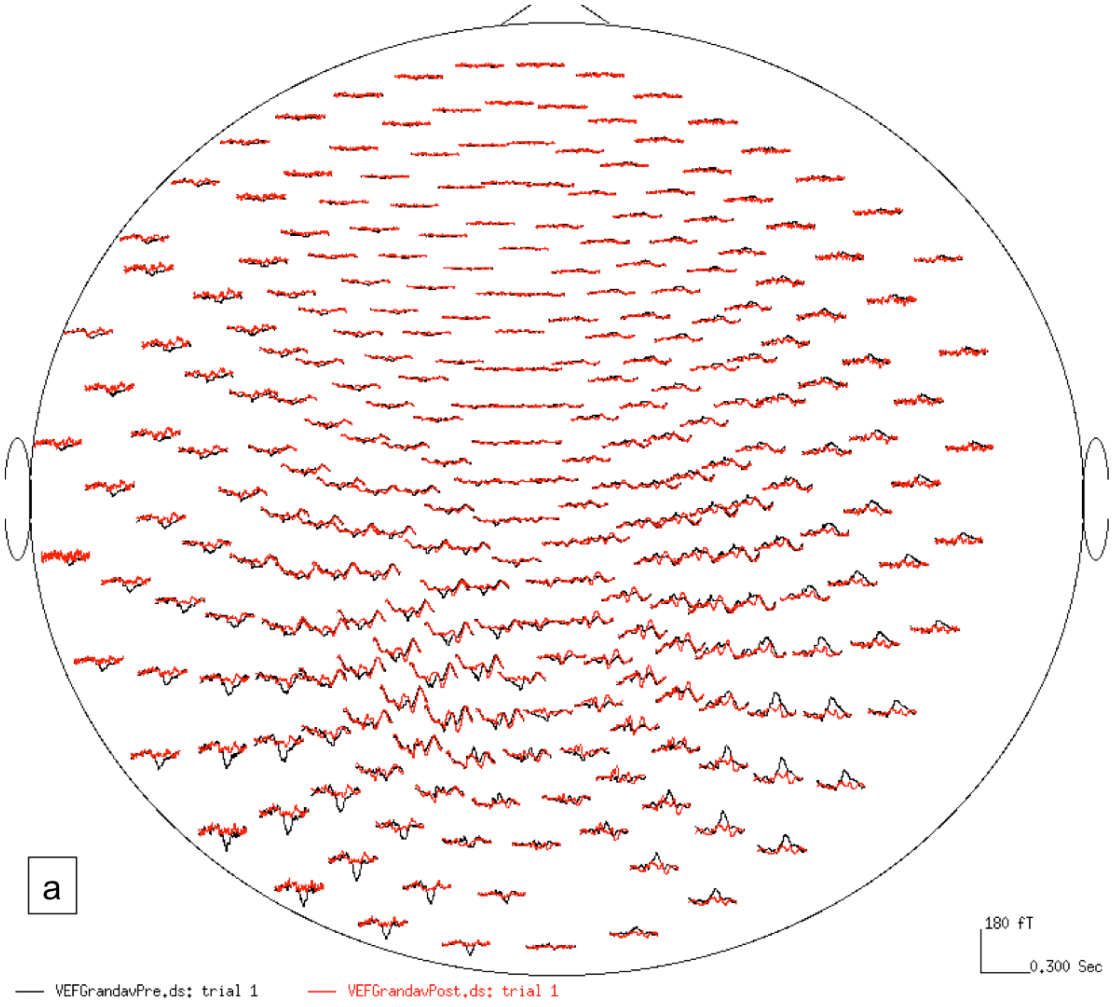

Figure 4-3: Summary of Visual evoked fields

(a) Topographical display of group-averaged evoked responses in sensor space, in both *Awake* (black) and *Sedated* (red) states. (b) Topographical plot of group-average amplitude at 0.12 s (maximum amplitude peak) in the *Awake* state. The topographic distribution is consistent with a single dipolar source in the occipital cortex. (c) Group-averaged evoked responses in the *Awake* state, showing peaks M70, M90 and M120. The vertical marker shows the latency of the response plotted in (b).

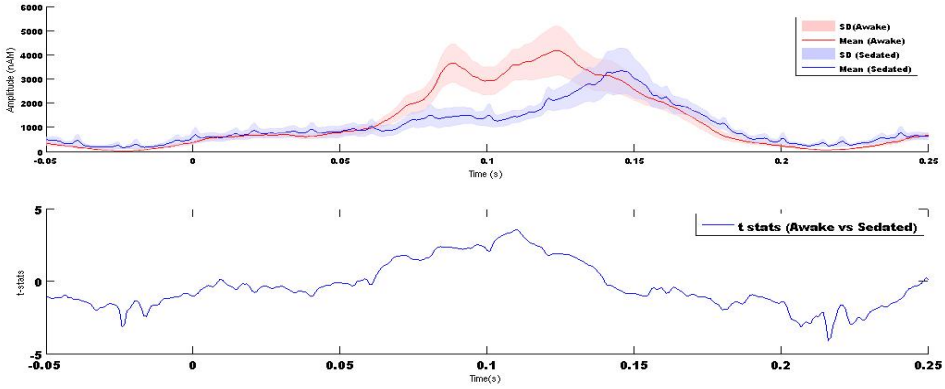

Figure 4-4: Summary of global field power differences in the Visual evoked fields. (Top) Global field power of the visual evoked field in *Awake* and *Sedated* states. (Bottom) t-stat image showing difference between *Awake* and *Sedated* states. t value of ≥1.8 corresponds to a significant difference between conditions ($p < 0.05$, one- tailed, paired t-test). There was a significant decrease in power between 0.08-0.12 s during the *Sedated* state relative to the *Awake* state.

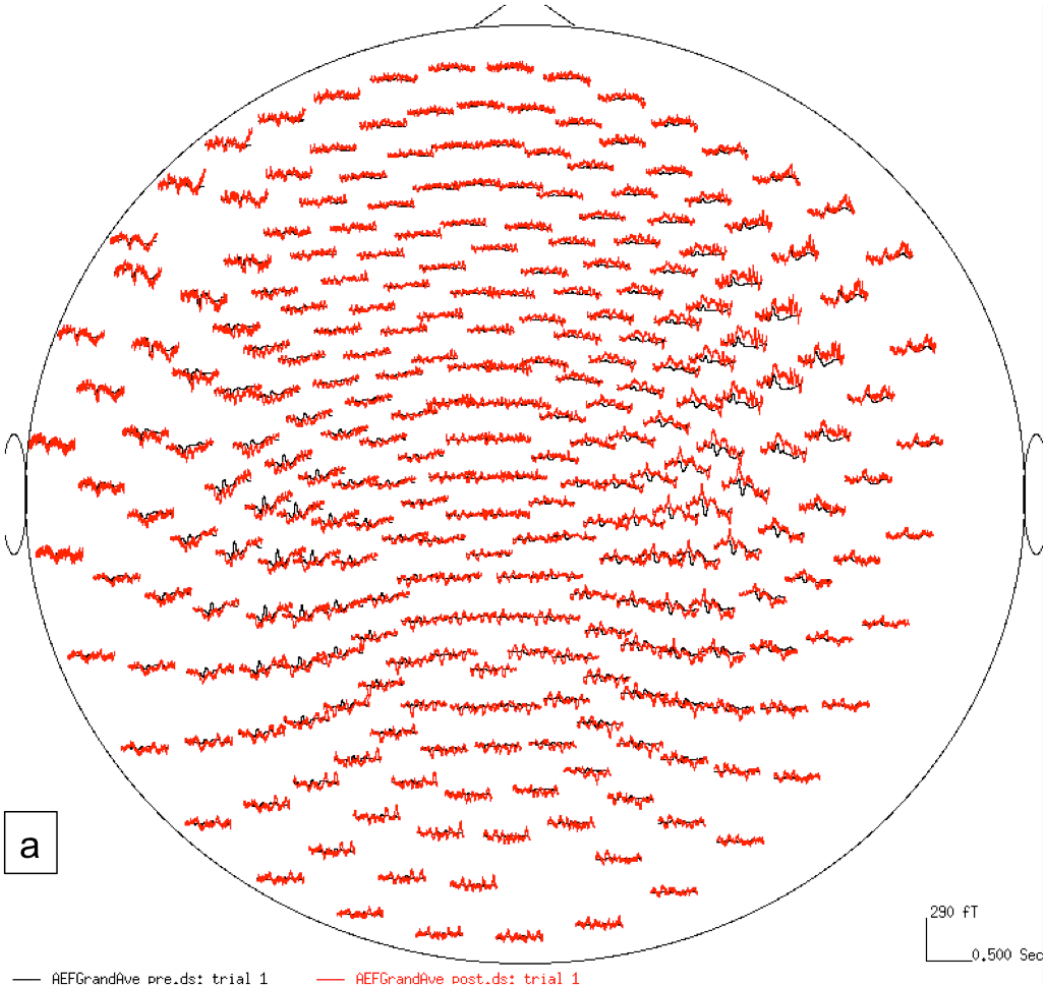

Figure 4-5: Summary of Auditory evoked fields
(a) Topographical display of group-averaged evoked responses in sensor space, in both *Awake* (black) and *Sedated* (red) states. (b) Topographical plot of group-average amplitude at 0.1 s (maximum amplitude peak) in the *Awake* state. The topographic distribution is consistent with bilateral dipolar sources in the temporal cortices. (c) Group-averages evoked responses in the *Awake* state, showing peaks M40, M65 and M100. The vertical marker shows the latency of the response plotted in (b).

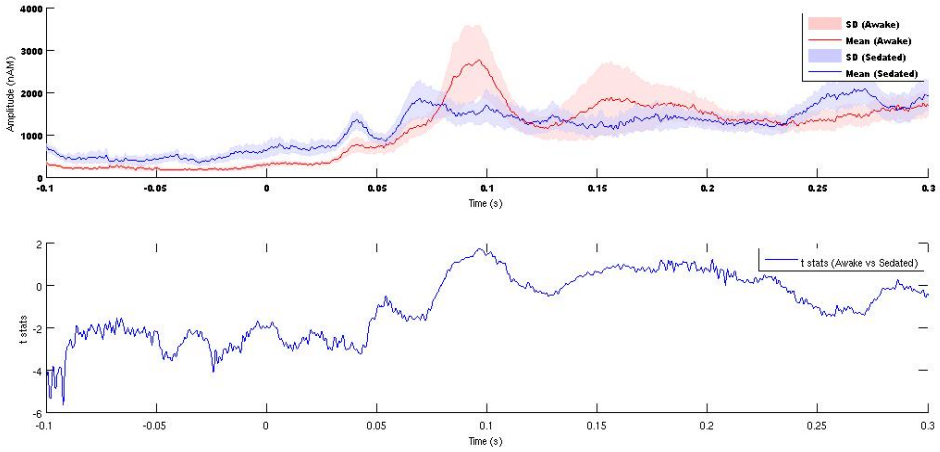

Figure 4-6: Summary of global field power differences in the Auditory evoked fields.

(Top) Global field power of the visual evoked field in *Awake* and *Sedated* states. (Bottom) t-stat image showing difference between *Awake* and *Sedated* states. t value of ≥1.8 corresponds to a significant difference between conditions ($p < 0.05$, one- tailed, paired t-test). There was a decrease in power around the latency of the M100 during the *Sedated* state relative to the *Awake* state but it was not statistically significant.

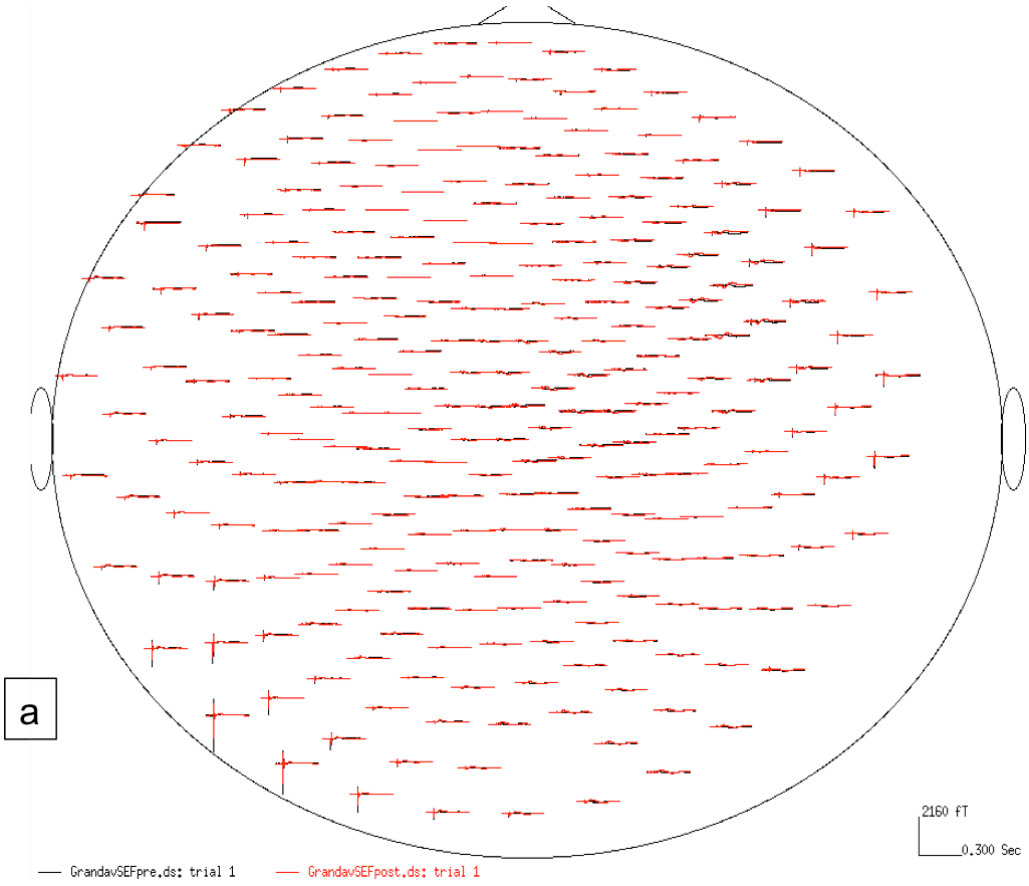

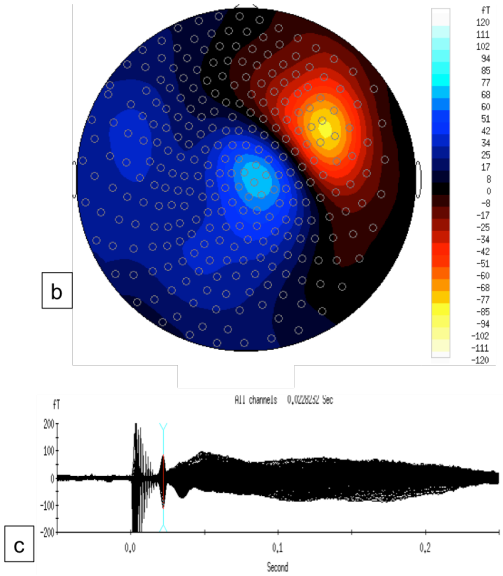

Figure 4-7: Summary of Somatosensory evoked fields
(a) Topographical display of group-averaged evoked responses in sensor space, in both *Awake* (black) and *Sedated* (red) states. (b) Topographical plot of group-average amplitude at 0.02 s (maximum amplitude peak) in the *Awake* state. The topographic distribution is consistent with a single dipolar source in the right sensorimotor cortex. (c) Group-average evoked responses in the *Awake* state. Note that the response present around stimulus onset is an artefact produced by the tactile stimulator.

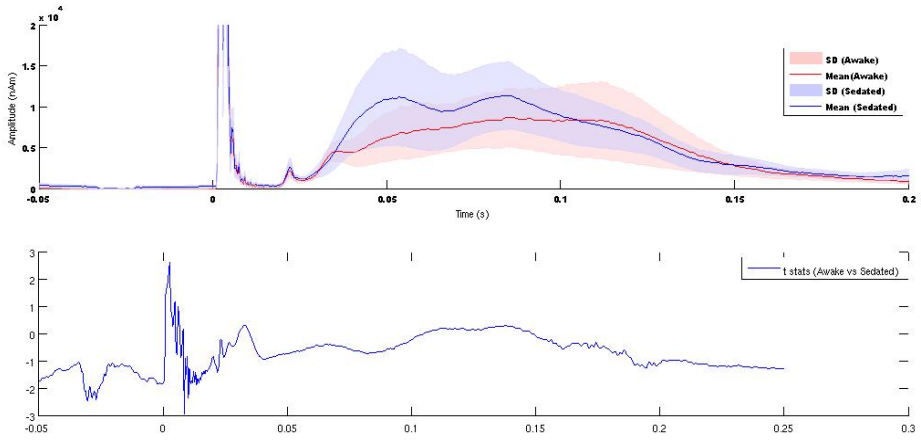

Figure 4-8: Summary of global field power differences in the Somatosensory evoked fields.
(Top) Global field power of the visual evoked field in *Awake* and *Sedated* states. (Bottom) t-stat image showing difference between *Awake* and *Sedated* states. t value of ≥1.8 corresponds to a significant difference between conditions ($p < 0.05$, one- tailed, paired t-test). There were no significant differences between the two conditions.

4.4.5 Discussion

This is the first ever report of the use of MEG to investigate alterations in evoked fields during propofol sedation. The findings of this experiment are comparable to those reported in the EEG literature with visual evoked responses showing a marked reduction, auditory responses undergoing a small change and somatosensory evoked responses remaining unchanged, during mild propofol sedation.

Studying visual evoked potentials, in relation to anaesthetic effects may be difficult, due to participants' inability to maintain an eye-open state (if required for the task). At levels of sedation used in this experiment, ability to keep eyes open remains grossly unaffected. All participants were therefore able to complete the tasks. As predicted, there was a significant and persistent decrease in VEF power in the time periods where the common peaks of M70 and M100 would be found. While statistical analysis of latencies was not possible, the second peak in the *Sedated* state appeared much delayed than during the *Awake* state, as predicted.

Auditory sensations are considered the most resistant to anaesthetic effects and some cortical reactivity persists even during deeper stages of anaesthesia. AERs have been used to monitor depth of anaesthesia/ sedation. Tooley et al (1996) found that mid-latency AERs such as Nb latency predicted propofol dose responsiveness better than Na. Ypparila et al (2004) showed that N100 could be used to discriminate between moderate and deep levels of sedation. However, mild propofol sedation (at the doses used in this experiment) have not been studied previously. In this experiment, peaks could be identified at 40, 65 and 100ms during the *Awake* state but they were less discernible during the *Sedated* state. This could represent noisy data or more widespread suppression. Significant global suppression of auditory activity at the doses used would be unlikely as auditory responses persist during deeper stages of sedation. The maximum difference between the *Awake* and *Sedated* state occurred around 100ms post-stimulus (M100), suggesting some reduction following propofol sedation, however this did not reach statistical significance.

No effect on the SSEF was found in this experiment. A reduction in tactile sensation is perceived during deeper levels of sedation, but is less likely during light sedation. Specifically, no behavioural tests were employed in the experiment to monitor tactile sensations or changes in those sensations. It is therefore difficult to establish if participants experienced a reduced sensation. Propofol has been shown to affect the SSEF less than other anaesthetics and it is therefore likely that at the levels of propofol infusion used in this experiment, lack of changes in SSEF mirrored a lack of change in perceived tactile sensation.

Since electrical stimulation was individually defined, there was a greater variance observed at the group level as compared to that during visual or auditory stimulation (Figure 4-4Figure 4-6Figure 4-8). VEFs showed the lowest variance and significant differences were seen between the *Awake* and *Sedated* states. It is possible that due to greater variability in individual responses, especially during SSEFs, potential group differences were missed.

4.5 Experiment 2

4.5.1 Introduction

Functional MRI based techniques allow studying of cortical reactivity to sedatives by studying changes in BOLD contrast in response to functional sensory tasks and changes occurring during sedation.

Mild to moderately sedative doses of isoflurane resulted in a reduction of cortical response to a vibrotactile stimulus (Antognini et al., 1997). Similarly, increasing doses of propofol reduces cortical blood flow increase in response to such tactile stimuli (Bonhomme et al., 2001). Reduced intensity and extent to noxious stimuli has also been reported with propofol (Hofbauer et al., 2004, Mhuircheartaigh et al., 2010). Reduction in visual responses have also been described with increasing doses of other anaesthetic drugs such as pentobarbital (Martin et al., 2000), isoflurane (Heinke and Schwarzbauer, 2001) and sevoflurane (Ramani et al., 2007), to tasks assessing simple and higher-order processing. Similarly, auditory perception and comprehension tasks have revealed loss of higher cortical areas activity at relatively lower doses of propofol and sevoflurane (Davis et al., 2007, Dueck et al., 2005, Heinke et al., 2004, Kerssens et al., 2005, Plourde et al., 2006, Veselis et al., 2005). The theme emerging from neuroimaging studies investigating cognitive processing of sensory stimuli suggest that higher order processing is lost relatively early on the path to unconsciousness, but the lower order processing may persist even at deeper stages of anaesthesia. While this suggests a dose dependent decline of sensory awareness with increasing anaesthetic doses; very few studies have specifically looked at the earliest stages of sedation to identify neural correlates of mild sedation.

Mild sedation is characterised by a state where participants are still responsive and communicative, but sluggish / lethargic in their response, have slurred speech and may also have amnesia. Most sensory abilities, although sluggish, are maintained. This experiment investigates the cortical reactivity in such sensory domains, in relation to mild propofol sedation.

4.5.2 Aims

The aims of experiment 2 were to

- Study the changes in cortical activity in response to visual, auditory and sensorimotor stimulation, following propofol sedation.

4.5.3 Methods

This experiment was performed as a part of the data collection for experiments described previously (Chapter 3) and therefore the methods for participant inclusions (same as Section 3.4.3.1) monitoring, drug administration and sedation assessment (Section 3.4.3.2) were the same.

4.5.3.1 MRI data collection

Functional MRI data were collected using gradient-echo echo- planar imaging at 3T (GE Healthcare HDx) using a blood oxygen level- dependent (BOLD) (T2*)-weighted imaging sequence (TR= 3 s, TE = 35 ms, matrix = 64 x 64, FOV/slice = 20.5 cm/3.2 mm, flip angle = 90°, 50 slices, 160 volumes). An eight-channel receive-only head coil was used. A T1-weighted whole-brain structural scan was also acquired (1 x1 x 1 mm voxels). For the purposes of accounting for physiological variance in the time-series data, end-tidal carbon dioxide, and end-tidal oxygen traces were recorded throughout the experiment using a nasal cannula attached to a capnograph (AEI Technologies). Cardiac and respiratory cycles were recorded using the scanner's built-in photoplethysmograph and a pneumatic chest belt, respectively.

All participants were instructed to keep their eyes open and follow the (passive) tasks.

4.5.3.2 Stimulation paradigm

During the *Awake* state and following steady-state sedation (*Sedated* state), the paradigm consisted of six alternating blocks of resting and task conditions. Each task block was composed of a pseudorandom sequence of three stimulations: Auditory,

Visual and Somatosensory, as below. Both resting and stimulation periods lasted for five volumes.

Somatosensory: For somatosensory stimulation, the median nerve was stimulated, transcutaneously, at the left wrist (duration 0.1 ms, inter-stimulus interval 0.4 ms) using a constant-current generator (Digitimer ^{TM}). The stimulus intensity exceeded the motor threshold producing a clear twitch of the thumb, although without being painful.

Visual: A checkerboard, reversing at 4Hz, was presented on a projection screen controlled by Presentation®. Participants were instructed to fixate on a small red cross at the middle of the screen for the entire experiment.

Auditory: Brief auditory tones were presented, binaurally (1 kHz sine tone pulses, n = 200, duration 150ms, rising/decay time 5ms, ISI 210 ms, NHL 90dB) and transmitted via acoustically shielded headphones.

4.5.3.3 MRI data analysis

Preprocessing

Same preprocessed data as used in Section 3.6.5 were used. Several sources of physiological variance were removed from each individual subject's time-series fMRI data. For each subject, physiological noise correction consisted of removal of time-locked cardiac and respiratory artefacts (two cardiac harmonics and two respiratory harmonics plus four interaction terms), using linear regression (Glover et al., 2000), and of low-frequency respiratory and heart rate effects (Birn et al., 2006; Shmueli et al., 2007; Chang and Glover, 2009). In addition, regressors formed from end-tidal CO_2 and O_2 traces were also removed (Murphy et al., 2011).

Analysis

fMRI data processing was carried out using FEAT (FMRI Expert Analysis Tool) Version 5.98, part of FSL (FMRIB's Software Library, www.fmrib.ox.ac.uk/fsl). The following pre-statistics processing was applied; motion correction using MCFLIRT

(Jenkinson et al., 2002), non brain removal using BET(Smith, 2002), spatial smoothing using a Gaussian kernel of FWHM 5mm; grand-mean intensity normalisation of the entire 4D dataset by a single multiplicative factor; high pass temporal filtering (Gaussian-weighted least-squares straight line fitting, with sigma=50.0s).

FMRIB's improved Linear Model (FILM) was used for first level analysis, where the haemodynamic response to each stimulus type, in relation to the physiological variations was explored for each subject, using the Resting-Auditory-Visual-Somatosensory design matrix (Figure 4-9).

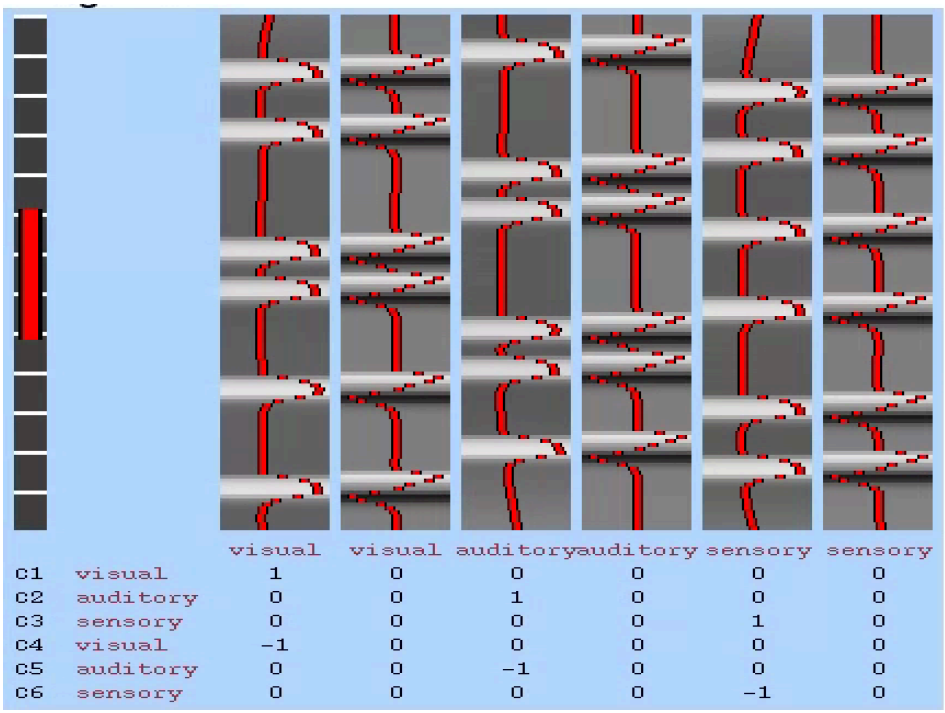

Figure 4-9: Design matrix as generated in FSL using general linear modelling.
The three explanatory variables are visual, sensory and auditory. The relevant contrasts use the 3 variables in two combinations; *Awake* > *Sedated* and *Seated* > *Awake*

Higher level analysis was carried out using FLAME (FMRIB's Local Analysis of Mixed Effects) stage 1 (Beckmann et al., 2003, Woolrich, 2008, Woolrich et al., 2004). Paired comparisons were performed to identify areas where responses to each stimulus type varied significantly with the sedation state. Z (Gaussianised T/F) statistic images were thresholded using clusters determined by Z>2.3 and a (corrected) cluster significance threshold of P=0.05 (Worsley, 2001).

FSLview was used to view the statistical parametric maps and the areas of BOLD signal differences were identified by using the Harvard-Oxford cortical and subcortical atlases.

4.5.4 Results

One participants' data could not be used due to excessive head motion and so the analysis was performed on 14 subjects' data. All participants were sedated to the desired level (OAA/S level of 4; mild sedation) during the *Sedated* state scanning. There was a significant slowing of the visual and auditory reaction times, as described previously in Section 3.4.4 (Table 3-2: Reaction times). There was no change in HR, BP, oxygen saturation or expired CO_2 as described previously in Section 3.4.4 (Table 3-1: Physiological Data). The mean (SD) propofol target concentration was 1.2 (0.2) mcg/ml. All the tasks were able to elicit the expected BOLD responses mainly in the respective primary sensory cortices (Figure 4-10, Figure 4-12, Figure 4-14).

Cortical responses to visual stimulation showed reduced activity in the superior frontal gyrus, paracingulate and cingulate gyri, left superior parietal lobule, left angular gyrus, left lateral occipital cortex and left supramarginal gyrus, following sedation. There was an increased activity in the cuneus, precuneus, supracalcarine and intracalcarine gyri, following sedation (Figure 5-1).

During the auditory stimulation task, decreased activity was seen in the superior and middle frontal gyri, paracingulate gyrus, right sensorimotor cortex and right anterior and posterior cingulate regions, following sedation. There was in increase in activity in left caudate, insula, anterior cingulate, right posterior cingulate, right lingual gyrus, and precuneus (Figure **4-13**), following sedation.

During the somatosensory task, propofol sedation resulted in a reduction in BOLD signal intensity in the contralateral somatosensory cortex, while an increase activity was seen in the left middle temporal gyrus, lateral occipital cortex, supracalcarine and intracalcarine cortex, posterior cingulate and precuneus regions (Figure 4-15).

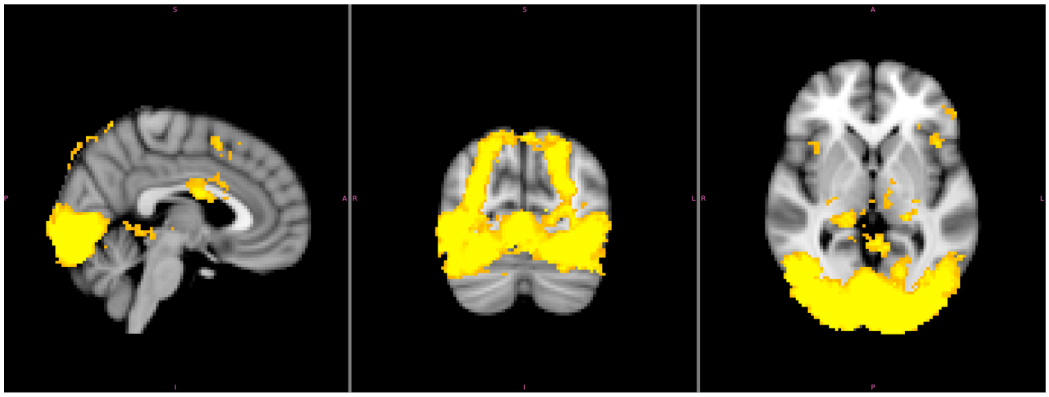

Figure 4-10: Group mean map showing activation of regions following a visual stimulus (*Awake* state)
Image only for diagrammatic representation, therefore, statistical colour bar not shown

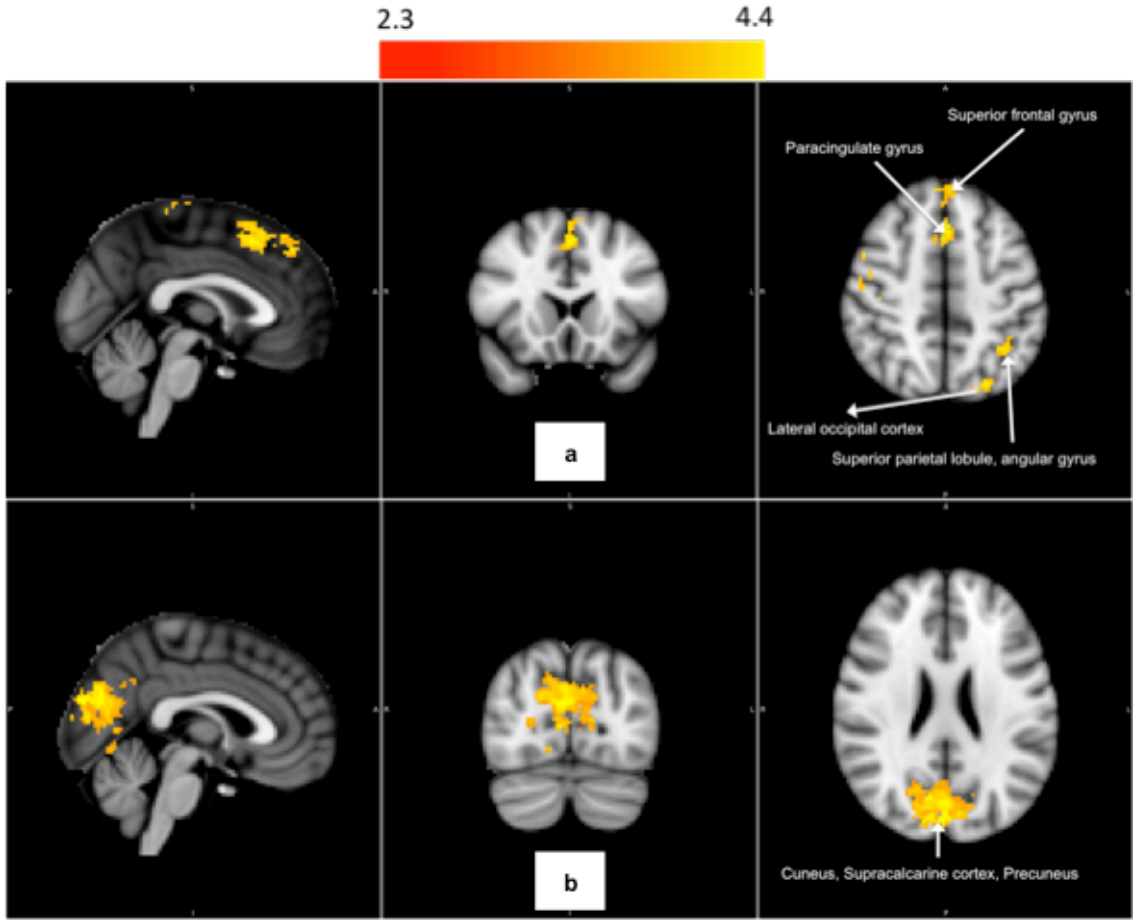

Figure 4-11: Group mean t-contrast maps showing differences in activation of regions following a visual stimulus.
a) *Awake*> *Sedated*: b) *Sedated* >*Awake* state. Z (Gaussianised T/F) statistic images were thresholded using clusters determined by Z > 2.3 and a corrected (cluster) significance threshold of P= 0.05. Colour bar shown above the figure.

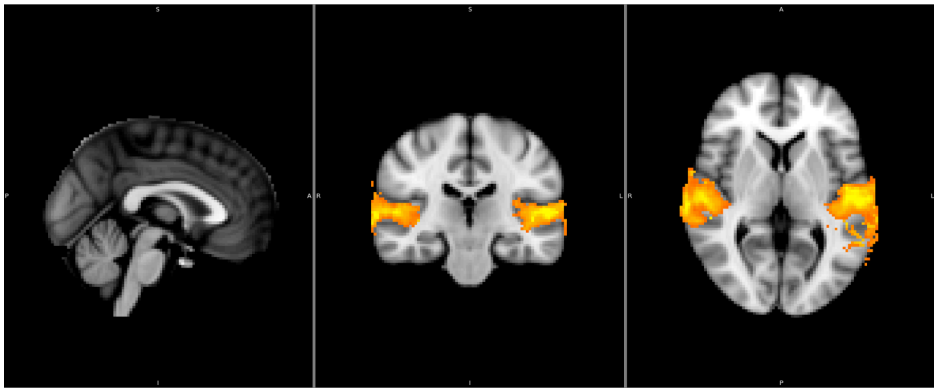

Figure 4-12: Group mean map showing activation of regions following an auditory stimulus (Awake state)
Image only for diagrammatic representation, therefore, statistical colour bar not shown.

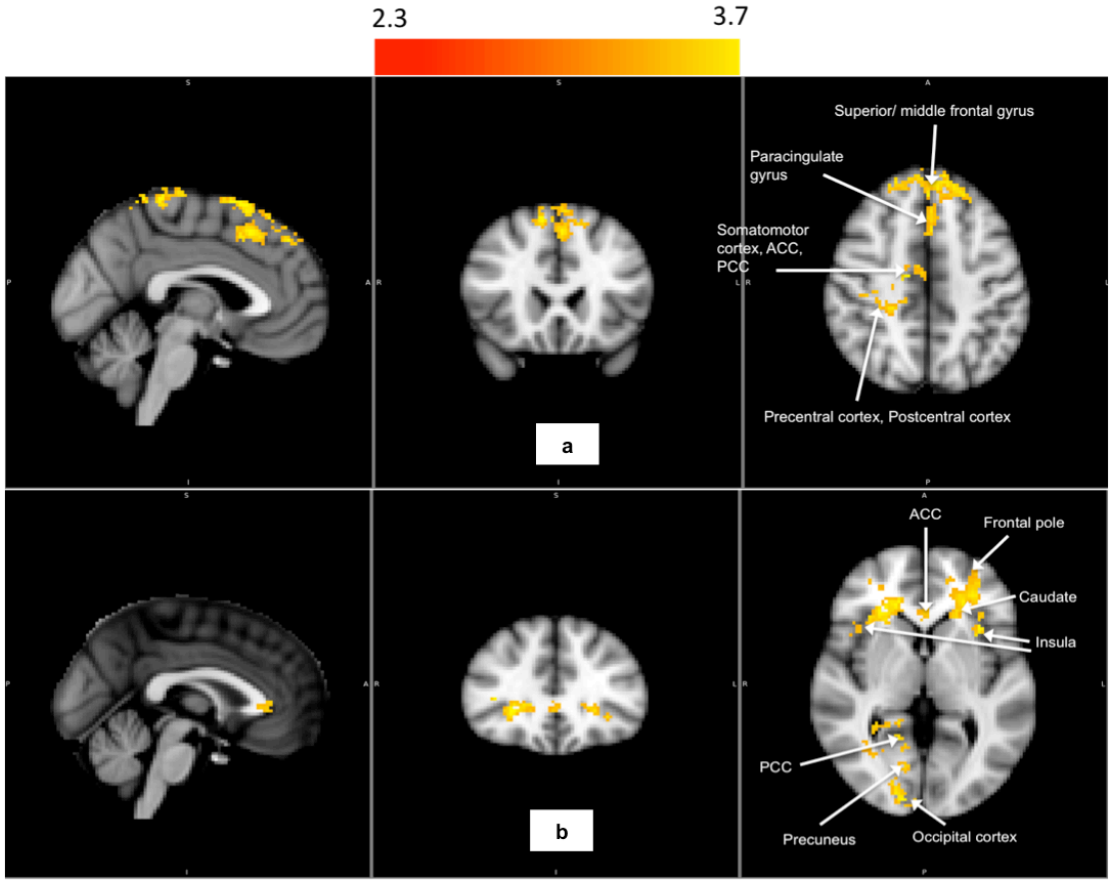

Figure 4-13**: Group mean t-contrast maps showing differences in activation of regions following an auditory stimulus.**
a) *Awake*> *Sedated*: b) *Sedated* >*Awake* state. Z (Gaussianised T/F) statistic images were thresholded using clusters determined by Z > 2.3 and a corrected (cluster) significance threshold of P= 0.05. Colour bar shown above the figure.

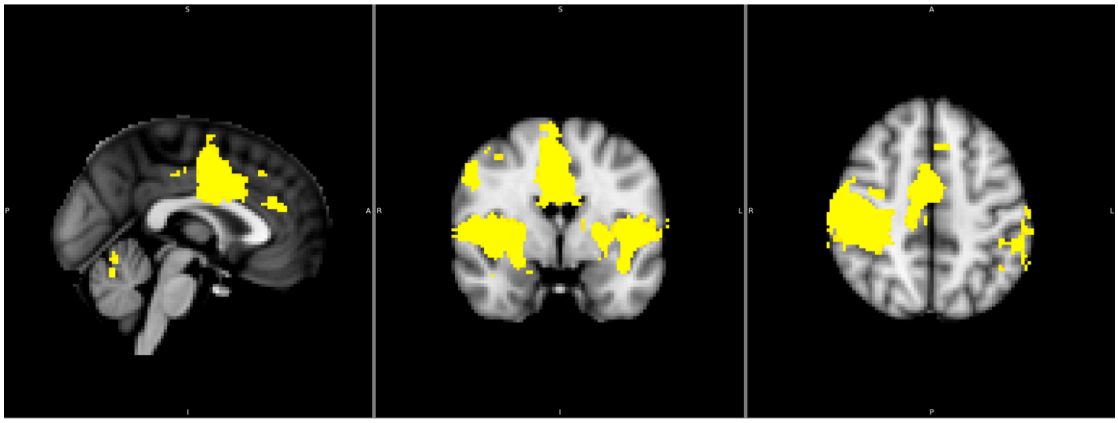

Figure 4-14: Group mean map showing activation of regions following median nerve stimulation (*Awake* state)
Image only for diagrammatic representation, therefore, statistical colour bar not shown

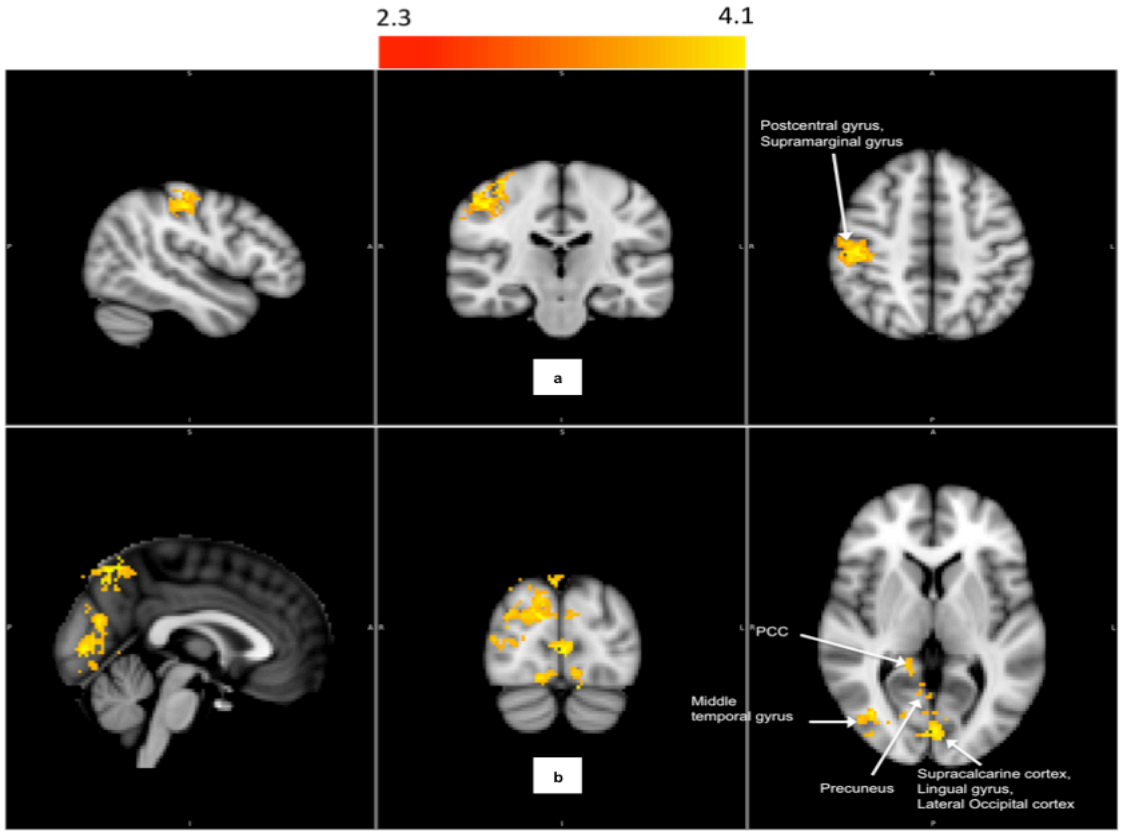

Figure 4-15: Group mean t-contrast maps showing differences in activation of regions following median nerve stimulation.
a) *Awake*> *Sedated*: b) *Sedated* >*Awake* state. Z (Gaussianised T/F) statistic images were thresholded using clusters determined by Z > 2.3 and a corrected (cluster) significance threshold of P= 0.05. Colour bar shown above the figure.

4.5.5 Discussion

As predicted, fMRI demonstrated a reduction in the activity of the primary sensorimotor cortex following propofol sedation. While significant reductions in activities of the primary visual or auditory cortices, were not seen, other areas of differences became apparent between the two states of consciousness.

Median nerve stimulation results in activation of the contralateral primary sensorimotor cortices and occasionally bilateral secondary sensorimotor cortices (Arthurs et al., 2000). Similar activations were seen in the *Awake* state in this experiment. Following mild propofol sedation primary somatosensory cortex showed a significant reduction in activity. This finding was predicted and supports the mechanism involved in a reduced sensation as a component of early stages of sedation. Similar, suppression of activity in the primary somatosensory cortex was reported with increasing levels of propofol sedation, studied using PET (Bonhomme et al., 2001). While Bonhomme et al (2001) did not report any increase in activity with sedation, the current experiment showed increased activity in PCC, precuneus, middle temporal gyrus and lateral occipital cortex. There is a relative paucity in literature of experiments studying earliest stages of sedation, as done in this experiment and therefore these findings are more difficult to explain. One explanation of an increased activity in these regions; precuneus (an important hub of the default mode network), middle temporal gyrus (key in auditory function) and lateral occipital cortex (key in visual function) may be a reflection of participants' attempts at compensation to mitigate some of the effects of sedation. Although, the tasks involved were passive, it is not uncommon in normal healthy volunteers, entering the light stages of sedation (where they can still follow commands and verbalize) to try and stay 'awake' and resist 'falling asleep', using alternative sensory modalities. While at deeper levels of sedation or anaesthetic levels this sub-conscious effort is impossible, at mild sedation, it is still possible. It is therefore possible that participants were using secondary modalities to compensate for the diminished perception of the primary (electrical) stimuli.

The auditory stimulation showed a reduced BOLD response in the superior and middle frontal gyrus, anterior cingulate and posterior cingulate cortices and the right

sensorimotor cortex, with propofol sedation. There was no reduction seen in the primary auditory cortical regions. During the *Sedated* state increased BOLD activity was seen in the cingulate cortex, insular cortex, left caudate, precuneus and occipital gyrus. The lack of change in BOLD activity in the auditory cortices was unexpected, but not completely surprising. Auditory activity is considered to be the most resistant of all sensations, to anaesthetics. Mhuircheartaigh et al (2010) demonstrated a reduction in BOLD activity in the auditory cortices, at similar levels of propofol sedation as used in this experiment. They had, however, used words instead of simple auditory tones. Veselis et al (2005) showed a 15% reduction in global CBF but no change in responsiveness to auditory stimuli during propofol sedation. In speech processing tasks, a dose-dependent reduction in activity in the auditory cortices has been shown (Davis et al., 2007, Dueck et al., 2005), however, some activity persists even in deeper stages of sedation / anaesthesia (Heinke et al., 2004, Plourde et al., 2006). This suggests that the step change in measurable auditory response, from awake to mild level of sedation is small and may depend on the dose studied and task involved. It is, therefore, possible that in this experiment the small degree of change in the activity, if any, for simple passive task, was not significant to appear in the analysis done. A small volume correction, focusing around the temporal cortices, may have been able to explore this further, but was not attempted.

A reduction in activity in frontal regions was also a surprising finding as the stimulus used in this experiment was a simple auditory tone task with no specific cognitive activity. Dueck et al (2005) studying auditory speech processing during propofol sedation found frontal activation, which was lost at 0.05mcg/ ml plasma level of propofol. Similarly, Davis et al (2007) also showed suppression of frontal and other areas involved in comprehension and recall. In the current experiment, suppression of frontal activity, possibly suggests a degree of unintended cognitive processing which the participants may have been engaging in during the *Awake* state, which was subsequently lost during the *Sedated* state. Diminished activity in the cingulate cortical regions and sensorimotor cortices, therefore, may reflect compensatory responses with those regions being engaged more in the *Awake* state. Similarly, increase in cortical and sub-cortical activity during the *Sedated* state, especially of the regions considered to be a part of the DMN (cingulate cortices and precuneus) is interesting. Functional

connectivity in the DMN regions is suppressed when performing a task. The possible explanation, for these findings, therefore would be that these DMN areas are successfully suppressed during the *Awake* state. However, during the *Sedated* state the ability to suppress these regions' connectivity is decreased leading to the emergence of a relative increase in BOLD activity in these regions.

Visual stimulation using a reversing checkerboard produces good, reliable activation of the primary and secondary visual cortices, as was found in the *Awake* state. There was a greater activation of the superior frontal gyrus, paracingulate gyrus and lateral occipital cortex in the *Awake* as compared to the *Sedated* state, while there was an increased BOLD response in the cuneus, precuneus and the supracalcarine and intraclacarine cortex. Lateral occipital cortex is involved in vision, especially in objection recognition (Grill-Spector et al., 2001, Nagy et al., 2012), while angular gyrus plays a role in semantic processing, cognition, attention and memory (Seghier, 2013). Similarly, paracingulate gyrus and superior frontal gyrus play an important part in cognition and attention as parts of key resting state networks. A decreased activity in these regions was unexpected but suggests some degree of attention and cognitive processing, during the *Awake* state, which was reduced during the *Sedated* state.

An increased activation of the cuneus and precuneus were seen during sedation. These regions are known to be an important part of the DMN and so an increase, possibly suggests (similar to the auditory stimulus) an emergence of activity in the DMN due to loss of inhibition, during the *Sedated* state. An increase in the supracalcarine and intraclacarine sulcus was more surprising. These regions are part of the secondary visual cortex and involved in higher level processing of visual stimuli. It has been shown that non-stimulated areas may be suppressed to facilitate precision activity of the stimulated areas (Bressler et al., 2007). This suppression of activity, in these regions may manifest as a negative BOLD response on fMRI (Pasley et al., 2007). While the mechanism of this remains poorly understood, it is one of the likely explanations of the findings in this experiment. It is possible that cortical areas around the primary visual cortex were suppressed during the visual checkerboard task and this suppression was lost at early stages of sedation, resulting in an increased BOLD response.

4.5.6 Comparing cortical responses from MEG and FMRI: potential limitations

This set of experiments was the first of its kind; studying neuromagnetic changes in brain's activity in response to simple sensory tasks and the changes associated with mild propofol sedation. Similarly, it is one of the few studies using BOLD-fMRI to investigate changes in cortical reactivity with mild propofol sedation and certainly, a novel attempt to compare the findings of the MEG experiment with BOLD-fMRI in a sequential experimental design.

Mild sedation is associated with changes in responsiveness and alertness, but there were no behavioural anchors used along with these passive tasks. However, the reaction times to visual and auditory stimuli, recorded separately (Chapter 3, section 3.4.4) between the scans can provide an objective measure of alterations in visual and auditory processing with sedation. Therefore changes in visual and auditory pathways were predicted using MEG and fMRI. The findings, however, were partly as predicted, but also somewhat conflicting when taking both the modalities into consideration. Visual stimulation resulted in reduced VEFs but no concomitant reduction in BOLD activity in the primary visual cortices. On the other hand, while there was no change in SSEFs, there was a reduction in BOLD activity in the primary somatosensory cortex. Auditory stimulation did not result in a significant change in either the AEF or the BOLD response. Experiment 2 (fMRI) also produced an interesting set of results, which are worthy of further research.

The differences between the results of MEG and fMRI may be attributable to the innate differences between the two modalities. The electromagnetic activity (as captured by MEG) of the brain and the haemodynamic activity (as captured by BOLD-fMRI) are best seen as complementary, originating from similar, but not limited to the same, sources. BOLD signal is linked to the local field potentials rather than multiunit activity or even neuronal spiking (Logothetis et al., 2001). Neurovascular coupling, manifesting as the BOLD response also depends on a number of variables, some of which continue to be poorly understood. In rats, regional heterogeneity of the neurovascular coupling has been shown (Sloan et al., 2010). Similar dependence of BOLD response to different

oscillatory bands and brain regions studied, has been demonstrated in humans (Conner et al., 2011, Ojemann et al., 2013).

Evoked responses and their haemodynamic responses (as in BOLD-fMRI) following repeated stimulations, habituate to different degrees. This is a reflection of the still incompletely understood mechanism of the BOLD response and its use as a surrogate of neural activity (more directly measurable as evoked responses). While habituation of BOLD response has been widely reported following repeated visual, auditory and sensory stimulations, it is not that common with evoked electrophysiological responses (Dirnberger et al., 2004, Fischer et al., 2000, Pfleiderer et al., 2002, Janz et al., 2001, Ai et al., 2013). Also, attention modulation of tasks may affect the BOLD response more variably than the evoked responses (Arthurs et al., 2004). The MR environment is substantially different from the MEG suite environment. The scanner noise itself can affect auditory tasks directly (more likely in complex auditory tasks than simple tasks) or even non-auditory tasks may engage other attentional modalities producing variable confounds (Peelle, 2014, Kobald et al., 2016). While these effects were expected to be less likely in these experiments involving lower order passive tasks, they cannot be completely ruled out.

The delivery of the stimulus paradigms was different in the two experiments. In MEG the three types of stimuli were presented in sequence, in a block design of 5 minutes each. In the MRI session, however, considering participant comfort (time spent undergoing MR scanning) and design efficiency; stimulus paradigm involved mixing the stimuli for the fMRI experiment (the total duration being about 8 minutes). It is possible that the pseudorandom sequence of the stimuli, their shorter duration and mixed design, produced some of the results as observed. However, no literature was found to identify a mechanism behind, differences in experimental designs, producing such differences.

Other factors, which may have contributed to the differences, could be the methodological factors such as the order effect (MRI sessions always followed the MEG session and the *Awake* session always preceded the *Sedated* session). The assessment of sedation was verbal and although done by a blinded anaesthetist, there

may have been subtle differences in assessing sedation (within the same objective level) resulting in some differences in the level of sedation between the two groups.

4.5.7 Conclusions

This is a novel attempt at combining different neuroimaging techniques to study neurophysiologic and haemodynamic changes associated with propofol sedation. The results of this sequential MEG/ fMRI can be summarized as follows

- There was a significant reduction in VEFs but no change in AEFs and SSEFs following mild propofol sedation.

- There was a reduction in activity of the primary somatosensory cortex in response to median nerve stimulation, but no change in primary cortical activity following visual or auditory tasks, following mild propofol sedation.

Chapter 5 : Effect of propofol sedation on resting state brain activity

5.1 Abstract

Neuroimaging of the resting brain has helped identify a number of networks indicating brain regions communicating with each other and have been shown to play an important role in regulating brain function.

In a series of experiments, using multimodal neuroimaging techniques, functional connectivity analyses were performed to study changes in resting state network (RSN) activity in response to mild propofol sedation.

Functional MRI revealed that functional connectivity of higher order networks changes with mild sedation. Posterior cingulate cortex (as a key hub of the default mode network- DMN) becomes less connected with the frontal pole while the thalamus becomes less connected with regions of the DMN, anterior cingulate cortex and motor cortex. Thalamus appears more connected with sensory cortices and superior temporal gyrus. Primary sensory and motor cortices show reduced connectivity with the occipital cortex but become more connected with the thalamus.

MEG analyses revealed that there was increased functional connectivity in bilateral frontal RSNs in the alpha, theta and delta frequency bands; increased functional connectivity in the bilateral parieto-occipital network (in the alpha band), and bilateral occipital network in the delta band. Bilateral motor networks were also identified, however, there was no change in those in the beta and gamma frequency bands.

5.2 Background and rationale

Task based fMRI has helped explore specific functions of the human brain, however, the discovery of task-unrelated activities of the brain (resting state) has opened up a whole new window into understanding of brain function. Raichle and Mintun (Raichle and Mintun, 2006), used positron emission tomography (PET) to demonstrate that in the resting (no task) state the human brain consumed a high amount of energy (20-25% of the body's basal oxygen/ glucose consumption), proving the brain to be fairly active even when not involved in any 'task'. Biswal et al (1995) had earlier demonstrated that during such a resting -state, the BOLD activity of the somatosensory cortex of one side was highly correlated with the activity of the other side. This 'resting state' activity was subsequently corroborated by other research groups and has led to the identification of numerous such 'resting state networks' (RSNs). These RSNs typically comprise of anatomically disparate regions, which appear to be active, synchronously (temporally related), i.e. functionally 'connected' in their activities. This co-activation of separate brain regions therefore suggests communication between regions as a marker of information integration/ processing between those regions. The presence and activity of these RSNs have been shown in animals such as rats and monkeys indicating their presence and relevance through various species (Vincent et al., 2007, Lu et al., 2012).

One of the most extensively investigated (and possibly the most fundamental) network is the Default Mode Network (DMN). This network has been shown to consist of brain regions including medial prefrontal, parietal, and posterior cingulate cortices and is active while the brain is not engaged in any active task (Greicius et al., 2003). Activity of the DMN tends to be suppressed during an active task. An 'Executive control network' (ECN: dorsolateral fronto-parietal network) has been identified as the network opposite to the DMN; this tends to be inactive at rest but becomes active during a task (and is usually anti-correlated to the DMN). Traditionally, DMN has been suggested to support a self-referential and internal mentation role. More recent literature, however, has shown that it may actually play an active role in higher order cognitive processing (Vatansever et al., 2018). Other networks commonly identifiable include the somato-motor, visual, somatosensory, auditory, language, dorsal and ventral attention networks. It has been suggested that about 10 consistent RSNs cover nearly 80% of the human

cortex, highlighting their potential importance in characterising brain function (Heine et al., 2012, Smith et al., 2009).

Studying brain's activity at rest provides an opportunity to interrogate physiological conditions and diseases where subject participation (to perform tasks) is not possible; such as unconsciousness, epilepsy and those in the paediatric age group (Lee et al., 2013a). Functional connectivity (fc) in the DMN has been shown to be inversely correlated to the level of consciousness impairment and also as a marker of recovery of consciousness in patients with "locked-in syndrome'' and vegetative states (Roquet et al., 2016). Similarly, pattern classification of RSN has been applied to distinguish patients with psychiatric disorders such as schizophrenia and depression. RSNs may also hold promise for future clinical applications in being able to identify patients with autism and attention deficit / hyperactivity disorder (Lee et al., 2013a).

5.2.1 Using multimodal imaging to study brain connectivity

Although, typically described using haemodynamic modalities, e.g. functional MRI (fMRI)/ PET, RSN fc has also been well described with electrophysiological modalities, including EEG and more recently MEG (Brookes et al., 2011b, Sockeel et al., 2016, Laufs, 2008).

As fMRI has temporal resolution in seconds, 'slow' temporal fluctuations have been studied in such temporal windows and network activity identified. However, the neurophysiological basis of resting-state dynamics occurring at faster time-scales and the nature of the coupling that binds cortical regions together cannot be accurately assessed using this technique. On the other hand, electrophysiological tools, with their excellent temporal sensitivity is much better at tracking dynamic changes in cognitive functions. If BOLD fluctuations are indeed a reliable, robust surrogate of neuronal function, it is expected that the electrophysiological signals will exhibit low-frequency spontaneous fluctuations with large-scale correlation patterns similar to those observed with resting-state fMRI.

Investigating the electrophysiological basis of these BOLD changes, it has been shown that the BOLD signal corresponds to the local neuronal field potential (Logothetis et al., 2001). Laufs et al, explored EEG changes and found that beta band correlated with BOLD activity of the DMN while alpha band activity was inversely correlated with the activity in the dorsal-attentional network (Laufs et al., 2003). Brookes et al used seed based connectivity correlations to identify sensorimotor networks and subsequently Independent Component Analysis (ICA) based techniques to investigate correlates of the envelopes of band-limited oscillations and demonstrated RSN with similar spatial localizations as those of fMRI (Brookes et al., 2011a, Brookes et al., 2011b). They also showed that most of the networks were best explained by beta band oscillations. However other authors have found different frequency bands related to different RSNs in different settings. Mantini et al found default-mode and lateral fronto-parietal networks and alpha and beta bands related to them in different directions (Mantini et al., 2007). Similarly they found auditory and visual networks to be related to most frequency bands, although somato-motor was still mainly related to the beta band. More recently comparing structural and functional connectivity with fMRI and MEG showed alpha and beta bands as the dominant bands in DMN and motor networks (Garces et al., 2016). These studies provide evidence of an electrophysiological basis of the commonly identifiable fMRI based RSN and therefore it appears useful combining the two modalities to investigate the modulation of these networks under propofol sedation. This combined technique is therefore likely to provide a better mechanistic understanding of the changes in the fMRI RSNs and their electrophysiological basis.

This experiment was performed as a two-part, sequential fMRI/ MEG study (as described previously in Section 2.4).

5.3 Hypotheses

Mild propofol sedation reduces the functional connectivity in the Default Mode networks and the thalamo-cortical networks without affecting the functional connectivity of the sensori-motor networks using fMRI.

5.4 Experiment 1

5.4.1 Introduction

While propofol's mechanism of action has been widely investigated using neuroimaging modalities, its resting-state fMRI or fc studies, investigating anaesthetic mechanisms have focused on loss of consciousness (i.e., 'anaesthetic' doses) and very few studies have looked at mild sedation and its impact on RSNs (see Appendix 1). Both higher order processing networks (those involved in cognition and higher order processing, for e.g. DMN, Executive control and salience networks) and basic/ lower order networks (visual, auditory, sensory and motor) have been well identified and studied.

In states of altered consciousness (including pharmacological, physiological e.g. sleep and disease conditions e.g. vegetative states) generally, the lower order- RSNs are more resistant to disruption than higher order RSN, and changes in their connectivities are related to the degree of change in consciousness. Anaesthetic / sedative studies also have shown similar changes but the results are not always consistent, either in magnitude of changes in connectivity or even its direction of change (increase or decrease). Functional connectivity of sensory, motor and other networks were maintained in isoflurane anaesthetised monkeys (Vincent et al., 2007). Similarly, in humans, at sedative concentrations of propofol (Boveroux et al., 2010) and sevoflurane, (Martuzzi et al., 2010), functional connectivity was maintained in sensory cortices. Functional connectivity of the key hubs of the DMN was decreased by propofol induced deep sedation (Martuzzi et al., 2010) and sevoflurane sedation (Martuzzi et al., 2010), while it was maintained, although slightly altered with midazolam (Greicius et al., 2008) or even increased with propofol sedation (Stamatakis et al., 2010). This may, however, reflect the differences between the choice of anaesthetic agent, analytic methods or differences in levels of sedation. Role of the thalamus and thalamo-cortical connectivity has been the focus of interest in many neuroimaging experiments. The thalamus has been proposed to act as a 'switch', (Alkire et al., 2000) which switches off consciousness by breaking down its connections with the cortex. Some groups argue that failure of thalamo-cortical connectivity is a cause of anaesthetic unconsciousness

while others argue that it is the cortico-cortical connectivity, failure of which results in unconsciousness (Boly et al., 2012, Boveroux et al., 2010, White and Alkire, 2003, Mashour and Alkire, 2013). While thalamo-cortical connectivity is certainly associated with anaesthesia; its precise role and sequence of impact, in relation to alterations in cortico-cortical connectivity, in causing sedation, is unclear.

5.4.2 Aims

The aims of experiment 1 were to

- Study the changes in functional connectivity in BOLD-signal based spatio-temporal, higher order (DMN) RSNs, lower order (sensory and motor) RSNs and thalmo-cortical networks, with mild propofol sedation.
- Identify other RSNs and evaluate changes in them, if any, with mild propofol sedation

5.4.3 Methods

This experiment was performed as a part of the data collection for experiments described previously (Chapter 3) and therefore the methods for participant inclusions (same as Section 3.4.3.1) monitoring, drug administration and sedation assessment (Section 3.4.3.2) were the same. The mean (SD) propofol target concentration was 0.95 (0.14) mcg/ml.

5.4.3.1 MRI data collection

Functional MRI data were collected using gradient-echo echo- planar imaging at 3T (GE Healthcare HDx) using a blood oxygen level- dependent (BOLD) (T2*)-weighted imaging sequence (TR =3 s, TE = 35 ms, matrix = 64 x 64, FOV/slice = 20.5 cm/3.2 mm, flip angle = 90°, 50 slices, 160 volumes). An eight-channel receive-only head coil was used. A T1-weighted whole-brain structural scan was also acquired (1 x1 x 1 mm voxels). For the purposes of accounting for physiological variance in the time-series data, end-tidal carbon dioxide, and end-tidal oxygen traces were recorded throughout

the experiment using a nasal cannula attached to a capnograph (AEI Technologies). Cardiac and respiratory cycles were recorded using the scanner's built-in photoplethysmograph and a pneumatic chest belt, respectively.

All participants were instructed to keep their eyes closed and try not to fall asleep and think of nothing in particular.

5.4.3.2 MRI data analysis

Preprocessing

Several sources of physiological variance were removed from each individual subject's time-series fMRI data. For each subject, physiological noise correction consisted of removal of time-locked cardiac and respiratory artefacts (two cardiac harmonics and two respiratory harmonics plus four interaction terms), using linear regression (Glover et al., 2000), and of low-frequency respiratory and heart rate effects (Birn et al., 2006; Shmueli et al., 2007; Chang and Glover, 2009). In addition, regressors formed from end-tidal CO_2 and O_2 traces were also removed (Murphy et al., 2011).

Following this part of preprocessing (physiological noise correction), this data was further analysed using three different and independent analytical approaches.

Low frequency BOLD correlations between different brain regions were investigated using

1. Seed based functional connectivity analyses
2. Independent components based– functional connectivity analysis

5.4.3.2.1 Seed based functional connectivity analysis

For group analysis, a two-step registration process was performed. fMRI data were registered first from functional space to individual subjects' structural space and then to a standard space (Montreal Neurological Institute MNI152 standard map) using FLIRT (FMRIB's Linear Registration Tool). Finally, data were spatially smoothed (5 x 5 x 5

mm full-width half-maximum Gaussian kernel). Connectivity analysis was done in standard space.

Bilateral motor cortex and bilateral sensory cortex seeds were derived from the Harvard-Oxford cortical probabilistic atlas. Similar region of interest (ROI) masks were generated for the following using the Harvard-Oxford subcortical probabilistic atlas.

- Posterior cingulate cortex (PCC)
- Thalamus

Voxel-wise correlation maps from the timeseries of each ROI with whole brain grey matter was generated using a Matlab based script, using NIFTY tools This correlation map was converted to a Z map by a Fisher's transformation.

These maps were then used for second level analysis in SPM 8, implemented in Matlab, and paired t-tests (between *Awake* and *Sedated* conditions) were performed. Results reported are of clusters that survived a random field cluster threshold of $p<0.05$ (family-wise error (FWE) corrected) for the entire brain (or cluster threshold of $p<0.001$, uncorrected, where stated). These results are reported using the height threshold *P* value less than 0.001 (uncorrected) at the voxel level and extent threshold *P* value less than 0.05 (FWE corrected) at the cluster level.

5.4.3.2.2 Independent Component (model free) functional connectivity analysis

Multivariate Exploratory Linear Optimized Decomposition into Independent Components (MELODIC) ICA (Independent Component Analysis) data exploration option was used in FSL. Multi-session temporal concatenation option was used and automatic dimensionality was used to identify possible components. No limit was set to the number of components to be identified. This was done due to the exploratory nature of this analysis. This decomposed the data into a set of 44 time courses and associated spatial maps that jointly describe the temporal and spatial characteristics of underlying hidden signals (components) using probabilistic independent component analysis. These

components were visually inspected and matched with previously reported RSNs and 6 probable networks identified, for further analysis.

In diseased brains (such as following stroke) the shape of the haemodynamic response may be altered (Carusone et al., 2002, Rossini et al., 2004). This may produce a reduced or even negative BOLD response. Similarly pharmacological conditions, which may reduce cerebrovascular reactivity or cerebral blood flow, may alter the BOLD response. These conditions may affect ICA based techniques where multi subject comparisons are being made. Forward estimation in multi subject group ICA employs various assumptions such as spatial and/ or temporal consistency at the group level. These assumptions may not be valid in diseased brains or those where networks are likely to be degraded. Single subject ICA followed by group analysis and then attempt to combine the output into a group *post hoc* by spatial correlation, or similar techniques, may be required in such scenarios (Calhoun and Adali, 2012). MELODIC, as used above, using temporal concatenation assumes spatial consistency, which is a valid assumption considering the healthy brains being studied, lack of effect of mild propofol sedation on haemodynamics and a within-subject comparison.

The set of spatial maps from the group-average analysis was used to generate subject-specific versions of the spatial maps, and associated timeseries, using dual regression (Filippini et al., 2009, Beckmann et al., 2009). First, for each subject, the group-average set of spatial maps is regressed (as spatial regressors in a multiple regression) into the subject's 4D space-time dataset. This results in a set of subject-specific timeseries, one per group-level spatial map. Next, those timeseries are regressed (as temporal regressors, again in a multiple regression) into the same 4D dataset, resulting in a set of subject-specific spatial maps, one per group-level spatial map. Voxel-wise analyses of the group differences between the *Awake* and the *Sedated* states (paired t-test) was carried out using FSL randomised nonparametric permutation-testing (Winkler et al., 2014) with 10000 permutations for each independent component of interest. Threshold-free cluster enhancement was used to control for multiple comparisons and the significance threshold was set to $P < 0.05$ corrected for family-wise error. The results characterised the probabilistic statistical maps, representing the group differences in functional connectivity for all RSNs of interest. The statistical maps were then

upsampled to a standard MNI 1-mm brain Montreal atlas to better localise the areas of RSN alterations. The Harvard–Oxford cortical and subcortical atlases (Harvard Centre for Morphometric Analysis), which are provided with the FSL software, were used to identify the anatomical representation of the clusters of the resulting probabilistic independent component analysis maps that showed significant differences between the two groups.

5.4.4 Results

All 15 participants were sedated to the desired level (OAA/S level of 4; mild sedation) during the *Sedated* state scanning. There was a significant slowing of the visual and auditory reaction times, as described previously in Section 3.4.4 (Table 3-2: Reaction times). There was no change in HR, BP, oxygen saturation or expired CO_2 as described previously in Section 3.4.4 (Table 3-1: Physiological Data). The mean (SD) propofol target concentration was 0.95 (0.14) mcg/ml.

5.4.4.1 ROI seed based functional connectivity

Seeds based in bilateral motor cortices showed a reduced connectivity with the right lateral occipital cortex but an increased connectivity with the right thalamus during sedation (Figure 5-1, Table 5-1). Sensory cortices showed a reduced connectivity with the lateral occipital cortices bilaterally, and middle temporal gyrus (right) while it showed an increased connectivity with the thalamus (Figure 5-2 , Table 5-2).

The seed based in the bilateral thalami showed a decreased connectivity with the left sided posterior cingulate and anterior cingulate cortices, paracingulate gyrus and superior frontal gyrus. There was an increase in connectivity with the superior temporal gyrus, planum temporale and postcentral gyrus (Figure 5-3, Table 5-3). The seed based in PCC (representing the key node of DMN) showed a reduced functional connectivity with the frontal pole and there was no increase in functional connectivity with sedation (Figure 5-4, Table 5-4).

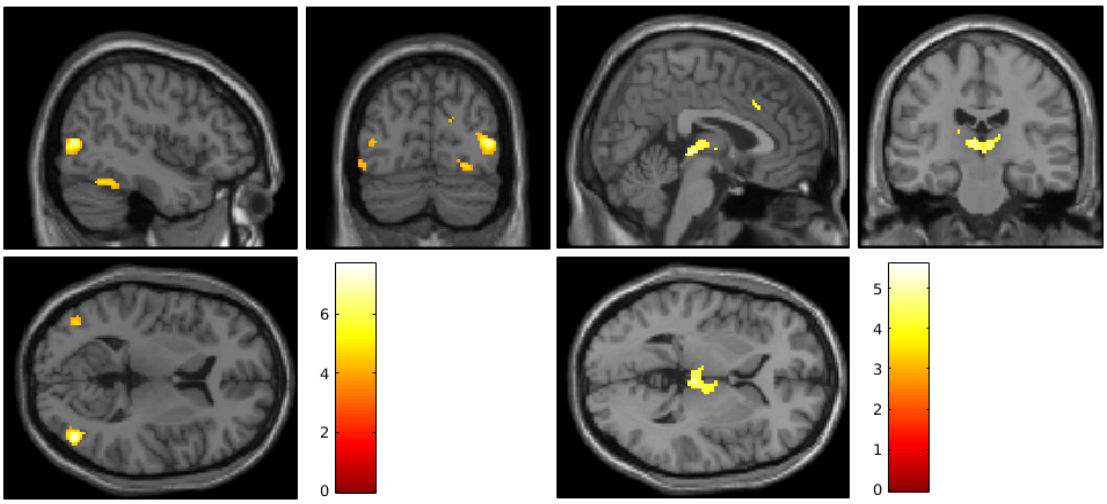

Figure 5-1: Significant Motor cortex connectivity for *Awake > Sedated* and *Sedated > Awake*)

Results shown superimposed on a standard T1 weighted structural image. Cluster level (extent threshold 10 voxels), FWE p≤0.05. Colour bar indicates strength of connectivity (t score).

Table 5-1: Significant connectivity peaks for the Motor network
Co-ordinates are reported, in MNI space (mm). L, Left; R, Right

Motor network						
	Brain regions	P value (FWE corrected : cluster level)	T values	MNI coordinates (mm)		
Awake > Sedated (i.e. functional connectivity reduces with sedation)	Lateral occipital cortex (R)	0.033		46	-76	8
Sedated > Awake (i.e. functional connectivity increases with sedation)	Thalamus (R)	0.001		4	-26	0

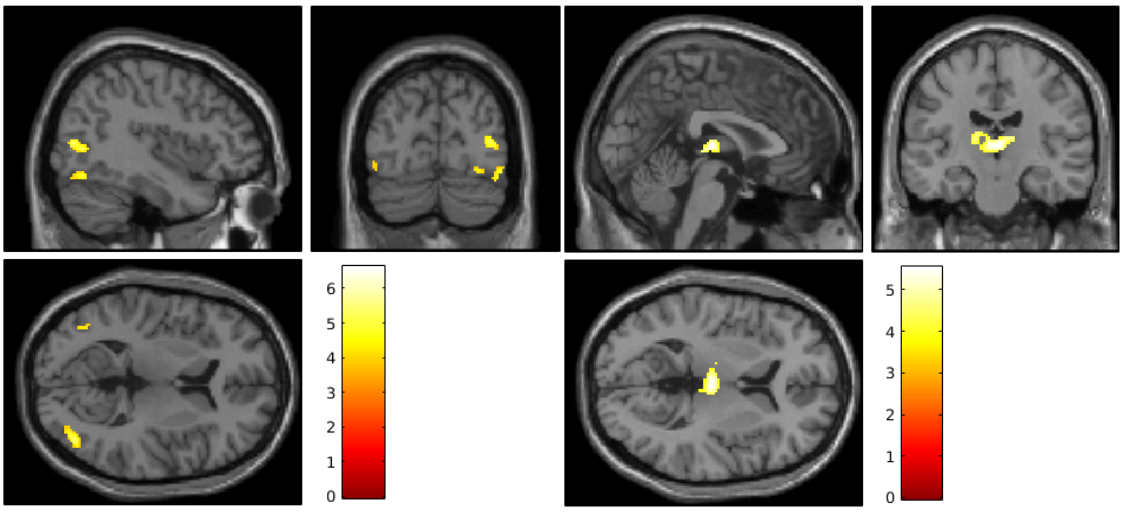

Awake > Sedated

Sedated > Awake

Figure 5-2: Significant Sensory cortex connectivity for *Awake > Sedated* and *Sedated > Awake*)

Results shown superimposed on a standard T1 weighted structural image. Cluster level (extent threshold 10 voxels), FWE p≤0.05. Colour bar indicates strength of connectivity (t score).

Table 5-2: Significant connectivity peaks for the Sensory network
Co-ordinates are reported, in MNI space (mm). L, Left; R, Right

Sensory network						
	Brain regions	P value (FWE < 0.05) (cluster level)	T values	MNI coordinates		
Awake > Sedated (i.e. functional connectivity reduces with sedation)	Lateral occipital cortex (L)	0.007		-52	-68	-4
	Lateral occipital cortex, middle temporal gyrus (R)	0.012		48	-70	-18
Sedated > Awake (i.e. functional connectivity increases with sedation)	Thalamus (R)	0.004		0	2	-18
	Thalamus (L)			0	-14	10

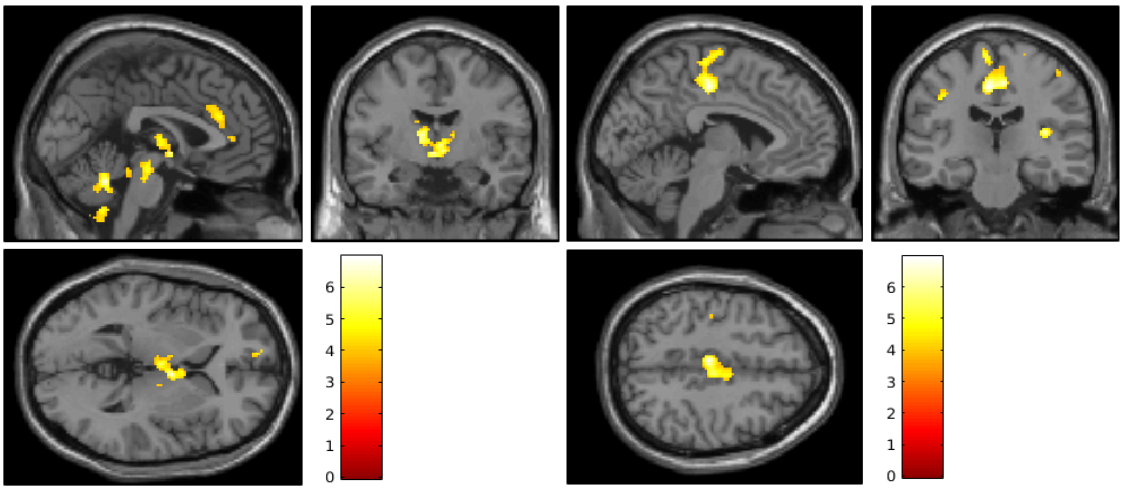

Awake > Sedated

Sedated > Awake

Figure 5-3: Significant Thalamus connectivity for *Awake > Sedated* and *Sedated > Awake*)

Results shown superimposed on a standard T1 weighted structural image. Cluster level (extent threshold 10 voxels), FWE p≤0.05. Colour bar indicates strength of connectivity (t score).

Table 5-3: Significant connectivity peaks for the Thalamus
Co-ordinates are reported, in MNI space (mm). L, Left; R, Right

Thalamus						
	Brain regions	P value (FWE < 0.05) (cluster level)	T values	MNI coordinates		
Awake > Sedated	PCC, ACC (L)	0.001	5.29	-4	18	32
	ACC, Paracingulate gyrus (L)	0.001	4.96	-2	30	24
	paracingulate, superior frontal gyrus (L)	0.001	4.71	-10	36	30
	PCC, precentral gyrus, ACC	0.000	6.8	-4	-22	46
	Precentral gyrus, PCC, SMA	0.000	6.6	6	-20	50
	precentral gyrus, SMA,	0.000	5.89	-6	-20	72

Sedated > Awake	anterior/ posterior superior temporal gyrus, planum temporale	0.043	5.28	66	-4	-4
	temporal pole,	0.043	4.83	60	10	-6
	central opercular cortex, postcentral gyrus, planum temporale	0.043	4.23	66	-10	10

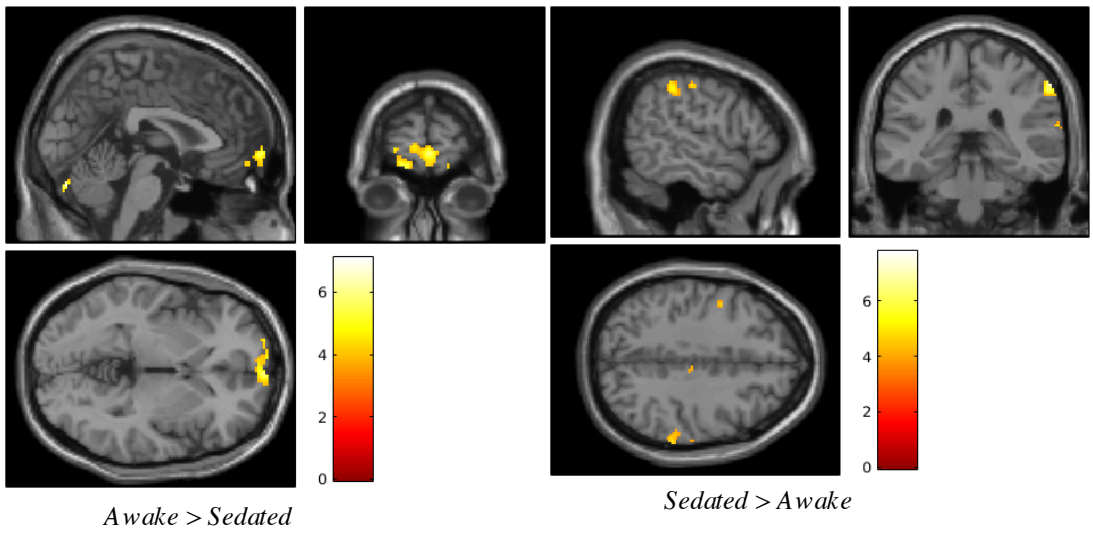

Awake > Sedated *Sedated > Awake*

Figure 5-4: Significant PCC connectivity for *Awake* > *Sedated* and *Sedated* > *Awake*)

Results shown superimposed on a standard T1 weighted structural image. Cluster level (extent threshold 10 voxels), FWE p≤0.05. Colour bar indicates strength of connectivity (t score).

Table 5-4: Significant connectivity peaks for the PCC
Co-ordinates are reported, in MNI space (mm). L, Left; R, Right

Posterior Cingulate Cortex						
	Brain regions	P value (FWE < 0.05) (cluster level)	T values	MNI coordinates		
Awake > Sedated	Frontal pole	0.008	5.97	4	66	16

5.4.4.2 ICA based RSN changes

Among the potential RSNs identified, Right fronto-parietal network (Figure 5-5) demonstrated a significant change (Figure 5-6) between the *Awake* and *Sedated* states.

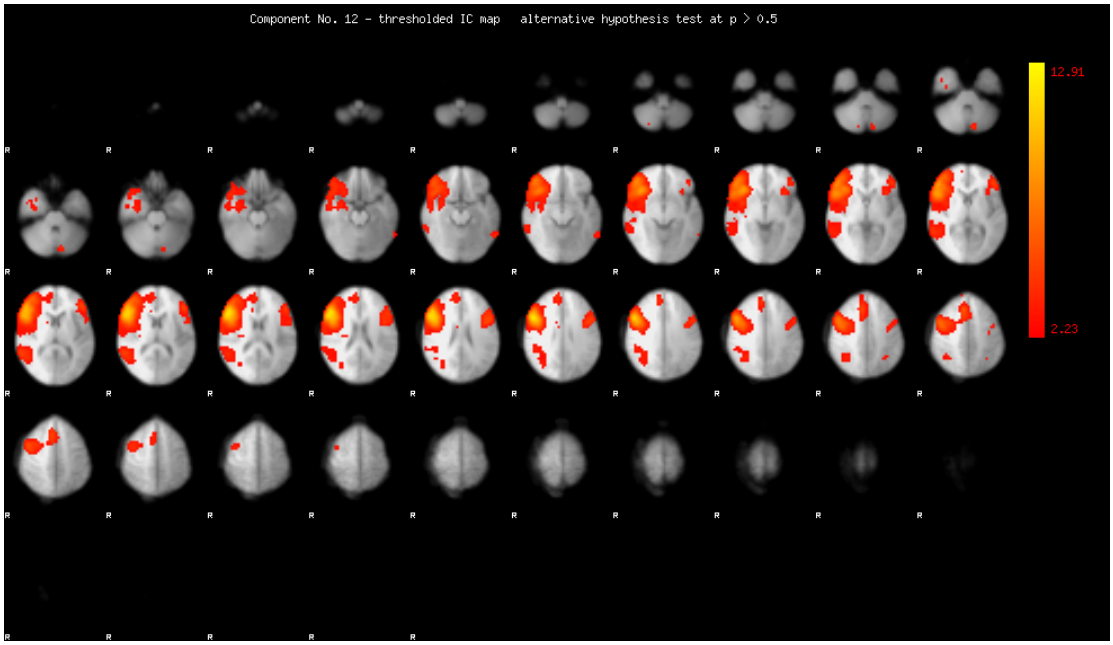

Figure 5-5: Right fronto-parietal network: IC map

Resting state network identified which was used for dual regression analysis. Results shown superimposed on a standard T1 weighted structural image. Colour bar indicates strength of connectivity (t score)

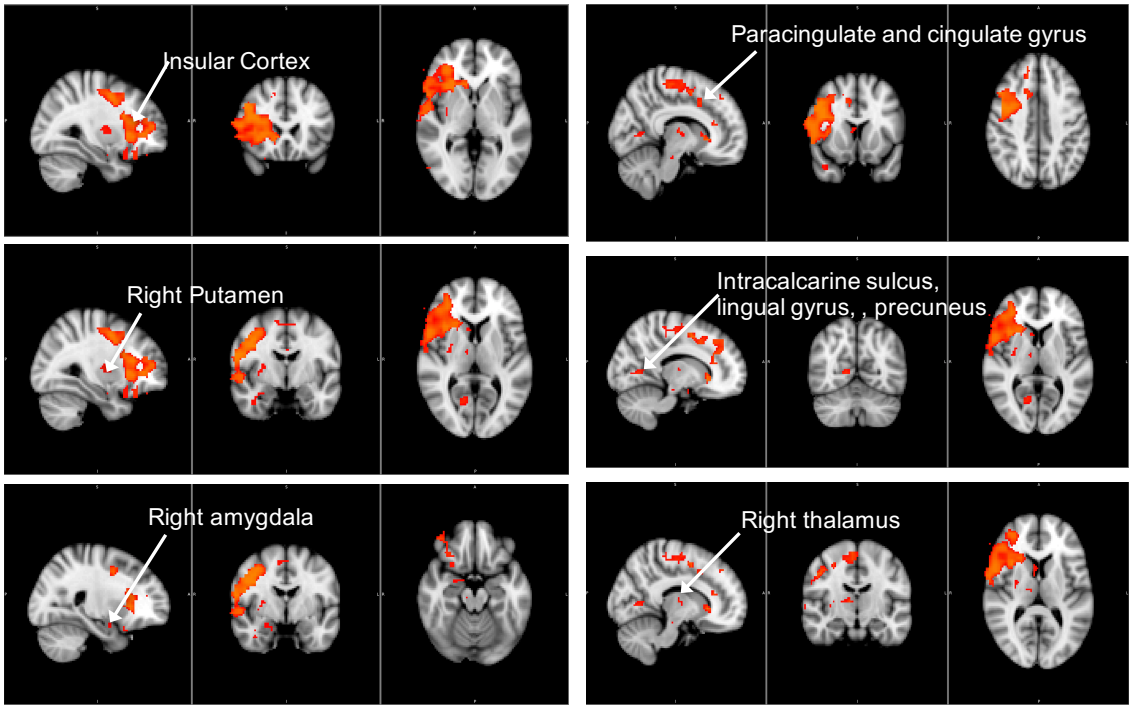

Figure 5-6: Changes in Right fronto-parietal network Fc: *Sedated > Awake*

Output of Randomise analysis. Shows the areas more connected with right fronto-parietal network. Results shown superimposed on a standard T1 weighted structural image. TFCE, FWE corrected at $p<0.05$.

5.4.5 Discussion

5.4.5.1 ROI seed based functional connectivity

The hypothesis driven (seed based) functional connectivity analysis revealed significant changes in the connectivity of the DMN and the thalamo-cortical connectivity. Functional connectivity of PCC (key region of the DMN) was reduced with the frontal pole with sedation while the thalamus was less functionally connected to the regions of the DMN, ACC, and the motor cortex. There was also increased thalamic connectivity with the superior temporal gyrus and sensory cortices. The primary sensory and motor cortices showed a reduced functional connectivity with the occipital cortex while it increased with the thalamus.

5.4.5.1.1 Lower order RSNs

Primary cortical regions are involved in the initial processing of their respective stimuli. However, further processing involves adjacent regions and further cross-regional interactions result in the overall perception. Haptic perception occurs through integration of different sensations, such as vision and touch. Lateral occipital cortex links with somatosensory cortices to facilitate this cross-modal integration (Lacey and Sathian, 2015, Negyessy et al., 2006). Sedation is commonly associated with loss of attention and perception (though not explicitly tested in this experiment). It is therefore not surprising to find a reduction in connectivity between the sensory cortex and the lateral occipital cortex. Similar cross-modal visuo-motor interaction allows for activities such as hand-eye coordination which are usually disrupted in states of altered consciousness (Sanders et al., 1991).

Previous work on propofol sedation has been lacking in this area, however neuroimaging studies with other sedative agents have shown similar results (Liang et al., 2015, Martuzzi et al., 2010). Sub-anaesthetic doses of sevoflurane, resulted in a decreased connectivity between the somatosensory cortex and the extra-striate visual areas while its connectivity with thalamus was increased (Martuzzi et al., 2010). Midazolam sedation resulted in an increased within network functional connectivity of

somato-motor and other primary networks (visual and auditory) (Liang et al., 2015, Greicius et al., 2003, Kiviniemi et al., 2005). Visual and auditory networks were shown to be maintained during varying doses of propofol sedation (Boveroux et al., 2010). Interestingly, Jordan et al (2013a) demonstrated an increased functional connectivity in the visual and auditory networks at higher (anaesthetic) doses of propofol. While the results from other research cannot be generalized to this experiment's results, due to differences in drugs, doses, methodology or analytic techniques, they generally point towards a maintained network connectivity of the primary RSNs.

5.4.5.1.2 Default mode network

PCC was used as a seed region (key hub of DMN) to assess changes in DMN functional connectivity with mild sedation. Once again, previous literature is variable in this respect. While Boveroux et al (2010) and Liu et al (2015) found a disruption in DMN functional connectivity, with propofol sedation, Guldenmund et al (2013) did not. A reduction in functional connectivity of the PCC with the frontal pole was observed in this experiment. Stamatakis et al (2010) also found a reduced connectivity of PCC with medial frontal areas, at mild sedation, however at deeper levels, surprisingly, they found increased connectivity of PCC with non-DMN areas, including motor/ sensory cortices, anterior thalamic nuclei and the reticular activating system. Co-activation patterns of PCC when studied with propofol demonstrated reduced frontal activations during sedative and anaesthetic doses, in a dose dependent manner (Amico et al., 2014). The authors also reported reduced co-activations with other cortical regions such as auditory, visual and motor cortices and thalamus. Increased connectivity of precuneus (another component of DMN) has also shown during propofol sedation, albeit during a non-resting state (auditory task) (Liu et al., 2014).

Other sedative drugs have also revealed similar results, midazolam (GABA-ergic drug, similar to propofol) sedation showing reduced functional connectivity in the DMN (Greicius et al., 2003) while there was no change with sevoflurane (Martuzzi et al., 2010). This suggests a dose or drug related effect on DMN's connectivity and the findings of this experiment are generally supported by previous literature.

5.4.5.1.3 Thalamo-cortical functional connectivity

In this experiment, functional connectivity of thalamus was reduced with the PCC (key hub of the DMN) and the ACC while it was increased with the superior temporal gyrus and the primary somatosensory cortex. This is in concordance with the results of Boveroux et al (Boveroux et al., 2010), who found preserved thalamo-cortical connectivity with primary RSNs, but reduced with the DMN. Their findings were more prominent at deeper stages of propofol sedation (although, not significant at mild sedation) but point in a similar direction of differential, thalamo-cortical dissociation associated with sedation. An increase in thalamic connectivity was found with auditory, insular, primary sensory, primary motor and SMA, during mild propofol sedation (Guldenmund et al., 2013), similar to the findings of this experiment, suggesting a dis-inhibitory influence of propofol in the thalamic relationship with these primary cortical regions. During an auditory and noxious stimulation, thalamo-cortical connectivity was found preserved, while putamen's connectivity was reduced (Mhuircheartaigh et al., 2010). Using graph- theoretical analyses and support vector machine classification, Monti et al (Monti et al., 2013) demonstrated an increased thalamo-cortical connectivity during sedation which was followed by a breakdown, during unconsciousness. While this study did not investigate the selectivity of thalamo-cortical connections, it suggested altering thalamo-cortical activity as sedation progressed. Breakdown of thalamo-cortical connectivity has been demonstrated in other studies too, although at higher doses of propofol (Schroter et al., 2012, White and Alkire, 2003).

These changes in thalamo-cortical connectivity with sedation may appear somewhat contradictory. While some of these variations can be accounted for by differences in experimental and analytic methodology, part of the problem may stem from treating the thalamus as a single entity and not discriminating between its different nuclei (specific and non-specific nuclei) which have different relationships with different cortical regions and therefore different roles. The specific thalamic nuclei are related to the visual, sensory and auditory pathways while the non-specific are more related to arousal, sleep-wake cycles. Liu et al (2013) studied the functional connectivity of the groups of thalamic nuclei specific (medial dorsal, ventral lateral, ventral posterior, and other) and nonspecific (centromedian and parafascicular) thalamic nuclei, under

propofol sedation. They found that specific thalamic nuclei had connectivity mainly with medial and bilateral frontal and temporal cortex while the non-specific nuclei had connectivity with the medial frontal and medial parietal cortex. Deep sedation was associated with greater changes in the functional connectivity of the non-specific nuclei than specific, suggesting a differential effect of propofol on these nuclei.

5.4.5.2 ICA based functional connectivity

Further exploratory analysis was done to detect changes, if any, in other networks, using independent components analysis.

5.4.5.2.1 Right lateral fronto-parietal network

ICA revealed a lateralized (right) fronto-parietal network, which showed an increased functional connectivity following sedation. This increase in connectivity occurred with regions within the network and also those outside the network (Figure 5-5, Figure 5-6).

Dorsolateral fronto-parietal networks are also known as executive control networks, which show increased connectivity as attention increases or a task is initiated. During deeper stages of sedation and unconsciousness, loss of attention correlates with this loss of fronto-parietal connectivity (Jordan et al., 2013b, Monti et al., 2013, Schrouff et al., 2011). Once again, there is paucity of literature specific to mild sedation. Boveroux et al (2010) found a decreased connectivity in lateralized fronto-parietal networks, correlating with the depth of propofol sedation. Similarly, a reduced fronto-parietal connectivity was shown with mild midazolam sedation (Liang et al., 2015).

The findings of this experiment are therefore surprising, but interesting. Boveroux et al (2010) used a ROI based analysis to study changes in RSNs. Their findings with fronto-parietal RSNs were more significant during the deeper stages of sedation but not during mild sedation. They had similar results with ICA based analysis where there was a trend towards significance, but not strong enough to survive multiple corrections. It is therefore likely that these changes in fronto-parietal networks are a dose (or sedation level) related effect but that these changes might not have been observable at mildly

sedative levels. If fronto-parietal functional connectivity is seen as a correlate of attention, it is possible that in this experiment, the volunteers, although mildly sedated, were 'trying to stay awake' and thus trying to be attentive, and potentially confounding the results. It is also possible that this may be a natural, compensatory mechanism of the brain to try and avoid loss of attention, before the 'breakdown' occurs. Alternatively, a dis-inhibitory effect on other influences on the fronto-parietal regions, as a precursor to deepening levels of sedation may be responsible for this emerging hyper-synchronicity in these regions, prior to a disruption in connectivity.

5.4.6 Potential limitations of the experiment

There are certain limitations of this experiment. Some of these, including the possibility of an order effect, lack of a range of doses etc. have been discussed previously (Section 3.6) and apply to this experiment too. Comparability of results with previous literature is limited by potential difference in drugs used, doses of propofol (when propofol was the drug) used and the methods of assessing sedation. The basis of BOLD signal depends on an assumption of neurovascular coupling. This may be altered in pharmacological studies. However, at mildly sedative doses of propofol, there were no significant change in haemodynamics or respiratory parameters and neurovascular coupling is likely to have been maintained.

Low frequency oscillations, arising from cardiac and respiratory fluctuations (physiological noise) may result in false connectivity results. In this experiment, physiological noise correction was performed to reduce such confounds. While physiological noise correction increases the robustness and validity of connectivity results, certain correction techniques can itself induce false correlations and may reduce inter and intra-subject variability (Birn et al., 2014, Khalili-Mahani et al., 2013).

The seed regions in the seed-based functional connectivity analyses, were chosen using standard atlas tools to delineate the regions of interest. Seed regions may be chosen based on anatomical knowledge or functional (determined following a functional task) and can range from a few voxels to well-defined anatomical regions. Different methods of choosing regions of interest can influence the connectivity results (Cole et al., 2010)

and can limit the comparability of results. ICA results reduce this element of 'subjectivity' by using a model free analysis. In this experiment, however, ICA did not produce similar results as the SCA did. The only significant change detected was also not corrected for the number of networks identified, due to the exploratory (no 'a priori' hypothesis) nature of the analysis. It is possible that this ICA result would not have survived such a correction.

5.5 Experiment 2

5.5.1 Introduction

MEG has been used to study neuro-pharmacological effects (Carhart-Harris et al., 2013) including that of benzodiazepines (Hall et al., 2010), however no previous study has targeted specific alterations in consciousness including sedation or anaesthesia. However, EEG changes induced with propofol sedation have been well studied. EEG changes during propofol sedation include a reduction in posterior alpha band power, an increase in frontal alpha and an increase in beta power. With increasing doses of sedation resulting in anaesthesia, alpha and beta bands disappear and an increase in delta and theta power occurs (Veselis, 1996).

Traditional EEG equipment is less likely to be able to provide enough spatial information to perform coherence analyses to identify RSNs. More recently, high density EEG equipment has allowed researchers to interrogate spatial coherence patterns successfully. MEG due to its large number of channels provides better spatial resolution and avoids potential artefacts due to conduction issues and possible muscle activity. This has allowed studies of functional connectivity. As discussed previously, RSNs similar to those found on BOLD-fMRI have been demonstrated using ICA based techniques (Brookes et al., 2011b).

Based on the fMRI literature (Section 5.2) it was expected to find reduction in functional connectivity of the higher order networks, such as the DMN. This experiment was an exploratory attempt to test if RSNs can be identified in different oscillatory bands, with MEG and whether their changes with sedation reflect those from the fMRI literature.

5.5.2 Aims

The aims of experiment 2 were to identify the MEG signal based spatio-temporal RSNs in the different frequency bands and evaluate the changes in those networks, with mild propofol sedation.

5.5.3 Methods

This experiment was performed as a part of the data collection for experiments described previously (Chapter 3) and therefore the methods for participant inclusions, monitoring, drug administration and sedation assessment were the same as stated in part (Section 3.4.3.2).

5.5.3.1 MEG acquisition and analysis

Whole head MEG recordings were made using a CTF 275-channel radial gradiometer system sampled at 1200 Hz (0–300 Hz bandpass). An additional 29 reference channels were recorded for noise cancellation purposes and the primary sensors were analysed as synthetic third-order gradiometers (Vrba and Robinson, 2001). Three of the 275 channels were turned off due to excessive sensor noise. At the onset of each stimulus presentation a TTL pulse was sent to the MEG system. Participants were fitted with three electromagnetic head coils (nasion and pre-auriculars), which were localised relative to the MEG system immediately before and after the recording session.

5.5.3.1.1 Pre-processing of resting state data.

Five minutes of resting state data was obtained during the *Awake* and *Sedated* sessions. Volunteers were instructed to keep their eyes closed and try not to think of anything in particular. This recording was high-pass filtered at 1Hz and segmented into epochs of 2s in length. There were therefore 150 epochs in each dataset for analysis. Each epoch was visually inspected, and those with gross artefacts (e.g., head movements, jaw clenches) were removed from the analysis. All subsequent analyses were performed on these cleaned datasets.

5.5.3.1.2 Frequency analysis: sensor space

Using the FieldTrip toolbox (Oostenveld et al., 2011) MEG data was converted to planar gradient configuration, and then a frequency analysis of the individual vector directions was conducted. Frequency analysis was conducted using Hanning windowed

fast Fourier transforms between 1 and 100 Hz at 0.5 Hz frequency intervals and then the planar directions combined to give local maxima under the sensors. Analysis of sensor-level MEG data in a planar gradient (spatial-derivative) configuration has the advantage of easy interpretability, because field maps can be interpreted as having a source directly underneath field maxima (Bastiaansen and Knosche, 2000). For statistical analysis, individual spectra were divided into the following frequency bands: delta (1–4 Hz), theta (4–8 Hz), alpha (8–13 Hz), beta (13–30 Hz), low gamma (30–49 Hz), and high gamma (51–99 Hz). The differences between *Sedated* and *Awake* states were tested using permutation testing of *t* statistics at each time point (Maris and Oostenveld, 2007, Nichols and Holmes, 2002). The Type 1 error rate was controlled using cluster randomization analysis with an initial cluster-forming threshold of $p = 0.05$ repeated >5000 permutations.

5.5.3.1.3 Independent component network analysis of functional connectivity

For analysis of oscillatory networks, methodology similar to that described in Brookes et al. (Brookes et al., 2011b) was utilised. For each participant and frequency band, beamformer weights were computed on an 8 mm grid based on the preprocessed dataset. Beamformer time courses were then generated at every voxel and normalized by an estimate of the projected noise amplitude at that voxel. The Hilbert transform was applied to each voxel time course, and the absolute value was computed to generate an amplitude envelope of the oscillatory signals in each frequency band. The data at each voxel was down-sampled to an effective sampling rate of 1 Hz, transformed to standard (MNI) space using FLIRT in FSL, and data from all subjects were concatenated in the time dimension across subjects. Temporal independent component analysis (ICA) was applied to the concatenated datasets (separately for all six frequency bands) using the fast ICA (research.ics.tkk.fi/ica/fastica) algorithm.

Prewhitening was applied to reduce the dimensionality of the source space Hilbert envelope signals to 20 principal components before ICA (Brookes et al., 2011b, Hall et al., 2013, Hyvarinen and Oja, 2000). Fifteen independent components were derived for

each frequency band. The spatial signature of each tIC (i.e., the maps shown in Fig. 1) was measured by Pearson correlation between the tIC and the time course of each voxel in the concatenated dataset. From these components we identified those that matched previous reports (Brookes et al., 2011b, Muthukumaraswamy et al., 2013). Five possible networks were identified. For these components, we computed the SD of the component time course for each subject and condition. Differences in the SD of the independent component time course between *Awake* and *Sedated* states were assessed using paired t-tests. Results are presented for those networks demonstrating statistical significance for change ($p < 0.01$, uncorrected for multiple comparisons). Other networks identified, without significant changes, have also been displayed for information purposes.

5.5.4 Results

There were no differences in the haemodynamic and ventilator parameters between the *Awake* and *Sedated* groups. The mean (SD) propofol target concentration was 1.07 (0.19) mcg/ml. There was a significant reduction in reaction times during the *Sedated* state (Section 3.5.6.1).

5.5.4.1 Sensor level changes

There was a significant reduction in the theta power in the frontoparietal regions and the alpha band power in the posterior (occipital) regions. There was a global increase in beta power, low gamma power and central increases in high gamma power, during sedation (**Error! Reference source not found.**).

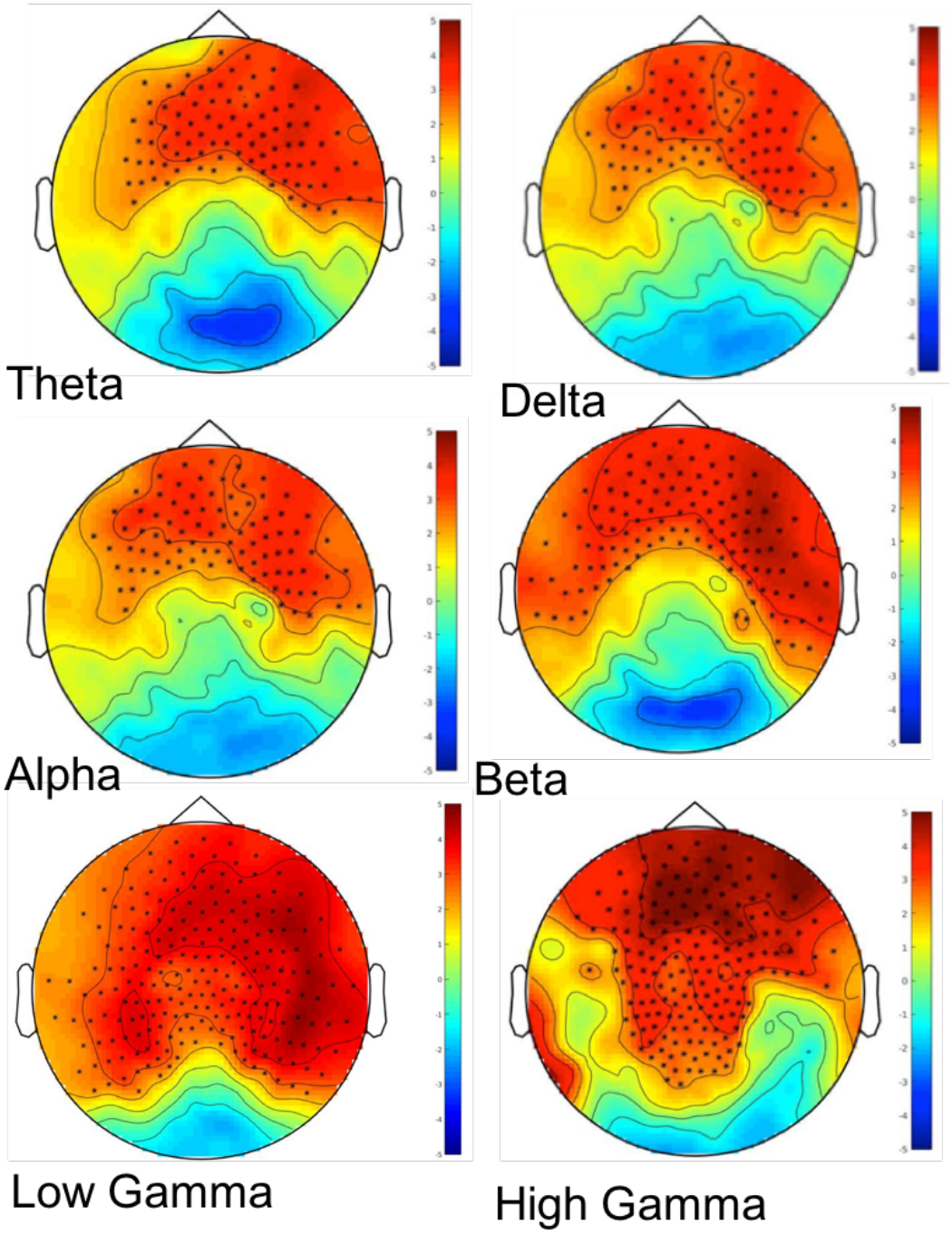

Figure 5-7: Sensor level oscillatory power changes (*Awake* vs *Sedated*)

Topographical maps of the planar gradiometer configured MEG data: Changes (paired t-tests between *Awake* and *Sedated* states): Delta= 1-4 Hz, Theta= 4-8 Hz, Alpha= 8-13 Hz, Beta= 13-30 Hz, Low gamma =30-50Hz, High gamma = 50-100 Hz. The colour bars represent the change in power, from baseline (warm colours represent an increase while cooler colours represent a decrease). Units are t statistics. Significant sensor clusters are marked with crosses, $p<0.05$.

5.5.4.2 Resting state networks

The ICA methodology revealed a number of functional brain networks. These spatial maps represent temporally independent time signals extracted from MEG Hilbert envelope data via temporal ICA. Networks in different frequency bands (identified, on visual matching with known networks (Brookes et al., 2011b, Muthukumaraswamy et al., 2013)) are displayed below (Figure 5-8, Figure 5-9, Figure 5-10, Figure 5-11) and their changes, listed in Table 5-5.These networks have been displayed as correlation maps between the temporal independent component and the time course of each voxel of the concatenated dataset, thresholded at 0.3 or 0.4 (for visualisation purposes).

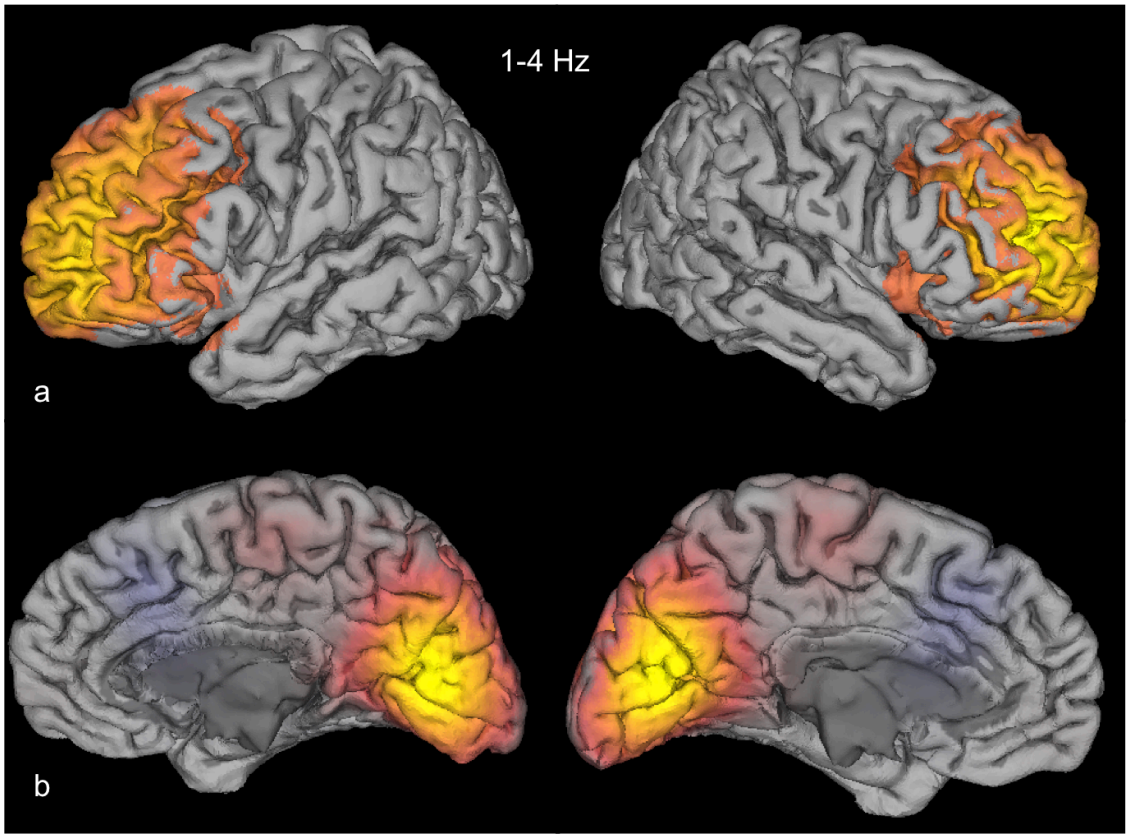

Figure 5-8: Localization of MEG resting-state networks altered by propofol sedation, for the delta band (1-4 Hz)
These consisted of bilateral frontal (a) and bilateral occipital (b) networks. Images show absolute ICA weights (in a.u.) thresholded at a correlation coefficient value of 0.3. Increased functional connectivity was seen in both networks: *Sedated* > *Awake*

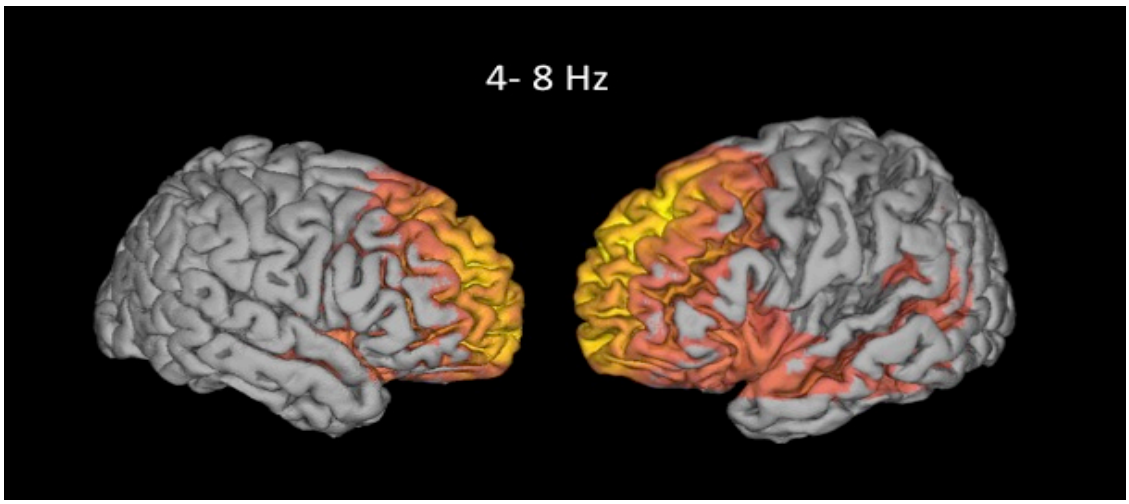

Figure 5-9: Localization of MEG resting-state networks altered by propofol sedation, for the theta band (4-8 Hz)
These consisted of bilateral frontal networks. Images show absolute ICA weights (in a.u.) thresholded at a correlation coefficient value of 0.4. Increased functional connectivity was seen: *Sedated > Awake*

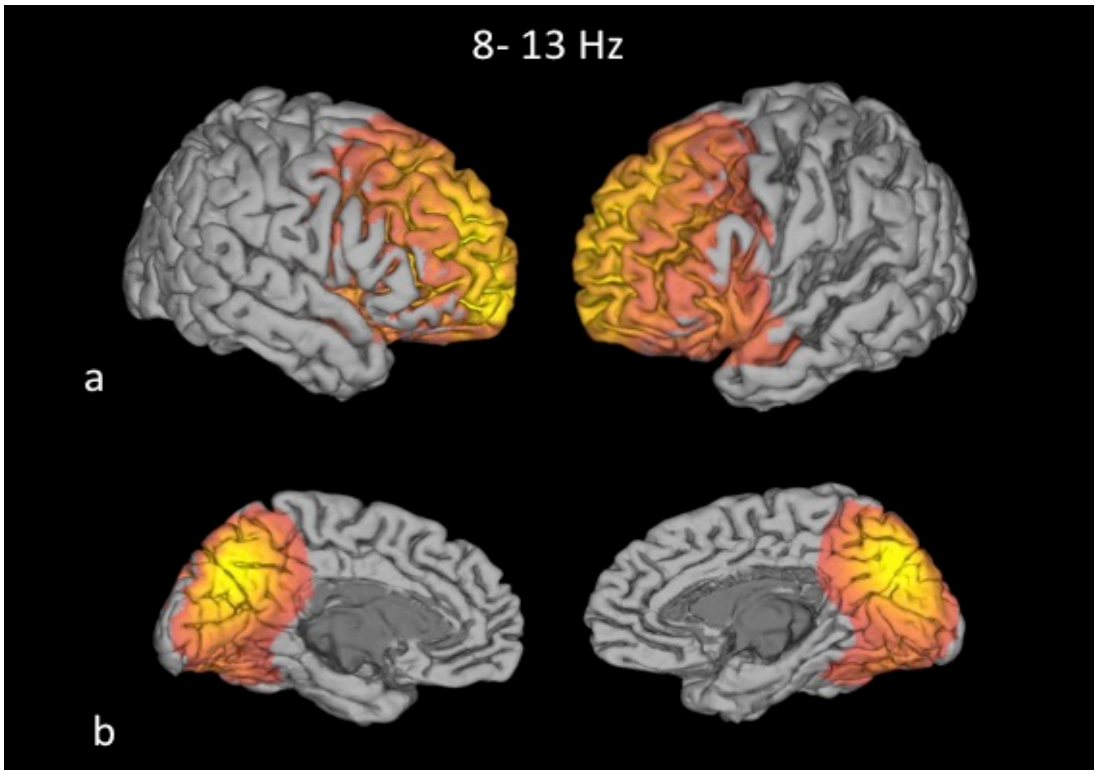

Figure 5-10: Localization of MEG resting-state networks altered by propofol sedation, for the alpha band (8-13 Hz)
These consisted of bilateral frontal (a) and bilateral parieto-occipital (b) networks. Images show absolute ICA weights (in a.u.) thresholded at a correlation coefficient value of 0.4. Increased functional connectivity was seen: *Sedated > Awake*

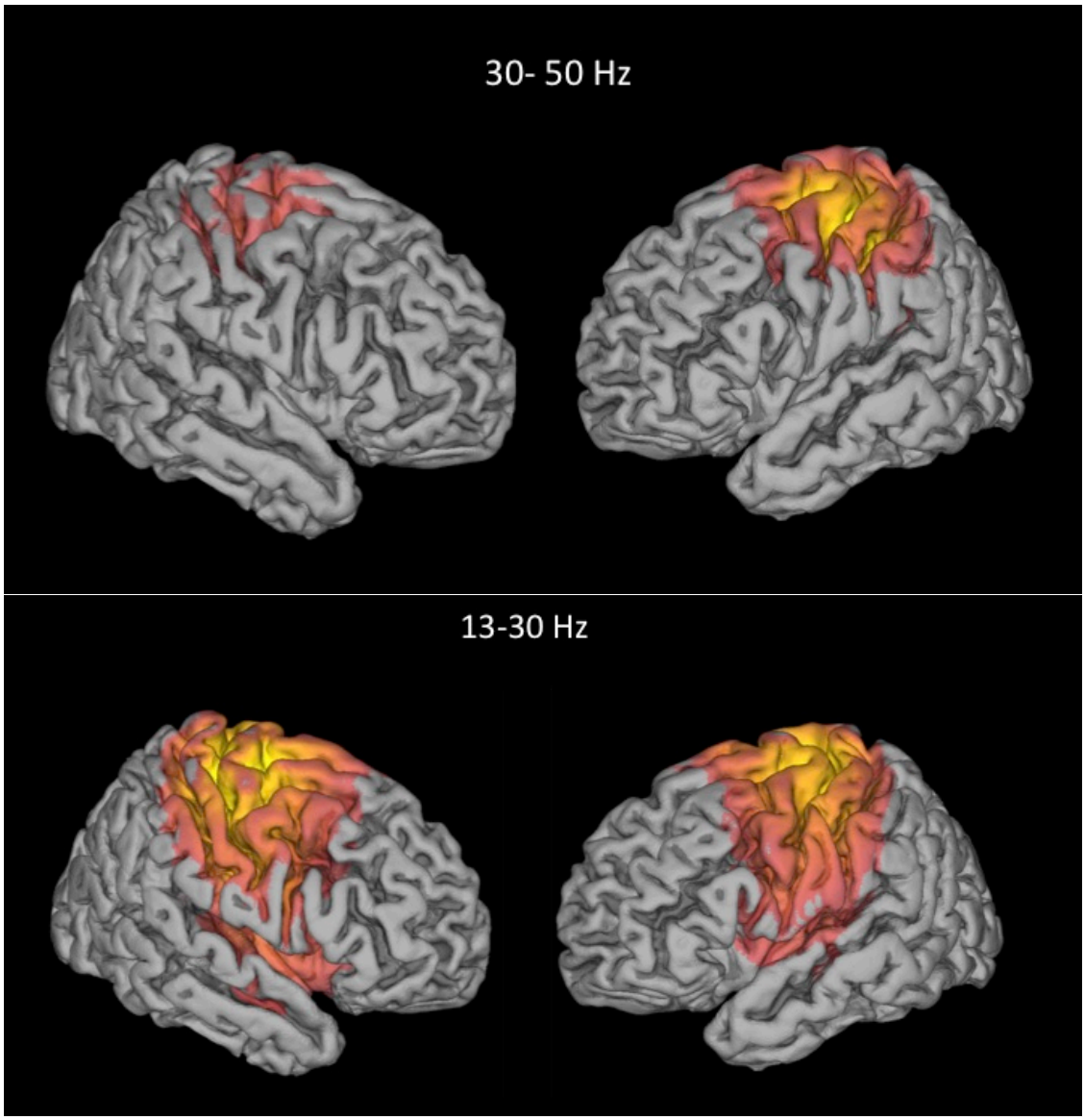

Figure 5-11: Localization of MEG resting-state networks altered by propofol sedation, for the beta band (13-30Hz) and gamma band (30-50 Hz)
These consisted of bilateral sensorimotor networks. Images show absolute ICA weights (in a.u.) thresholded at a correlation coefficient value of 0.3. No change in functional connectivity was seen.

Table 5-5: Summary of sensor space oscillatory power changes and independent component networks' functional connectivity changes: *Sedated* vs *Awake*

Sig= significant change. P values as stated, not corrected for multiple comparisons

	1-4 Hz	4-8 Hz	8-13 Hz	13-30 Hz	30-50 Hz
Sensor power	Increase fronto-parietal (sig)	Increase frontal (sig)	Increase frontal (sig)	Increase fronto-parietal and central (sig)	Increase frontal and central (sig)
Networks					
B/l frontal	Increase P = 0.0253	Increase P = 0.0064	Increase P = 0.0041		
B/l occipital	Increase P = 0.0268	No change			
B/l parietal		No change			
B/l occipito-parietal			Increase P = 0.0082		
B/l sensori-motor				No change	No change

5.5.5 Discussion

5.5.5.1 Spectral analysis of spontaneous activity

In this experiment mild propofol sedation resulted in a decrease in posterior alpha power while the anterior alpha power increases ('anteriorization' of alpha). There was also a global increase in beta power, decrease in fronto-parietal delta power while the frontoparietal theta activity increased.

While there are no MEG based studies in the literature, the findings here are broadly similar to those reported from EEG literature in relation to propofol sedation and effects of other GABA-ergic drugs. Propofol sedation has been associated with a decrease (Greene et al., 2007, Hashemi et al., 2015, Kishimoto et al., 1995, Doenicke et al., 2007), complete disappearance (Veselis, 1996) or no change (Sneyd et al., 1994) in the alpha band activity. The commonly reported decrease in typical (occipital) alpha is also associated with an increased frontal (anterior) alpha activity and this 'anteriorization' of the alpha band is similar to that found in this experiment. The neuronal mechanisms of these alpha rhythms have been well investigated. Both thalamo-cortical models (Ching and Brown, 2014, Ching et al., 2010b, Hashemi et al., 2015, Vijayan et al., 2013b) and cortical (Hutt, 2013, Spiegler et al., 2011) have been suggested to explain the generation and modulation of these rhythms. It has been suggested that the posterior (occipital) alpha and anterior (frontal) alpha rhythms are produced by two distinct mechanisms (Ching and Brown, 2014, Vijayan et al., 2013b). It has been suggested that increased GABA-A conductance and decreased lag time, by propofol, induces this alpha activity. Increased GABA-A conductance further involves the thalamus resulting in cortical synchrony (in the alpha range) and that the cells in the reticular nucleus synchronise disparate relay nuclei enabling synchrony over larger cortical areas. This is then further enhanced by reciprocal thalamo-cortical feedback loops (Ching et al., 2010b). Regarding the posterior alpha rhythm, it has been suggested that propofol attenuates the h-currents which alters the dynamics of the high threshold thalamo-cortical neurons which generate the posterior alpha, without affecting the frontal projecting neurons (Ching and Brown, 2014, Vijayan et al., 2013b). This differential response represents a distinct effect of propofol on the different thalamic nuclei resulting in different effects,

possibly similar to those reported in BOLD FMRI based studies (Liu et al., 2013). On similar lines, Hashemi et al (2015) proposed that alpha anteriorisation occurs due to fronto-occipital differences in non-linear gain function in cortico-thalamic relay circuits suggesting a role of propofol on those circuits.

Increased frontal beta band power was also demonstrated in this experiment as has previously been described by others (Feshchenko et al., 1996, Greene et al., 2007, Kishimoto et al., 1995, Sneyd et al., 1994, Veselis, 1996, Veselis and Reinsel, 1992). It has been suggested that an increase beta activity at sedative doses of propofol may be a result of the interactions between pyramidal cells with two types of interneurons (Ching and Brown, 2014, McCarthy et al., 2008, Jensen et al., 2005). As propofol increases the conductance and time constant of the GABA-A synaptic current, this then interacts with the M-current (a slow potassium current) in low threshold spiking interneurons. This causes a transition from synchrony to anti-synchrony at the inter-neuronal network level, which then shifts the frequency of oscillation of the pyramidal neurons, in to the beta band level at the population level.

Lower frequency oscillations usually become prominent at deeper stages of sedation/ anaesthesia (Gugino et al., 2001). At mildly sedative doses, the results are more variable. A decrease in theta band activity has been shown with GABA-ergic compunds such as diazepam (Hall et al., 2010) and alcohol (Rosen et al., 2014). A decrease in theta band activity, with propofol, has been reported by some authors (Wang et al., 1997), while no change has been reported by others (Breshears et al., 2010, Greene et al., 2007, Kishimoto et al., 1995). Doenicke et al (2007) reported an increase in theta band at light hypnosis, which was then replaced, by an increased delta band at moderate sedation. A similar increase in frontal theta band was found in this experiment. Theta oscillations are closely linked to hippocampal activity (Buzsaki, 2002, Canolty et al., 2006) and play an important role in memory formation, especially linking with high frequency oscillations (Canolty et al., 2006, Klimesch, 1996). While the generation of theta oscillations is not completely clear, during computational modelling to predict alpha and delta oscillations (originating from thalamo-cortical neuronal activity) it has been suggested that theta oscillations may originate from spectral leakage from alpha and delta bands (Hindriks and van Putten, 2012). Theta band oscillations are also

suggested to be the mediator of fronto-parietal connectivity (Hillebrand et al., 2016) and so effects on theta band may offer a mechanism of altered cortico-cortical connectivity with sedation.

Increase in delta band activity with propofol sedation has been widely reported (Hashemi et al., 2015, Kishimoto et al., 1995, Veselis and Reinsel, 1992). In this experiment also delta band power increased in the frontal regions. A thalamic role has been implicated in the generation of the delta bands too. Alkire et al (2000) proposed that effect of anaesthetics on the thalamus resulted in hyperpolarization of the thalamo-cortical neurons resulting in their changing from a burst to a tonic pattern of firing. Further modelling work (Hashemi et al., 2015) has supported the role of thalamo-cortical generation of the delta rhythm and its increase being a reflection of the cortico-reticular-relay-cortical feedback loop due to a prominent enforced thalamic-reticular-relay interaction. These findings, therefore, further support the role of propofol sedation on thalamic neuronal activity.

5.5.5.2 Resting state networks

Functional connectivity analyses revealed a number of typical RSNs. There were significant changes (increased functional connectivity) found in bilateral frontal RSNs in the alpha, theta and delta frequency bands; increased functional connectivity in the bilateral parieto-occipital network (in the alpha band), and bilateral occipital network in the delta band. Bilateral sensori-motor networks were also identified. However, there was no change in those in the beta and gamma frequency bands.

Maintained functional connectivity in the motor RSN is similar to that expected from fMRI-based studies investigating sedative and anaesthetic effects of propofol, wherein primary RSNs retain their connectivity within the networks and with other regions (Boveroux et al., 2010, Schroter et al., 2012).

Increased functional connectivity in the frontal networks in the alpha, theta and delta bands was perhaps, more surprising as fMRI based studies would have predicted a reduced/ maintained connectivity in these networks. Despite the obvious prediction,

fMRI studies are somewhat contradictory in this respect (see Appendix 1). Yet again, very few experiments have focused only on the early stages of sedation. Interestingly, increased regional connectivity has been reported in most EEG based connectivity studies investigating both propofol induced sedation and anaesthesia. Supp et al (2011) described an increased synchronicity in the alpha band, in the frontal areas, with increasing doses of propofol resulting in loss of consciousness. This was a result of both an increase in alpha power and also phase coherence. Cimenser et al (2011) have reported a similar increase in alpha band coherence in the frontal regions along with increased frontal alpha and delta bands, again, similar to the findings of this experiment. Effective / directional connectivity analyses go a step further in trying to establish a causal role of brain regions in synchronizing their activities with other brain regions. Using Granger Causality based analysis, to explore directional connectivity between ACC and PCC during propofol induced loss of consciousness an increased coherence in these areas, especially in the beta (Barrett et al., 2012) and gamma bands (Murphy et al., 2011b) was shown. While these studies focused on loss of consciousness, it is likely that sedative concentrations may have similar, albeit less prominent, changes. On those lines, Boly et al (2012), using dynamic causal modelling (DCM) to explore directed effective connectivity between brain regions, showed that sedation was related to thalamic excitability, but not changes in cortico-cortical connectivity. Cortico-cortico connectivity was however reduced with further doses of propofol, as consciousness was lost. Using a different measure of directional connectivity (renormalized partial directed coherence), Makismow et al (2014) found a reduced occipital to frontal coherence (in 8-16 Hz band) and an increased frontal to occipital coherence (in 10-20 Hz band) during propofol sedation. These findings did not change with further increase in propofol doses. It is likely that similar mechanisms resulted in an increase in connectivity in bilateral occipital and parieto-occipital networks in alpha and delta bands respectively in this experiment.

Even within the same experimental conditions different analytic methods may produce discordant results. In a recent MEG study (Muthukumaraswamy et al., 2015), investigating the effects of ketamine, DCM based effective connectivity was reduced in fronto-parietal networks, however the functional connectivity based on band pass power correlates (similar to that used in this experiment) did not change. This reflects the

different sensitivities of these methods to different signal elements. Since, computation of band pass power envelopes involves discarding all phase information and further down-sampling, which is not the case with DCM based measures, it can confound some estimates of functional connectivity such as phase locking factors. Lee et al (2011) used graph theory to reduce the potential confound induced by increase band power, appearing as an increased strength of connection during anaesthesia. They found that parietal networks are most affected while frontal networks are least affected, with propofol-induced unconsciousness. While they did not study mild sedation, it is likely that frontal networks show similar resistance to disintegration during lower doses of propofol and explaining some of the findings of this experiment.

5.5.6 Potential limitations of this experiment

The spontaneous temporal fluctuations in neuronal oscillatory power present as spatial networks that are similar to the RSNs as observed with BOLD-fMRI. Recent experiments have confirmed the presence of these networks in various frequency bands, thus providing a sense of electrophysiological basis of the haemodynamic RSNs.

However, there are certain limitations of studying RSN functional connectivity with MEG. Apart from the common factors, as with fMRI (see section 5.4.6), such as influence of order of experiment and head motion, recently, it has been shown that physiological changes also can affect neuronal power (Driver et al., 2016). Therefore experimental designs affecting haemodynamics and ventilation may affect the results. In this experiment the physiological changes between the two states was not significant and therefore unlikely to have any influence on the results. Co-registration of the MEG data to an anatomical brain scan itself can induce significant variations, even with slight errors.

Another emerging factor in this type of MEG/EEG analysis is the choice of technique correlating neuronal activity. While most experiments use covariance of envelopes of oscillations or in some cases, phase synchrony of these oscillations. BOLD, however, is a much more complex phenomenon and so expecting the haemodynamic fluctuations to

be related to a single frequency band would be over-simplistic. Indeed, it has been shown that cross-frequency communication may be responsible for some of these BOLD changes. Tewarie et al (2016), have recently investigated linear and non-linear cross frequency interactions in an attempt to predict haemodynamic networks. Their modelling showed that cross frequency interactions and connectivity profiles of adjacent regions also influenced regional connectivity beyond the electrophysiological activity of those regions. It is likely that the changes in choice of frequency range or use of cross frequency interactions may produce different results and offer a better insight into drug-induced changes in functional connectivity.

5.5.7 Combining RSN functional connectivity results of the MRI and MEG; limitations and future directions

As discussed earlier, while there are numerous fMRI studies investigating functional connectivity changes with propofol induced LOC, relatively few have studied functional connectivity changes with mild sedation. An even smaller number have attempted to combine electrophysiological studies along with fMRI data (combined EEG/fMRI studies). There have been no previous studies using MEG with fMRI to study mild propofol sedation.

The results of these experiments were broadly in line with the (limited) published literature available. While the BOLD based connectivity analyses revealed changes (both increases and decreases) in the networks studied, as predicted; the results of the MEG RSN functional connectivity analyses were different and revealed increases in connectivity in some of the identified networks. Some of the MEG RSN findings mirrored, increased BOLD-based frontoparietal network connectivity found using ICA technique. In the motor networks, functional connectivity was maintained with both MEG (in the beta and gamma bands) and fMRI, as predicted.

It can be considered ambitious trying to combine the two modalities to study changes in resting state functional networks, with sedation. The possible reasons for the apparent differences in the results between the two techniques are multifactorial. While MEG

data have shown RSNs similar in spatial location to those found with BOLD fMRI, very few studies have tried to compare the results of the two techniques, and when done, have shown similar but not completely consistent results (Demuru et al., 2014). Also, no previous study has tried to track and compare the changes in these RSNs using these two distinct modalities following a modifying intervention. This lack of difference in modifiability of the RSNs identified through these two sources may represent some key underlying differences between the two techniques. It is possible that the fMRI RSN changes are a result of cross-frequency changes due to sedation/ drug effects, which may not present itself in the broadband frequency change (in MEG RSN) to the same extent or even in the same direction.

The MEG and MRI session had to be done in a sequential manner rather than simultaneously and therefore despite the best efforts there may be differences in experimental conduct. In this case an 'order effect' (MEG session always preceded the MRI session) cannot be ruled out. Also, although all subjects were sedated to the same level (OAA/S), the assessment is subjective, so other factors (including order effects due to participants having experienced sedation previously) could have contributed to differences in the level of sedation achieved. While this may continue to be an issue with other MEG/ fMRI studies, simultaneous EEG-fMRI can obviate some of these concerns.

Identification of anatomical sites in MEG data depends on the registration process and despite best efforts errors may be induced during the co-registration process. While this can magnify the usual limitation of MEG i.e. relatively limited spatial resolution; this can result in even more significant differences in resting state connectivity analyses.

As discussed previously, the analysis of electrophysiological data in a band limited format might not fully explain the BOLD related haemodynamic changes. Also the analysis method used in Experiment 2 uses temporal down-sampling of the oscillatory envelopes of the frequency bands and while fairly robust and valid for identifying RSN, does not take into account phase synchrony and therefore may lose out on valuable information which may be partly responsible for drug induced modulations of RSNs. It is therefore plausible that while the neuronal synchrony increases in a particular band,

the changes in other neuronal bands result in a de-synchronous response in the haemodynamics, presenting as a decreased BOLD related functional connectivity. Also, as the understanding of the electrophysiological basis of BOLD haemodynamic changes is still incomplete, there may be yet other confounding factors that may contribute to this divergence of responses. It is likely that analysis methods, in future will take into account the other dimensions of oscillatory changes to relate them to BOLD changes.

5.5.8 Conclusions

This is a novel attempt at combining different neuroimaging techniques to study neurophysiologic and haemodynamic changes associated with propofol sedation. The results of this sequential MEG/ fMRI can be summarized as follows

- Functional connectivity of higher order networks changes with mild sedation. PCC (as a key hub of DMN) becomes less connected with the frontal pole while the thalamus becomes less connected with regions of the DMN, ACC and motor cortex. Thalamus appears more connected with sensory cortices and superior temporal gyrus. Primary sensory and motor cortices show reduced connectivity with the occipital cortex but become more connected with the thalamus.

- There was increased functional connectivity found in bilateral frontal RSN in the alpha, theta and delta frequency bands; increased functional connectivity in the bilateral parieto-occipital network (in the alpha band), and bilateral occipital network in the delta band. Bilateral motor networks were also identified however there was no change in those in the beta and gamma frequency bands.

Chapter 6 : Changes in cerebral perfusion with mild sedation observed using Arterial Spin Labelling fMRI

6.1 Abstract

Arterial spin labelling involves using endogenous water (in circulating blood) as a magnetically modifiable contrast, to study perfusion changes in the brain. This can then be used to calculate cerebral blood flow (providing information comparable to the gold standard, i.e. positron emission tomography). ASL based changes in cerebral blood flow can also be used to study changes in neuronal functions and may have certain advantages over BOLD based fMRI.

In this experiment relative changes in cerebral perfusion were studied, using ASL-fMRI, during mild propofol sedation.

Mild propofol sedation resulted in a decreased global cerebral perfusion by about 9%. Regional cerebral perfusion decreases by about 24%, mainly in the key frontal regions, with 9- 14% reduction in the precuneus, posterior cingulate cortex and the thalamus. This was predicted, based on existing literature and the known functions of these regions in pharmacological modulation of consciousness.

6.2 Background and rationale

The strengths of various neuroimaging techniques and their combinations have been exploited over the years to explore anaesthetic related changes in consciousness and arousal. The excellent sensitivity and specificity of positron emission tomography (PET) is limited by the potential hazards associated with radioactivity and the associated difficulties with repetition. With the development of blood oxygen level dependent (BOLD) contrast based functional MRI (fMRI) some of the challenges of PET were overcome at the cost of some loss of specificity and information. BOLD-fMRI still relies on an incompletely understood mechanism of neurovascular coupling and although quite robust for most applications, still has some limitations in situations in which underlying cerebrovascular physiology may be altered (Iannetti and Wise, 2007). Arterial spin labelling (ASL) cerebral blood flow measurement uses an endogenous tracer (water in the blood) thus avoiding the risks associated with exogenous radioactive tracers. ASL uses magnetically labelled water in arterial blood to measure cerebral perfusion. ASL has certain distinct advantages over the BOLD-contrast. While the spatial localisation during BOLD-fMRI results from a complex interplay between the blood flow, blood volume and neuronal oxygen consumption, ASL is more specific to local (perfusion) changes. ASL can also provide absolute quantification of perfusion values and since it involves pair-wise subtraction of control and tagged images, it is less affected by baseline drift and may be less susceptible to motion artefacts, making it more suitable for long term repetitive studies or those with low frequency changes (Detre and Wang, 2002).

ASL based techniques are especially suited for physiological and pharmacological fMRI studies on neuronal activity where there may be an independent, physiological condition/ drug action related confounding effect on perfusion that would make use of BOLD difficult or in studies in which cerebral perfusion is the primary functional parameter of interest.

6.2.1 ASL application in studying central drug effects

ASL is increasingly being used to bridge the gap between the information derived from BOLD-fMRI and PET in relation to pharmacological neuroimaging studies. Notably, it has been used to study centrally acting drugs, which may have confounding effect on systemic vasculature and have provided confirmatory evidence (similar to BOLD – fMRI/ PET) or additional, new, information about drug effects. Pulsed ASL (PASL) when used in chronic heroin users to study the effects of acute heroin administration showed reduced perfusion in the left and right insula, left ACC and left medial prefrontal cortex (mPFC) suggesting a role of these regions in the self and emotional regulation of these patients in the heroin maintenance program (Denier et al., 2013). Carhart-Harris et al (2012) studied the effects of psilocybin (a psychedelic drug causing altered consciousness) and reported decreased CBF in the higher level association areas and important connector hubs (such as ACC, PCC, mPFC and thalamus) related to their behavioural effects. These findings challenged the previously reported PET results that had showed an increase in metabolism with psilocybin rather than a reduction. Similarly, another consciousness altering drug, 3,4-methylenedioxymethamphetamine (MDMA), was shown to reduce the CBF in the amygdala, hippocampus and medial temporal lobe (areas with known high density of 5-HT-1A receptors) and this correlated with the intensity of the drug effects (Carhart-Harris et al., 2014).

ASL has also been applied to study the effects of anaesthetic drugs and has contributed to existing knowledge about anaesthetic actions. Remifentanil, an ultra-short acting opioid, which produces analgesia and sedation was shown to increase global CBF in a dose related manner (Kofke et al., 2007). This was similar to the findings of increased CBF, during reminfentanil infusions, as studied with PET (Lorenz et al., 2000). There was a relative CBF (regional CBF change/global CBF change) increase in the cingulate cortices while CBF decreased in the amygdala and hippocampus. Macintosh et al (2008), similarly, using GRASE (Gradient and Spin Echo) ASL technique demonstrated a global increase in CBF with remifentanil infusion with a relative increase in the anterior cingulate, insula and the thalamus. While these results may have been confounded by increased CO_2 secondary to respiratory depression induced by remifentanil, the technique of ASL was demonstrably sensitive to regional changes.

Studies with sevoflurane, a commonly used inhalational anaesthetic, failed to show any regional CBF changes at sedative doses (0.25 MAC) (during rest), but, reduced CBF during visual and motor tasks, was seen in primary cortical areas and its unimodal association areas, sensorimotor area, along with thalamus and hippocampus (Ramani et al., 2007). This suggested a sensitivity effect of PASL, which increased during tasks to be able to discriminate between regional effects during sedation and un-sedated states. It may also suggest that the areas such as thalamus are not normally inhibited at sedative doses in the resting state and this may be an activity-state related suppression. Midazolam, a selective GABA agonist sedative drug, was studied at sedative concentrations using ASL and showed reduced CBF in the left middle frontal gyrus, left cingulate gyrus, left PCC and left precuneus (Liang et al., 2012). Of these, the changes in the left middle frontal gyrus correlated with memory test performance, demonstrating its role in midazolam-induced amnesia.

6.2.2 CBF and anaesthesia

Cerebral blood flow changes may occur during sedation and anaesthesia through different mechanisms. Anaesthetic drugs, usually cause a depression in blood pressure, which could result in a reduction in global CBF. Also, respiratory depression induced by anaesthesia would result in hypercarbia (unless ventilation is controlled) that might itself result in changes in CBF. However, the autoregulatory mechanisms maintain cerebral perfusion within a normal range, within quite wide ranges of systemic blood pressure and CO_2 changes (Cipolla, 2009). Changes in these systemic variables are usually dependent on anaesthetic dose and therefore CBF changes are even less likely to occur at sedative doses.

Another mechanism of CBF alteration, of most interest to neuroimaging researchers, relies on neurovascular coupling such that a suppression of neuronal/ regional activity by anaesthetic drugs would result in a concomitant reduction in regional CBF (Section 1.6.1). While the exact mechanism of this neurovascular coupling is unclear, it is unlikely that this coupling is altered at sedative doses of propofol (Veselis et al., 2005). If haemodynamic and ventilatory parameters do not change (with mild levels of

sedation) the CBF changes can therefore be considered representative of changes in neuronal activity.

At low doses, anaesthetic agents preferentially affect the cortical areas; especially higher association areas and the primary cortical areas are affected subsequently, as the dose increases (Heinke and Schwarzbauer, 2002). Thalamus (Alkire et al., 2000) and more recently the precuneus (Cavanna, 2007) have been suggested as the 'consciousness' switch due to their roles in modulating arousal and consciousness. However, at sedative doses, the effect on these structures is less clear. Brain regions of the resting state networks including the default mode network (DMN: medial prefrontal cortex, precuneus, posterior cingulate cortex) (Greicius et al., 2003) and frontoparietal networks are likely to be affected as alterations in the synchrony of these networks is commonly associated with sedation. A suppression of neuronal activity in these brain regions is therefore likely to be associated with a reduction in regional cerebral perfusion.

6.3 Hypothesis

Mild propofol sedation will be associated with a reduction in CBF in the frontal cortex, precuneus, posterior cingulate cortex and the thalamus.

6.4 Aims

To use ASL based perfusion MRI to study CBF changes during mild propofol sedation.

6.5 Methods

This experiment was performed as a part of the data collection for fMRI experimental session (Section 2.4.2) and therefore the methods for participant inclusions, monitoring, drug administration and sedation assessment are the same as stated in part 3.4.3. All participants were instructed to lie still with their eyes closed and to try and stay awake. The sequence of data acquisition was always *Awake* state followed by *Sedated* state.

6.5.1 MRI – ASL acquisition

MRI data were collected at 3 T (HDx, General Electric) using an eight-channel receive-only head coil. CBF was estimated using single-shot, proximal inversion with a control for off-resonance effects – quantitative imaging of perfusion using single subtraction II (PICORE-QUIPSS II) (Wong et al., 1998). Imaging parameters were: TR/TE/ = 2200 ms/19.8 ms; TI = 1500 ms; field of view, 24 cm x 24 cm; twelve slices, 7 mm thick, with a 1-mm gap between slices; matrix, 64 x 64. Each scan included 130 repetitions. With the same slice prescription, calibration scans were acquired to provide an estimate of M0 (fully relaxed blood water magnetization) (Liau et al., 2008). T1-weighted whole-brain structural scan was also acquired (1 x 1 x 1 mm voxels).

6.5.2 ASL-MRI analysis

General linear modelling was used to evaluate the drug-induced modulation of the perfusion signal. In the first-level analysis, the difference between tag and control images was explicitly modelled as one regressor representing the voxel-wise signal proportional to the mean perfusion. Given the global scaling in FEAT of each dataset to the same value, the parameter estimates were assumed to represent relative perfusion at each voxel, permitting a paired (within-subject) comparison of sedation related to relative perfusion changes.

fMRI data processing was carried out using FEAT (FMRI Expert Analysis Tool) Version 5.98, part of FSL (FMRIB's Software Library, www.fmrib.ox.ac.uk/fsl). The following pre-statistics processing was applied; motion correction using MCFLIRT (Jenkinson et al., 2002), nonbrain removal using BET (Smith, 2002), spatial smoothing using a Gaussian kernel of FWHM 5mm; grand-mean intensity normalisation of the entire 4D dataset by a single multiplicative factor; highpass temporal filtering (Gaussian-weighted least-squares straight line fitting, with sigma=7.5s). Time-series statistical analysis was carried out using FILM with local autocorrelation correction (Woolrich et al., 2001). Z (Gaussianised T/F) statistic images were thresholded using clusters determined by Z>2.3 and a (corrected) cluster significance threshold of P=0.05 (Worsley, 2001). Registration to high resolution structural and standard space images

was carried out using FLIRT (Jenkinson et al., 2002, Jenkinson and Smith, 2001). Registration from high resolution structural to standard space was then further refined using FNIRT nonlinear registration (Andersson et al., 2007a, Andersson et al., 2007b).
The results of fitting this model at the first level were combined in a higher-level within-subjects analysis to compare modulation of perfusion during propofol sedation. Higher level analysis was carried out using FLAME (FMRIB's Local Analysis of Mixed Effects) stage 1 (Beckmann et al., 2003, Woolrich, 2008, Woolrich et al., 2004). Z (Gaussianised T/F) statistic images were thresholded using clusters determined by $Z>2.3$ and a (corrected) cluster significance threshold of $P=0.05$ (Worsley, 2001). To assist with this process, perfusion data underwent unwarping for B0 field distortions and were registered to the T1-weighted high-resolution ($1 \times 1 \times 1$ mm) structural scan which was itself registered to a 1-mm resolution Montreal Neurological Institute (MNI) standard brain, using nonlinear registration.

6.6 Results

All 15 participants were sedated to the desired level (OAA/S level of 4; mild sedation) during the *Sedated* state scanning. All 15 participants' data was available and used for analysis. There was a significant slowing of the visual and auditory reaction times, as described previously in Section 3.4.4 (Table 3-2: Reaction times). There was no change in HR, BP, oxygen saturation or expired CO_2, as described previously in Section 3.4.4 (Table 3-1: Physiological Data). The mean (SD) propofol target concentration was 1.2 (0.2) mcg/ml.

The group level results revealed significant CBF decreases, during sedation, in the frontal lobe, inferior frontal gyrus, precuneus, posterior cingulate gyrus and the thalamus, with most changes being bilateral. As hypothesized, these decreases were localized to the higher association areas (e.g. the PCC, inf. frontal gyrus, frontal pole) and important connector hubs (e.g. the precuneus, PCC and thalamus).

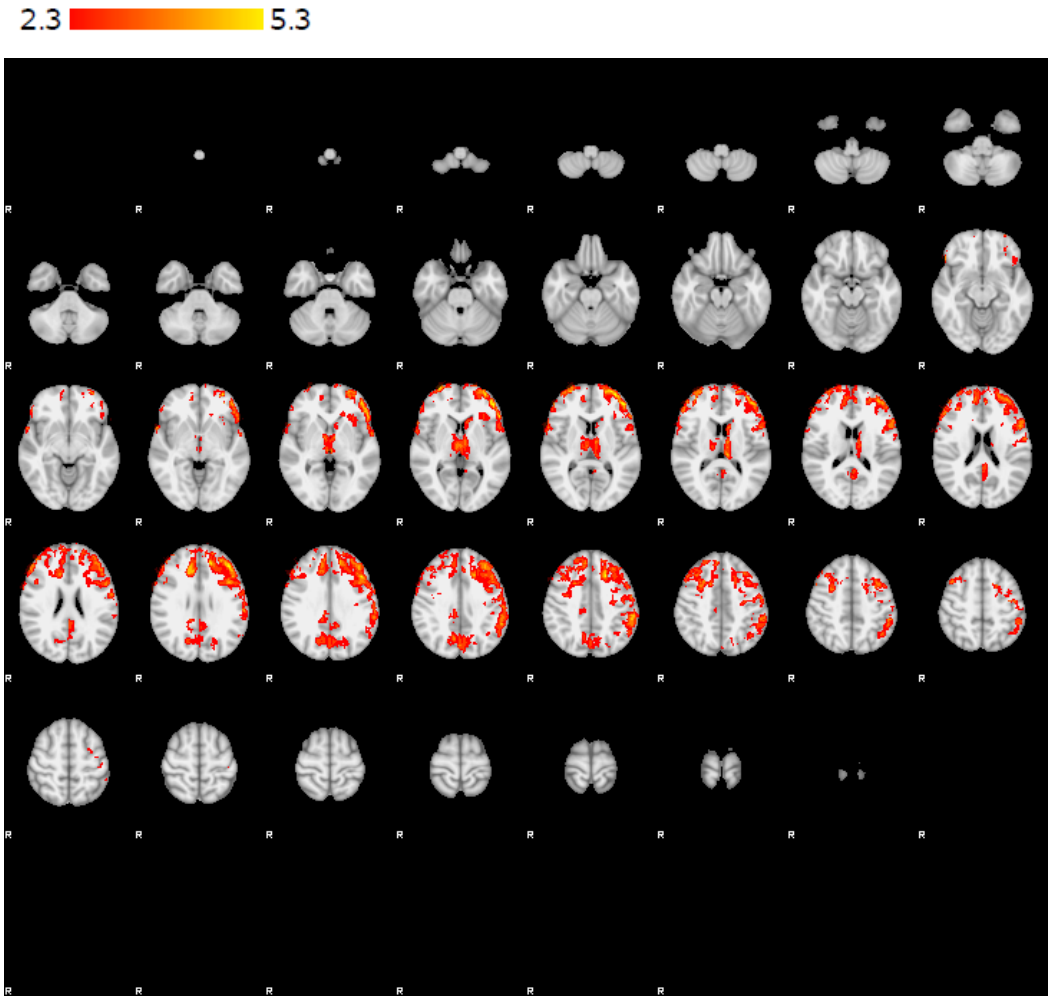

Figure 6-1: Perfusion maps (*Sedated- Awake*)
Analysis carried out using FEAT version 5.98, part of FSL. Z (Gaussianised T/F) statistic images were thresholded using clusters determined by Z > 2.3 and a corrected (cluster) significance threshold of P= 0.05.

Table 6-1: Peak voxel coordinates showing change in perfusion during mild sedation.
Co-ordinates are reported, in MNI space. L, Left; R, Right

		Voxel Coordinates		
Brain region	Voxel (z)	x	y	z
Frontal pole (L)	5.32	52	84	51
Frontal pole (L)	5.16	68	85	37
Frontal pole (L)	5.12	61	92	34
Frontal pole (L)	5.04	66	86	39
Inferior frontal gyrus (L)	5.04	70	80	37
Frontal pole (L)	5.01	62	92	38
Precuneus cortex (L)	3.84	40	31	54
Precuneus cortex	3.72	45	27	55
Posterior cingulate gyrus (L)	3.54	46	38	43
Posterior cingulate gyrus (R)	3.51	41	48	53
Precuneus cortex (L)	3.5	48	29	55
Posterior cingulate gyrus	3.49	45	41	47
Thalamus (L)	4.38	46	52	37
Thalamus (L)	4.18	49	50	42
Thalamus (R)	4.14	42	56	39
Thalamus (R)	4.08	44	57	37
Thalamus (R)	4.07	43	54	37
Thalamus (L)	3.98	48	60	37

6.6.1 Functional region of interest (ROI) CBF changes

In order to quantify the level of significant perfusion changes observed, a functional ROI mask was derived from the contrast of parameter estimates (COPE) image (derived from the voxel clusters passing the $Z > 2.3$ threshold) and the fractional change in perfusion was estimated, (Fig. 6-2; suprathreshold regions). This change was about 23.7%.

The whole brain (global) perfusion decreased by 9% during sedation.

6.6.2 Anatomical ROI CBF changes

CBF changes in the thalamus, PCC and precuneus were estimated using ROI masks derived from the Harvard Cortical atlas. The relative decreases in the CBF in the thalamus, the PCC and the precuneus, from *Awake* to *Sedated* state were 9.6%, 10.6% and 13.4% respectively.

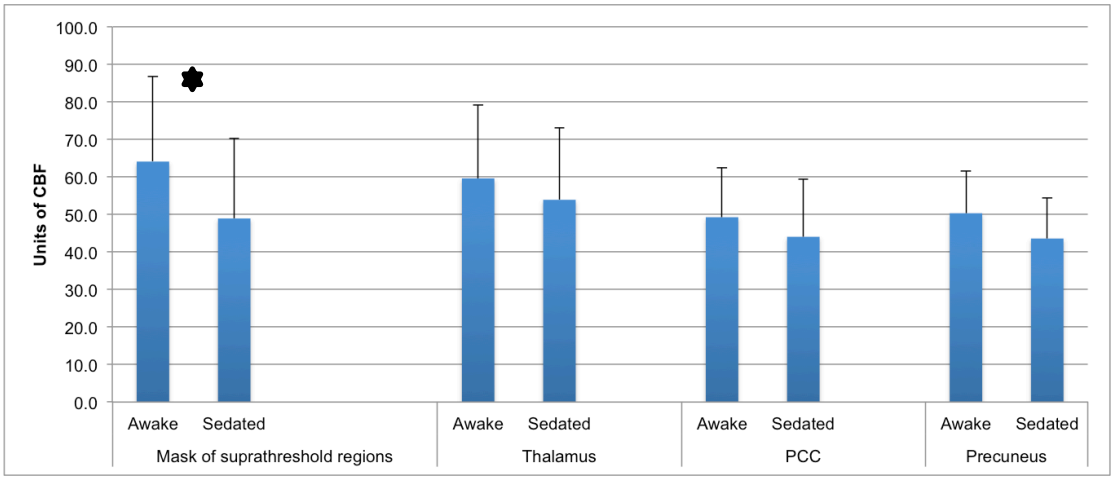

Figure 6-2: Changes in CBF (arbitrary units)
Comparisons done in functional ROI (based on statistical thresholded z map) and anatomical ROIs (thalamus, PCC and precuneus). Error bars represent SD of values. *denotes significant change ($p<0.05$, paired t-test, one tailed)

6.7 Discussion

In this experiment, ASL has been used to map the changes in CBF associated with propofol-induced sedation. It was found that mild propofol sedation is associated with a reduction in CBF in some of the key frontal cortical areas, regions of the DMN and the thalamus.

6.7.1 Anaesthetic effects on global cerebral perfusion

Previous quantitative studies of CBF changes have used PET imaging and most of the research has been focused on anaesthetic induced unconsciousness, with only a few studying mild sedation. Global reductions in CBF follow global suppression of metabolic activity at anaesthetic doses producing unconsciousness. Propofol anaesthesia has been shown to suppress global activity ranging from 20% (Fiset et al., 1999), up to 70% (Kaisti et al., 2002). This is similar to the reduction in global brain metabolism of around 55% during propofol anaesthesia (Alkire et al., 1995b). Sedation with propofol decreased the global CBF by about 17% (Veselis et al., 2004b) paralleling an expected, dose related, reduction in metabolic/ neuronal activity. In this experiment, mild propofol sedation reduced the global CBF by about 9%.

6.7.2 Regional perfusion

In this experiment, a reduction in regional CBF was predicted on the basis of previous CBF literature (PET/ ASL based studies) and those of BOLD based fMRI, demonstrating key cortical and subcortical regions involved in sedation. Specifically, frontal cortex, regions involved in the DMN and the thalamus were investigated and found to have reduced CBF during sedation.

Frontal cortical regions (including prefrontal cortex) have been shown to be involved in sedation (Byas-Smith et al., 2002, Sun et al., 2008, Veselis et al., 2004b). Intuitively, this would be expected, as the prefrontal cortex is well known to be involved in attention, cognition and working memory; alterations of all of which characterise mild sedation. Mild sedation, as objectively defined using the OAA/S grading, is

behaviourally characterized by a slurred speech, sluggish response to verbal commands and sluggish visual and auditory reaction times (Chernik et al., 1990). Veselis et al (Veselis et al., 2004a) showed a reduction in CBF in the right sided anterior brain (inferior frontal gyrus, insula and superior temporal gyrus) with propofol dosing similar to those in this study. Sun et al (Sun et al., 2008) reported a reduction in frontal lobe metabolism by about 10+/- 3% and temporal lobe metabolism by 13.1 +/- 2% during light propofol sedation but, simultaneously, a greater reduction in activity of the occipital lobe, a change which was not found in this study. While the occipital lobe has quite a high density of GABA receptors (similar to the frontal lobe) (Alkire and Haier, 2001), its deactivation with sedation has not been universally reported. In this experiment, the subjects were instructed to keep their eyes closed, which may have contributed to a reduced baseline activation of the occipital lobe to limit further significant changes. Byas-Smith (Byas-Smith et al., 2002) also showed a reduction in CBF of the middle and inferior frontal gyrus with propofol-sedation. As prefrontal cortex plays an important role in attention and working memory, propofol sedation related amnesia has been shown to be associated with suppression of prefrontal cortical activity (Veselis et al., 2002).

As further evidence of their involvement in maintaining consciousness, dorsolateral prefrontal cortex is also functionally connected to parietal cortical regions forming the lateral frontoparietal attentional functional network, also called executive control network (ECN), which becomes activated during executive tasks. Loss of feedback frontoparietal connectivity is associated with anaesthetic induced unconsciousness (Lee et al., 2009a).

Similar to the frontal cortex, PCC and precuneus, which are highly connected and metabolically active cortical structures, also play a significant role in maintaining consciousness. PCC is involved in cognition and attention by participating in the DMN (Fransson and Marrelec, 2008) and interacting with the ECN (Leech and Sharp, 2014). DMN may have a role in internally attentive tasks but is suppressed during external, attention demanding tasks. PCC's metabolism and connectedness is also related to the unconsciousness during vegetative states and return of normal function (Laureys et al., 2000). Its connectivity with prefrontal cortex also reduces with deepening stages of

sleep (Horovitz et al., 2009). Precuneus plays an important role in visuo-spatial imagery, episodic memory retrieval and self-processing operations (Cavanna and Trimble, 2006) and forms an integral node of the DMN. Thalamus is the gateway of most incoming sensory stimuli to be processed in the cortex and its reciprocal thalamo-cortical connections makes it a key area in arousal and consciousness (Mashour and Alkire, 2013). Indeed, these brain networks have been shown to have high resting metabolism and therefore increased CBF. Networks with longer range connectivity such as DMN and ECC are associated with higher CBF changes than networks with shorter range changes (Liang 2013). Although CBF and its relationship with functional connectivity was not studied in this experiment it corroborates the importance of these connector hubs in maintaining consciousness, which is then altered by sedation.

PET and BOLD-fMRI studies, investigating propofol effects, have shown that at sedative concentrations of propofol a dose related reduction in CBF occurs in the PCC, precuneus and the thalamus (Fiset et al., 1999, Byas-Smith et al., 2002). Bonhomme et al (2001) also showed a dose related reduction in BOLD response activity of these structures to a sensory stimulus with increasing doses of sedation. Reduced thalamic metabolism (glucose consumption) has been shown at sedative (Sun et al., 2008) and anaesthetic concentrations (Alkire et al., 1995b). These CBF changes, in this experiment, ranged from 9.6- 13.4 % from the baseline.

While there are alternative mechanisms of reduced CBF such as systemic hypotension or effects of hypercarbia; in this experiment the systemic blood pressure and ventilatory parameters remained unaltered during sedation (Table 3-1: Physiological Data). Propofol is also unlikely to alter neurovascular coupling (Veselis et al., 2005) therefore the changes in CBF mirror the expected changes in neuronal responses to propofol.

6.8 Conclusions

Since there is no previous published report on the use of ASL perfusion technique to study CBF during mild propofol sedation, this experiment provides novel information. Pulsed ASL was used, in this experiment, to map the changes in CBF during propofol sedation. Mild propofol sedation resulted in a decreased global CBF by about 9%.

Regional CBF decreases by about 24% mainly in the key frontal regions and also in the precuneus, PCC and the thalamus by about 9-14%. These findings corroborate similar findings with other, well established techniques including PET (including quantifying CBF) and BOLD-fMRI (in identifying brain regions and networks involved in sedation) and, therefore, provide confirmatory evidence of the potential of ASL based perfusion and fMRI studies in investigating central pharmacological actions.

Chapter 7 : Discussion, conclusions and future recommendations

Pharmacological sedation is commonly used in clinical practice both by anaesthetists and non-anaesthetists. While anaesthetic-induced unconsciousness has been an area of wide interest, early stages of sedation have received less attention. Understanding neural mechanisms of early stages of sedation is expected to improve understanding of consciousness and early stages of altered consciousness, in both physiological and pathological conditions. A greater knowledge of these neural mechanisms is likely to avoid complications of sedation and anaesthesia (such as ICU-delirium), help develop better and safer drugs and potentially develop monitoring systems to track brain function independent of the choice of anaesthetic drugs. This was the motivation behind this thesis.

Gamma-aminobutyric acid (GABA), being the most prevalent inhibitory neurotransmitter in the brain is the key modulator of inhibition. Most common anaesthetic drugs facilitate this inhibitory activity. The focus of this thesis was therefore to understand better the neural correlates of GABA-ergic pharmacological sedation. Propofol was chosen as the GABA-ergic compound being one of the commonest clinically used drug for this purpose. Advanced neuroimaging techniques were used to study the haemodynamic, neurophysiologic and spectroscopic neural changes associated with mild levels of propofol sedation and the relationships between those findings were explored.

7.1 Main findings

In Chapter 3, in a series of experiments, GABA MR Spectroscopy, magnetoencephalography (MEG) and blood oxygen level dependent –fMRI (BOLD-fMRI) were used to explore the complex relationship between neurochemistry (GABA concentration), electrophysiology (gamma band response (GBR)) and haemodynamic activity (BOLD signal) and their modulation with mild propofol sedation.

Mild propofol sedation did not result in any significant changes in MRS detectable GABA+ (GABA plus co-edited macromolecules) concentration in either the cortical (occipital) or subcortical (thalamic) regions. There was also a reduced BOLD signal, in the peak voxel of the visual cortex, during a high intensity visual stimulation, during sedation. At similar levels of mild propofol sedation, MEG revealed an increase in visually-induced gamma band (30- 50 Hz) responses, increased alpha amplitude suppression, and a concurrent reduction in the visually evoked response compared to the *Awake* state. While there was a trend towards an inverse relationship between GABA+ concentration and BOLD signal change (during visual activation), in the *Awake* state, no clear relationship existed during sedation, nor was there a well-defined relationship between the BOLD response and GBR. A significant negative correlation between the peak spike gamma frequency with occipital GABA+ concentration during the *Sedated* state (and a trend towards significance between the occipital GABA+ and peak spike gamma frequency during the *Awake* state) but no relationship was found between the GABA + concentration and the sustained gamma band frequencies.

In Chapter 4 cortical responses to multisensory stimulation were investigated using MEG and BOLD fMRI, during propofol sedation. Evoked oscillatory activity in response to visual stimulation was decreased but not in response to auditory or somatosensory stimulation. The haemodynamic response (BOLD-fMRI) showed a reduction in activity of the primary somatosensory cortex in response to median nerve stimulation but no changes in primary cortical responses to visual or auditory stimulation.

In Chapter 5 functional connectivity was explored in the higher-order and lower-order known resting state networks (RSNs) using BOLD-fMRI. Using seed based connectivity measures; posterior cingulate cortex (as a key hub of the Default mode network - DMN) became less connected with the frontal pole while the thalamus became less connected with the regions of the DMN, anterior cingulate cortex and the motor cortex. Thalamus, however, showed an increased connectivity with sensory cortices and superior temporal gyrus. Primary sensory and motor cortices showed reduced connectivity with the occipital cortex but became more connected with the thalamus.

Oscillatory activity was explored to identify RSNs within frequency bands and connectivity changes in those networks explored, using MEG. There was increased functional connectivity found in bilateral frontal RSNs in the alpha, theta and delta frequency bands; increased functional connectivity in the bilateral parieto-occipital network (in the alpha band), and bilateral occipital network in the delta band. Bilateral motor networks were also identified however there was no change in those in the beta and gamma frequency bands.

In chapter 6, pulsed arterial spin labelling (ASL) was used to map the changes in CBF during propofol sedation. Mild propofol sedation resulted in a decreased global CBF by about 9%. Regional CBF decreases by about 24%, mainly in the frontal regions, and in other key regions precuneus, PCC and the thalamus by around 9- 14%.

7.2 Neural correlates of mild propofol sedation

The focus of these experiments was to identify the neural correlates of mild sedation induced by the GABA-ergic drug, propofol. Mild propofol sedation, as the earliest (objectively) measurable, change in consciousness is characterised by an increasing loss of attentiveness, slurred speech and reduced responsiveness. This stage may also be associated with amnesia. Participants undergoing sedation respond with a lethargic response to verbal commands but are able to carry out most tasks as commanded. While sedation was assessed using the Objective assessment of alertness/ sedation (OAA/S) scoring system, reaction times were also measured. *Sedated* state was associated with slower auditory and visual reaction times as compared to the *Awake* state.

7.2.1 Attentional modulation

One of the key findings of this thesis was the effect of propofol on visual-gamma oscillations. Task induced gamma oscillations have been implicated in 'binding' of percepts and cognition resulting in higher order functioning and may play a critical role in maintaining consciousness. On examining visual task induced gamma oscillations it was shown that propofol resulted in a dissociation of evoked and induced responses,

whereby evoked gamma power was reduced while the induced gamma power increased. This suggests that the two MEG responses may reflect the activity of different generator populations in primary visual cortex or that these generators are differentially pharmacologically sensitive. Indeed, in primary visual cortex gamma band responses are primarily generated in layers II, III and IV (Xing et al., 2012), whereas early evoked responses are mostly generated in layer IV (Kraut et al., 1985). Due to its temporal characteristics, the gamma spike (evoked) is considered to represent the early visual pathway while the sustained (induced) gamma represents a cortico-cortical synchronous response to the visual stimulation (Castelo-Branco et al., 1998). The dissociation between evoked and induced found in this experiment is similar to the difference Privman et al found with implanted subdural electrodes where evoked responses decreased while the gamma band responses were maintained under anaesthesia (Privman et al., 2011).

7.2.2 Primary cortical functions

The primary sensory cortices, including the occipital (visual) cortex, temporal (auditory) and somatosensory cortices are involved in sensory processing. They provide lower-order processing following transmission of impulses through the primary and secondary order neurons gated through the thalamus. They then lead the impulses up to higher association areas resulting in the overall sensory experience. These functions were studied in Chapters 3, 4 and 5.

The fMRI response to the visual attention task (Chapter 3) resulted in activation of the visual cortex. The BOLD response in the peak voxel of the visual cortex showed a reduction in the BOLD response suggestive of a reduction in neuronal activity during sedation. A suppression of primary cortical function is expected during pharmacological sedation and anaesthesia, usually in a dose-dependent manner, although complete suppression of the activity in primary cortex does not occur even at high doses.

The findings from the MEG and fMRI experiment (Chapter 4) were, however, mixed. In this experiment simple passive tasks were presented to stimulate the primary sensory cortices. Visual function is considered most sensitive to anaesthetics while auditory

functions are most resistant. This was apparent in the MEG results where visual evoked fields showed a reduction with sedation while the auditory evoked fields persisted. There was no effect on somatosensory evoked fields.

While BOLD response to somatosensory stimulation was reduced in the contralateral somatosensory cortex, during sedation, visual and auditory stimulation did not show any changes in their primary cortical BOLD responses. Visual stimulation showed reduced activity in the superior frontal gyrus, paracingulate and cingulate gyri, left superior parietal lobule, left angular gyrus, left lateral occipital cortex and left supramarginal gyrus, while there was an increased activity in the cuneus, precuneus, supracalcarine and intracalcarine gyri, following sedation. During the auditory stimulation task, decreased activity was seen in the superior and middle frontal gyri, paracingulate gyrus, right sensorimotor cortex and right anterior and posterior cingulate regions while there was in increase in activity in left caudate, insula, anterior cingulate, right posterior cingulate, right lingual gyrus, and precuneus, following sedation. While some of these findings can be explained by the existing literature on the role of other brain regions such as the frontal lobe, precuneus and PCC in the form of emergence of activity in related regions due to a compensatory mechanism, some may have been due to a compensatory engagement of other regions to maintain wakefulness during sedation. These findings would need further exploration in future studies.

Propofol sedation also modulates the way in which primary cortices are connected with other brain regions. In Chapter 5, functional connectivity of primary cortical areas (sensory and motor cortex) was shown to be reduced with the occipital cortex while it increased with thalamus. Similar results have been shown by other groups with other anaesthetic drugs at sedative levels (Liang et al., 2015, Martuzzi et al., 2010, Greicius et al., 2003, Kiviniemi et al., 2005).

MEG data revealed bilateral sensori-motor networks but there was no change in their functional connectivity in the beta and gamma frequency band networks. Beta and gamma band oscillations are most relevant to the BOLD RSNs and therefore these findings reflect the reported findings from the fMRI literature.

7.2.3 Actions on precueus and PCC

Precuneus and PCC are adjoining regions of the posteromedial parietal cortex and play a crucial role in maintaining consciousness related functions (Roquet et al., 2016)

Chapter 6 showed a reduced perfusion in the precuneus and PCC. PCC forms an integral part of perhaps the most basic RSN (Greicius et al., 2003). Chapter 5 showed a decrease in functional connectivity of the PCC with the frontal pole as a correlate of mild propofol sedation as has been reported by previous reports investigating DMN connectivity with sedation (Boveroux et al., 2010, Liu et al., 2015, Stamatakis et al., 2010, Greicius et al., 2003). Interestingly functional connectivity of the right PCC increased with pons, as pons appeared to become more relevant during mild sedation (Gili et al., 2013).

7.2.4 Actions on thalamus

Thalamus has been known to play a crucial role as the sensory gateway. Most neuroimaging studies have focused on thalamus as a potential consciousness switch. Indeed thalamus and its cortical connections appeared as a key neural correlate of mild propofol sedation.

Perfusion fMRI using pulsed ASL (Chapter 6) revealed nearly a 10% reduction in thalamic blood flow showing an effect of propofol sedation on thalamus. Seed based connectivity from those thalamic regions showed a reduced connectivity with multiple cortical and sub-cortical structures while there were no regions with increased connectivity (Gili et al., 2013).

7.2.5 Action on frontal cortical regions

The frontal cortical regions including the prefrontal cortex play a key role in higher order processing of sensory function and cognition. They are also closely linked to RSN especially the DMN and executive control network (ECN).

It was therefore not a surprise that the frontal brain regions showed a decrease in perfusion (Chapter 6) with mild propofol sedation. Studying functional connectivity of the higher-order networks in Chapter 5 also revealed interesting results. Previous literature has shown a decrease in frontoparietal functional connectivity with deeper stages of sedation (Jordan et al., 2013b, Monti et al., 2013, Schrouff et al., 2011, Boveroux et al., 2010, Liang et al., 2015). Mild sedation, as used in this thesis, has not been studied as extensively. Using independent component analysis an increase in functional connectivity of the right frontoparietal network was seen, although it was not corrected for multiple networks. Therefore the changes in frontal network connectivity is unclear from this thesis, although there may be a trend for an increased connectivity.

MEG based measures, however, clearly showed an increased functional connectivity in the frontal networks in the alpha, theta and delta frequency bands. The functional connectivity in oscillatory frequency bands, it appears, do not follow the same change pattern as the BOLD-fMRI based measures. This reflects the gap in understanding of the interplay between different neuronal frequency bands resulting in the observed BOLD response. Increased regional connectivity, especially in the frontal areas, has been reported in most EEG based connectivity studies investigating both propofol induced sedation and anaesthesia (Supp et al., 2011, Cimenser et al., 2011), demonstrating a similar increase in alpha band coherence in the frontal regions along with increased frontal alpha and delta bands, again, similar to the findings of this experiment.

7.2.6 Alterations in GABA levels

The GABA-ergic activity of propofol was expected to alter MRS detectable GABA concentration during propofol administration. This hypothesis was based on the known mechanisms of propofol increasing both phasic and tonic activity, through GABA receptors. While, unlike drugs which reduce the breakdown of GABA (and thus increasing its amount available in synaptic areas); propofol induced GABA activity may be considered more akin to a relative redistribution of GABA in the synaptic context. The only previously published study using GABA-MR Spectroscopy showed an increase in MRS detectable GABA at anaesthetic doses of propofol but not at sedative

doses (Zhang et al., 2009). It was expected that using a more sensitive technique as used in Chapter 3 would be more likely to identify changes in GABA+ concentration at sedative doses of propofol.

The absence of a significant detectable change in GABA+ concentration suggested either a lack of change or a lack of sensitivity of the current MRS analyses pipelines. Placing these findings in the context of Zhang et al's study (Zhang et al., 2009) it is possible that the change in MRS detectable concentration occurs only at anaesthetic doses of propofol. This would warrant further investigation with studies of larger samples at different doses of propofol.

The relationship between GABA, the BOLD signal and the gamma band revealed interesting trends but no conclusive findings, partly due to absence of change in GABA measures. These relationships would need further investigation.

7.2.7 Perfusion effects of propofol sedation

Perfusion fMRI (using ASL) is emerging as a robust and reliable non-invasive neuroimaging modality to study cerebral perfusion. Although limited by a smaller signal than BOLD-fMRI it has the advantages of providing absolute perfusion values. This makes this technique uniquely useful in studying conditions that can have an independent effect on cerebral blood flow thus confounding BOLD signal responses. ASL has been used to study perfusion changes with other drugs including anaesthetic drugs (sevoflurane and midazolam) (Ramani et al., 2007, Liang et al., 2012). This thesis provides the first report of the use of pulsed ASL, during propofol sedation. There was a decrease in global CBF by about 9%. There were also regional decreases in perfusion, especially in the frontal regions, the thalamus (9.6%), the PCC (10.6%) and the precuneus (13.4%) regions. The magnitude of the changes found using pulsed ASL were similar to those reported previously in neuroimaging literature and therefore validates the use of pharmacological study of perfusion fMRI.

As propofol does not affect neurovascular coupling and, at the doses studied in this experiment, there were no significant haemodynamic and ventilatory changes and

therefore the perfusion changes can be considered to be a reflection of neuronal effects of propofol. Indeed the key areas, which showed decreased perfusion, included the frontal lobe, PCC, precuneus and thalamus. These areas are the key components of the networks involved in higher-order functioning, such as the DMN and the frontal regions.

7.3 Limitations of the experiments

The experiments conducted as part of this thesis involved a range of advanced multimodal neuroimaging techniques in a sequential study design. This design included healthy volunteers undergoing a MEG session followed a few days later, by an MRI session. Each session involved collecting data during the awake state followed by propofol sedation. The findings of these experiments were then interrogated to identify similarities, differences and to inform each others' results to provide a picture of the GABA-ergic mechanisms of sedation.

Combining the findings of different neuroimaging tools with their unique advantages is one of the key strength of this thesis. However, this also presented a few challenges.

Chapters 3, 4 and 5 have tried to bring together the results obtained from MEG and fMRI following similar tasks or during a resting state. The relationship between electrophysiological activity and its haemodynamic response in not completely understood. BOLD signal is linked to the local field potentials rather than multiunit activity or even neuronal spiking (Logothetis et al., 2001). Neurovascular coupling, manifesting as the BOLD response also depends on a number of variables, some of which continue to be poorly understood. In rats, regional heterogeneity of the neurovascular coupling has been shown (Sloan et al., 2010). Similar dependence of BOLD response to different oscillatory bands and brain regions studied has been demonstrated in humans (Conner et al., 2011, Ojemann et al., 2013). Similarly, in the context of MEG, the sources of oscillatory activity and the interactions between different frequency bands is not completely clear. Therefore the findings of the two modalities cannot simply be extrapolated to each other and are best seen as

complementary. Future studies would benefit from improvements in the understanding of this neurovascular coupling.

There was a fixed order of the experiments: MRI always followed the MEG session and *Sedated* always followed the *Awake* session. The sequence of the MEG and MRI scans was chosen due to safety reasons, where the MEG scan due to easier access, would have made it easier for the monitoring anaesthetist to manage complications if any. Similarly the *Awake* and *Sedated* sessions could not have been counterbalanced due to the study design. This meant that there was always a potential for an 'order effect' in terms of participants' responsiveness. Following the safe conduct of this set of experiments (these were the first sedation experiments of this nature in CUBRIC), future experimenters will have more confidence in counterbalancing MEG and MRI sessions. Similarly a placebo-controlled, crossover design (placebo and drug administered on different occasions) could limit the order effect of sedation. While this was considered for this experiment, it was not considered appropriate given the complexity of set up and limits of time and potential inconvenience to participants.

The delivery of the stimulus paradigms was somewhat different in the two experiments. This was due to the considerations of participant comfort (time spent undergoing MR scanning), design efficiency and the additional experiments (MRS and perfusion components) during the MR scanning.

Only one level of sedation was assessed in this study. While this was intentional, it is possible that adding a level of deeper sedation and / or studying recovery from these levels of sedation would have added more useful information. The MRS based experiment (Chapter 3) did not reveal any measurable change in GABA concentration. At deeper levels of sedation there may have been more pronounced changes making them detectable. While this remains speculative, the task based and resting state changes are likely to have been more pronounced at deeper levels of sedation. Recovery from anaesthesia follows a different trajectory to anaesthesia induction and can provide further valuable information about mechanisms of anaesthesia and consciousness (MacDonald et al., 2015, Tarnal et al., 2016). Studying recovery from sedation may have offered further similar insights. All these options were discussed at the planning

stages but considering the complexities of the design it was decided to limit to a single level of sedation.

These experiments focused on studying mild sedation, which was assessed objectively using the OAA/S scale. This involved calling out participants' names and assessing their responsiveness. Despite the blinding of the anaesthetist the scale has subjective variability, which could have resulted in different levels of sedation between the two sessions. Also, environmental factors can play a part in participant's experience of sedation. With the MRI scan environment being different to that of MEG this could have contributed to differences in sedation. Other researchers have targeted a pre-defined plasma concentration and not limited themselves to clinical assessment. The priority for us, however, was a similar behavioural endpoint and so a clinical assessment scale was chosen.

The order effect imposed by the sequential design and the potential differences in methodology and sedation assessments can be limited by a concurrent design. While combined MEG/ fMRI scanning is still in its infancy, combined EEG/ fMRI may offer solutions. Simultaneous EEG was collected with the fMRI experiments. However the data obtained was of a poor quality and therefore further analysis was not considered possible. As the main hypotheses involved MEG based parameters, it was unlikely that the MEG sessions could have been avoided without significantly compromising on the results.

7.4 Future directions

7.4.1 Visual gamma as a potential biomarker to investigate sedative drug effects

One of the main findings in these series of experiments was the discovery of modifiability of human visual gamma in response to sedation. Propofol sedation resulted in an increase in the power of induced gamma while the evoked gamma was reduced in power. This observation has shed light on the potential sources of visual

gamma generation in humans and the differential effects of propofol on those potential generators.

Gamma band observations are difficult with EEG due to the potential interference with EMG artefacts. Visual attention tasks also require participants to keep eyes open and therefore cannot be used to test deeper stages of unconsciousness. Therefore, this finding is unlikely to be easily directly translated into clinical practice (for e.g. depth of sedation monitoring systems). However, this may be a valuable tool in understanding mechanisms of different sedative drugs and then using them as a biomarker to monitor molecular activity of pharmacological agents in a non-invasive way.

The next obvious step would be to compare a non-GABA-ergic drug with propofol and establish the differences in the visual gamma responses between those. In fact, our group has recently performed this experiment and compared sedation with propofol and dexmedetomidine (which is non-GABA-ergic sedative) and shown that enhancement of induced gamma power is a feature of propofol while dexmedetomidine does not do so (Figure **7-1**). Dexmedetomidine at mildly sedative doses resulted in a decreased evoked and induced power of visual gamma.

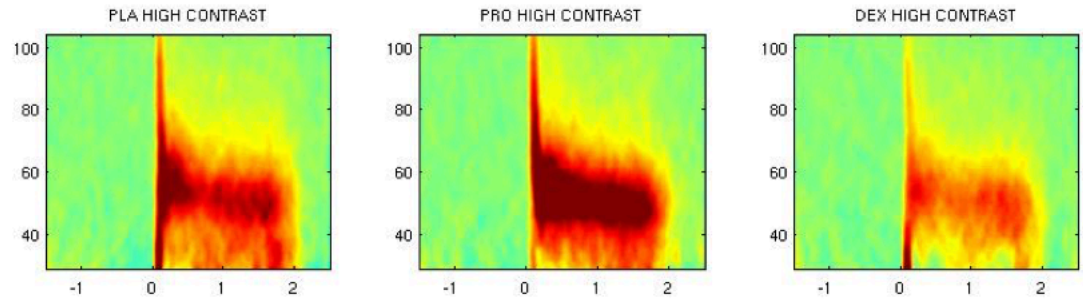

Figure 7-1: Time frequency spectrograms of visual gamma band responses.
Placebo controlled crossover design. Three groups; PLA = placebo, PRO= propofol, DEX= dexmedetomidine. Time on x –axis, power on y axis. 0 sec is onset of stimulus (unpublished results)

This experiment confirmed the findings of Experiment 2 (in Chapter 3) and hold promise for the future application of these findings. The next step would be to repeat this experiment with other GABA-ergic and non-GABA-ergic sedative drugs.

7.4.2 Application of perfusion fMRI

Application of pulsed ASL to measure perfusion changes has been successfully applied in this thesis. Recent developments in brainstem perfusion is expected to provide another avenue of interrogating brainstem function in sedation/ anaesthesia. Since pons appeared as an important brainstem structure, it would be interesting to explore perfusion changes in pons during sedation. Anaesthetic actions of other drugs, such as dexmedetomidine which have subcortical functions, would be better informed using such techniques. We are currently planning such a study.

7.4.3 Magnetic resonance spectroscopy for GABA concentration

The results of MRS experiment did not reveal any significant change in GABA related measurable activity. Interestingly there have been no other reports of the use of GABA MRS in investigating anaesthesia, during the period of this thesis. This perhaps reflects the intrinsic limitations of the existing MRS techniques. With further progress in MRS techniques it would be desirable to employ larger sample sizes to study different stages of sedation and anaesthesia to further explore the role of MR measures of GABA and its role in anaesthesia.

References

Abel, K. M., Allin, M. P., Kucharska-Pietura, K., Andrew, C., Williams, S., David, A. S. & Phillips, M. L. 2003a. Ketamine and fMRI BOLD signal: distinguishing between effects mediated by change in blood flow versus change in cognitive state. *Hum Brain Mapp,* 18**,** 135-45.

Abel, K. M., Allin, M. P., Kucharska-Pietura, K., David, A., Andrew, C., Williams, S., Brammer, M. J. & Phillips, M. L. 2003b. Ketamine alters neural processing of facial emotion recognition in healthy men: an fMRI study. *Neuroreport,* 14**,** 387-91.

Absalom, A. R., Mani, V., De Smet, T. & Struys, M. M. 2009. Pharmacokinetic models for propofol--defining and illuminating the devil in the detail. *Br J Anaesth,* 103**,** 26-37.

Achard, S., Salvador, R., Whitcher, B., Suckling, J. & Bullmore, E. 2006. A resilient, low-frequency, small-world human brain functional network with highly connected association cortical hubs. *J Neurosci,* 26**,** 63-72.

Adjamian, P., Holliday, I. E., Barnes, G. R., Hillebrand, A., Hadjipapas, A. & Singh, K. D. 2004. Induced visual illusions and gamma oscillations in human primary visual cortex. *European Journal of Neuroscience,* 20**,** 587-592.

Ai, L., Oya, H., Howard, M. & Xiong, J. 2013. Functional MRI detection of hemodynamic response of repeated median nerve stimulation. *Magn Reson Imaging,* 31**,** 550-4.

Akeju, O., Loggia, M. L., Catana, C., Pavone, K. J., Vazquez, R., Rhee, J., Contreras Ramirez, V., Chonde, D. B., Izquierdo-Garcia, D., Arabasz, G., Hsu, S., Habeeb, K., Hooker, J. M., Napadow, V., Brown, E. N. & Purdon, P. L. 2014. Disruption of thalamic functional connectivity is a neural correlate of dexmedetomidine-induced unconsciousness. *Elife,* 4**,** e04499.

Alkire, M. & Haier, R. 2001. Correlating in vivo anaesthetic effects with ex vivo receptor density data supports a GABAergic mechanism of action for propofol, but not for isoflurane. *Br J Anaesth,* 86**,** 618-26.

Alkire, M. T., Haier, R. J., Barker, S. J., Shah, N. K., Wu, J. C. & Kao, J. Y. 1995a. Cerebral Metabolism during Propofol Anesthesia in Humans Studied with Positron Emission Tomography. *Anesthesiology,* 82**,** 393-403.

Alkire, M. T., Haier, R. J., Barker, S. J., Shah, N. K., Wu, J. C. & Kao, Y. J. 1995b. Cerebral metabolism during propofol anesthesia in humans studied with positron emission tomography. *Anesthesiology,* 82**,** 393-403.

Alkire, M. T., Haier, R. J. & Fallon, J. H. 2000. Toward a Unified Theory of Narcosis: Brain Imaging Evidence for a Thalamocortical Switch as the Neurophysiologic Basis of Anesthetic-Induced Unconsciousness. *Consciousness and Cognition,* 9**,** 370-386.

Alkire, M. T., Haier, R. J., Shah, N. K. & Anderson, C. T. 1997. Positron emission tomography study of regional cerebral metabolism in humans during isoflurane anesthesia. *Anesthesiology,* 86**,** 549-557.

Alkire, M. T., Mcreynolds, J. R., Hahn, E. L. & Trivedi, A. N. 2007. Thalamic microinjection of nicotine reverses sevoflurane-induced loss of righting reflex in the rat. *Anesthesiology,* 107**,** 264-272.

Alkire, M. T., Pomfrett, C. J., Haier, R. J., Gianzero, M. V., Chan, C. M., Jacobsen, B. P. & Fallon, J. H. 1999. Functional brain imaging during anesthesia in humans: effects of halothane on global and regional cerebral glucose metabolism. *Anesthesiology,* 90**,** 701-709.

Amico, E., Gomez, F., Di Perri, C., Vanhaudenhuyse, A., Lesenfants, D., Boveroux, P., Bonhomme, V., Brichant, J. F., Marinazzo, D. & Laureys, S. 2014. Posterior cingulate cortex-related co-activation patterns: A resting state fMRI study in propofol-induced loss of consciousness. *PLoS ONE,* 9.

Andersson, J. L. R., Jenkinson, M. & Smith, S. M. 2007a. Non-linear optimisation. . *FMRIB technical report TR07JA1.*

Andersson, J. L. R., Jenkinson, M. & Smith, S. M. 2007b. Non-linear registration, aka Spatial normalisation. *FMRIB technical report TR07JA1.*

Antognini, J. F., Buonocore, M. H., Disbrow, E. A. & Carstens, E. 1997. Isoflurane anesthesia blunts cerebral responses to noxious and innocuous stimuli: a fMRI study. *Life Sci,* 61**,** PL 349-54.

Arthurs, O. J. & Boniface, S. J. 2003. What aspect of the fMRI BOLD signal best reflects the underlying electrophysiology in human somatosensory cortex? *Clin Neurophysiol,* 114**,** 1203-9.

Arthurs, O. J., Johansen-Berg, H., Matthews, P. M. & Boniface, S. J. 2004. Attention differentially modulates the coupling of fMRI BOLD and evoked potential signal amplitudes in the human somatosensory cortex. *Exp Brain Res,* 157**,** 269-74.

Arthurs, O. J., Williams, E. J., Carpenter, T. A., Pickard, J. D. & Boniface, S. J. 2000. Linear coupling between functional magnetic resonance imaging and evoked potential amplitude in human somatosensory cortex. *Neuroscience,* 101**,** 803-6.

Baars, B. J. & Gage, N. M. 2010. Vision. *In:* BAARS, B. J. & GAGE, N. M. (eds.) *Cognition, Brain, and Consciousness. Introduciton to cognitive neuroscience.* Second ed.: Elsevier.

Baars, B. J., Ramsoy, T. Z. & Laureys, S. 2003. Brain, conscious experience and the observing self. *Trends Neurosci,* 26**,** 671-675.

Bagary, M., Fluck, E., File, S. E., Joyce, E., Lockwood, G. & Grasby, P. 2000. Is benzodiazepine-induced amnesia due to deactivation of the left prefrontal cortex? *Psychopharmacology (Berl),* 150**,** 292-9.

Bai, D., Zhu, G., Pennefather, P., Jackson, M. F., Macdonald, J. F. & Orser, B. A. 2001. Distinct functional and pharmacological properties of tonic and quantal inhibitory postsynaptic currents mediated by gamma-aminobutyric acid(A) receptors in hippocampal neurons. *Mol Pharmacol,* 59**,** 814-824.

Barrett, A. B., Murphy, M., Bruno, M. A., Noirhomme, Q., Boly, M., Laureys, S. & Seth, A. K. 2012. Granger causality analysis of steady-state electroencephalographic signals during propofol-induced anaesthesia. *PLoS One,* 7**,** e29072.

Bartos, M., Vida, I. & Jonas, P. 2007. Synaptic mechanisms of synchronized gamma oscillations in inhibitory interneuron networks. *Nature Reviews Neuroscience,* 8**,** 45-56.

Barttfeld, P., Bekinschtein, T. A., Salles, A., Stamatakis, E. A., Adapa, R., Menon, D. K. & Sigman, M. 2015. Factoring the brain signatures of anesthesia concentration and level of arousal across individuals. *Neuroimage Clin,* 9**,** 385-91.

Bastiaansen, M. C. & Knosche, T. R. 2000. Tangential derivative mapping of axial MEG applied to event-related desynchronization research. *Clin Neurophysiol,* 111**,** 1300-5.

Beckmann, C. F., Jenkinson, M. & Smith, S. M. 2003. General multilevel linear modeling for group analysis in FMRI. *Neuroimage,* 20**,** 1052-63.

Beckmann, C. F., Mackay, C. E., Filippini, N. & Smith, S. M. Group comparison of resting-state FMRI data using multi-subject ICA and dual regression. OHBM, 2009.

Beecher, H. K. 1947. Anesthesia's Second Power: Probing the Mind. *Science,* 105**,** 164-6.

Berridge, C. W. 2008. Noradrenergic modulation of arousal. *Brain Res Rev,* 58**,** 1-17.

Bianchi, M. T., Haas, K. F. & Macdonald, R. L. 2002. Alpha1 and alpha6 subunits specify distinct desensitization, deactivation and neurosteroid modulation of GABA(A) receptors containing the delta subunit. *Neuropharmacology,* 43**,** 492-502.

Biel, M., Wahl-Schott, C., Michalakis, S. & Zong, X. 2009. Hyperpolarization-activated cation channels: from genes to function. *Physiol Rev,* 89**,** 847-885.

Birn, R., Diamond, J., Smith, M. & Bandettini, P. 2006. Separating respiratory-variation-related fluctuations from neuronal-activity-related fluctuations in fMRI. *Neuroimage,* 31**,** 1536-48.

Birn, R. M., Cornejo, M. D., Molloy, E. K., Patriat, R., Meier, T. B., Kirk, G. R., Nair, V. A., Meyerand, M. E. & Prabhakaran, V. 2014. The influence of physiological noise correction on test-retest reliability of resting-state functional connectivity. *Brain Connect,* 4**,** 511-22.

Biswal, B., Yetkin, F. Z., Haughton, V. M. & Hyde, J. S. 1995. Functional connectivity in the motor cortex of resting human brain using echo-planar MRI. *Magn Reson Med,* 34**,** 537-541.

Bogner, W., Gruber, S., Doelken, M., Stadlbauer, A., Ganslandt, O., Boettcher, U., Trattnig, S., Doerfler, A., Stefan, H. & Hammen, T. 2010. In vivo quantification of intracerebral GABA by single-voxel (1)H-MRS-How reproducible are the results? *Eur J Radiol,* 73**,** 526-31.

Boisseau, N., Madany, M., Staccini, P., Armando, G., Martin, F., Grimaud, D. & Raucoules-Aime, M. 2002. Comparison of the effects of sevoflurane and propofol on cortical somatosensory evoked potentials. *Br J Anaesth,* 88**,** 785-9.

Boiten, F., Sergeant, J. & Geuze, R. 1992. Event-related desynchronization: the effects of energetic and computational demands. *Electroencephalogr Clin Neurophysiol,* 82**,** 302-9.

Boly, M., Moran, R., Murphy, M., Boveroux, P., Bruno, M. A., Noirhomme, Q., Ledoux, D., Bonhomme, V., Brichant, J. F., Tononi, G., Laureys, S. & Friston, K. 2012. Connectivity changes underlying spectral EEG changes during propofol-induced loss of consciousness. *J Neurosci,* 32**,** 7082-90.

Boly, M., Sanders, R. D., Mashour, G. A. & Laureys, S. 2013. Consciousness and responsiveness: lessons from anaesthesia and the vegetative state. *Curr Opin Anaesthesiol,* 26**,** 444-9.

Bonhomme, V., Boveroux, P., Vanhaudenhuyse, A., Hans, P., Brichant, J. F., Jaquet, O., Boly, M. & Laureys, S. 2011. Linking sleep and general anesthesia mechanisms: this is no walkover. *Acta Anaesthesiol Belg,* 62**,** 161-71.

Bonhomme, V., Fiset, P., Meuret, P., Backman, S., Plourde, G., Paus, T., Bushnell, M. & Evans, A. 2001. Propofol anesthesia and cerebral blood flow changes elicited by vibrotactile stimulation: a positron emission tomography study. *J Neurophysiol,* 85**,** 1299-308.

Bonhomme, V., Maquet, P., Phillips, C., Plenevaux, A., Hans, P., Luxen, A., Lamy, M. & Laureys, S. 2008. The effect of clonidine infusion on distribution of regional cerebral blood flow in volunteers. *Anesth Analg,* 106**,** 899-909.

Boveroux, P., Vanhaudenhuyse, A., Bruno, M. A., Noirhomme, Q., Lauwick, S., Luxen, A., Degueldre, C., Plenevaux, A., Schnakers, C., Phillips, C., Brichant, J. F., Bonhomme, V., Maquet, P., Greicius, M. D., Laureys, S. & Boly, M. 2010. Breakdown of within- and between-network resting state functional magnetic resonance imaging connectivity during propofol-induced loss of consciousness. *Anesthesiology,* 113**,** 1038-53.

Breshears, J. D., Roland, J. L., Sharma, M., Gaona, C. M., Freudenburg, Z. V., Tempelhoff, R., Avidan, M. S. & Leuthardt, E. C. 2010. Stable and dynamic cortical electrophysiology of induction and emergence with propofol anesthesia. *Proc Natl Acad Sci U S A,* 107**,** 21170-5.

Bressler, D., Spotswood, N. & Whitney, D. 2007. Negative BOLD fMRI response in the visual cortex carries precise stimulus-specific information. *PLoS One,* 2**,** e410.

Brookes, M. J., Gibson, A. M., Hall, S. D., Furlong, P. L., Barnes, G. R., Hillebrand, A., Singh, K. D., Holliday, I. E., Francis, S. T. & Morris, P. G. 2005. GLM-beamformer method demonstrates stationary field, alpha ERD and gamma ERS co-localisation with fMRI BOLD response in visual cortex. *Neuroimage,* 26**,** 302-8.

Brookes, M. J., Hale, J. R., Zumer, J. M., Stevenson, C. M., Francis, S. T., Barnes, G. R., Owen, J. P., Morris, P. G. & Nagarajan, S. S. 2011a. Measuring functional connectivity using MEG: methodology and comparison with fcMRI. *Neuroimage,* 56**,** 1082-104.

Brookes, M. J., Woolrich, M., Luckhoo, H., Price, D., Hale, J. R., Stephenson, M. C., Barnes, G. R., Smith, S. M. & Morris, P. G. 2011b. Investigating the electrophysiological basis of resting state networks using magnetoencephalography. *Proc Natl Acad Sci U S A,* 108**,** 16783-8.

Brunel, N. & Wang, X. J. 2003. What determines the frequency of fast network oscillations with irregular neural discharges? I. Synaptic dynamics and excitation-inhibition balance. *J Neurophysiol,* 90**,** 415-30.

Brunner, M. D., Nel, M. R., Fernandes, R., Thornton, C. & Newton, D. E. 2002. Auditory evoked response during propofol anaesthesia after pre-induction with midazolam. *Br J Anaesth,* 89**,** 325-7.

Brunner, M. D., Umo-Etuk, J., Sharpe, R. M. & Thornton, C. 1999. Effect of a bolus dose of midazolam on the auditory evoked response in humans. *Br J Anaesth,* 82**,** 633-4.

Buzsaki, G. 2002. Theta oscillations in the hippocampus. *Neuron,* 33**,** 325-40.

Byas-Smith, M., Frolich, M. A., Votaw, J. R., Faber, T. L. & Hoffman, J. M. 2002. Cerebral blood flow during propofol induced sedation. *Mol Imaging Biol,* 4**,** 139-46.

Byas–Smith, M. 2002. Cerebral Blood Flow During Propofol Induced Sedation. *Molecular Imaging & Biology,* 4**,** 139-146.

Calhoun, V. D. & Adali, T. 2012. Multisubject independent component analysis of fMRI: a decade of intrinsic networks, default mode, and neurodiagnostic discovery. *IEEE Rev Biomed Eng,* 5**,** 60-73.

Canolty, R. T., Edwards, E., Dalal, S. S., Soltani, M., Nagarajan, S. S., Kirsch, H. E., Berger, M. S., Barbaro, N. M. & Knight, R. T. 2006. High gamma power is phase-locked to theta oscillations in human neocortex. *Science,* 313**,** 1626-8.

Cardin, J. A., Carlen, M., Meletis, K., Knoblich, U., Zhang, F., Deisseroth, K., Tsai, L. H. & Moore, C. I. 2009. Driving fast-spiking cells induces gamma rhythm and controls sensory responses. *Nature,* 459**,** 663-7.

Carhart-Harris, R. L., Erritzoe, D., Williams, T., Stone, J. M., Reed, L. J., Colasanti, A., Tyacke, R. J., Leech, R., Malizia, A. L., Murphy, K., Hobden, P., Evans, J., Feilding, A., Wise, R. G. & Nutt, D. J. 2012. Neural correlates of the psychedelic state as determined by fMRI studies with psilocybin. *Proc Natl Acad Sci U S A,* 109**,** 2138-43.

Carhart-Harris, R. L., Leech, R., Erritzoe, D., Williams, T. M., Stone, J. M., Evans, J., Sharp, D. J., Feilding, A., Wise, R. G. & Nutt, D. J. 2013. Functional connectivity measures after psilocybin inform a novel hypothesis of early psychosis. *Schizophr Bull,* 39**,** 1343-51.

Carhart-Harris, R. L., Murphy, K., Leech, R., Erritzoe, D., Wall, M. B., Ferguson, B., Williams, L. T., Roseman, L., Brugger, S., De Meer, I., Tanner, M., Tyacke, R., Wolff, K., Sethi, A., Bloomfield, M. A., Williams, T. M., Bolstridge, M., Stewart, L., Morgan, C., Newbould, R. D., Feilding, A., Curran, H. V. & Nutt, D. J. 2014. The Effects of Acutely Administered 3,4-Methylenedioxymethamphetamine on Spontaneous Brain Function in Healthy Volunteers Measured with Arterial Spin Labeling and Blood Oxygen Level-Dependent Resting State Functional Connectivity. *Biol Psychiatry*.

Carusone, L. M., Srinivasan, J., Gitelman, D. R., Mesulam, M. M. & Parrish, T. B. 2002. Hemodynamic response changes in cerebrovascular disease: implications for functional MR imaging. *AJNR Am J Neuroradiol,* 23**,** 1222-8.

Castelo-Branco, M., Neuenschwander, S. & Singer, W. 1998. Synchronization of visual responses between the cortex, lateral geniculate nucleus, and retina in the anesthetized cat. *J Neurosci,* 18**,** 6395-410.

Cauli, B., Tong, X.-K., Rancillac, A., Serluca, N., Lambolez, B., Rossier, J. & Hamel, E. 2004. Cortical GABA interneurons in neurovascular coupling: relays for subcortical vasoactive pathways. *J Neurosci,* 24**,** 8940-8949.

Cavanna, A. E. 2007. The precuneus and consciousness. *CNS Spectr,* 12**,** 545-52.

Cavanna, A. E. & Trimble, M. R. 2006. The precuneus: a review of its functional anatomy and behavioural correlates. *Brain,* 129**,** 564-83.

Chalmers, D. J. 1995. Facing up to the problem of consciousness. *Journal of Consciousness Studies,* 2**,** 200-219.

Chambers, J. D., Bethwaite, B., Diamond, N. T., Peachey, T., Abramson, D., Petrou, S. & Thomas, E. A. 2012. Parametric computation predicts a multiplicative interaction between synaptic strength parameters that control gamma oscillations. *Front Comput Neurosci,* 6**,** 53.

Chandra, D., Jia, F., Liang, J., Peng, Z., Suryanarayanan, A., Werner, D. F., Spigelman, I., Houser, C. R., Olsen, R. W., Harrison, N. L. & Homanics, G. E. 2006. GABAA receptor alpha 4 subunits mediate extrasynaptic inhibition in thalamus and dentate gyrus and the action of gaboxadol. *Proc Natl Acad Sci U S A,* 103**,** 15230-15235.

Checketts, M. R., Alladi, R., Ferguson, K., Gemmell, L., Handy, J. M., Klein, A. A., Love, N. J., Misra, U., Morris, C., Nathanson, M. H., Rodney, G. E., Verma, R., Pandit, J. J., Association of Anaesthetists of Great, B. & Ireland 2016. Recommendations for standards of monitoring during anaesthesia and recovery 2015: Association of Anaesthetists of Great Britain and Ireland. *Anaesthesia,* 71**,** 85-93.

Chen, X., Shu, S. & Bayliss, D. A. 2009. HCN1 channel subunits are a molecular substrate for hypnotic actions of ketamine. *J Neurosci,* 29**,** 600-609.

Chen, Z., Silva, A. C., Yang, J. & Shen, J. 2005. Elevated endogenous GABA level correlates with decreased fMRI signals in the rat brain during acute inhibition of GABA transaminase. *J Neurosci Res,* 79**,** 383-391.

Chernik, D. A., Gillings, D., Laine, H., Hendler, J., Silver, J. M., Davidson, A. B., Schwam, E. M. & Siegel, J. L. 1990. Validity and reliability of the Observer's Assessment of Alertness/Sedation Scale: study with intravenous midazolam. *J Clin Psychopharmacol,* 10**,** 244-51.

Ching, S. & Brown, E. N. 2014. Modeling the dynamical effects of anesthesia on brain circuits. *Current Opinion in Neurobiology,* 25**,** 116-122.

Ching, S., Cimenser, A., Purdon, P. L., Brown, E. N. & Kopell, N. J. 2010a. Thalamocortical model for a propofol-induced -rhythm associated with loss of consciousness. *Proceedings of the National Academy of Sciences,* 107**,** 22665-22670.

Ching, S., Cimenser, A., Purdon, P. L., Brown, E. N. & Kopell, N. J. 2010b. Thalamocortical model for a propofol-induced alpha-rhythm associated with loss of consciousness. *Proc Natl Acad Sci U S A,* 107**,** 22665-70.

Chu, D. C., Albin, R. L., Young, A. B. & Penney, J. B. 1990. Distribution and kinetics of GABAB binding sites in rat central nervous system: a quantitative autoradiographic study. *Neuroscience,* 34**,** 341-57.

Cimenser, A., Purdon, P. L., Pierce, E. T., Walsh, J. L., Salazar-Gomez, A. F., Harrell, P. G., Tavares-Stoeckel, C., Habeeb, K. & Brown, E. N. 2011. Tracking brain states under general anesthesia by using global coherence analysis. *Proc Natl Acad Sci U S A,* 108**,** 8832-7.

Cipolla, M. J. 2009. The Cerebral Circulation. *Morgan & Claypool Life Sciences.* San Rafael (CA).

Claeys, M. A., Gepts, E. & Camu, F. 1988. Haemodynamic changes during anaesthesia induced and maintained with propofol. *Br J Anaesth,* 60**,** 3-9.

Cohen, M. S. & Bookheimer, S. Y. 1994. Localization of brain function using magnetic resonance imaging. *Trends Neurosci,* 17**,** 268-77.

Cole, D. M., Smith, S. M. & Beckmann, C. F. 2010. Advances and pitfalls in the analysis and interpretation of resting-state FMRI data. *Front Syst Neurosci,* 4**,** 8.

Collins, G. G. 1988. Effects of the anaesthetic 2,6-diisopropylphenol on synaptic transmission in the rat olfactory cortex slice. *Br J Pharmacol,* 95**,** 939-949.

Concas, A., Santoro, G., Serra, M., Sanna, E. & Biggio, G. 1991. Neurochemical action of the general anaesthetic propofol on the chloride ion channel coupled with GABAA receptors. *Brain Research,* 542**,** 225-232.

Conner, C. R., Ellmore, T. M., Pieters, T. A., Disano, M. A. & Tandon, N. 2011. Variability of the relationship between electrophysiology and BOLD-fMRI across cortical regions in humans. *J Neurosci,* 31**,** 12855-65.

Cook, T. M., Andrade, J., Bogod, D. G., Hitchman, J. M., Jonker, W. R., Lucas, N., Mackay, J. H., Nimmo, A. F., O'connor, K., O'sullivan, E. P., Paul, R. G., Palmer, J. H., Plaat, F., Radcliffe, J. J., Sury, M. R., Torevell, H. E., Wang, M., Hainsworth, J., Pandit, J. J., Royal College Of, A., Association of Anaesthetists of Great, B. & Ireland 2014. 5th National Audit Project (NAP5) on accidental awareness during general anaesthesia:

patient experiences, human factors, sedation, consent, and medicolegal issues. *Br J Anaesth,* 113**,** 560-74.

Davis, M. H., Coleman, M. R., Absalom, A. R., Rodd, J. M., Johnsrude, I. S., Matta, B. F., Owen, A. M. & Menon, D. K. 2007. Dissociating speech perception and comprehension at reduced levels of awareness. *Proc Natl Acad Sci U S A,* 104**,** 16032-7.

Demuru, M., Van Duinkerken, E., Fraschini, M., Marrosu, F., Snoek, F. J., Barkhof, F., Klein, M., Diamant, M. & Hillebrand, A. 2014. Changes in MEG resting-state networks are related to cognitive decline in type 1 diabetes mellitus patients. *Neuroimage Clin,* 5**,** 69-76.

Denier, N., Gerber, H., Vogel, M., Klarhofer, M., Riecher-Rossler, A., Wiesbeck, G. A., Lang, U. E., Borgwardt, S. & Walter, M. 2013. Reduction in cerebral perfusion after heroin administration: a resting state arterial spin labeling study. *PLoS One,* 8**,** e71461.

Detre, J. A. & Wang, J. 2002. Technical aspects and utility of fMRI using BOLD and ASL. *Clin Neurophysiol,* 113**,** 621-34.

Di Russo, F., Martinez, A., Sereno, M. I., Pitzalis, S. & Hillyard, S. A. 2002. Cortical sources of the early components of the visual evoked potential. *Hum Brain Mapp,* 15**,** 95-111.

Dickinson, R., Peterson, B. K., Banks, P., Simillis, C., Martin, J. C. S., Valenzuela, C. A., Maze, M. & Franks, N. P. 2007. Competitive inhibition at the glycine site of the N-methyl-D-aspartate receptor by the anesthetics xenon and isoflurane: evidence from molecular modeling and electrophysiology. *Anesthesiology,* 107**,** 756-767.

Dirnberger, G., Duregger, C., Lindinger, G. & Lang, W. 2004. Habituation in a simple repetitive motor task: a study with movement-related cortical potentials. *Clin Neurophysiol,* 115**,** 378-84.

Doenicke, A. W., Kugler, J., Kochs, E., Rau, J., Muckter, H., Hoernecke, R., Conzen, P., Bromber, H. & Schneider, G. 2007. The Narcotrend monitor and the electroencephalogram in propofol-induced sedation. *Anesth Analg,* 105**,** 982-92, table of contents.

Donahue, M. J., Near, J., Blicher, J. U. & Jezzard, P. 2010. Baseline GABA concentration and fMRI response. *Neuroimage,* 53**,** 392-398.

Driver, I. D., Whittaker, J. R., Bright, M. G., Muthukumaraswamy, S. D. & Murphy, K. 2016. Arterial CO2 Fluctuations Modulate Neuronal Rhythmicity: Implications for MEG and fMRI Studies of Resting-State Networks. *J Neurosci,* 36**,** 8541-50.

Dueck, M. H., Petzke, F., Gerbershagen, H. J., Paul, M., Hesselmann, V., Girnus, R., Krug, B., Sorger, B., Goebel, R., Lehrke, R., Sturm, V. & Boerner, U. 2005. Propofol attenuates responses of the auditory cortex to acoustic stimulation in a dose-dependent manner: a FMRI study. *Acta Anaesthesiol Scand,* 49**,** 784-791.

Dujardin, K., Derambure, P., Defebvre, L., Bourriez, J. L., Jacquesson, J. M. & Guieu, J. D. 1993. Evaluation of event-related desynchronization (ERD) during a recognition task: effect of attention. *Electroencephalogr Clin Neurophysiol,* 86**,** 353-6.

Edden, R. A. & Barker, P. B. 2007. Spatial effects in the detection of gamma-aminobutyric acid: improved sensitivity at high fields using inner volume saturation. *Magn Reson Med,* 58**,** 1276-82.

Edden, R. A., Intrapiromkul, J., Zhu, H., Cheng, Y. & Barker, P. B. 2012. Measuring T2 in vivo with J-difference editing: application to GABA at 3 Tesla. *J Magn Reson Imaging,* 35**,** 229-34.

Epperson, C. N., Gueorguieva, R., Czarkowski, K. A., Stiklus, S., Sellers, E., Krystal, J. H., Rothman, D. L. & Mason, G. F. 2006. Preliminary evidence of reduced occipital GABA concentrations in puerperal women: a 1H-MRS study. *Psychopharmacology (Berl),* 186**,** 425-33.

Epperson, C. N., Haga, K., Mason, G. F., Sellers, E., Gueorguieva, R., Zhang, W., Weiss, E., Rothman, D. L. & Krystal, J. H. 2002. Cortical gamma-aminobutyric acid levels across the menstrual cycle in healthy women and those with premenstrual dysphoric disorder: a proton magnetic resonance spectroscopy study. *Arch Gen Psychiatry,* 59**,** 851-858.

Epperson, C. N., O'malley, S., Czarkowski, K. A., Gueorguieva, R., Jatlow, P., Sanacora, G., Rothman, D. L., Krystal, J. H. & Mason, G. F. 2005. Sex, GABA, and nicotine: the impact of smoking on cortical GABA levels across the menstrual cycle as measured with proton magnetic resonance spectroscopy. *Biol Psychiatry,* 57**,** 44-8.

European Delirium, A. & American Delirium, S. 2014. The DSM-5 criteria, level of arousal and delirium diagnosis: inclusiveness is safer. *BMC Med,* 12**,** 141.

Evans, C. J., Mcgonigle, D. J. & Edden, R. a. E. 2010. Diurnal stability of gamma-aminobutyric acid concentration in visual and sensorimotor cortex. *J Magn Reson Imaging,* 31**,** 204-209.

Evans, C. J., Puts, N. A., Robson, S. E., Boy, F., Mcgonigle, D. J., Sumner, P., Singh, K. D. & Edden, R. A. 2013. Subtraction artifacts and frequency (mis-)alignment in J-difference GABA editing. *J Magn Reson Imaging,* 38**,** 970-5.

Farrant, M. & Nusser, Z. 2005. Variations on an inhibitory theme: phasic and tonic activation of GABA(A) receptors. *Nat Rev Neurosci,* 6**,** 215-229.

Feng, H. J. & Macdonald, R. L. 2004. Multiple actions of propofol on alphabetagamma and alphabetadelta GABAA receptors. *Mol Pharmacol,* 66**,** 1517-24.

Ferrarelli, F., Massimini, M., Sarasso, S., Casali, A., Riedner, B. A., Angelini, G., Tononi, G. & Pearce, R. A. 2010. Breakdown in cortical effective connectivity during midazolam-induced loss of consciousness. *Proc Natl Acad Sci U S A,* 107**,** 2681-2686.

Ferre, J. C., Bannier, E., Raoult, H., Mineur, G., Carsin-Nicol, B. & Gauvrit, J. Y. 2013. Arterial spin labeling (ASL) perfusion: techniques and clinical use. *Diagn Interv Imaging,* 94**,** 1211-23.

Feshchenko, V., Veselis, R. & Reinsel, R. 1996. EFFECTS OF ANESTHETIC SEDATION ON THE OSCILLATORY SYSTEM UNDERLYING EEG ALPHA-RHYTHM: B201. *J Clin Neurophysiol,* 13**,** 439.

Feshchenko, V. A., Veselis, R. A. & Reinsel, R. A. 2004. Propofol-induced alpha rhythm. *Neuropsychobiology,* 50**,** 257-66.

Filippini, N., Macintosh, B. J., Hough, M. G., Goodwin, G. M., Frisoni, G. B., Smith, S. M., Matthews, P. M., Beckmann, C. F. & Mackay, C. E. 2009. Distinct patterns of brain activity in young carriers of the APOE-epsilon4 allele. *Proc Natl Acad Sci U S A,* 106**,** 7209-14.

Fischer, H., Furmark, T., Wik, G. & Fredrikson, M. 2000. Brain representation of habituation to repeated complex visual stimulation studied with PET. *Neuroreport,* 11**,** 123-6.

Fiset, P., Paus, T., Daloze, T., Plourde, G., Meuret, P., Bonhomme, V., Hajj-Ali, N., Backman, S. B. & Evans, A. C. 1999. Brain mechanisms of propofol-induced loss of consciousness in humans: a positron emission tomographic study. *J Neurosci,* 19**,** 5506-5513.

Fox, P. T. & Raichle, M. E. 1984. Stimulus rate dependence of regional cerebral blood flow in human striate cortex, demonstrated by positron emission tomography. *J Neurophysiol,* 51**,** 1109-1120.

Franks, N. P. & Zecharia, A. Y. 2011. Sleep and general anesthesia. *Can J Anaesth,* 58**,** 139-48.

Fransson, P. & Marrelec, G. 2008. The precuneus/posterior cingulate cortex plays a pivotal role in the default mode network: Evidence from a partial correlation network analysis. *Neuroimage,* 42**,** 1178-84.

Freund, T. F. & Meskenaite, V. 1992. gamma-Aminobutyric acid-containing basal forebrain neurons innervate inhibitory interneurons in the neocortex. *Proc Natl Acad Sci U S A,* 89**,** 738-742.

Fries, P., Scheeringa, R. & Oostenveld, R. 2008. Finding gamma. *Neuron,* 58**,** 303-305.

Fuller, P. M., Saper, C. B. & Lu, J. 2007. The pontine REM switch: past and present. *J Physiol,* 584**,** 735-741.

Gaetz, W., Roberts, T. P., Singh, K. D. & Muthukumaraswamy, S. D. 2012. Functional and structural correlates of the aging brain: relating visual cortex (V1) gamma band responses to age-related structural change. *Hum Brain Mapp,* 33**,** 2035-46.

Galarreta, M. & Hestrin, S. 1999. A network of fast-spiking cells in the neocortex connected by electrical synapses. *Nature,* 402**,** 72-75.

Gallopin, T., Luppi, P. H., Cauli, B., Urade, Y., Rossier, J., Hayaishi, O., Lambolez, B. & Fort, P. 2005. The endogenous somnogen adenosine excites a subset of sleep-promoting neurons via A2A receptors in the ventrolateral preoptic nucleus. *Neuroscience,* 134**,** 1377-1390.

Garces, P., Pereda, E., Hernandez-Tamames, J. A., Del-Pozo, F., Maestu, F. & Pineda-Pardo, J. A. 2016. Multimodal description of whole brain connectivity: A comparison of resting state MEG, fMRI, and DWI. *Hum Brain Mapp,* 37**,** 20-34.

Gauss, A., Heinrich, H. & Wilder-Smith, O. H. 1991. Echocardiographic assessment of the haemodynamic effects of propofol: a comparison with etomidate and thiopentone. *Anaesthesia,* 46**,** 99-105.

Ghita, A. M., Parvu, D., Sava, R., Georgescu, L. & Zagrean, L. 2013. Analysis of the visual evoked potential in anesthesia with sevoflurane and chloral hydrate : (Variability of amplitudes, latencies and morphology of VEP with the depth of anesthesia). *J Med Life,* 6**,** 214-25.

Ghoneim, M. M. 2000. Awareness during anesthesia. *Anesthesiology,* 92**,** 597-602.

Gili, T., Saxena, N., Diukova, A., Murphy, K., Hall, J. E. & Wise, R. G. 2013. The thalamus and brainstem act as key hubs in alterations of human brain network connectivity induced by mild propofol sedation. *J Neurosci,* 33**,** 4024-31.

Girard, T. D., Pandharipande, P. P. & Ely, E. W. 2008. Delirium in the intensive care unit. *Crit Care,* 12 Suppl 3**,** S3.

Glover, G., Li, T. & Ress, D. 2000. Image-based method for retrospective correction of physiological motion effects in fMRI: RETROICOR. *Magn Reson Med,* 44**,** 162-7.

Glover, G. H. 2011. Overview of functional magnetic resonance imaging. *Neurosurg Clin N Am,* 22**,** 133-9, vii.

Goddard, A. W., Mason, G. F., Appel, M., Rothman, D. L., Gueorguieva, R., Behar, K. L. & Krystal, J. H. 2004a. Impaired GABA neuronal response to acute benzodiazepine administration in panic disorder. *Am J Psychiatry,* 161**,** 2186-93.

Goddard, A. W., Mason, G. F., Rothman, D. L., Behar, K. L., Petroff, O. A. & Krystal, J. H. 2004b. Family psychopathology and magnitude of reductions in occipital cortex GABA levels in panic disorder. *Neuropsychopharmacology,* 29**,** 639-40.

Goodman, N. W., Black, A. M. & Carter, J. A. 1987. Some ventilatory effects of propofol as sole anaesthetic agent. *Br J Anaesth,* 59**,** 1497-503.

Gray, A. T., Winegar, B. D., Leonoudakis, D. J., Forsayeth, J. R. & Yost, C. S. 1998. TOK1 is a volatile anesthetic stimulated K+ channel. *Anesthesiology,* 88**,** 1076-1084.

Gray, C. M., Engel, A. K., Konig, P. & Singer, W. 1990. Stimulus-Dependent Neuronal Oscillations in Cat Visual Cortex: Receptive Field Properties and Feature Dependence. *Eur J Neurosci,* 2**,** 607-619.

Greene, B. R., Mahon, P., Mcnamara, B., Boylan, G. B. & Shorten, G. 2007. Automated estimation of sedation depth from the EEG. *Conf Proc IEEE Eng Med Biol Soc,* 2007**,** 3188-91.

Greicius, M. D., Kiviniemi, V., Tervonen, O., Vainionpaa, V., Alahuhta, S., Reiss, A. L. & Menon, V. 2008. Persistent default-mode network connectivity during light sedation. *Hum Brain Mapp,* 29**,** 839-47.

Greicius, M. D., Krasnow, B., Reiss, A. L. & Menon, V. 2003. Functional connectivity in the resting brain: a network analysis of the default mode hypothesis. *Proc Natl Acad Sci U S A,* 100**,** 253-258.

Grill-Spector, K., Kourtzi, Z. & Kanwisher, N. 2001. The lateral occipital complex and its role in object recognition. *Vision Res,* 41**,** 1409-22.

Gross, J., Baillet, S., Barnes, G. R., Henson, R. N., Hillebrand, A., Jensen, O., Jerbi, K., Litvak, V., Maess, B., Oostenveld, R., Parkkonen, L., Taylor, J. R., Van Wassenhove, V., Wibral, M. & Schoffelen, J. M. 2012. Good-practice for conducting and reporting MEG research. *NeuroImage*.

Gugino, L., Chabot, R., Prichep, L., John, E., Formanek, V. & Aglio, L. 2001. Quantitative EEG changes associated with loss and return of consciousness in healthy adult volunteers anaesthetized with propofol or sevoflurane. *Br J Anaesth,* 87**,** 421-8.

Guldenmund, P., Demertzi, A., Boveroux, P., Boly, M., Vanhaudenhuyse, A., Bruno, M. A., Gosseries, O., Noirhomme, Q., Brichant, J. F., Bonhomme, V., Laureys, S. & Soddu, A. 2013. Thalamus, brainstem and salience network connectivity changes during propofol-induced sedation and unconsciousness. *Brain Connect,* 3**,** 273-85.

Gyulai, F. E., Firestone, L. L., Mintun, M. A. & Winter, P. M. 1996. In vivo imaging of human limbic responses to nitrous oxide inhalation. *Anesth Analg,* 83**,** 291-298.

Hadjipapas, A., Adjamian, P., Swettenham, J. B., Holliday, I. E. & Barnes, G. R. 2007. Stimuli of varying spatial scale induce gamma activity with distinct temporal characteristics in human visual cortex. *Neuroimage,* 35**,** 518-530.

Hall, E. L., Woolrich, M. W., Thomaz, C. E., Morris, P. G. & Brookes, M. J. 2013. Using variance information in magnetoencephalography measures of functional connectivity. *Neuroimage,* 67**,** 203-12.

Hall, S. D., Barnes, G. R., Furlong, P. L., Seri, S. & Hillebrand, A. 2010. Neuronal network pharmacodynamics of GABAergic modulation in the human cortex determined using pharmaco-magnetoencephalography. *Hum Brain Mapp,* 31**,** 581-94.

Hall, S. D., Holliday, I. E., Hillebrand, A., Furlong, P. L., Singh, K. D. & Barnes, G. R. 2005a. Distinct contrast response functions in striate and extra-striate regions of visual cortex revealed with magnetoencephalography (MEG). *Clinical Neurophysiology,* 116**,** 1716-1722.

Hall, S. D., Holliday, I. E., Hillebrand, A., Singh, K. D., Furlong, P. L., Hadjipapas, A. & Barnes, G. R. 2005b. The missing link: analogous human and primate cortical gamma oscillations. *Neuroimage,* 26**,** 13-7.

Harada, M., Kubo, H., Nose, A., Nishitani, H. & Matsuda, T. 2010. Measurement of variation in the human cerebral GABA level by in vivo MEGA-editing proton MR spectroscopy using a clinical 3 T instrument and its dependence on brain region and the female menstrual cycle. *Hum Brain Mapp*.

Haridas, R. P. 2016. "Gentlemen! This Is No Humbug": Did John Collins Warren, M.D., Proclaim These Words on October 16, 1846, at Massachusetts General Hospital, Boston? *Anesthesiology,* 124**,** 553-60.

Harris, A. D., Glaubitz, B., Near, J., John Evans, C., Puts, N. A., Schmidt-Wilcke, T., Tegenthoff, M., Barker, P. B. & Edden, R. A. 2014. Impact of frequency drift on gamma-aminobutyric acid-edited MR spectroscopy. *Magn Reson Med,* 72**,** 941-8.

Hasenstaub, A., Shu, Y., Haider, B., Kraushaar, U., Duque, A. & Mccormick, D. A. 2005. Inhibitory postsynaptic potentials carry synchronized frequency information in active cortical networks. *Neuron,* 47**,** 423-35.

Hashemi, M., Hutt, A. & Sleigh, J. 2015. How the cortico-thalamic feedback affects the EEG power spectrum over frontal and occipital regions during propofol-induced sedation. *Journal of Computational Neuroscience,* 39**,** 155-179.

Hashimoto, I., Mashiko, T., Yoshikawa, K., Mizuta, T., Imada, T. & Hayashi, M. 1995. Neuromagnetic measurements of the human primary auditory response. *Electroencephalogr Clin Neurophysiol,* 96**,** 348-56.

Heine, L., Soddu, A., Gomez, F., Vanhaudenhuyse, A., Tshibanda, L., Thonnard, M., Charland-Verville, V., Kirsch, M., Laureys, S. & Demertzi, A. 2012. Resting state networks and consciousness: alterations of multiple resting state network connectivity in physiological, pharmacological, and pathological consciousness States. *Front Psychol,* 3**,** 295.

Heinke, W., Kenntner, R., Gunter, T. C., Sammler, D., Olthoff, D. & Koelsch, S. 2004. Sequential effects of increasing propofol sedation on frontal and temporal cortices as indexed by auditory event-related potentials. *Anesthesiology,* 100**,** 617-25.

Heinke, W. & Schwarzbauer, C. 2001. Subanesthetic isoflurane affects task-induced brain activation in a highly specific manner: a functional magnetic resonance imaging study. *Anesthesiology,* 94**,** 973-981.

Heinke, W. & Schwarzbauer, C. 2002. In vivo imaging of anaesthetic action in humans: approaches with positron emission tomography (PET) and functional magnetic resonance imaging (fMRI). *Br J Anaesth,* 89**,** 112-22.

Henry, P. G., Dautry, C., Hantraye, P. & Bloch, G. 2001. Brain GABA editing without macromolecule contamination. *Magn Reson Med,* 45**,** 517-20.

Hernandez, B. A., Lindroth, H., Rowley, P., Boncyk, C., Raz, A., Gaskell, A., García, P. S., Sleigh, J. & Sanders, R. D. 2017. Post-anaesthesia care unit delirium: incidence, risk factors and associated adverse outcomes. *British Journal of Anaesthesia,* 119**,** 288 - 290.

Hevers, W. & Luddens, H. 1998. The diversity of GABAA receptors. Pharmacological and electrophysiological properties of GABAA channel subtypes. *Mol Neurobiol,* 18**,** 35-86.

Hillebrand, A. & Barnes, G. R. 2002. A quantitative assessment of the sensitivity of whole-head MEG to activity in the adult human cortex. *Neuroimage,* 16**,** 638-650.

Hillebrand, A., Tewarie, P., Van Dellen, E., Yu, M., Carbo, E. W., Douw, L., Gouw, A. A., Van Straaten, E. C. & Stam, C. J. 2016. Direction of information flow in large-scale resting-state networks is frequency-dependent. *Proc Natl Acad Sci U S A*.

Hindriks, R., Bijma, F., Van Dijk, B. W., Van Der Werf, Y. D., Van Someren, E. J. & Van Der Vaart, A. W. 2011. Dynamics underlying spontaneous human alpha oscillations: a data-driven approach. *Neuroimage,* 57**,** 440-51.

Hindriks, R. & Van Putten, M. J. 2012. Meanfield modeling of propofol-induced changes in spontaneous EEG rhythms. *Neuroimage,* 60**,** 2323-34.

Hofbauer, R. K., Fiset, P., Plourde, G., Backman, S. B. & Bushnell, M. C. 2004. Dose-dependent effects of propofol on the central processing of thermal pain. *Anesthesiology,* 100**,** 386-94.

Hoge, R. D. & Pike, G. B. 2001. Quantitative measurement using fMRI. *Functional MRI: An introduction to methods.* Oxford University Press.

Hoogenboom, N., Schoffelen, J. M., Oostenveld, R., Parkes, L. M. & Fries, P. 2006. Localizing human visual gamma-band activity in frequency, time and space. *Neuroimage,* 29**,** 764-773.

Horovitz, S. G., Braun, A. R., Carr, W. S., Picchioni, D., Balkin, T. J., Fukunaga, M. & Duyn, J. H. 2009. Decoupling of the brain's default mode network during deep sleep. *Proc Natl Acad Sci U S A,* 106**,** 11376-11381.

Houston, C. M., Mcgee, T. P., Mackenzie, G., Troyano-Cuturi, K., Rodriguez, P. M., Kutsarova, E., Diamanti, E., Hosie, A. M., Franks, N. P. & Brickley, S. G. 2011. Are extrasynaptic GABAA receptors important targets for sedative/hypnotic drugs? *J Neurosci,* 32**,** 3887-97.

Hu, Y., Chen, X., Gu, H. & Yang, Y. 2013. Resting-state glutamate and GABA concentrations predict task-induced deactivation in the default mode network. *J Neurosci,* 33**,** 18566-18573.

Huang, M. X., Mosher, J. C. & Leahy, R. M. 1999. A sensor-weighted overlapping-sphere head model and exhaustive head model comparison for MEG. *Physics in Medicine and Biology,* 44**,** 423-440.

Huang, Z., Wang, Z., Zhang, J., Dai, R., Wu, J., Li, Y., Liang, W., Mao, Y., Yang, Z., Holland, G., Zhang, J. & Northoff, G. 2014. Altered temporal variance and neural synchronization of spontaneous brain activity in anesthesia. *Human Brain Mapping,* 35**,** 5368-78.

Hutt, A. 2013. The anesthetic propofol shifts the frequency of maximum spectral power in EEG during general anesthesia: analytical insights from a linear model. *Front Comput Neurosci,* 7**,** 2.

Hyvarinen, A. & Oja, E. 2000. Independent component analysis: algorithms and applications. *Neural Netw,* 13**,** 411-30.

Iannetti, G. D. & Wise, R. G. 2007. BOLD functional MRI in disease and pharmacological studies: room for improvement? *Magnetic Resonance Imaging,* 25**,** 978-88.

Iidaka, T., Yamashita, K., Kashikura, K. & Yonekura, Y. 2004. Spatial frequency of visual image modulates neural responses in the temporo-occipital lobe. An investigation with event-related fMRI. *Brain Res Cogn Brain Res,* 18**,** 196-204.

Imas, O. A., Ropella, K. M., Ward, B. D., Wood, J. D. & Hudetz, A. G. 2005. Volatile anesthetics disrupt frontal-posterior recurrent information transfer at gamma frequencies in rat. *Neurosci Lett,* 387**,** 145-150.

Inui, K., Wang, X., Tamura, Y., Kaneoke, Y. & Kakigi, R. 2004. Serial processing in the human somatosensory system. *Cereb Cortex,* 14**,** 851-7.

Iohom, G., Collins, I., Murphy, D., Awad, I., O'connor, G., Mccarthy, N. & Shorten, G. 2001. Postoperative changes in visual evoked potentials and cognitive function tests following sevoflurane anaesthesia. *Br J Anaesth,* 87**,** 855-9.

Janz, C., Heinrich, S. P., Kornmayer, J., Bach, M. & Hennig, J. 2001. Coupling of neural activity and BOLD fMRI response: new insights by combination of fMRI and VEP experiments in transition from single events to continuous stimulation. *Magn Reson Med,* 46**,** 482-6.

Jenkinson, M., Bannister, P., Brady, M. & Smith, S. 2002. Improved optimization for the robust and accurate linear registration and motion correction of brain images. *Neuroimage,* 17**,** 825-41.

Jenkinson, M. & Smith, S. 2001. A global optimisation method for robust affine registration of brain images. *Med Image Anal,* 5**,** 143-56.

Jensen, O., Gips, B., Bergmann, T. O. & Bonnefond, M. 2014. Temporal coding organized by coupled alpha and gamma oscillations prioritize visual processing. *Trends Neurosci,* 37**,** 357-69.

Jensen, O., Goel, P., Kopell, N., Pohja, M., Hari, R. & Ermentrout, B. 2005. On the human sensorimotor-cortex beta rhythm: sources and modeling. *Neuroimage,* 26**,** 347-55.

Jensen, O., Kaiser, J. & Lachaux, J. P. 2007. Human gamma-frequency oscillations associated with attention and memory. *Trends in Neurosciences,* 30**,** 317-324.

Jeong, J. A., Kim, E. J., Jo, J. Y., Song, J. G., Lee, K. S., Kim, H. W., Lee, S. D., Jeon, B. H., Lee, J. U. & Park, J. B. 2011. Major role of GABA(A)-receptor mediated tonic inhibition in propofol suppression of supraoptic magnocellular neurons. *Neurosci Lett,* 494**,** 119-23.

Jeong, Y. B., Kim, J. S., Jeong, S. M., Park, J. W. & Choi, I. C. 2006. Comparison of the effects of sevoflurane and propofol anaesthesia on regional cerebral glucose metabolism in humans using positron emission tomography. *J Int Med Res,* 34**,** 374-84.

John, E. R. & Prichep, L. S. 2005. The anesthetic cascade: a theory of how anesthesia suppresses consciousness. *Anesthesiology,* 102**,** 447-471.

John, J., Wu, M.-F., Boehmer, L. N. & Siegel, J. M. 2004. Cataplexy-active neurons in the hypothalamus: implications for the role of histamine in sleep and waking behavior. *Neuron,* 42**,** 619-634.

Jones, B. E. & Cuello, A. C. 1989. Afferents to the basal forebrain cholinergic cell area from pontomesencephalic--catecholamine, serotonin, and acetylcholine--neurons. *Neuroscience,* 31**,** 37-61.

Jordan, D., Ilg, R., Riedl, V., Schorer, A., Grimberg, S., Neufang, S., Omerovic, A., Berger, S., Untergehrer, G., Preibisch, C., Schulz, E., Schuster, T., Schroter, M., Spoormaker, V., Zimmer, C., Hemmer, B., Wohlschlager, A., Kochs, E. F. & Schneider, G. 2013a. Simultaneous electroencephalographic and functional magnetic resonance imaging indicate impaired cortical top-down processing in association with anesthetic-induced unconsciousness. *Anesthesiology,* 119**,** 1031-42.

Jordan, D., Ilg, R., Untergehrer, G., Schneider, G. & Kochs, E. 2013b. Propofol-induced changes of cortical auditory processing. *Journal of Neurosurgical Anesthesiology,* Conference**,** 41st Annual Meeting of the Society for Neuroscience in Anesthesiology and Critical Care San Francisco, CA United States. Conference Start: 20131011 Conference End: 20131011. Conference Publication: (var.pagings). 25 (4) (pp 472-473).

Kahlbrock, N., Butz, M., May, E. S. & Schnitzler, A. 2012. Sustained gamma band synchronization in early visual areas reflects the level of selective attention. *Neuroimage,* 59**,** 673-81.

Kaisti, K. K., Metsahonkala, L., Teras, M., Oikonen, V., Aalto, S., Jaaskelainen, S., Hinkka, S. & Scheinin, H. 2002. Effects of surgical levels of propofol and sevoflurane anesthesia on cerebral blood flow in healthy subjects studied with positron emission tomography. *Anesthesiology,* 96**,** 1358-1370.

Kawamura, T., Nakasato, N., Seki, K., Kanno, A., Fujita, S., Fujiwara, S. & Yoshimoto, T. 1996. Neuromagnetic evidence of pre- and post-central cortical sources of somatosensory evoked responses. *Electroencephalogr Clin Neurophysiol,* 100**,** 44-50.

Kayser, C., Kim, M., Ugurbil, K., Kim, D.-S. & Konig, P. 2004. A comparison of hemodynamic and neural responses in cat visual cortex using complex stimuli. *Cereb Cortex,* 14**,** 881-891.

Kelz, M. B., Sun, Y., Chen, J., Cheng Meng, Q., Moore, J. T., Veasey, S. C., Dixon, S., Thornton, M., Funato, H. & Yanagisawa, M. 2008. An essential role for orexins in emergence from general anesthesia. *Proc Natl Acad Sci U S A,* 105**,** 1309-1314.

Kerssens, C., Hamann, S., Peltier, S., Hu, X. P., Byas-Smith, M. G. & Sebel, P. S. 2005. Attenuated brain response to auditory word stimulation with sevoflurane: a functional magnetic resonance imaging study in humans. *Anesthesiology,* 103**,** 11-19.

Khalili-Mahani, N., Chang, C., Van Osch, M. J., Veer, I. M., Van Buchem, M. A., Dahan, A., Beckmann, C. F., Van Gerven, J. M. & Rombouts, S. A. 2013. The impact of "physiological correction" on functional connectivity analysis of pharmacological resting state fMRI. *Neuroimage,* 65**,** 499-510.

Kim, K. M., Jeon, W. J., Lee, D. H., Kang, W. C., Kim, J. H. & Noh, G. J. 2004. Changes in visual and auditory response time during conscious sedation with propofol. *Acta Anaesthesiol Scand,* 48**,** 1033-7.

Kirsch, M. M. D., Wannez, S. M., Thibaut, A. P., Laureys, S. M. D. P., Brichant, J. F. M. D. P. & Bonhomme, V. M. D. P. 2016. Positron Emission Tomography: Basic Principles, New Applications, and Studies Under Anesthesia. *International Anesthesiology Clinics Winter,* 54**,** 109-128.

Kirschstein, T. & Kohling, R. 2009. What is the source of the EEG? *Clin EEG Neurosci,* 40**,** 146-9.

Kishimoto, T., Kadoya, C., Sneyd, R., Samra, S. K. & Domino, E. F. 1995. Topographic electroencephalogram of propofol-induced conscious sedation. *Clin Pharmacol Ther,* 58**,** 666-74.

Kiviniemi, V. J., Haanpaa, H., Kantola, J. H., Jauhiainen, J., Vainionpaa, V., Alahuhta, S. & Tervonen, O. 2005. Midazolam sedation increases fluctuation and synchrony of the resting brain BOLD signal. *Magn Reson Imaging,* 23**,** 531-7.

Klimesch, W. 1996. Memory processes, brain oscillations and EEG synchronization. *Int J Psychophysiol,* 24**,** 61-6100.

Kobald, S. O., Getzmann, S., Beste, C. & Wascher, E. 2016. The impact of simulated MRI scanner background noise on visual attention processes as measured by the EEG. *Sci Rep,* 6**,** 28371.

Kofke, W. A., Blissitt, P. A., Rao, H., Wang, J., Addya, K. & Detre, J. 2007. Remifentanil-induced cerebral blood flow effects in normal humans: dose and ApoE genotype. *Anesth Analg,* 105**,** 167-75.

Koht, A., Schutz, W., Schmidt, G., Schramm, J. & Watanabe, E. 1988. Effects of etomidate, midazolam, and thiopental on median nerve somatosensory evoked potentials and the additive effects of fentanyl and nitrous oxide. *Anesth Analg,* 67**,** 435-41.

Kopp Lugli, A., Yost, C. S. & Kindler, C. H. 2009. Anaesthetic mechanisms: update on the challenge of unravelling the mystery of anaesthesia. *Eur J Anaesthesiol,* 26**,** 807-20.

Kraut, M. A., Arezzo, J. C. & Vaughan, H. G. 1985. Intracortical generators of the flash VEP in monkeys. *Electroencephalography and Clinical Neurophysiology/Evoked Potentials Section,* 62**,** 300-312.

Kreis, R., Ernst, T. & Ross, B. D. 1993. Development of the human brain: in vivo quantification of metabolite and water content with proton magnetic resonance spectroscopy. *Magn Reson Med,* 30**,** 424-37.

Ku, S. W., Lee, U., Noh, G. J., Jun, I. G. & Mashour, G. A. 2011. Preferential inhibition of frontal-to-parietal feedback connectivity is a neurophysiologic correlate of general anesthesia in surgical patients. *PLoS One,* 6**,** e25155.

Lacey, S. & Sathian, K. 2015. Crossmodal and Multisensory Interactions between Vision and Touch. *Scholarpedia J,* 10**,** 7957.

Langsjo, J. W., Kaisti, K. K., Aalto, S., Hinkka, S., Aantaa, R., Oikonen, V., Sipila, H., Kurki, T., Silvanto, M. & Scheinin, H. 2003. Effects of subanesthetic doses of ketamine on regional cerebral blood flow, oxygen consumption, and blood volume in humans. *Anesthesiology,* 99**,** 614-623.

Langsjo, J. W., Maksimow, A., Salmi, E., Kaisti, K., Aalto, S., Oikonen, V., Hinkka, S., Aantaa, R., Sipila, H., Viljanen, T., Parkkola, R. & Scheinin, H. 2005. S-ketamine anesthesia increases cerebral blood flow in excess of the metabolic needs in humans. *Anesthesiology,* 103**,** 258-268.

Langsjo, J. W., Salmi, E., Kaisti, K. K., Aalto, S., Hinkka, S., Aantaa, R., Oikonen, V., Viljanen, T., Kurki, T., Silvanto, M. & Scheinin, H. 2004. Effects of subanesthetic ketamine on regional cerebral glucose metabolism in humans. *Anesthesiology,* 100**,** 1065-1071.

Laufs, H. 2008. Endogenous brain oscillations and related networks detected by surface EEG-combined fMRI. *Hum Brain Mapp,* 29**,** 762-9.

Laufs, H., Krakow, K., Sterzer, P., Eger, E., Beyerle, A., Salek-Haddadi, A. & Kleinschmidt, A. 2003. Electroencephalographic signatures of attentional and cognitive default modes in spontaneous brain activity fluctuations at rest. *Proc Natl Acad Sci U S A,* 100**,** 11053-8.

Laureys, S., Faymonville, M. E., Luxen, A., Lamy, M., Franck, G. & Maquet, P. 2000. Restoration of thalamocortical connectivity after recovery from persistent vegetative state. *Lancet,* 355**,** 1790-1791.

Laureys, S., Giacino, J. T., Schiff, N. D., Schabus, M. & Owen, A. M. 2006. How should functional imaging of patients with disorders of consciousness contribute to their clinical rehabilitation needs? *Curr Opin Neurol,* 19**,** 520-7.

Le Van Quyen, M., Foucher, J., Lachaux, J. P., Rodriguez, E., Lutz, A., Martinerie, J. & Varela, F. J. 2001. Comparison of Hilbert transform and wavelet methods for the analysis of neuronal synchrony. *Journal of Neuroscience Methods,* 111**,** 83-98.

Lee, M. H., Smyser, C. D. & Shimony, J. S. 2013a. Resting-state fMRI: a review of methods and clinical applications. *AJNR Am J Neuroradiol,* 34**,** 1866-72.

Lee, U., Kim, S., Noh, G.-J., Choi, B.-M., Hwang, E. & Mashour, G. A. 2009a. The directionality and functional organization of frontoparietal connectivity during consciousness and anesthesia in humans. *Conscious Cogn,* 18**,** 1069-1078.

Lee, U., Ku, S., Noh, G., Baek, S., Choi, B. & Mashour, G. A. 2013b. Disruption of frontal-parietal communication by ketamine, propofol, and sevoflurane. *Anesthesiology,* 118**,** 1264-75.

Lee, U., Mashour, G. A., Kim, S., Noh, G. J. & Choi, B. M. 2009b. Propofol induction reduces the capacity for neural information integration: implications for the mechanism of consciousness and general anesthesia. *Conscious Cogn,* 18**,** 56-64.

Leech, R. & Sharp, D. J. 2014. The role of the posterior cingulate cortex in cognition and disease. *Brain,* 137**,** 12-32.

Levin, J. M., Ross, M. H., Mendelson, J. H., Kaufman, M. J., Lange, N., Maas, L. C., Mello, N. K., Cohen, B. M. & Renshaw, P. F. 1998. Reduction in BOLD fMRI response to primary visual stimulation following alcohol ingestion. *Psychiatry Res,* 82**,** 135-46.

Liang, P., Manelis, A., Liu, X., Aizenstein, H. J., Gyulai, F., Quinlan, J. J. & Reder, L. M. 2012. Using arterial spin labeling perfusion MRI to explore how midazolam produces anterograde amnesia. *Neurosci Lett,* 522**,** 113-7.

Liang, P., Zhang, H., Xu, Y., Jia, W., Zang, Y. & Li, K. 2015. Disruption of cortical integration during midazolam-induced light sedation. *Hum Brain Mapp,* 36**,** 4247-61.

Liau, J., Perthen, J. E. & Liu, T. T. 2008. Caffeine reduces the activation extent and contrast-to-noise ratio of the functional cerebral blood flow response but not the BOLD response. *Neuroimage,* 42**,** 296-305.

Licata, S. C., Jensen, J. E., Penetar, D. M., Prescot, A. P., Lukas, S. E. & Renshaw, P. F. 2009. A therapeutic dose of zolpidem reduces thalamic GABA in healthy volunteers: a proton MRS study at 4 T. *Psychopharmacology (Berl),* 203**,** 819-29.

Licata, S. C., Lowen, S. B., Trksak, G. H., Maclean, R. R. & Lukas, S. E. 2011. Zolpidem reduces the blood oxygen level-dependent signal during visual system stimulation. *Prog Neuropsychopharmacol Biol Psychiatry,* 35**,** 1645-52.

Lin, Y. Y. & Forss, N. 2002. Functional characterization of human second somatosensory cortex by magnetoencephalography. *Behav Brain Res,* 135**,** 141-5.

Liu, X., Li, H., Luo, F., Zhang, L., Han, R. & Wang, B. 2015. Variation of the default mode network with altered alertness levels induced by propofol. *Neuropsychiatric Disease and Treatment,* 11**,** 2573-2581.

Liu, X., Li, S. J. & Hudetz, A. G. 2014. Increased precuneus connectivity during propofol sedation. *Neurosci Lett,* 561**,** 18-23.

Liu, X. P. D., Lauer, K. K. M. D., Ward, B. D. M. S., Li, S.-J. P. D. & Hudetz, A. G. D. B. M. P. D. 2013. Differential Effects of Deep Sedation with Propofol on the Specific and Nonspecific Thalamocortical Systems: A Functional Magnetic Resonance Imaging Study. *Anesthesiology January,* 118**,** 59-69.

Logothetis, N. K., Pauls, J., Augath, M., Trinath, T. & Oeltermann, A. 2001. Neurophysiological investigation of the basis of the fMRI signal. *Nature,* 412**,** 150-157.

Lohmann, G., Margulies, D. S., Horstmann, A., Pleger, B., Lepsien, J., Goldhahn, D., Schloegl, H., Stumvoll, M., Villringer, A. & Turner, R. 2010. Eigenvector centrality mapping for analyzing connectivity patterns in fMRI data of the human brain. *PLoS One,* 5**,** e10232.

Lopes Da Silva, F. H. 2010. Electrophysiological Basis of MEG Signals. *In:* HANSEN, P. C., KRINGELBACH, M. L. & SALMELIN, R. (eds.) *MEG. An introduction to methods.* Oxford: Oxford University Press.

Lorenz, I. H., Kolbitsch, C., Schocke, M., Kremser, C., Zschiegner, F., Hinteregger, M., Felber, S., Hormann, C. & Benzer, A. 2000. Low-dose remifentanil increases regional cerebral blood flow and regional cerebral blood volume, but decreases regional mean transit time and regional cerebrovascular resistance in volunteers. *Br J Anaesth,* 85**,** 199-204.

Loughnan, B. L., Sebel, P. S., Thomas, D., Rutherfoord, C. F. & Rogers, H. 1987. Evoked potentials following diazepam or fentanyl. *Anaesthesia,* 42**,** 195-8.

Lu, H., Zou, Q., Gu, H., Raichle, M. E., Stein, E. A. & Yang, Y. 2012. Rat brains also have a default mode network. *Proc Natl Acad Sci U S A,* 109**,** 3979-84.

Lu, J., Jhou, T. C. & Saper, C. B. 2006. Identification of wake-active dopaminergic neurons in the ventral periaqueductal gray matter. *J Neurosci,* 26**,** 193-202.

Lynch, J. C. 2013. Cerebral Cortex. *In:* HAINES, D. H. (ed.) *Fundamental Neuroscience for Basic and Clinical Applications.* Philadelphia: Elsevier Saunders.

Macdonald, A. A., Naci, L., Macdonald, P. A. & Owen, A. M. 2015. Anesthesia and neuroimaging: investigating the neural correlates of unconsciousness. *Trends Cogn Sci,* 19**,** 100-7.

Macintosh, B. J., Pattinson, K. T., Gallichan, D., Ahmad, I., Miller, K. L., Feinberg, D. A., Wise, R. G. & Jezzard, P. 2008. Measuring the effects of remifentanil on cerebral blood flow and arterial arrival time using 3D GRASE MRI with pulsed arterial spin labelling. *J Cereb Blood Flow Metab,* 28**,** 1514-22.

Maddock, R. J. & Buonocore, M. H. 2012. MR spectroscopic studies of the brain in psychiatric disorders. *Curr Top Behav Neurosci,* 11**,** 199-251.

Maksimow, A., Silfverhuth, M., Langsjo, J., Kaskinoro, K., Georgiadis, S., Jaaskelainen, S. & Scheinin, H. 2014. Directional connectivity between frontal and posterior brain regions is altered with increasing concentrations of propofol. *PLoS One,* 9**,** e113616.

Mann, E. O. & Mody, I. 2011. Control of hippocampal gamma oscillation frequency by tonic inhibition and excitation of interneurons. *Nat Neurosci,* 13**,** 205-12.

Mantini, D., Perrucci, M., Del Gratta, C., Romani, G. & Corbetta, M. 2007. Electrophysiological signatures of resting state networks in the human brain. *Proc Natl Acad Sci U S A,* 104**,** 13170-5.

Maris, E. & Oostenveld, R. 2007. Nonparametric statistical testing of EEG- and MEG-data. *J Neurosci Methods,* 164**,** 177-90.

Marsh, B., White, M., Morton, N. & Kenny, G. N. 1991. Pharmacokinetic model driven infusion of propofol in children. *Br J Anaesth,* 67**,** 41-8.

Martel, J. P. & Barnett, S. R. 2015. Sedation: definitions and regulations. *Int Anesthesiol Clin,* 53**,** 1-12.

Martin, E., Thiel, T., Joeri, P., Loenneker, T., Ekatodramis, D., Huisman, T., Hennig, J. & Marcar, V. L. 2000. Effect of pentobarbital on visual processing in man. *Hum Brain Mapp,* 10**,** 132-9.

Martuzzi, R., Ramani, R., Qiu, M., Rajeevan, N. & Constable, R. T. 2010. Functional connectivity and alterations in baseline brain state in humans. *Neuroimage,* 49**,** 823-834.

Mashour, G. A. 2013. Cognitive unbinding: a neuroscientific paradigm of general anesthesia and related states of unconsciousness. *Neurosci Biobehav Rev,* 37**,** 2751-9.

Mashour, G. A. & Alkire, M. T. 2013. Consciousness, anesthesia, and the thalamocortical system. *Anesthesiology,* 118**,** 13-5.

Mccarthy, M. M., Brown, E. N. & Kopell, N. 2008. Potential network mechanisms mediating electroencephalographic beta rhythm changes during propofol-induced paradoxical excitation. *J Neurosci,* 28**,** 13488-504.

Mescher, M., Merkle, H., Kirsch, J., Garwood, M. & Gruetter, R. 1998. Simultaneous in vivo spectral editing and water suppression. *NMR Biomed,* 11**,** 266-272.

Mhuircheartaigh, R. N., Rosenorn-Lanng, D., Wise, R., Jbabdi, S., Rogers, R. & Tracey, I. 2010. Cortical and subcortical connectivity changes during decreasing levels of consciousness in humans: a functional magnetic resonance imaging study using propofol. *J Neurosci,* 30**,** 9095-9102.

Mihic, S. J., Ye, Q., Wick, M. J., Koltchine, V. V., Krasowski, M. D., Finn, S. E., Mascia, M. P., Valenzuela, C. F., Hanson, K. K., Greenblatt, E. P., Harris, R. A. & Harrison, N. L. 1997. Sites of alcohol and volatile anaesthetic action on GABA(A) and glycine receptors. *Nature,* 389**,** 385-389.

Mileykovskiy, B. Y., Kiyashchenko, L. I. & Siegel, J. M. 2005. Behavioral correlates of activity in identified hypocretin/orexin neurons. *Neuron,* 46**,** 787-798.

Modirrousta, M., Mainville, L. & Jones, B. E. 2004. Gabaergic neurons with alpha2-adrenergic receptors in basal forebrain and preoptic area express c-Fos during sleep. *Neuroscience,* 129**,** 803-810.

Mody, I., De Koninck, Y., Otis, T. S. & Soltesz, I. 1994. Bridging the cleft at GABA synapses in the brain. *Trends Neurosci,* 17**,** 517-525.

Mohler, H. 2002. Pathophysiological aspects of diversity in neuronal inhibition: a new benzodiazepine pharmacology. *Dialogues Clin Neurosci,* 4**,** 261-9.

Molyneaux, B. J., Arlotta, P., Menezes, J. R. & Macklis, J. D. 2007. Neuronal subtype specification in the cerebral cortex. *Nat Rev Neurosci,* 8**,** 427-37.

Monti, M. M., Lutkenhoff, E. S., Rubinov, M., Boveroux, P., Vanhaudenhuyse, A., Gosseries, O., Bruno, M. A., Noirhomme, Q., Boly, M. & Laureys, S. 2013. Dynamic change of global and local information processing in propofol-induced loss and recovery of consciousness. *PLoS Computational Biology,* 9**,** e1003271.

Monti, M. M., Vanhaudenhuyse, A., Coleman, M. R., Boly, M., Pickard, J. D., Tshibanda, L., Owen, A. M. & Laureys, S. 2010. Willful modulation of brain activity in disorders of consciousness. *N Engl J Med,* 362**,** 579-89.

Moore, J. & Kelz, M. 2011. Brain anatomy of relevance to the anesthesiologist. *In:* MASHOUR, G. A. & LYDIC, R. (eds.) *Neuroscientific Foundations of Anesthesiology.* Oxford University Press.

Mountcastle, V. B. 1997. The columnar organization of the neocortex. *Brain,* 120 (Pt 4)**,** 701-722.

Mullins, P. G., Mcgonigle, D. J., O'gorman, R. L., Puts, N. A., Vidyasagar, R., Evans, C. J., Cardiff Symposium On, M. R. S. O. G. & Edden, R. A. 2014. Current practice in the use of MEGA-PRESS spectroscopy for the detection of GABA. *Neuroimage,* 86**,** 43-52.

Murphy, K., Harris, A. D. & Wise, R. G. 2011a. Robustly measuring vascular reactivity differences with breath-hold: normalising stimulus-evoked and resting state BOLD fMRI data. *Neuroimage,* 54**,** 369-79.

Murphy, M., Bruno, M. A., Riedner, B. A., Boveroux, P., Noirhomme, Q., Landsness, E. C., Brichant, J. F., Phillips, C., Massimini, M., Laureys, S., Tononi, G. & Boly, M. 2011b. Propofol anesthesia and sleep: a high-density EEG study. *Sleep,* 34**,** 283-91A.

Murray, M. M., Brunet, D. & Michel, C. M. 2008. Topographic ERP analyses: a step-by-step tutorial review. *Brain Topogr,* 20**,** 249-64.

Muthukumaraswamy, S. & Singh, K. 2009. Functional decoupling of BOLD and gamma-band amplitudes in human primary visual cortex. *Hum Brain Mapp,* 30**,** 2000-7.

Muthukumaraswamy, S. D. 2010. Functional properties of human primary motor cortex gamma oscillations. *Journal of Neurophysiology,* 104**,** 2873-2885.

Muthukumaraswamy, S. D., Carhart-Harris, R. L., Moran, R. J., Brookes, M. J., Williams, T. M., Errtizoe, D., Sessa, B., Papadopoulos, A., Bolstridge, M., Singh, K. D., Feilding, A., Friston, K. J. & Nutt, D. J. 2013. Broadband cortical desynchronization underlies the human psychedelic state. *J Neurosci,* 33**,** 15171-83.

Muthukumaraswamy, S. D., Edden, R. A., Jones, D. K., Swettenham, J. B. & Singh, K. D. 2009. Resting GABA concentration predicts peak gamma frequency and fMRI

amplitude in response to visual stimulation in humans. *Proc Natl Acad Sci U S A,* 106**,** 8356-61.

Muthukumaraswamy, S. D., Evans, C. J., Edden, R. A., Wise, R. G. & Singh, K. D. 2012. Individual variability in the shape and amplitude of the BOLD-HRF correlates with endogenous GABAergic inhibition. *Hum Brain Mapp,* 33**,** 455-65.

Muthukumaraswamy, S. D., Shaw, A. D., Jackson, L. E., Hall, J., Moran, R. & Saxena, N. 2015. Evidence that Subanesthetic Doses of Ketamine Cause Sustained Disruptions of NMDA and AMPA-Mediated Frontoparietal Connectivity in Humans. *J Neurosci,* 35**,** 11694-706.

Muthukumaraswamy, S. D. & Singh, K. D. 2008. Spatiotemporal frequency tuning of BOLD and gamma band MEG responses compared in primary visual cortex. *Neuroimage,* 40**,** 1552-1560.

Muthukumaraswamy, S. D., Singh, K. D., Swettenham, J. B. & Jones, D. K. 2010. Visual Gamma Oscillations and Evoked Responses: Variability, Repeatability and structural MRI correlates. *NeuroImage,* 49**,** 3349-3357.

Nagy, K., Greenlee, M. W. & Kovacs, G. 2012. The lateral occipital cortex in the face perception network: an effective connectivity study. *Front Psychol,* 3**,** 141.

Near, J., Ho, Y. C., Sandberg, K., Kumaragamage, C. & Blicher, J. U. 2014. Long-term reproducibility of GABA magnetic resonance spectroscopy. *Neuroimage,* 99**,** 191-6.

Negyessy, L., Nepusz, T., Kocsis, L. & Bazso, F. 2006. Prediction of the main cortical areas and connections involved in the tactile function of the visual cortex by network analysis. *Eur J Neurosci,* 23**,** 1919-30.

Nelson, L. E., Guo, T. Z., Lu, J., Saper, C. B., Franks, N. P. & Maze, M. 2002. The sedative component of anesthesia is mediated by GABA(A) receptors in an endogenous sleep pathway. *Nat Neurosci,* 5**,** 979-984.

Ni Mhuircheartaigh, R., Warnaby, C., Rogers, R., Jbabdi, S. & Tracey, I. 2013. Slow-wave activity saturation and thalamocortical isolation during propofol anesthesia in humans. *Sci Transl Med,* 5**,** 208ra148.

Nichols, T. E. & Holmes, A. P. 2002. Nonparametric permutation tests for functional neuroimaging: A primer with examples. *Human Brain Mapping,* 15**,** 1-25.

Niessing, J., Ebisch, B., Schmidt, K. E., Niessing, M., Singer, W. & Galuske, R. a. W. 2005. Hemodynamic signals correlate tightly with synchronized gamma oscillations. *Science,* 309**,** 948-951.

Noirhomme, Q., Soddu, A., Lehembre, R., Vanhaudenhuyse, A., Boveroux, P., Boly, M. & Laureys, S. 2010. Brain connectivity in pathological and pharmacological coma. *Front Syst Neurosci,* 4**,** 160.

Noll, D. C. 2001. *A Primer on MRI and Functional MRI* [Online]. Available: http://fmri.research.umich.edu/documents/fmri_primer.pdf [Accessed].

Nusser, Z., Sieghart, W., Benke, D., Fritschy, J. M. & Somogyi, P. 1996. Differential synaptic localization of two major gamma-aminobutyric acid type A receptor alpha subunits on hippocampal pyramidal cells. *Proc Natl Acad Sci U S A,* 93**,** 11939-11944.

Nutt, D. 2006. GABAA receptors: subtypes, regional distribution, and function. *J Clin Sleep Med,* 2**,** S7-11.

Ojemann, G. A., Ojemann, J. & Ramsey, N. F. 2013. Relation between functional magnetic resonance imaging (fMRI) and single neuron, local field potential (LFP) and electrocorticography (ECoG) activity in human cortex. *Front Hum Neurosci,* 7**,** 34.

Oke, O. O., Magony, A., Anver, H., Ward, P. D., Jiruska, P., Jefferys, J. G. & Vreugdenhil, M. 2010. High-frequency gamma oscillations coexist with low-frequency gamma oscillations in the rat visual cortex in vitro. *Eur J Neurosci,* 31**,** 1435-45.

Oostenveld, R., Fries, P., Maris, E. & Schoffelen, J. M. 2011. FieldTrip: Open source software for advanced analysis of MEG, EEG, and invasive electrophysiological data. *Comput Intell Neurosci,* 2011**,** 156869.

Orser, B. A., Wang, L. Y., Pennefather, P. S. & Macdonald, J. F. 1994. Propofol modulates activation and desensitization of GABAA receptors in cultured murine hippocampal neurons. *J Neurosci,* 14**,** 7747-7760.

Osipova, D., Hermes, D. & Jensen, O. 2008. Gamma power is phase-locked to posterior alpha activity. *PLoS One,* 3**,** e3990.

Owen, A. M., Coleman, M. R., Boly, M., Davis, M. H., Laureys, S. & Pickard, J. D. 2006. Detecting awareness in the vegetative state. *Science,* 313**,** 1402.

Pandharipande, P. P., Pun, B. T., Herr, D. L., Maze, M., Girard, T. D., Miller, R. R., Shintani, A. K., Thompson, J. L., Jackson, J. C., Deppen, S. A., Stiles, R. A., Dittus, R. S., Bernard, G. R. & Ely, E. W. 2007. Effect of sedation with dexmedetomidine vs lorazepam on acute brain dysfunction in mechanically ventilated patients: the MENDS randomized controlled trial. *JAMA,* 298**,** 2644-53.

Pasley, B. N., Inglis, B. A. & Freeman, R. D. 2007. Analysis of oxygen metabolism implies a neural origin for the negative BOLD response in human visual cortex. *Neuroimage,* 36**,** 269-76.

Peelle, J. E. 2014. Methodological challenges and solutions in auditory functional magnetic resonance imaging. *Front Neurosci,* 8**,** 253.

Pelizzone, M., Hari, R., Makela, J. P., Huttunen, J., Ahlfors, S. & Hamalainen, M. 1987. Cortical origin of middle-latency auditory evoked responses in man. *Neurosci Lett,* 82**,** 303-7.

Perry, G., Hamandi, K., Brindley, L. M., Muthukumaraswamy, S. D. & Singh, K. D. 2013. The properties of induced gamma oscillations in human visual cortex show individual variability in their dependence on stimulus size. *Neuroimage,* 68**,** 83-92.

Petroff, O. A., Behar, K. L., Mattson, R. H. & Rothman, D. L. 1996. Human brain gamma-aminobutyric acid levels and seizure control following initiation of vigabatrin therapy. *J Neurochem,* 67**,** 2399-2404.

Petroff, O. A., Hyder, F., Collins, T., Mattson, R. H. & Rothman, D. L. 1999a. Acute effects of vigabatrin on brain GABA and homocarnosine in patients with complex partial seizures. *Epilepsia,* 40**,** 958-64.

Petroff, O. A., Hyder, F., Mattson, R. H. & Rothman, D. L. 1999b. Topiramate increases brain GABA, homocarnosine, and pyrrolidinone in patients with epilepsy. *Neurology,* 52**,** 473-8.

Petroff, O. A. & Rothman, D. L. 1998. Measuring human brain GABA in vivo: effects of GABA-transaminase inhibition with vigabatrin. *Mol Neurobiol,* 16**,** 97-121.

Peyron, C., Tighe, D. K., Van Den Pol, A. N., De Lecea, L., Heller, H. C., Sutcliffe, J. G. & Kilduff, T. S. 1998. Neurons containing hypocretin (orexin) project to multiple neuronal systems. *J Neurosci,* 18**,** 9996-99910015.

Pfleiderer, B., Ostermann, J., Michael, N. & Heindel, W. 2002. Visualization of auditory habituation by fMRI. *Neuroimage,* 17**,** 1705-10.

Pfurtscheller, G. & Lopes Da Silva, F. H. 1999. Event-related EEG/MEG synchronization and desynchronization: basic principles. *Clin Neurophysiol,* 110**,** 1842-57.

Pinotsis, D. A., Schwarzkopf, D. S., Litvak, V., Rees, G., Barnes, G. & Friston, K. J. 2013. Dynamic causal modelling of lateral interactions in the visual cortex. *Neuroimage,* 66**,** 563-76.

Plourde, G., Belin, P., Chartrand, D., Fiset, P., Backman, S. B., Xie, G. & Zatorre, R. J. 2006. Cortical processing of complex auditory stimuli during alterations of consciousness with the general anesthetic propofol. *Anesthesiology,* 104**,** 448-457.

Plourde, G., Chartrand, D., Fiset, P., Font, S. & Backman, S. B. 2003. Antagonism of sevoflurane anaesthesia by physostigmine: effects on the auditory steady-state response and bispectral index. *Br J Anaesth,* 91**,** 583-586.

Poldrack, R. A., Mumford, J. A. & Nichols, T. E. 2011. Statistical modeling: SIingle subject analysis. *In:* POLDRACK, R. A., MUMFORD, J. A. & NICHOLS, T. E. (eds.) *Handbook of Functional MRI Data Analysis.* Cambridge University Press.

Pourtois, G., Delplanque, S., Michel, C. & Vuilleumier, P. 2008. Beyond conventional event-related brain potential (ERP): exploring the time-course of visual emotion processing using topographic and principal component analyses. *Brain Topogr,* 20**,** 265-77.

Prielipp, R. C., Wall, M. H., Tobin, J. R., Groban, L., Cannon, M. A., Fahey, F. H., Gage, H. D., Stump, D. A., James, R. L., Bennett, J. & Butterworth, J. 2002. Dexmedetomidine-induced sedation in volunteers decreases regional and global cerebral blood flow. *Anesth Analg,* 95**,** 1052-9, table of contents.

Privman, E., Fisch, L., Neufeld, M. Y., Kramer, U., Kipervasser, S., Andelman, F., Yeshurun, Y., Fried, I. & Malach, R. 2011. Antagonistic relationship between gamma power and visual evoked potentials revealed in human visual cortex. *Cereb Cortex,* 21**,** 616-24.

Puts, N. A. & Edden, R. A. 2012. In vivo magnetic resonance spectroscopy of GABA: a methodological review. *Prog Nucl Magn Reson Spectrosc,* 60**,** 29-41.

Puts, N. A., Edden, R. A., Evans, C. J., Mcglone, F. & Mcgonigle, D. J. 2011. Regionally specific human GABA concentration correlates with tactile discrimination thresholds. *J Neurosci,* 31**,** 16556-60.

Quine, M. A., Bell, G. D., Mccloy, R. F., Charlton, J. E., Devlin, H. B. & Hopkins, A. 1995. Prospective audit of upper gastrointestinal endoscopy in two regions of England: safety, staffing, and sedation methods. *Gut,* 36**,** 462-7.

Ramani, R., Qiu, M. & Constable, R. T. 2007. Sevoflurane 0.25 MAC preferentially affects higher order association areas: a functional magnetic resonance imaging study in volunteers. *Anesth Analg,* 105**,** 648-55.

Ramani, R., Rose, M., Qiu, M. & Constable, R. T. 2011. *A1164: Propofol Infusion Decreases rCBF and Increases GABA Level in the Thalamus - fMRI, MRS Study in Volunteers* [Online]. American Society of Anesthesiologists. Available: http://www.asaabstracts.com/strands/asaabstracts/abstract.htm ?year=2011&index=10&absnum=4236 [Accessed 2018].

Rao, Y., Wang, Y.-L., Chen, Y.-Q., Zhang, W.-S. & Liu, J. 2009. Protective effects of emulsified isoflurane after myocardial ischemia-reperfusion injury and its mechanism in rabbits. *Chin J Traumatol,* 12**,** 18-21.

Rasmussen, L. S., Larsen, K., Houx, P., Skovgaard, L. T., Hanning, C. D., Moller, J. T. & Dysfunction, I. G. T. I. S. O. P. C. 2001. The assessment of postoperative cognitive function. *Acta Anaesthesiol Scand,* 45**,** 275-89.

Ray, S. & Maunsell, J. H. 2010. Differences in gamma frequencies across visual cortex restrict their possible use in computation. *Neuron,* 67**,** 885-96.

Reade, M. C. & Finfer, S. 2014. Sedation and delirium in the intensive care unit. *N Engl J Med,* 370**,** 444-54.

Reinsel, R. A., Veselis, R. A., Dnistrian, A. M., Feshchenko, V. A., Beattie, B. J. & Duff, M. R. 2000. Midazolam decreases cerebral blood flow in the left prefrontal cortex in a dose-dependent fashion. *Int J Neuropsychopharmacol,* 3**,** 117-127.

Reinstrup, P., Ryding, E., Algotsson, L., Messeter, K., Asgeirsson, B. & Uski, T. 1995. Distribution of cerebral blood flow during anesthesia with isoflurane or halothane in humans. *Anesthesiology,* 82**,** 359-366.

Rex, S., Meyer, P. T., Baumert, J. H., Rossaint, R., Fries, M., Bull, U. & Schaefer, W. M. 2008. Positron emission tomography study of regional cerebral blood flow and flow-metabolism coupling during general anaesthesia with xenon in humans. *Br J Anaesth,* 100**,** 667-75.

Rex, S., Schaefer, W., Meyer, P. H., Rossaint, R., Boy, C., Setani, K., Bull, U. & Baumert, J. H. 2006. Positron emission tomography study of regional cerebral metabolism during general anesthesia with xenon in humans. *Anesthesiology,* 105**,** 936-43.

Reynolds, D. S., Rosahl, T. W., Cirone, J., O'meara, G. F., Haythornthwaite, A., Newman, R. J., Myers, J., Sur, C., Howell, O., Rutter, A. R., Atack, J., Macaulay, A. J., Hadingham, K. L., Hutson, P. H., Belelli, D., Lambert, J. J., Dawson, G. R., Mckernan, R., Whiting, P. J. & Wafford, K. A. 2003. Sedation and anesthesia mediated by distinct GABA(A) receptor isoforms. *J Neurosci,* 23**,** 8608-8617.

Ribary, U., Ioannides, A. A., Singh, K. D., Hasson, R., Bolton, J. P., Lado, F., Mogilner, A. & Llinas, R. 1991. Magnetic field tomography of coherent thalamocortical 40-Hz oscillations in humans. *Proc Natl Acad Sci U S A,* 88**,** 11037-41.

Robinson, B. J., Ebert, T. J., O'brien, T. J., Colinco, M. D. & Muzi, M. 1997. Mechanisms whereby propofol mediates peripheral vasodilation in humans. Sympathoinhibition or direct vascular relaxation? *Anesthesiology,* 86**,** 64-72.

Robinson, S. E. Localization of Event-Related Activity by SAM(erf). *In:* HALGREN, E., AHLFORS, S., HAMALAINEN, M. & COHEN, D., eds. Biomag 2004: Proceedings of the 14th International Conference on Biomagnetism, 2004 Boston, USA. Biomag 2004 Ltd.

Robinson, S. E. & Vrba, J. 1999. Functional neuroimaging by synthetic aperture manetometry (SAM). *In:* YOSHIMOTO, T., KOTANI, M., KURIKI, S., KARIBE, H. & NAKASATO, N. (eds.) *Recent Advances in Biomagnetism.* Sendai: Tohoku University Press.

Rodriguez, R., Kallenbach, U., Singer, W. & Munk, M. H. 2004. Short- and long-term effects of cholinergic modulation on gamma oscillations and response synchronization in the visual cortex. *J Neurosci,* 24**,** 10369-78.

Rogers, R., Wise, R. G., Painter, D. J., Longe, S. E. & Tracey, I. 2004. An investigation to dissociate the analgesic and anesthetic properties of ketamine using functional magnetic resonance imaging. *Anesthesiology,* 100**,** 292-301.

Roquet, D., Foucher, J. R., Froehlig, P., Renard, F., Pottecher, J., Besancenot, H., Schneider, F., Schenck, M. & Kremer, S. 2016. Resting-state networks distinguish locked-in from vegetative state patients. *Neuroimage Clin,* 12**,** 16-22.

Rosen, B. Q., O'hara, R., Kovacevic, S., Schulman, A., Padovan, N. & Marinkovic, K. 2014. Oscillatory spatial profile of alcohol's effects on the resting state: anatomically-constrained MEG. *Alcohol,* 48**,** 89-97.

Rossini, P. M., Altamura, C., Ferretti, A., Vernieri, F., Zappasodi, F., Caulo, M., Pizzella, V., Del Gratta, C., Romani, G. L. & Tecchio, F. 2004. Does cerebrovascular disease affect the coupling between neuronal activity and local haemodynamics? *Brain,* 127**,** 99-110.

Rudolph, U. & Antkowiak, B. 2004. Molecular and neuronal substrates for general anaesthetics. *Nat Rev Neurosci,* 5**,** 709-720.

Rudolph, U., Crestani, F., Benke, D., Brünig, I., Benson, J., Fritschy, J., Martin, J., Bluethmann, H. & Möhler, H. 1999. Benzodiazepine actions mediated by specific gamma-aminobutyric acid(A) receptor subtypes. *Nature,* 401**,** 796-800.

Sanacora, G., Mason, G. F., Rothman, D. L., Behar, K. L., Hyder, F., Petroff, O. A., Berman, R. M., Charney, D. S. & Krystal, J. H. 1999. Reduced cortical gamma-aminobutyric acid levels in depressed patients determined by proton magnetic resonance spectroscopy. *Arch Gen Psychiatry,* 56**,** 1043-7.

Sanders, L. D., Clyburn, P. A., Rosen, M. & Robinson, J. O. 1991. Propofol in short gynaecological procedures. Comparison of recovery over 2 days after anaesthesia with propofol or thiopentone as sole anaesthetic agent. *Anaesthesia,* 46**,** 451-5.

Sanders, R. D., Pandharipande, P. P., Davidson, A. J., Ma, D. & Maze, M. 2011. Anticipating and managing postoperative delirium and cognitive decline in adults. *BMJ,* 343**,** d4331.

Sanders, R. D., Tononi, G., Laureys, S. & Sleigh, J. W. 2012. Unresponsiveness not equal unconsciousness. *Anesthesiology,* 116**,** 946-59.

Sanna, E., Mascia, M. P., Klein, R. L., Whiting, P. J., Biggio, G. & Harris, R. A. 1995. Actions of the general anesthetic propofol on recombinant human GABAA receptors: influence of receptor subunits. *J Pharmacol Exp Ther,* 274**,** 353-360.

Savoia, G., Esposito, C., Belfiore, F., Amantea, B. & Cuocolo, R. 1988. Propofol infusion and auditory evoked potentials. *Anaesthesia,* 43 Suppl**,** 46-9.

Scherg, M., Vajsar, J. & Picton, T. W. 1989. A source analysis of the late human auditory evoked potentials. *J Cogn Neurosci,* 1**,** 336-55.

Schiff, N. D. 2008. Central thalamic contributions to arousal regulation and neurological disorders of consciousness. *Ann N Y Acad Sci,* 1129**,** 105-118.

Schiff, N. D. 2009. Central thalamic deep-brain stimulation in the severely injured brain: rationale and proposed mechanisms of action. *Ann N Y Acad Sci,* 1157**,** 101-16.

Schnakers, C., Vanhaudenhuyse, A., Giacino, J., Ventura, M., Boly, M., Majerus, S., Moonen, G. & Laureys, S. 2009. Diagnostic accuracy of the vegetative and minimally conscious state: clinical consensus versus standardized neurobehavioral assessment. *BMC Neurol,* 9**,** 35.

Schnider, T. W., Minto, C. F., Gambus, P. L., Andresen, C., Goodale, D. B., Shafer, S. L. & Youngs, E. J. 1998. The influence of method of administration and covariates on the pharmacokinetics of propofol in adult volunteers. *Anesthesiology,* 88**,** 1170-82.

Schreckenberger, M., Lange-Asschenfeldt, C., Lange-Asschenfeld, C., Lochmann, M., Mann, K., Siessmeier, T., Buchholz, H.-G., Bartenstein, P. & Grunder, G. 2004. The thalamus as the generator and modulator of EEG alpha rhythm: a combined PET/EEG study with lorazepam challenge in humans. *Neuroimage,* 22**,** 637-644.

Schroter, M. S., Spoormaker, V. I., Schorer, A., Wohlschlager, A., Czisch, M., Kochs, E. F., Zimmer, C., Hemmer, B., Schneider, G., Jordan, D. & Ilg, R. 2012. Spatiotemporal reconfiguration of large-scale brain functional networks during propofol-induced loss of consciousness. *Journal of Neuroscience,* 32**,** 12832-12840.

Schrouff, J., Perlbarg, V., Boly, M., Marrelec, G., Boveroux, P., Vanhaudenhuyse, A., Bruno, M. A., Laureys, S., Phillips, C., Pelegrini-Issac, M., Maquet, P. & Benali, H.

2011. Brain functional integration decreases during propofol-induced loss of consciousness. *NeuroImage,* 57**,** 198-205.

Schwarzkopf, D. S., Robertson, D. J., Song, C., Barnes, G. R. & Rees, G. 2012. The frequency of visually induced gamma-band oscillations depends on the size of early human visual cortex. *J Neurosci,* 32**,** 1507-12.

Sebel, P. S., Flynn, P. J. & Ingram, D. A. 1984. Effect of nitrous oxide on visual, auditory and somatosensory evoked potentials. *Br J Anaesth,* 56**,** 1403-7.

Sebel, P. S., Ingram, D. A., Flynn, P. J., Rutherfoord, C. F. & Rogers, H. 1986. Evoked potentials during isoflurane anaesthesia. *Br J Anaesth,* 58**,** 580-5.

Seghier, M. L. 2013. The angular gyrus: multiple functions and multiple subdivisions. *Neuroscientist,* 19**,** 43-61.

Singer, W. 2001. Consciousness and the binding problem. *Ann N Y Acad Sci,* 929**,** 123-46.

Singh, K. D. 2006. Magnetoencephalography. *In:* SENIOR, C., RUSSELL, T. & GAZZANIGA, M. S. (eds.) *Methods in Mind.*

Singh, K. D. 2012. Which "neural activity" do you mean? fMRI, MEG, oscillations and neurotransmitters. *Neuroimage,* 62**,** 1121-30.

Sloan, H. L., Austin, V. C., Blamire, A. M., Schnupp, J. W., Lowe, A. S., Allers, K. A., Matthews, P. M. & Sibson, N. R. 2010. Regional differences in neurovascular coupling in rat brain as determined by fMRI and electrophysiology. *Neuroimage,* 53**,** 399-411.

Slotnick, S. D., Klein, S. A., Carney, T., Sutter, E. & Dastmalchi, S. 1999. Using multi-stimulus VEP source localization to obtain a retinotopic map of human primary visual cortex. *Clin Neurophysiol,* 110**,** 1793-800.

Smith, S. M. 2002. Fast robust automated brain extraction. *Hum Brain Mapp,* 17**,** 143-55.

Smith, S. M., Fox, P. T., Miller, K. L., Glahn, D. C., Fox, P. M., Mackay, C. E., Filippini, N., Watkins, K. E., Toro, R., Laird, A. R. & Beckmann, C. F. 2009. Correspondence of the brain's functional architecture during activation and rest. *Proc Natl Acad Sci U S A,* 106**,** 13040-5.

Sneyd, J. R., Samra, S. K., Davidson, B., Kishimoto, T., Kadoya, C. & Domino, E. F. 1994. Electrophysiologic effects of propofol sedation. *Anesth Analg,* 79**,** 1151-8.

Sockeel, S., Schwartz, D., Pelegrini-Issac, M. & Benali, H. 2016. Large-Scale Functional Networks Identified from Resting-State EEG Using Spatial ICA. *PLoS One,* 11**,** e0146845.

Sperling, R., Greve, D., Dale, A., Killiany, R., Holmes, J., Rosas, H. D., Cocchiarella, A., Firth, P., Rosen, B., Lake, S., Lange, N., Routledge, C. & Albert, M. 2002. Functional MRI detection of pharmacologically induced memory impairment. *Proc Natl Acad Sci U S A,* 99**,** 455-460.

Spiegler, A., Knosche, T. R., Schwab, K., Haueisen, J. & Atay, F. M. 2011. Modeling brain resonance phenomena using a neural mass model. *PLoS Comput Biol,* 7**,** e1002298.

Sporns, O. & Honey, C. J. 2006. Small worlds inside big brains. *Proc Natl Acad Sci U S A,* 103**,** 19219-20.

Stagg, C. J., Bachtiar, V. & Johansen-Berg, H. 2011. What are we measuring with GABA magnetic resonance spectroscopy? *Commun Integr Biol,* 4**,** 573-5.

Stamatakis, E. A., Adapa, R. M., Absalom, A. R. & Menon, D. K. 2010. Changes in resting neural connectivity during propofol sedation. *PLoS One,* 5.

Steriade, M. 2003. The corticothalamic system in sleep. *Front Biosci,* 8**,** d878-99.

Steriade, M., Datta, S., Pare, D., Oakson, G. & Curro Dossi, R. C. 1990. Neuronal activities in brain-stem cholinergic nuclei related to tonic activation processes in thalamocortical systems. 10**,** 2541-2559.

Suffczynski, P., Kalitzin, S., Pfurtscheller, G. & Lopes Da Silva, F. H. 2001. Computational model of thalamo-cortical networks: dynamical control of alpha rhythms in relation to focal attention. *Int J Psychophysiol,* 43**,** 25-40.

Sumner, P., Edden, R. A., Bompas, A., Evans, C. J. & Singh, K. D. 2010. More GABA, less distraction: a neurochemical predictor of motor decision speed. *Nat Neurosci,* 13**,** 825-7.

Sun, X., Zhang, H., Gao, C., Zhang, G., Xu, L., Lv, M. & Chai, W. 2008. Imaging the effects of propofol on human cerebral glucose metabolism using positron emission tomography. *J Int Med Res,* 36**,** 1305-10.

Suntsova, N., Szymusiak, R., Alam, M. N., Guzman-Marin, R. & Mcginty, D. 2002. Sleep-waking discharge patterns of median preoptic nucleus neurons in rats. *J Physiol,* 543**,** 665-677.

Supp, G. G., Siegel, M., Hipp, J. F. & Engel, A. K. 2011. Cortical hypersynchrony predicts breakdown of sensory processing during loss of consciousness. *Curr Biol,* 21**,** 1988-93.

Sur, C., Fresu, L., Howell, O., Mckernan, R. M. & Atack, J. R. 1999. Autoradiographic localization of alpha5 subunit-containing GABAA receptors in rat brain. *Brain Res,* 822**,** 265-270.

Swettenham, J. B., Muthukumaraswamy, S. D. & Singh, K. D. 2009. Spectral properties of induced and evoked gamma oscillations in human early visual cortex to moving and stationary stimuli. *J Neurophysiol,* 102**,** 1241-53.

Szymusiak, R. & Mcginty, D. 2008. Hypothalamic regulation of sleep and arousal. *Ann N Y Acad Sci,* 1129**,** 275-286.

Tallon-Baudry, C. & Bertrand, O. 1999. Oscillatory gamma activity in humans and its role in object representation. *Trends in Cognitive Sciences,* 3**,** 151-162.

Tarnal, V., Vlisides, P. E. & Mashour, G. A. 2016. The Neurobiology of Anesthetic Emergence. *J Neurosurg Anesthesiol,* 28**,** 250-5.

Tewarie, P., Bright, M. G., Hillebrand, A., Robson, S. E., Gascoyne, L. E., Morris, P. G., Meier, J., Van Mieghem, P. & Brookes, M. J. 2016. Predicting haemodynamic networks using electrophysiology: The role of non-linear and cross-frequency interactions. *Neuroimage,* 130**,** 273-92.

Teyler, T. J., Cuffin, B. N. & Cohen, D. 1975. The visual evoked magnetoencephalogram. *Life Sci,* 17**,** 683-91.

Thomas, C. G. & Menon, R. S. 1998. Amplitude response and stimulus presentation frequency response of human primary visual cortex using BOLD EPI at 4 T. *Magn Reson Med,* 40**,** 203-209.

Thomson, A. J., Nimmo, A. F., Tiplady, B. & Glen, J. B. 2009. Evaluation of a new method of assessing depth of sedation using two-choice visual reaction time testing on a mobile phone. *Anaesthesia,* 64**,** 32-8.

Thornton, C., Creagh-Barry, P., Jordan, C., Luff, N. P., Dore, C. J., Henley, M. & Newton, D. E. 1992. Somatosensory and auditory evoked responses recorded simultaneously: differential effects of nitrous oxide and isoflurane. *Br J Anaesth,* 68**,** 508-14.

Thornton, C. & Sharpe, R. M. 1998. Evoked responses in anaesthesia. *Br J Anaesth,* 81**,** 771-81.

Tononi, G. 2004. An information integration theory of consciousness. *BMC Neurosci,* 5**,** 42-42.

Tooley, M. A., Greenslade, G. L. & Prys-Roberts, C. 1996. Concentration-related effects of propofol on the auditory evoked response. *Br J Anaesth,* 77**,** 720-6.

Trapani, G., Altomare, C., Liso, G., Sanna, E. & Biggio, G. 2000. Propofol in anesthesia. Mechanism of action, structure-activity relationships, and drug delivery. *Curr Med Chem,* 7**,** 249-71.

Traub, R. D., Whittington, M. A., Colling, S. B., Buzsaki, G. & Jefferys, J. G. R. 1996. Analysis of gamma rhythms in the rat hippocampus in vitro and in vivo. *Journal of Physiology-London,* 493**,** 471-484.

Uhlhaas, P. J. & Singer, W. 2010. Abnormal neural oscillations and synchrony in schizophrenia. *Nat Rev Neurosci,* 11**,** 100-13.

Urban, B. W. & Bleckwenn, M. 2002. Concepts and correlations relevant to general anaesthesia. *Br J Anaesth,* 89**,** 3-16.

Van Den Heuvel, M. P. & Hulshoff Pol, H. E. 2010. Exploring the brain network: a review on resting-state fMRI functional connectivity. *Eur Neuropsychopharmacol,* 20**,** 519-34.

Vanini, G., Watson, C., Lydic, R. & Baghdoyan, H. 2008. Gamma-aminobutyric acid-mediated neurotransmission in the pontine reticular formation modulates hypnosis, immobility, and breathing during isoflurane anesthesia. *Anesthesiology,* 109**,** 978-88.

Vatansever, D., Manktelow, A. E., Sahakian, B. J., Menon, D. K. & Stamatakis, E. A. 2018. Default Mode Network Engagement Beyond Self-Referential Internal Mentation. *Brain Connect*.

Vaucher, E., Tong, X. K., Cholet, N., Lantin, S. & Hamel, E. 2000. GABA neurons provide a rich input to microvessels but not nitric oxide neurons in the rat cerebral cortex: a means for direct regulation of local cerebral blood flow. *J Comp Neurol,* 421**,** 161-171.

Verma, R., Alladi, R., Jackson, I., Johnston, I., Kumar, C., Page, R., Smith, I., Stocker, M., Tickner, C., Williams, S. & Young, R. 2011. Day case and short stay surgery: 2. *Anaesthesia,* 66**,** 417-34.

Veselis, R., Reinsel, R., Feshchenko, V., Beattie, B. & Akhurst, T. 2004a. Auditory rCBF covariation with word rate during drug-induced sedation and unresponsiveness: a H2015 PET study. *Brain Cogn,* 54**,** 142-4.

Veselis, R. A. 1996. The EEG as a monitor of sedation: encouraging progress. *J Clin Anesth,* 8**,** 81S-87S.

Veselis, R. A., Feshchenko, V. A., Reinsel, R. A., Beattie, B. & Akhurst, T. J. 2005. Propofol and thiopental do not interfere with regional cerebral blood flow response at sedative concentrations. *Anesthesiology,* 102**,** 26-34.

Veselis, R. A., Feshchenko, V. A., Reinsel, R. A., Dnistrian, A. M., Beattie, B. & Akhurst, T. J. 2004b. Thiopental and propofol affect different regions of the brain at similar pharmacologic effects. *Anesth Analg,* 99**,** 399-408, table of contents.

Veselis, R. A. & Reinsel, R. A. 1992. Electroencephalographic effects of sedative hypnotics. *Anesthesiology,* 77**,** 837-8.

Veselis, R. A., Reinsel, R. A., Feshchenko, V. A. & Dnistrian, A. M. 2002. A neuroanatomical construct for the amnesic effects of propofol. *Anesthesiology,* 97**,** 329-37.

Vijayan, S., Ching, S., Purdon, P. L., Brown, E. N. & Kopell, N. J. 2013a. Thalamocortical Mechanisms for the Anteriorization of Alpha Rhythms during Propofol-Induced Unconsciousness. *Journal of Neuroscience,* 33**,** 11070-11075.

Vijayan, S., Ching, S., Purdon, P. L., Brown, E. N. & Kopell, N. J. 2013b. Thalamocortical mechanisms for the anteriorization of alpha rhythms during propofol-induced unconsciousness. *J Neurosci,* 33**,** 11070-5.

Vincent, J. L., Patel, G. H., Fox, M. D., Snyder, A. Z., Baker, J. T., Van Essen, D. C., Zempel, J. M., Snyder, L. H., Corbetta, M. & Raichle, M. E. 2007. Intrinsic functional architecture in the anaesthetized monkey brain. *Nature,* 447**,** 83-86.

Vrba, J. & Robinson, S. E. 2001. Signal processing in magnetoencephalography. *Methods,* 25**,** 249-271.

Wang, B., Bai, Q., Jiao, X., Wang, E. & White, P. F. 1997. Effect of sedative and hypnotic doses of propofol on the EEG activity of patients with or without a history of seizure disorders. *J Neurosurg Anesthesiol,* 9**,** 335-40.

Wang, X. J. & Buzsaki, G. 1996. Gamma oscillation by synaptic inhibition in a hippocampal interneuronal network model. *Journal of Neuroscience,* 16**,** 6402-6413.

Warnaby, C. E. P. D., Seretny, M. M. D., Ni Mhuircheartaigh, R. M. D. D. P., Rogers, R. M. D., Jbabdi, S. P. D., Sleigh, J. M. D. & Tracey, I. M. a. D. P. F. R. C. a. F. M. S. 2016. Anesthesia-induced Suppression of Human Dorsal Anterior Insula Responsivity at Loss of Volitional Behavioral Response. *Anesthesiology April,* 124**,** 766-778.

Watts, D. J. & Strogatz, S. H. 1998. Collective dynamics of 'small-world' networks. *Nature,* 393**,** 440-2.

Webster, M. 2017. https://fsl.fmrib.ox.ac.uk/fsl/fslwiki/FEAT/UserGuide [Online]. FMRIB. [Accessed 17.08.2017].

White, N. S. & Alkire, M. T. 2003. Impaired thalamocortical connectivity in humans during general-anesthetic-induced unconsciousness. *Neuroimage,* 19**,** 402-411.

Whitham, E. M., Lewis, T., Pope, K. J., Fitzgibbon, S. P., Clark, C. R., Loveless, S., Delosangeles, D., Wallace, A. K., Broberg, M. & Willoughby, J. O. 2008. Thinking activates EMG in scalp electrical recordings. *Clinical Neurophysiology,* 119**,** 1166-1175.

Whitham, E. M., Pope, K. J., Fitzgibbon, S. P., Lewis, T., Clark, C. R., Loveless, S., Broberg, M., Wallace, A., Delosangeles, D., Lillie, P., Hardy, A., Fronsko, R., Pulbrook, A. & Willoughby, J. O. 2007. Scalp electrical recording during paralysis: quantitative evidence that EEG frequencies above 20 Hz are contaminated by EMG. *Clin Neurophysiol,* 118**,** 1877-88.

Whittington, M. A., Jefferys, J. G. & Traub, R. D. 1996. Effects of intravenous anaesthetic agents on fast inhibitory oscillations in the rat hippocampus in vitro. *Br J Pharmacol,* 118**,** 1977-1986.

Winkler, A. M., Ridgway, G. R., Webster, M. A., Smith, S. M. & Nichols, T. E. 2014. Permutation inference for the general linear model. *Neuroimage,* 92**,** 381-97.

Wong, E. C., Buxton, R. B. & Frank, L. R. 1998. Quantitative imaging of perfusion using a single subtraction (QUIPSS and QUIPSS II). *Magn Reson Med,* 39**,** 702-8.

Woolrich, M. 2008. Robust group analysis using outlier inference. *Neuroimage,* 41**,** 286-301.

Woolrich, M. W., Behrens, T. E., Beckmann, C. F., Jenkinson, M. & Smith, S. M. 2004. Multilevel linear modelling for FMRI group analysis using Bayesian inference. *Neuroimage,* 21**,** 1732-47.

Woolrich, M. W., Ripley, B. D., Brady, M. & Smith, S. M. 2001. Temporal autocorrelation in univariate linear modeling of FMRI data. *Neuroimage,* 14**,** 1370-86.

Worsley, K. J. 2001. Statistical analysis of activation images. *In:* JEZZARD, P., MATTHEWS, P. M. & SMITH, S. M. (eds.) *Functional MRI: An Introduction to Methods.* OUP.

Wu, X., Zou, Q., Hu, J., Tang, W., Mao, Y., Gao, L., Zhu, J., Jin, Y., Wu, X., Lu, L., Zhang, Y., Zhang, Y., Dai, Z., Gao, J. H., Weng, X., Zhou, L., Northoff, G., Giacino, J. T., He, Y. & Yang, Y. 2015. Intrinsic Functional Connectivity Patterns Predict Consciousness Level and Recovery Outcome in Acquired Brain Injury. *J Neurosci,* 35**,** 12932-46.

Xie, G., Deschamps, A., Backman, S. B., Fiset, P., Chartrand, D., Dagher, A. & Plourde, G. 2011. Critical involvement of the thalamus and precuneus during restoration of consciousness with physostigmine in humans during propofol anaesthesia: a positron emission tomography study. *Br J Anaesth,* 106**,** 548-57.

Xing, D., Yeh, C. I., Burns, S. & Shapley, R. M. 2012. Laminar analysis of visually evoked activity in the primary visual cortex. *Proc Natl Acad Sci U S A,* 109**,** 13871-6.

Yarkoni, T., Barch, D. M., Gray, J. R., Conturo, T. E. & Braver, T. S. 2009. BOLD correlates of trial-by-trial reaction time variability in gray and white matter: a multi-study fMRI analysis. *PLoS One,* 4**,** e4257.

Yip, G. M., Chen, Z. W., Edge, C. J., Smith, E. H., Dickinson, R., Hohenester, E., Townsend, R. R., Fuchs, K., Sieghart, W., Evers, A. S. & Franks, N. P. 2013. A propofol binding site on mammalian GABAA receptors identified by photolabeling. *Nat Chem Biol,* 9**,** 715-20.

Ypparila, H., Korhonen, I., Tarvainen, M., Musialowicz, T., Jakob, S. M. & Partanen, J. 2004. N100 auditory potential and electroencephalogram discriminate propofol-induced sedation levels. *J Clin Monit Comput,* 18**,** 163-70.

Yuval-Greenberg, S., Tomer, O., Keren, A. S., Nelken, I. & Deouelll, L. Y. 2008. Transient induced gamma-band response in EEG as a manifestation of miniature saccades. *Neuron,* 58**,** 429-441.

Yvert, B., Crouzeix, A., Bertrand, O., Seither-Preisler, A. & Pantev, C. 2001. Multiple supratemporal sources of magnetic and electric auditory evoked middle latency components in humans. *Cereb Cortex,* 11**,** 411-23.

Zaehle, T., Frund, I., Schadow, J., Tharig, S., Schoenfeld, M. A. & Herrmann, C. S. 2009. Inter- and intra-individual covariations of hemodynamic and oscillatory gamma responses in the human cortex. *Front Hum Neurosci,* 3**,** 8.

Zeller, A., Arras, M., Jurd, R. & Rudolph, U. 2007. Mapping the contribution of beta3-containing GABAA receptors to volatile and intravenous general anesthetic actions. *BMC Pharmacol,* 7**,** 2-2.

Zhang, H., Wang, W., Gao, W., Ge, Y., Zhang, J., Wu, S. & Xu, L. 2009. Effect of propofol on the levels of neurotransmitters in normal human brain: a magnetic resonance spectroscopy study. *Neurosci Lett,* 467**,** 247-51.

Appendices

Appendix 1: Spatial connectivity studies with propofol sedation and anaesthesia

(Stamatakis et al., 2010)	Propofol	light/ deep sedation	PCC fc increases/ changes with sedation
(Boveroux et al., 2010)	Propofol	sedation	Diminished fc in DMN and FP, not sensory networks
(Mhuircheartaigh et al., 2010)	propofol	sedation	Thalam-cortical fc preserved, loss of putamen fc
(Schrouff et al., 2011)	Propofol	deep sedation	Reduced/ preserved fc, decrease in fronto-parietal is the key change
(Schroter et al., 2012)	propofol	anaesthesia	Loss of thalamo-cortical fc, fc of sensory cortices maintained
(Jordan et al., 2013a)	propofol	anaesthesia	Decreased Fc in DMN, increased in sensory networks under anaesthesia; Directional connectivity reduced in Fronto-parietal networks
(Liu et al., 2013)	propofol	light/ deep sedation	Nonspecific and specific thalamic nuclei have different fc; NS relevant for consciousness
(Monti et al., 2013)	propofol	anaesthesia/sedation	Increased cortico-cortico and thalam-cortical fc during sedation, Cortico-cortico fc responsible for unconsciousness
(Guldenmund et al., 2013)	propofol	anaesthesia	Decreased fc of DMN and salience networks. Thalamus, disconnected but increased fc with sensori-motor, auditory and insular. Brainstem disconnected
(Amico et	propofol	anaesthesia/s	Reduced PCC fc with frontal areas

al., 2014)		edation	
(Huang et al., 2014)	propofol / sevoflurane	anaesthesia	Decreased fc in DMN, TC,; reduced with midline structures but increased with lateral structures
(Barttfeld et al., 2015)	propofol	light and deep sedation	Reduced FP connectivity with sedation and loss of TC fc with unconsciousness, but increase TC fc with occipital and temporal regions
(Liu et al., 2015)	propofol	light and deep sedation	DMN fc reduced by light and deep sedation